LIÈGE université
Gembloux
Agro-Bio Tech

Profiling and fingerprinting of volatiles by advanced analytical techniques

Steven MASCREZ

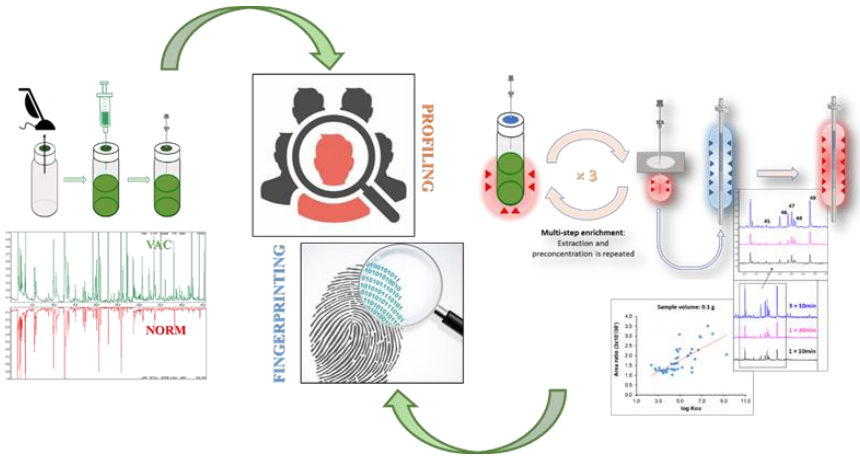

COMMUNAUTÉ FRANÇAISE DE BELGIQUE
UNIVERSITÉ DE LIÈGE – GEMBLOUX AGRO-BIO TECH

Profiling and fingerprinting of volatiles by advanced analytical techniques

Steven Patrick Roger Joseph Mascrez

Dissertation originale présentée (ou essai présenté) en vue de l'obtention du grade de doctorat en sciences agronomiques et ingénierie biologique

Promoteur(s) : Professeur Giorgia Purcaro
Année civile (= année du dépôt) : 2024

Abstract

Food is a highly heterogeneous matrix made up of various biochemical components. Food product characterization can be used for a variety of goals, including ensuring food safety, authenticity, and/or quality. For instance, flavor, which combines taste and olfaction, is a key element in determining whether or not a food will be accepted by consumers. Organoleptic perception is closely correlated with volatile compounds.

The most widely used headspace-based sampling technique is headspace-solid phase microextraction (HS-SPME). This is a solvent-free, quick, affordable, easy to use, versatile, and automatable sample preparation technique for pre-concentration of (semi)volatile compounds. The adsorption is based on the partition equilibrium among the three-phase system constituted by sample, headspace over the sample, and fibre. Equilibrium can be reached from several minutes to hours. In HS-SPME method development, compromise has to be done between sensitivity and analysis throughput.

In this thesis alternative HS-SPME approaches have been investigated to enhance the level of information extractable without extending the extraction time.

The first method involved increasing the kinetics of extraction by decreasing the pressure in the SPME-vial (Vac-SPME). As a result, more compounds are extracted in shorter time, than they would in a conventional HS-SPME, and at milder temperatures.

The second strategy involved exploiting the multiple cumulative trapping SPME method (MCT-SPME) by means of cooled trap. Multiple extractions from a single vial were performed, and each extract was concentrated in a cold trap before desorption of the cumulated extract into a gas chromatographic column.

The performances of the different sampling approaches were evaluated considering both the extraction yield of targeted compounds and the discrimination ability in a cross-sample comparison (translated into the level of information extracted).

The third part of the thesis attempts to combine the two previous approaches. The goal was to highlight the synergistic potentiality of merging vacuum assisted extraction and MCT- HS-SPME. Olive oil was the main case study used in this thesis due to the importance of its volatile profile, which reflects in the sensory evaluation determining the commercial classification of the final product in extra virgin, virgin, and lampante oil.

Résumé

Les aliments sont une matrice très hétérogène composée de divers éléments biochimiques. La caractérisation des produits alimentaires peut être utilisée à diverses fins, notamment pour garantir la sécurité du consommateur, l'authenticité et/ou la qualité des aliments. Par exemple, la saveur, qui combine le goût et l'olfaction, est un élément clé pour déterminer si un aliment sera accepté ou non par les consommateurs. La perception organoleptique est étroitement liée aux composés volatils.

La technique d'échantillonnage basée sur l'espace de tête la plus utilisée est la microextraction en phase solide dans l'espace de tête (HS-SPME). Il s'agit d'une technique de préparation d'échantillons sans solvant, rapide, abordable, facile à utiliser, polyvalente et automatisable pour la préconcentration des composés (semi-) volatils. L'adsorption est basée sur le partage à l'équilibre dans un système triphasé constitué par l'échantillon, l'espace de tête et la fibre. L'équilibre peut être atteint en quelques minutes ou en quelques heures. Dans le développement de méthodes de HS-SPME, il faut trouver un compromis entre la sensibilité et le débit d'analyse.

Dans cette thèse, d'autres approches HS-SPME ont été étudiées pour améliorer le niveau d'information extractible sans allonger le temps d'analyse.

La première méthode a consisté à augmenter la cinétique d'extraction en diminuant la pression dans le flacon de SPME (Vac-SPME). Ainsi, davantage de composés sont extraits en moins de temps que dans une HS-SPME conventionnelle, et à des températures plus basses.

La deuxième stratégie consiste à exploiter la méthode SPME à piégeage cumulatif multiple (MCT-SPME) au moyen d'un piège à froid. Des extractions multiples à partir d'un seul flacon ont été réalisées, et chaque extrait a été concentré avant la désorption de l'ensemble des extraits dans une colonne de chromatographie en phase gazeuse.

Les performances des différentes approches d'échantillonnage ont été évaluées en tenant compte à la fois du rendement d'extraction des composés ciblés et de la capacité de discrimination dans une comparaison inter-échantillons (traduite en niveau d'information extraite).

La troisième partie de la thèse tente de combiner les deux approches précédentes. L'objectif était de mettre en évidence le potentiel synergique de la fusion de l'extraction assistée sous vide et de la MCT-HS-SPME. L'huile d'olive a été le principal cas d'étude utilisé dans cette thèse en raison de l'importance de son profil volatil qui, reflété dans l'évaluation sensorielle, détermine la classification commerciale du produit final en huile extra vierge, vierge et lampante.

Acknolwedgements

I would like to thank the people who contributed to the completion of this thesis, as well as those who supported me during this long-term project.

To Professor Giorgia Purcaro, for her support, her availability and her involvement with my thesis subject. It allowed me to improve considerably in many aspects related to the world of research. She helped give me exceptional training to prepare me for post-doctoral work, which resulted in me getting a job with one of our colleagues.

To the members of the thesis committee, for their advice and collaboration on various projects.

To all the people I met in our Analytical Chemistry laboratory with whom I shared so many things, and more particularly with Sophie Vancraenenbroeck and Alex Glieneur who have been there since the start of my thesis.

And then to the other members or visitors of our lab:
Damien Eggermont, Aleksandra Gorska, Maurine Collard, Grégory Bauwens, Marta Cialiè Rosso, Nicola Sdrigotti, Angelica Fina, Nicolo Salgarella, Yening Qiao, Andrea Schincaglia, Silvia Pranteddu, Paula Albendea, and of course, Donatella Ferrara.

To all colleagues in the faculty, in particular Philippe Maesen and the members of BEAGx, the entomoligists and the members of Terra with whom I had the pleasure of collaborating.

I thank my family and friends for their unwavering support.

I also thank all those who have been part of my life directly or indirectly from my PhD student life. I could not name them because the list would be very long. However, I do not forget them.

Table of contents

List of figures

List of tables

Table 6-6: List of the top discriminatory compounds extrapolated after RF analysis to discriminate between EVO and VO, reported in order of elution, along with the CAS number, their octanol air partition (K_{oa}), linear retention index (LRI_{exp}) experimentally calculated and reported in the literature (LRI_{lib}).

List of acronyms

CCD: central composite design

DHS: dynamic headspace

DI: direct immersion

DOE: design of experiment

DVB/CAR/PDMS: divinylbenzene/carboxen/polydimethylsiloxane

EVO: extra virgin oil

FID: flame ionization detector

GC: gas chromatography

HCA: hierarchical cluster analysis

HCC: high concentration capacity

HS: headspace

LO: lampante oil

LRI: linear retention index

MCT: multiple cumulative trapping

MS: mass spectrometry

PCA: principal component analysis

PIL: polymeric ionic liquid

PQN: probabilistic quotient normalization

RF: random forest

RSD: relative standard deviation

SBSE: stir bar sorptive extraction

SPME: solid-phase microextraction

TOF: time of flight

VO: virgin oil

VOC: volatile organic compound

Chapter 1

Thesis introduction

Introduction

Volatile substances are an essential fraction of foods that generally compose the odorants that characterize the volatiles of a food product, but not only. The volatile profile of food has been used to describe different quality parameters, such as different authenticity aspects (e.g., geographical or botanical origin), transformation procedure (e.g., roasting), storage, and volatile profile or spoilage.

The analysis of volatiles is generally performed in the headspace (HS) above the sample, and can be performed in static-headspace (SHS) and dynamic-headspace (DHS). In the early 90's solid-phase microextraction (SPME) was introduce by Pawliszyn and co-authors. SPME HS represents a bridge between S- and DHS, being simple, fast, easy to automate, and reliable as the former but allowing a high concentration factor as DHS.

For the identification and quantification of the volatile compounds trapped in the HS, gas chromatography (GC) and even better multidimensional chromatography represent the main analytical techniques used over the years, thanks to the capability to provide fingerprinting and profiling information simultaneously [1]. In particular, comprehensive multidimensional GC (GC×GC) can generate chromatographic fingerprints that can be treated completely unbiased through chemometrics tools. But, if necessary, a profiling of the compounds present can be performed to obtain a targeted characterization of possible markers of specific scientific questions.

In this thesis, an introduction part is devoted to the introduction to the theory of SPME and GC×GC , followed by an overview of the powerful marriage of the two techniques in the field of food analysis (Chapter 2). Then the discussion enters in the experimental work performed during this PhD thesis, which was focused on enhancing the extraction ability and in particular the level of information obtained by implementing different sampling strategies in SPME. The first strategy was the application of vacuum-assisted (Vac) HS-SPME applied to olive oil and to fresh fish to investigate the use of sub-ambient temperature (Chapter 4). Then the possibility to perform multiple-cumulative trapping (MCT)-HS-SPME and the impact on the overall volatile profile was investigated (Chapter 5). Finally the two preview approaches were merged into MCT-Vac-HS-SPME to study the synergic effect of the two (Chapter 6).

An overall scheme of the thesis is reported in Figure 1.1.

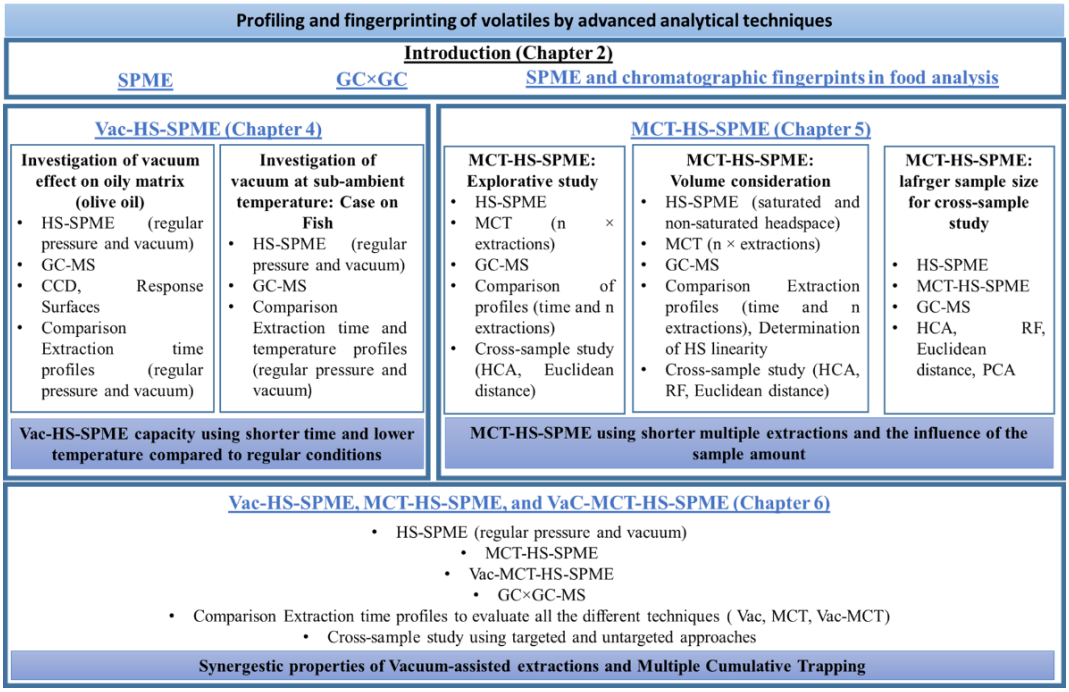

Figure 1-1 : Structure of the thesis.

Chapter 2

Introduction

1. SPME

Pawliszyn et al. [1, 2] developed Solid Phase Microextraction (SPME) to meet the exigency for expeditious sample preparation both within laboratory settings and on-site investigative procedures. The nomenclature "SPME" originates from its inaugural application, which involved extracting substances from solid fused silica fibers. Subsequently, the term was adjusted to reflect the appearance of the extraction phase in contrast to liquid or gaseous donor phases, notwithstanding the extraction phase's variable composition. SPME merges sampling, isolation, concentration, and sample introduction into a singular procedural step [3, 4].

The methodology employs a short, slender, solid fused silica rod, typically measuring 1 cm in length and 0.11 mm in outer diameter, coated with a polymer of approximately 1 µL volume. This fiber exhibits exceptional stability even under elevated temperatures and shares the same chemically inert characteristics as fused silica used in fabricating capillary GC columns. During periods of inactivity, the coated fused silica (SPME fiber) is shielded by a metal sheath, ensuring the safety of both the silica rod and the coated polymer. The SPME fiber is affixed to a metal rod, presenting a configuration akin to a modified syringe, conveniently housed within a fiber holder as depicted in Figure 2-1.

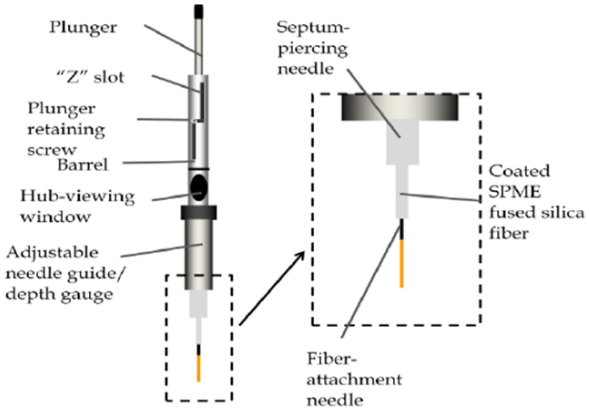

Figure 2-1 : Design and enlarged view of the commercial SPME device.

SPME involves initial partitioning of analytes between the sample and the fiber coating (mediated or not by the headspace), followed by desorption of the analytes from the coated fiber into an analytical instrument. A liquid or solid sample is sealed within a vial using a cap and septum. The fiber is either submerged directly into the liquid sample (resembling an aqueous environment) or exposed to the sample's headspace (either of liquid and solid samples) by lowering the plunger after puncturing the septum with the SPME protective sheath. Following an appropriate extraction duration, the fiber is retracted into the protective sheath, which is then removed from the sampling vial.

Subsequently, the sheath is inserted into the GC injector and the plunger is lowered to expose the fiber. The high temperature in the injector liner (GC) facilitates the thermal desorption of the sorbed analytes, which are subsequently refocused onto the head of the GC column. Thereafter, the fiber is withdrawn into the protective sheath and removed from the injector.

1.1. Principles of SPME

Solid-phase microextraction operates on an equilibrium basis, where analytes are not fully extracted from the matrix. Upon placement of a sample in a sealed vial, the equilibrium is established among three phases: (1) the fiber coating, (2) the headspace, and (3) the sample. The prediction of analyte recovery in SPME relies on the overall equilibrium which comprises two distinct equilibria: one between the sample and headspace, and another between the headspace and fiber, within the sampling vial. The total analyte amount remains constant throughout the extraction process. The distribution of the three phases post-equilibrium can be represented by the equation:

$$C_0 V_s = C_h V_h + C_s V_s + C_f V_f \quad \text{(Eq. 2.1)}$$

Where C_0 is the analyte's initial concentration in the aqueous solution; C_h, C_s, and C_f represent the equilibrium concentrations of analyte in the headspace, sample, and fiber coating respectively; and V_h, V_s, and V_f are the volumes of the headspace, sample, and fiber coating, respectively [5]. In cases where there is no headspace in the closed vial, the term involving the headspace, C_hV_h, is excluded, and equilibrium is established solely between the sample and the fiber.

This section delves into the theory developed for fibers coated with liquid polymers, known as the absorption mechanism. Another category of SPME coating is the porous polymer, which relies on adsorption rather than absorption. Its properties will be discussed in the subsequent section on SPME coatings.

First, the principles of direct liquid sampling, involving the immersion of the fiber directly into the aqueous sample, will be addressed. Subsequently, the principles of headspace sampling will be elucidated.

Furthermore, a third mode, SPME with membrane protection, entails the use of a selective membrane to separate the fiber from the sample, allowing analytes to permeate while impeding interference. The primary role of the membrane barrier is to safeguard the fiber from the adverse effects of high-molecular-weight compounds when analyzing exceptionally contaminated samples. Although achieving a similar outcome as headspace extraction, membrane protection facilitates the analysis of less volatile compounds.

1.1.1. Direct liquid sampling

The partitioning phenomenon occurring between the fiber coating (stationary phase) and the sample is characterized by the distribution constant, K_{fs}, which is defined as:

$$K_{fs} = \frac{C_f}{C_s} \qquad \text{(Eq. 2.2)}$$

Where: C_f is the concentration of analyte in the fiber coating and C_s is the concentration of analyte in the sample [6]. This parameter serves as a distinctive measure of the fiber coating's properties and its selectivity towards specific analytes as opposed to other components within the matrix.

The partition ratio, k′ is:

$$k' = \frac{C_f V_f}{C_s V_s} = \frac{n_f}{n_s} = \frac{K_{fs} V_f}{V_s} \qquad \text{(Eq. 2.3)}$$

where n_f and ns are the number of moles in the aqueous and fiber coating phases, respectively, and V_f and V_s are the volumes of the fiber coating and sample. The K_{fs} values of the targeted analytes are comparatively high because the coatings used in SPME have strong affinities for organic compounds. This suggests that SPME produces good sensitivity and has a very high concentrating effect [7]. Nevertheless, K_{fs} values are too small to completely extract most analytes from the matrix. Instead, SPME is an equilibrium sampling method that can be used to accurately determine the concentration of target analytes in a sample matrix after it has been properly calibrated.

Two different equations are used to determine the amount absorbed by the fiber, depending on the sample volume. For big sample volumes, the amount of analyte absorbed by the fiber coating at equilibrium is exactly proportional to the initial sample concentration, or C_0. The following formula is used when the volume of the sample, V_s, is much larger than the stationary phase volume ($V_s >> K_{fs}V_f$), or when its volume is almost infinite in respect to the fiber volume.

$$n_f = K_{fs} V_f C_0 \quad \text{(Eq. 2.4)}$$

Where n_f represents the amount that the fiber coating has extracted. Because the sample volume in this instance is relatively infinite, it does not need to be known, which makes it perfect for field sampling and streamlining laboratory procedures. But when drawing from a limited sample volume, the sample may become severely reduced, and the amount absorbed turns into:

$$n_f = \frac{K_{fs} V_f V_s C_0}{K_{fs} V_f + V_s} \quad \text{(Eq. 2.5)}$$

The amount of analyte absorbed by the fiber coating is directly proportional to the initial analyte concentration, C_0, just as in the case of an infinitely aqueous volume. Nonetheless, the denominator now includes the extra $K_{fs}V_f$ term. The significance of this new term lies only in its comparison to the sample volume, or V_s, as it reduces the amount of analyte that the fiber coating absorbs.

In practical terms, this reduction is primarily observed in cases of large distribution constants, Kfs, attributable to the minute volume of the fiber stationary phase, V_f. If $K_{fs}V_f >> V_s$ [8], most of the analyte will indeed transfer to the fiber coating.

1.1.2. Headspace sampling

In HS-SPME mode, a fused silica fiber coated with polymeric organic liquid is inserted into the headspace above the sample. The coating extracts and concentrates the volatile organic analytes, which are then transferred to the analytical instrument for desorption and analysis. This modification to the solid-phase microextraction method reduces extraction time and makes it easier to use for solid sample analysis. At room temperature, the headspace SPME technique is very effective for isolating compounds with Henry's constants greater than 90 $atm.cm^3.mol^{-1}$, and it can also be used to sample less volatile compounds if high sensitivity is achieved without reaching equilibrium. The equilibration time for less volatile compounds can be significantly reduced by agitating both the aqueous phase and the headspace, reducing the headspace volume, and increasing the sampling temperature.

The geometry of the SPME headspace extraction is shown in Figure 2-2a. A sample contaminated with organic compounds is placed in a closed container with headspace. Chemical equilibrium is established between the sample and the headspace before inserting a fused silica fiber coated with a thin layer of a selected liquid organic polymer into the container's headspace (the fiber has no direct contact with the sample). The fiber's liquid coating begins to absorb organic analytes from the headspace. Analytes move through a series of transport processes, from sample to gas phase and finally to the coating, until the system reaches equilibrium. The diffusion process occurs in both the axial and radial directions. A simple one-dimensional diffusion model, as shown in Figure 2-2b, can provide adequate insight into this diffusion problem. In the model shown in Figure 2-2b, diffusion occurs only in one direction (x-axis); a is the thickness of the polymeric coating, b-a is the length of the headspace, and c-b is the length of the sample.

Though the headspace SPME technique can be used to analyze organic compounds in a variety of matrices, and the fiber coating can be solid or liquid, its equilibrium and kinetic theory can be better understood by looking at a three-phase system that includes a liquid polymeric coating, a headspace, and an aqueous solution. The amount of analytes absorbed by the liquid polymeric coating is proportional to the overall balance of analytes in the three-phase system. Since the total amount of an analyte must be the same during the extraction, we obtain the Equation 2.1.

If we define fiber coating/headspace partition coefficients as $K_{fh} = Cf/C_h$ and headspace/sample partition coefficient as $K_{hs} = C_h/C_s$, the amount of the analyte absorbed by the coating (i.e., the capacity of the coating), can be expressed as

$$n = \frac{C_0 V_f K_{fs} K_{hs}}{V_f K_{fh} K_{hs} + V_h K_{hs} + V_s} \quad \text{(Eq. 2.6)}$$

where n is the mass of the analyte extracted by the coating, C_0 is the initial concentration of the analyte in the sample; V_f, V_s and V_h are the volumes of the coating, the sample, and the headspace, respectively; K_{fh} is the coated fiber/headspace partition coefficient and K_{hs} the headspace/sample partition coefficient.

Equation 2.6 describes the mass extracted by the polymeric coating once equilibrium has been achieved. The driving force in a multiphase equilibrium is the difference among an analyte's chemical potentials in the three phases. At equilibrium conditions in a three-phase system, the amount of analyte extracted is not affected by the fiber's location in the system. As long as the volume of the fiber coating, headspace, and sample remains constant, the fiber can be placed in either the headspace or the sample. The three terms in the denominator of Equation 2.6 represent the analyte capacity of each phase: fiber ($V_f K_{fh} K_{hs}$), headspace ($V_h K_{hs}$), and sample (V_s). Assuming that the vial containing the sample is completely filled with aqueous matrix (no headspace), the term in the denominator can be removed, yielding Equation 2.5 (two phase system).

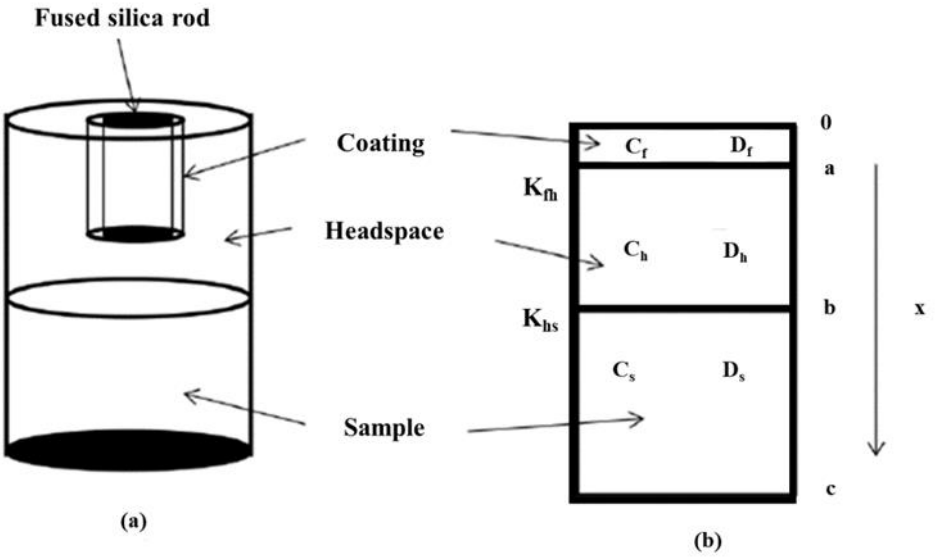

Figure 2-2 : (a) Geometry of the headspace SPME method. (b) One – dimensional model of the three – phase diffusion process; K_{fh} and K_{hs} are the coating/gas and gas/sample partition coefficients, respectively: D_f, D_h, and D_s are the diffusion coefficients of the analyte in the coating, the headspace, and sample, respectively; C_f, C_h and C_s, are the concentrations of the analyte in the coating, the headspace, and sample, respectively; a, b-a, and c-b are the thicknesses of the coating, the headspace, and sample, respectively [5].

The headspace SPME technique is based on analyte equilibrium in the involved phases. Equation 2.4 calculates the mass of analytes absorbed by the liquid polymeric coating once equilibrium has been achieved. The kinetics of mass transport, in which analytes move from the sample phase to the headspace and then to the coating, must also be addressed, as this process determines the sampling time of the headspace SPME method.

1.2. Mass transfer

The transfer of analytes in the headspace is one of the main limiting factors in HS-SPME sampling. A two-resistance theory can be used to explain the mass transfer of molecules into headspace from an aqueous liquid sample [9, 10]. This theory has been derived from the method used to describe the rate at which water bodies evaporate into the atmosphere [11]. A representation of the model is shown in Figure 2-3. The model makes the following assumptions:

- An inter-phase effectively separates the headspace and aqueous liquid sample.
- On either side of the inter-phase, two nearly stationary films (liquid and gas) are present.
- These films contain the majority of the diffusion resistance.
- These films contain the majority of the gradient's concentration

In this model, extraction involves a number of processes. The molecules in the aqueous liquid sample first migrate to the liquid film. Following that, they move to the gas-film via molecular diffusion. Molecules are moved from the gas-film closer to the coating of the fiber. Depending on the nature of the coating, they migrate into the bulk or remain on the coating surface after becoming adsorbed on the surface [10, 12]. The chemical mass balance is expressed as follows when the extraction is carried out before the equilibration state is reached [13]:

$$V_s \frac{dC_s}{dt} = -K_L A(C_s - C_i) \quad \text{(Eq. 2.8)}$$

Where,

C_i: analyte concentration in the inter-phase between liquid and gas.

A: interfacial contact area between liquid and gas.

K_L: overall mass transfer coefficient.

K_L can be described using the 2-resistance theory mentioned above as [11, 13]:

$$K_L = \left[\frac{1}{k_l} + \frac{RT}{K_H k_g}\right] \quad \text{(Eq. X.9)}$$

k_l and k_g: mass transfer coefficient of the liquid-film and gas-film, respectively.
K_H: Henry's law constant (ratio of the partial pressure to aqueous concentration).
R: gas constant (8.2057×10^{-5} $m^3.atm.mol^{-1}.K^{-1}$).
T: temperature.

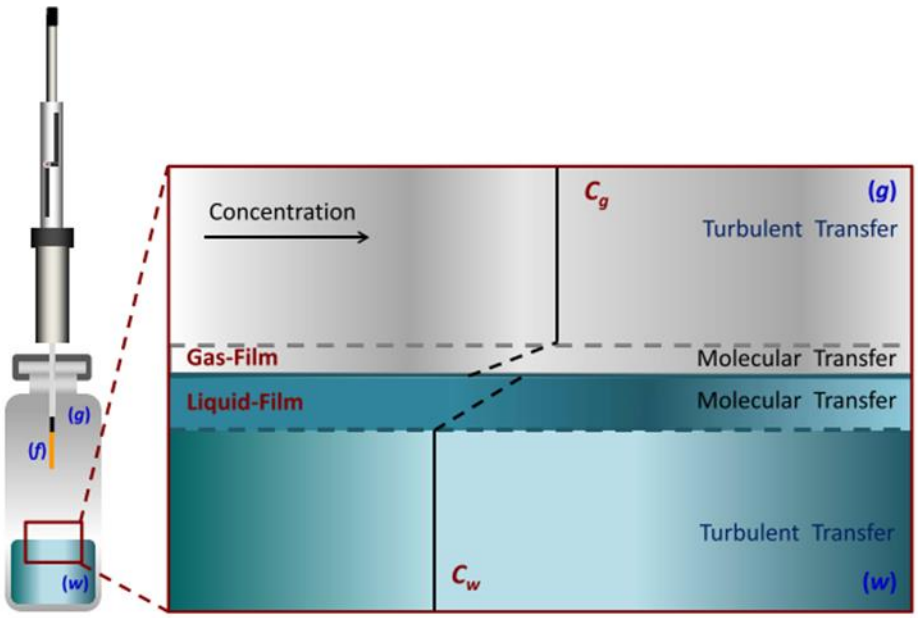

Figure 2-1: Headspace SPME experimental setup and diagram of the 2-resistance model (gas-liquid) [9].

1.3. Desorption

After the extraction is finished, the coated fiber containing the analytes is transferred to the instrument's injection port. The analyte diffuses from the coating into the carrier fluid stream during the desorption process. As a result, when the concentration of an analyte at the coating/fluid interface is zero, this process is the inverse of absorption from a well-agitated aqueous phase. A high linear flow rate must be generated to ensure that this condition is met. The high flow rate is required to ensure that the desorbed analyte is removed from the vicinity of the coating as soon as possible so that it does not interact with the coating and slow down the desorption process. At the beginning of desorption, analyte is removed from the layer of coating closest to the interface, followed by the deeper parts of the coating.

To prevent carry-over, parameters (such as temperature, exposition time, or injection depth) are optimized so that everything desorbs quickly. GCs have a dedicated liner for SPME desorption which simplifies the overall process [14].

1.4. SPME fibers

Commonly utilized SPME fiber materials include polydimethylsiloxane (PDMS), polyacrylate (PA), Carboxen (CAR), polyethylene glycol (PEG or polyethylene oxide, PEO, or Carbowax, CW), and divinylbenzene (DVB). To enhance selectivity, commercially available coatings often consist of blends of materials, such as PDMS/DVB, PDMS/CAR, and CW/DVB [15]. A comprehensive list of these commercially available fiber coatings and their recommended applications can be found in Table 2-1. The selection of fiber depends on the analyte, in accordance with the general rule "like dissolves like". Typical thickness of the coatings is from 7 – 150 μm. The thicker the phase, the larger is the amount extracted resulting, though, in longer extraction times.

Thick coating is also ideal for highly volatile analytes while thin layers are a better choice for less volatile compounds.

Table 2-1: Properties of commercially available SPME fibers.

Stationary phase	**Extraction mechanism**	**Physical state**	**Polarity**	**Thickness**
PDMS	Absorption	Liquid	Non-polar	7 to 100
PDMS/DVB	Adsorption	Porous solid	Semi-polar	65
PA	Absorption	Liquid	Polar	85
CAR/PDMS	Adsorption	Porous solid	Semi-polar	75, 85
CW/DVB	Adsorption	Porous solid	Polar	65
DVB/CAR/PDMS	Adsorption	Porous solid	Semi-polar	50/30

The fibers are also characterized as polar and non – polar. The PDMS fiber has a non – polar coating while the PA and PEG have a polar coating [16].

The fiber coatings are classified as liquid or solid based on their sorption mechanism toward the bulk of the fiber (Figure 2-4). The analytes in liquid coatings partition into the extraction phase, where the molecules are solvated by the coating molecules. Their diffusion coefficients enable molecules to penetrate the entire

volume of the coating in a reasonable extraction time, depending on thickness. A thicker coating will retain larger amounts of analyte than a thin one, but the time to reach equilibrium in the former case is correspondingly longer. Thick coatings are usually used for sampling volatile analytes since they can be transferred to the injector of the measuring instrument without loss, whereas thin SPME fiber coatings ensure good recoveries of high-molecular-weight molecules and nonpolar compounds.
The PDMS, PA, and PEG are considered liquid fibers, and extraction is achieved through absorption. In the case of solid coatings, the well-defined crystalline structure, which is dense, significantly reduces diffusion coefficients within the structure. Therefore, compounds with lower affinity are detected after short extraction times while longer extraction times may result in the displacement of analytes with lower affinity. This effect is due to the limited surface area available for adsorption [5, 17]. Porous polymer fibers are constituted of, at least, a mix of two different polymers.

The performances of liquid and solid coatings exhibit notable disparities, as depicted in Figure 2-4. A comparison elucidating the differences between adsorptive and absorptive equilibrium extraction proves instructive. In both scenarios, the extraction process commences with the adsorption of analytes at the interface between the extraction phase and the matrix, succeeded by analyte diffusion into the bulk of the extraction phase. When analytes possess high diffusion coefficients within the extraction phase, complete partitioning between the two phases occurs, leading to absorptive extraction. This process is facilitated by thin coatings of the extraction phase or convective movement within the sample matrix. Conversely, if the diffusion coefficient is low, analytes persist at the interface, where adsorption predominates.

An inherent advantage of absorption extraction (partitioning) lies in the attainment of a linear isotherm across a broad spectrum of analyte and interference concentrations. This uniformity arises from the negligible alteration in the properties of the extraction phase until the extracted amount approaches approximately 1% of the weight of the extraction phase. Conversely, in adsorption extraction, the isotherm becomes highly nonlinear at elevated concentrations, particularly when substantial surface coverage occurs. This nonlinearity poses a specific challenge in equilibrium methods, as the fiber's response to analytes at high sample concentrations hinges upon the concentrations of both analytes and interferences. Solid sorbents offer increased selectivity and capacity for polar and volatile analytes. SPME fibers are coated with either a liquid polymer or a porous solid sorbent

through the immobilization of fused silica fibers as non-bonded, bonded, partially cross-linked, or highly cross-linked films. Non-bonded films exhibit stability with some water-miscible organic solvents, although they may undergo swelling upon exposure to nonpolar solvents. Bonded phases, with few exceptions, remain stable across all organic solvents. Partially cross-linked phases demonstrate stability in most water-miscible organic solvents and select non-polar solvents. Highly cross-linked phases share similarities with partially cross-linked phases, although some bonding to the core may occur under specific circumstances [17].

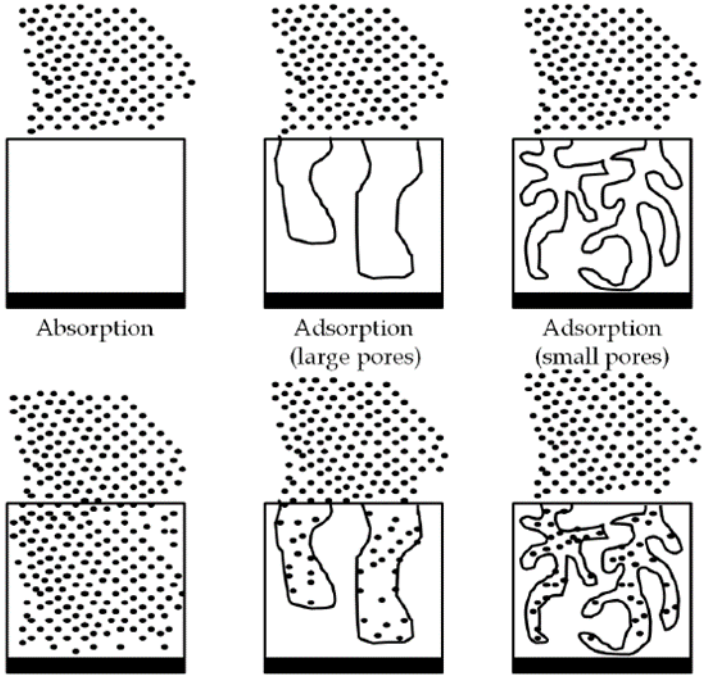

Figure 2-4: Schematic representation of absorptive versus adsorptive extraction and adsorption in small versus large porous [12].

1.5. Effect of extraction parameters

Theoretical thermodynamics offers predictions regarding the impacts of altering specific extraction conditions on partitioning and delineates the parameters necessitating control for ensuring reproducibility. This theoretical framework serves as a tool for optimizing extraction conditions through a minimal number of

experiments and facilitates the correction of variations in extraction conditions, obviating the necessity for repeating calibration tests under new conditions. For instance, when conducting SPME analysis of outdoor air, which may entail considerable temperature fluctuations, the relationship elucidating the temperature's influence on the extracted analyte amount facilitates calibration without the need for extensive experimentation.

1.5.1. Effect of sample volume

The effect of sample volume on quantification and precision of results can be neglected only in rare cases. In headspace analysis, extraction kinetics rely on headspace capacity. The analyte is almost exclusively extracted from the gaseous phase if it is large enough, and equilibration can happen quickly. However, this results in a loss of sensitivity. It is important to make sure that the volumes of the standard solutions and samples for calibration are equivalent in order to prevent mistakes or lower precision [18, 19].

The amount of the analyte extracted by the fiber at equilibrium in a three – phase system is the same independently of where the fiber is located, be it in the headspace or the liquid. The amount of analyte extracted by the fiber regardless of where the fiber is located can be calculated from the Equation 2.10.

$$n = C_f V_f = \frac{V_f V_s K_{fh} K_{hs}}{V_f K_f K_{hs} + V_h K_{hs} + V_s} C_s^0 \qquad \text{(Eq. 2.10)}$$

K_{hs} is typically close to 1 for volatile compounds, meaning that headspace volume can only be disregarded in two-phase systems where it is nearly zero. K_{hs} values for semi-volatile compounds are substantially lower. As a result, the $K_{hs}V_h$ term might not be very small. Such an assumption, though, ought to be confirmed at all times. In three-phase systems with headspace, the magnitude of the effect of sample volume on the extracted amount is determined by the combination of K_{hs} and K_{fh} K_{hs} for a given compound.

Assuming that less than 1% of the initial amount present in the sample is extracted by the fiber, i.e., Eq. (2.10) can yield

$$V_s \geq \frac{99 V_f K_{fs} K_{hs}}{1 + \alpha K_{hs}} \qquad \text{(Eq. 2.11)}$$

where $\alpha = V_h/V_s$. From Eq. (2.11) can be calculated the minimum sample volume that does not affect the amount of the analyte extracted by the fiber.

If the analyte has a very high affinity for the SPME polymer phase, that means that $K_{hs}K_{fs}$ is very large and $K_{hs}K_{fs}V_f >> V_hK_{hs}+V_s$ and Eq. (2.11) becomes:

$$\boldsymbol{n \approx V_s C_s^0} \qquad \text{(Eq. 2.12)}$$

1.5.2. Effect of temperature and extraction time

Temperature and extraction time represent the main parameters governing the efficacy of the extraction process. Elevating the extraction temperature can markedly diminish equilibration time, thereby expediting the entire extraction procedure. However, the impact of raising extraction temperature entails two opposing phenomena: (1) an advantageous enhancement in headspace capacity and/or analyte diffusion coefficient, bolstering the extraction rate, and (2) a contrary effect on the fiber/headspace distribution constant , K_{fh}. Balancing these antagonistic effects is imperative for maximizing sensitivity. The decision to utilize elevated sampling temperatures hinges on whether the primary objective of the analysis is a screening analysis or maximizing achievable sensitivity. Notably, the amount of analyte extracted at a given time (prior to equilibrium) at higher temperatures surpasses that extracted at lower temperatures. Conversely, at equilibrium, the amount extracted at lower temperatures surpasses that at higher temperatures.

A judicious approach to SPME analysis entails allowing the analyte to attain equilibrium between the sample and the fiber coating. Equilibration time denotes the duration after which the extracted analyte amount stabilizes and corresponds, within the confines of experimental error, to the amount extracted after an infinite time. Caution is warranted when determining equilibration times, as substantial reduction in the slope of the curve may erroneously be construed as the point of equilibrium. This occurrence is common in headspace SPME determinations of aqueous samples, where a swift ascent of the equilibration curve, corresponding to extraction from the gaseous phase alone, is succeeded by a slow increase related to analyte transfer from water through the headspace to the fiber. Determining the amount extracted at equilibrium facilitates the calculation of distribution constants.

In instances where equilibration times are excessively protracted, shorter extraction times are mostly employed to work in pre-equilibrium stage. However, meticulous control of extraction conditions (time, temperature, stirring) is imperative to ensure precision. At equilibrium, minor variations in extraction time do not impact the amount of analyte extracted by the fiber. Conversely, during the abrupt part of the curve slope, even slight deviations in extraction time may yield significant variations in the amount extracted. Notably, shorter extraction times entail larger relative errors.

1.5.3. Effect of agitation

A compound with a high coating/sample partition coefficient ($K_{fh}K_{hs}$) may require a longer sampling time. Indirectly sampling analytes from the headspace above the sample results in significantly shorter extraction times. Analytes diffuse four orders of magnitude more readily in the vapor phase than in the liquid phase. It is possible to quickly reach an equilibrium between the vapor and liquid phases by continuously stirring the liquid sample, which creates a continuously new surface. Additionally, the SPME technique can be expanded to more complex samples containing solid or high molecular weight materials by sampling from the headspace [5, 16].

In addition to effectively agitating the liquid phase, a high sample stirring rate may also cause convection in the headspace. To achieve good precision in these types of experiments, it is crucial to maintain consistent agitation conditions and appropriate extraction times [5, 16, 20].

1.5.4. Effect of pH adjustment

Modulating the pH of the sample presents an avenue for enhancing the sensitivity of the method towards both acidic and basic analytes. This enhancement stems from the inherent limitation of SPME, which, lacking ion exchange coatings, can solely extract neutral non-ionic species (undissociated) from aqueous samples. Achieving complete conversion of analytes into neutral forms through pH adjustment markedly augments method sensitivity. Consequently, acidic compounds exhibit enhanced extraction efficiency at low pH values, whereas basic compounds demonstrate improved extraction efficiency at high pH levels.

Proper adjustment of the pH enables the SPME fiber to extract weak acids and bases effectively. To ensure that at least 99% of the acidic compound remains in neutral form, the pH should be set two units below the analyte's pKa. Conversely, for basic compounds, the pH should be adjusted two units higher than the pKa [20].

During pH adjustment of the sample, headspace sampling mode is preferred for extraction to mitigate potential damage to the fiber coating resulting from direct contact with the sample at extreme pH levels. Alternatively, when employing the direct immersion sampling mode, it is advisable to avoid employing excessively high or low pH values, as these may lead to degradation of the coating.

1.5.5. Ion strength

The addition of salt serves to elevate the ionic strength of the sample solution, consequently augmenting the K_{fs} constant and enhancing sensitivity across various applications, barring those involving exceedingly polar analytes. This augmentation is attributed to the salting-out effect, wherein analyte molecules exhibit increased propensity to migrate from the sample matrix to the headspace, a phenomenon commonly leveraged in headspace (HS)-SPME. Notably, the presence of significant salt quantities leads to diminished aqueous solubilities of many organic compounds. However, for compounds exhibiting unchanged aqueous solubility, salt addition may induce a reduction in the extracted amount by lowering the activity coefficients of the analytes, thereby adversely impacting the partition coefficient between the sample and the SPME coating.

In certain scenarios, high ionic strength facilitates the extraction efficiency of the target analyte while concurrently improving the extraction of interfering compounds, an outcome typically undesirable, particularly when employing a solid (adsorbent) type of coating [21].

Although NaCl stands as the best and more common choice for adjusting ionic strength, alternative salts can also be employed. For instance, the incorporation of Na_2SO_4 has demonstrated potential in yielding superior extraction efficiency [22].

1.5.6. Extraction with derivatization

Performing derivatization before and/or during extraction can enhance the sensitivity and selectivity of both extraction and detection processes. It also enables the determination of analytes using SPME, especially those analytes that are polar or ionic and would otherwise be difficult to extract or analyze using this method. The primary goal of derivatization is twofold: firstly, to convert the native analytes into less-polar derivatives, thereby increasing their efficiency in extraction; and secondly, to label them for improved detection and/or chromatography.

Post-extraction methods are limited to improving chromatographic behavior and detection, while derivatization offers the added advantage of enhancing both extraction and detection. However, incorporating a derivatization step can add complexity to the SPME procedure and, therefore, should only be considered when absolutely necessary. Selective reactions that produce specific analogues can significantly reduce interference during quantitation, making this approach particularly useful for analyte determination in complex matrices. Moreover, sensitivity enhancement can be achieved when the derivatizing reagent contains functional groups that enhance detection.

1.5.7. Effect of pressure

The time required to reach equilibrium in HS-SPME is primarily determined by the properties of the analytes and matrix, with volatiles reaching this state more quickly at room temperature than semi-volatile analytes. (Semi-volatile organic compounds (SVOC) are distinct from volatile organic compounds (VOC) in that they have higher molecular weights, higher boiling point (>200 °C), a vapour pressure between 10^{-9} and 10^{-3} Pa at room temperature). Volatile analytes are effectively transported through the headspace to the extraction phase. For the semi-volatiles, heating the sample is a common analytical strategy for increasing headspace concentrations while shortening sampling times. Nonetheless, some issues may arise, such as a reduction in analyte affinity for the SPME fibre or changes in sample composition as a result of heating.

Sampling under reduced pressure conditions is an alternative method for improving HS-SPME extraction kinetics, known as vacuum-assisted HS-SPME (Vac-HS-SPME). Brunton et al. [23] first proposed the use of low pressures during HS-SPME sampling in 2001, and Darrouzes et al. [24] and Groenewold et al. [25] later confirmed their findings. Psillakis et al. [13, 26] developed the theoretical basis for the technique in 2012, triggering a more systematic and rigorous investigation of the vacuum approach. Current findings conclude that Vac-HS-SPME sampling has no effect on the final analyte amount extracted at equilibrium but significantly accelerates the extraction of analytes with long equilibration times under standard atmospheric pressure (see Figure 2-5) [9]. Vac-HS-SPME has successfully been used to extract various analytes from different matrices such as water, solids, and food. In all cases, the use of Vac-HS-SPME resulted in higher extraction efficiencies

and very good sensitivities at shorter extraction times and lower sampling temperatures than the standard HS-SPME procedure.

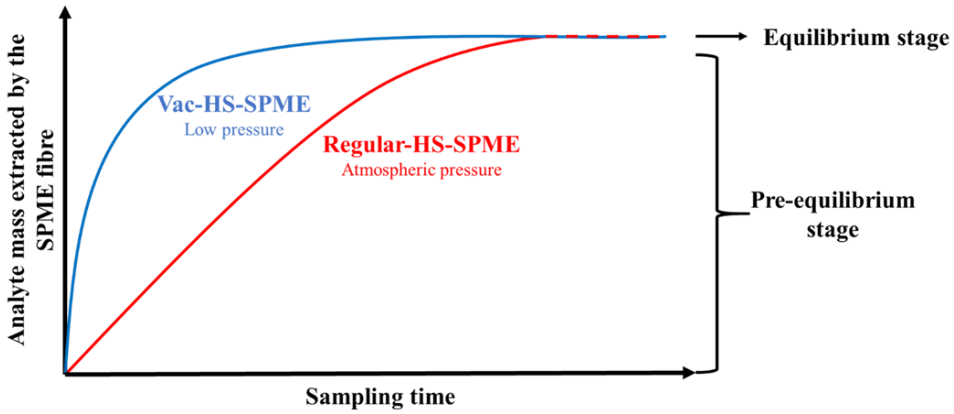

Figure 2-5: Graphical representation of the extraction time profile curves of compounds with a low affinity for the headspace obtained with Vac-HS-SPME (blue line) and regular HS-SPME (red line) also indicating the pressure dependence of the pre-equilibrium and equilibrium HS-SPME sampling stages. Adapted from [9].

As shown previously, HS-SPME principle is based on the analyte's equilibrium partitioning between three phases (the sample or condensed phase, its headspace, and the extraction phase of the SPME fiber) [5]. Assuming that sufficient sampling time has been allowed to achieve equilibrium, it is well established [1, 5, 27] that the amount of analyte extracted by a liquid fiber is given by equation 2.10.

Thermodynamic theory states that equilibrium concentrations and partial pressures are independent of the total pressure because Henry's constants and partition coefficients are only impacted at high operating pressures (P > 500 kPa). Since the amount of analyte extracted by the fiber under reduced or regular pressure sampling conditions is expected to be the same at equilibrium. The sampling pressure can exert influence on the efficacy of compound extraction, contingent upon their inherent properties such as boiling point, vapor pressure, and polarity, which govern their volatilization tendencies. Lower pressure conditions can enhance the volatilization of semi-volatile compounds, thereby positively impacting their extraction rate.

HS-SPME is regarded as a multi-stage process that involves mass transfer in the three phases involved and across two interfaces (sample/headspace and headspace/fiber) in a closed three-phase system of limited volume [5, 18, 19]. It is reasonable to assume that equilibrium has been reached and the analyte(s) have partitioned between the sample and the headspace prior to SPME fiber insertion. Analytes from the gas phase are quickly absorbed by the fiber as soon as it is exposed to headspace. Consequently, the analyte concentration in the headspace decreases quickly and is subsequently restored by the analyte that is moved from the sample to the headspace [12]. Typically, mass transfer in the headspace is considered as a rapid process [19]. For semi-volatile compounds, the rate-determining step for HS-SPME is analyte evaporation from the sample to the headspace, whereas mass transfer at the headspace/SPME polymer interface is considered as a relatively fast process [18, 19].

According to the two-film model, analyte mass transfer occurs solely through molecular diffusion at the interface, where two thin films of liquid sample and air separate uniformly mixed liquid and gas bulk phases (see Figure 2-3) [9]. Additionally, the model assumes that the total resistance to evaporation will be the sum of the resistances discovered during transfer through the liquid- and gas-films. This resistance is defined as the reciprocal of the overall mass-transfer coefficient for volatilization based on the liquid phase, K_{OL} [28]. Next, using resistance formulation, the evaporation of organic solutes from the water sample is expressed as :

$$\frac{1}{K_{OL}} = \frac{1}{k_l} + \frac{RT}{K_H k_g} \qquad \text{(Eq. 2.13)}$$

where K_H is the Henry's law constant, which is defined as the ratio of the compound's partial pressure and its concentration in water at a given temperature. T is the absolute temperature, R is the gas constant, and the liquid- and gas-film mass-transfer coefficients are k_l and k_g. According to equation (2.13), in the case of a high K_H solute, the second term will be insignificant, and the analyte's primary mass-transfer resistance will be found in the liquid phase, specifically $K_{OL} \approx k_l$. On the other hand, evaporation for a low K_H organic solute will be regulated by gas-phase limitations and a small liquid-sided resistance, or $K_{OL} = K_H k_g/RT$.

The mass transfer coefficient kg of a compound is proportionally related to the gas-phase diffusion coefficient (D_g) raised to a power m (typical values of m: 0.5, 2/3

and 1) [26]. Moreover, according to the Fuller-Schettler-Giddings correlation given below [26], D_g is related to the reciprocal of the total pressure (P):

$$D_g = \frac{0.001 \times T^{1.75} \sqrt{\frac{1}{M_{air}} + \frac{1}{M_A}}}{P[(\sum V_{air})^{1/3} + (\sum V_A)^{1/3}]^2} \qquad \text{(Eq. 2.14)}$$

where M_{air}, M_A, V_{air} and V_A are the molecular weights and molar volumes of the air and the analyte, respectively. When the total pressure is lowered from 1 atm to 0.04 atm (the typical pressure taken into consideration in Vac-HSPME sampling from water-containing samples), calculations using equation. 2.14 produce an improvement in D_g for any given analyte of more than 25 times [29, 30]. Because of the increased k_g resulting from this improvement in gas diffusivity, gas-sided resistance (represented as $1/k_g$ in equation 2.13) will decrease. Consequently, using a low sampling pressure will increase evaporation rates for analytes where mass transfer from the liquid sample to the gas phase is governed by gas-sided constraints. Assuming that evaporation from the sample is the limiting step in the overall extraction process, this will lead to a faster response of the sample to the analyte's concentration drops occurring at the headspace and a faster equilibration time compared to regular atmospheric pressure. On the other hand, because these kinds of constraints are pressure-independent, lowering the overall pressure will not have an impact on the extraction kinetics for analytes where liquid-sided limitations regulate evaporation. It should be mentioned that faster analyte transport in the bulk gas phase will also be brought about by the improvement in D_g values; however, this does not signify a rate-limiting step in the extraction process.

In the case of solid samples, a modified form of Fick's law of diffusion was used to describe the pressure dependence of pre-equilibrium HS-SPME sampling from solid samples, as well as related gas-phase diffusivities to the vapor flux assumed to diffuse through a stagnant boundary layer connecting solid and air [30]. According to the formulation, lowering the total pressure during the pre-equilibrium stage of HS-SPME sampling will improve D_g values and thus increase the vapor flux of chemicals at the solid surface, resulting in a faster overall HS-SPME process.

1.6. Quantification using headspace extraction

The extraction and quantitative analysis of volatile and semi-volatile compounds in solid or complex matrices poses a formidable analytical challenge. Various liquid-solid extraction methodologies, such as Soxhlet extraction, microwave-assisted extraction (MAE), supercritical fluid extraction (SFE), and sonication, are commonly employed to extract analytes from solid samples. However, these techniques are often characterized by high cost, time and labor intensiveness, and/or necessitate large quantities of toxic organic solvents.

When employing headspace techniques, the partition of analytes from solid samples into the gaseous phase is frequently hindered due to interactions between the analytes and the matrix [31]. Consequently, internal and external calibration techniques frequently yield unsatisfactory results owing to matrix effects, which induce significant variations in partition coefficients and release rates among different analytes. In 1977, Kolb and Pospisil introduced a technique termed discontinuous gas extraction, subsequently renamed multiple headspace extraction (MHE) [32]. This method circumvents matrix effects, thereby enabling direct quantitative determination of analytes in solid matrices using headspace techniques.

The principle of MHE is elucidated below and subsequently expanded to encompass multiple headspace solid-phase microextraction.

1.6.1. Multiple headspace extraction

Sequential headspace extraction is a systematic approach employed to quantitatively analyze volatile components within solid or complex liquid samples. This method involves a series of extractions in order to calculate the total quantity of analytes present in a sample through a few successive extractions, enabling volatile quantification [32].

Initially, during the first extraction, a portion of the headspace is extracted, disrupting the equilibrium between the analyte in the condensed sample and the headspace. Subsequently, as the sample re-equilibrates, additional analytes migrate from the condensed phase to the headspace. Consequently, concentrations in both phases decrease relative to the initial extraction, while the ratio of analyte concentrations remains consistent.

With each subsequent extraction, the peak obtained becomes smaller as more analytes are transferred to the headspace. Through iterative repetition of this process,

it becomes possible to extract all volatile components from the sample. Continuation of this procedure ultimately leads to the aggregation of peak areas corresponding to various analytes, culminating in the determination of the total peak area, which correlates with the total amount of analyte present in the sample.

Importantly, this exhaustive extraction eliminates the influence of the sample matrix. Utilizing a logarithmic function, the sequential extractions do not necessitate completion until all analytes are entirely removed from the sample matrix. Instead, logarithms of area values from successive analyses are plotted against the number of analyses on a linear scale, and the total area value is calculated via regression from areas obtained in a few extraction steps [33].

The total amount of a volatile compound in a sample can be determined by summarizing all individual peak areas (A_i), where i is the number of the extraction. As this is a converging geometrical progression, the sum can be derived as:

$$\sum_{i=1}^{i=\infty} A_i = \frac{A_1}{1-e^{-q}} \qquad \text{(Eq. 2.15)}$$

The sum of all peak areas can, thus, be calculated from two values: the peak area obtained in the first extraction, A_1 and the exponent q′, which describes the exponential decline of the peak areas during the stepwise MHE procedure. A_1 is a measured value and the exponent q′ is obtained from the linear regression analysis:

$$\ln A_i = -q'(i-1) + \ln A_1 \qquad \text{(Eq. 2.16)}$$

Where the q′ value is equal to the slope of the linear regression line and ln A_1 is given by the y-intercept.

The quantity of analytes within the system is crucial; an exponential decline in peak area should be evident with an increasing number of extractions. If this decline is minimal, there is inadequate depletion of the SPME. This indicates that the amount of analytes extracted is negligible compared to the existing content in the vial. Consequently, after the extraction, the amount in the vial remains constant, as does the area for subsequent extractions. Consequently, the logarithm of peak areas does not follow a linear correlation with the number of extractions. To achieve linearity, the quantity of analytes extracted by the fiber must be significant in comparison to the content in the vial before each extraction. Figure 2-7, presented in the following

section, shows cases when an exponential decline is observed after several extractions and when it is not.

1.6.2. Multiple headspace solid-phase microextraction

MHS-SPME is a stepwise procedure involving successive HS-SPME iterations on the identical sample. It can be perceived as a combination of MHE and SPME techniques. The theoretical groundwork for this combined technique under equilibrium conditions was exposed by Ezquerro et al [34].

The quantity of analyte present in the fiber coating at equilibrium following the ni extraction can be expressed as:

$$n_i = n_1 \beta^{i-1} \quad \text{(Eq. 2.17)}$$

where n_1 is the equilibrium amount of analyte in the fiber coating after the first extraction, and β is the remaining fraction of the analyte in the system after one equilibration with a value between zero and unity ($0 \leq \beta < 1$), and is given by:

$$\beta = 1 - \frac{K_{fs} V_f}{K_{fs} V_f + K_{hs} V_h + V_s} \qquad \text{(Eq. 2.18)}$$

Presuming a linear correlation between peak area and the quantity of analyte injected into the instrument, equation (2.17) can be reformulated as:

$$A_i = A_1 \beta^{i-1} \quad \text{(Eq. 2.19)}$$

The sequential peak areas form a geometric progression, the total of which, representing the complete extraction's total area, can be calculated utilizing equation (2.20):

$$A_T = \sum_{i=0}^{i=\infty} A_i = \frac{A_1}{1-\beta} \qquad \text{(Eq. 2.20)}$$

According to equation 2.20, the overall peak area can be calculated from the initial extraction's peak area, A_1, and the constant β, which can be determined through linear regression analysis of the logarithmic representation of equation 2.19:

$$\log A_i = (i-1) \log \beta + \log A_1 \qquad \text{(Eq. 2.21)}$$

where the logarithm of β is the slope of the linear plot of the logarithm of Ai against the number of extractions (i-1) obtained from a few (three or four) consecutive HS-SPME-GC analysis.

1.6.3. Multiple cumulative trapping (MCT) HS-SPME

This approach developed along the thesis can be considered a technical modification of MHE, although with different purpose. On contrary of MHE which requires one analysis for each extraction, MCT-HS-SPME requires one single analysis. Prior the chromatographic analysis, the compounds from the n extraction cycles (extraction and desorption) are focused on a refrigerated sorbent (called “cold trap”) which allows to perform the desired number of extraction. The only limitation is the capacity of the cold trap sorbent.

Then, the cold trap is quickly heated up. The overall extract is transferred to the GC. Figure 2-6 represents the overall process.

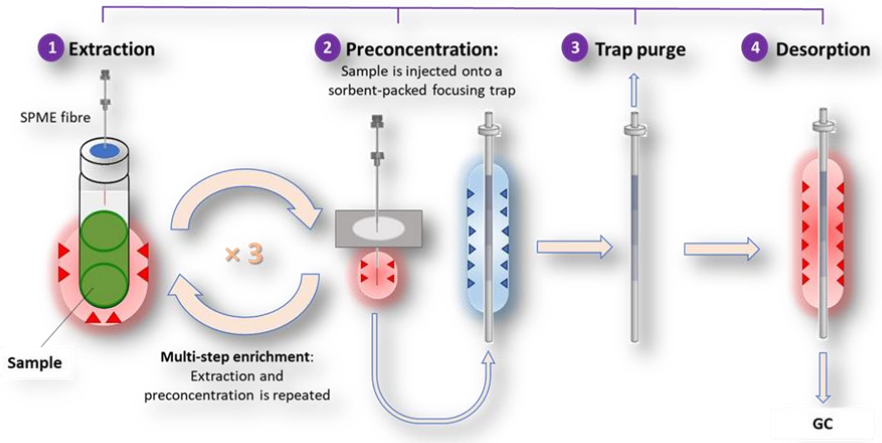

Figure 2-6: Steps of MCT-HS-SPME.

Figure 2-7 illustrates a comparison between the profiles of MHE and MCT under both saturated and unsaturated headspace conditions. In the context of MHE, each data point represents a distinct extraction and subsequent injection process. Therefore, the initial data point reflects the outcome of the first extraction followed by injection, with subsequent points indicating results from subsequent extractions and injections conducted sequentially within the same vial. Conversely, in the case of MCT, the initial data point corresponds to a single extraction followed by injection, while subsequent data points represent the cumulative effect of results from multiple successive extractions performed in the same vial prior to injection.

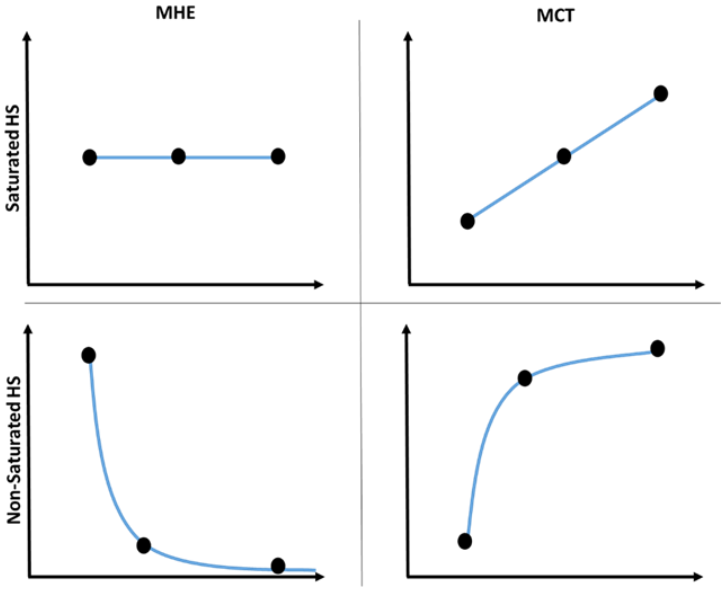

Figure 2-7: Representation of the extraction profile between one and three extractions. On left side, the profiles obtained with MHE, on the right side ones obtained with MCT. Then top profiles correspond to a saturated HS and bottom profiles, a non-saturated headspace.

According to these plots, only non-saturated headspace can be used for quantitative purpose because the totality of the analyte is extracted, or at least an exponential model can be used to determine it because 0 is reached using MHE or a maximum with MCT, allowing the estimation of the absolute intensity.

1.7. References

[1] Pawliszyn J (1997) Solid Phase Microextraction: Theory and Practice - Janusz Pawliszyn - Google Libros

[2] Pawliszyn J (1995) New directions in sample preparation for analysis of organic compounds. Trends Anal Chem 14:113–122. https://doi.org/10.1016/0165-9936(95)94044-F.

[3] Grote C, Pawliszyn J (1997) Solid-Phase Microextraction for the Analysis of Human Breath. Anal Chem 69:587–596. https://doi.org/10.1021/ac960749l.

[4] Ouyang G, Pawliszyn J (2006) Recent developments in SPME for on-site analysis and monitoring. TrAC - Trends Anal Chem 25:692–703. https://doi.org/10.1016/j.trac.2006.05.005.

[5] Zhang Z, Pawliszyn J (1993) Headspace Solid-Phase Microextraction. Anal Chem 65:1843–1852. https://doi.org/10.1021/ac00062a008.

[6] Arthur CL, Pawliszyn J (1990) Solid phase microextraction with thermal desorption using fused silica optical fibers. Anal Chem 62:2145–2148. https://doi.org/10.1021/ac00218a019.

[7] Zhang Z, Yang MJ, Pawliszyn J (1994) Solid-Phase Microextraction. Anal Chim Acta 66:844–853.

[8] Louch D, Motlagh S, Pawliszyn J (1992) Dynamics of Organic Compound Extraction from Water Using Liquid-Coated Fused Silica Fibers. Anal Chem 64:1187–1199. https://doi.org/10.1021/ac00034a020.

[9] Psillakis E (2017) Vacuum-assisted headspace solid-phase microextraction: A tutorial review. Anal Chim Acta 986:12–24. https://doi.org/10.1016/j.aca.2017.06.033.

[10] Zhakupbekova A, Baimatova N, Kenessov B (2019) A critical review of vacuum-assisted headspace solid-phase microextraction for environmental analysis. Trends Environ Anal Chem 22:. https://doi.org/10.1016/j.teac.2019.e00065.

[11] Mackay D, Leinonen PJ (1975) Rate of Evaporation of Low-Solubility Contaminants from Water Bodies to Atmosphere. Environ Sci Technol 9:1178–1180. https://doi.org/10.1021/es60111a012.

[12] Górecki T, Yu X, Pawliszyn J (1999) Theory of analyte extraction by selected porous polymer SPME fibres. Analyst 124:643–649. https://doi.org/10.1039/a808487d.

[13] Psillakis E, Mousouraki A, Yiantzi E, Kalogerakis N (2012) Effect of Henry's law constant and operating parameters on vacuum-assisted headspace solid phase microextraction. J Chromatogr A 1244:55–60. https://doi.org/10.1016/j.chroma.2012.05.006.

[14] Xu CH, Chen GS, Xiong ZH, Fan YX, Wang XC, Liu Y (2016) Applications of solid-phase microextraction in food analysis. TrAC - Trends Anal Chem 80:12–29. https://doi.org/10.1016/j.trac.2016.02.022.

[15] Fontanals N, Marcé RM, Borrull F (2007) New materials in sorptive extraction techniques for polar compounds. J Chromatogr A 1152:14–31. https://doi.org/10.1016/j.chroma.2006.11.077.

[16] Lord H, Pawliszyn J (2000) Evolution of solid-phase microextraction technology

[17] Kataoka H, Saito K (2011) Recent advances in SPME techniques in biomedical analysis. J Pharm Biomed Anal 54:926–950. https://doi.org/10.1016/j.jpba.2010.12.010.

[18] Ai J (1997) Solid Phase Microextraction for Quantitative Analysis in Nonequilibrium Situations. Anal Chem 69:1230–1236. https://doi.org/10.1021/ac9609541.

[19] Ai J (1997) Headspace Solid Phase Microextraction. Dynamics and Quantitative Analysis before Reaching a Partition Equilibrium. Anal Chem 69:3260–3266. https://doi.org/10.1021/ac970024x.

[20] Pawliszyn J (2000) Theory of Solid-Phase Microextraction. J Chromatogr Sci 38:270–278.

[21] De Oliveira ARM, Cesarino EJ, Bonato PS (2005) Solid-phase microextraction and chiral HPLC analysis of ibuprofen in urine. J Chromatogr B Anal Technol Biomed Life Sci 818:285–291. https://doi.org/10.1016/j.jchromb.2005.01.010.

[22] Sánchez-Ortega A, Sampedro MC, Unceta N, Goicolea MA, Barrio RJ (2005) Solid-phase microextraction coupled with high performance liquid chromatography using on-line diode-array and electrochemical detection for the determination of fenitrothion and its main metabolites in environmental water samples. J Chromatogr A 1094:70–76. https://doi.org/10.1016/j.chroma.2005.07.089.

[23] Brunton NP, Cronin DA, Monahan FJ (2001) The effects of temperature and pressure on the performance of Carboxen/PDMS fibres during solid phase microextraction (SPME) of headspace volatiles from cooked and raw turkey breast. Flavour Fragr J 16:294–302. https://doi.org/10.1002/ffj.1000.

[24] Darrouzès J, Bueno M, Pécheyran C, Holeman M, Potin-Gautier M (2005) New approach of solid-phase microextraction improving the extraction yield of butyl and phenyltin compounds by combining the effects of pressure and type of agitation. J Chromatogr A 1072:19–27. https://doi.org/10.1016/j.chroma.2005.02.026.

[25] Groenewold GS, Scott JR, Rae C (2011) Recovery of phosphonate surface contaminants from glass using a simple vacuum extractor with a solid-phase microextraction fiber. Anal Chim Acta 697:38–47. https://doi.org/10.1016/j.aca.2011.04.034.

[26] Psillakis E, Yiantzi E, Sanchez-Prado L, Kalogerakis N (2012) Vacuum-assisted headspace solid phase microextraction: Improved extraction of semivolatiles by non-equilibrium headspace sampling under reduced pressure conditions. Anal Chim Acta 742:30–36. https://doi.org/10.1016/j.aca.2012.01.019.

[27] Górecki T, Pawliszyn J (1997) Effect of sample volume on quantitative analysis by solid-phase microextraction: Part 1. Theoretical considerations. Analyst 122:1079–1086. https://doi.org/10.1039/a701303e.

[28] Psillakis E (2023) Chapter 3: The effect of vacuum on headspace SPME: Theory and practice.

[29] Psillakis E, Koutela N, Colussi AJ (2019) Vacuum-assisted headspace single-drop microextraction: Eliminating interfacial gas-phase limitations. Anal Chim Acta 1092:9–16. https://doi.org/10.1016/j.aca.2019.09.056.

[30] Yiantzi E, Kalogerakis N, Psillakis E (2015) Vacuum-assisted headspace solid phase microextraction of polycyclic aromatic hydrocarbons in solid samples. Anal Chim Acta 890:108–116. https://doi.org/10.1016/j.aca.2015.05.047.

[31] Gröning M, Hakkarainen M (2004) Multiple headspace solid-phase microextraction of 2-cyclopentyl- cyclopentanone in polyamide 6.6: Possibilities and limitations in the headspace analysis of solid hydrogen-bonding matrices. J Chromatogr A 1052:61–68. https://doi.org/10.1016/j.chroma.2004.08.112.

[32] Kolb B, Pospisil P (1977) A gas chromatographic assay for quantitative analysis of volatiles in solid materials by discontinuous gas extraction. Chromatographia 10:705–711. https://doi.org/10.1007/BF02263080.

[33] Kolb B (1982) Multiple headspace extraction-A procedure for eliminating the influence of the sample matrix in quantitative headspace, gas chromatography. Chromatographia 15:587–594. https://doi.org/10.1007/BF02280380.

[34] Ezquerro Ó, Pons B, Tena MT (2003) Multiple headspace solid-phase microextraction for the quantitative determination of volatile organic compounds in multilayer packagings. J Chromatogr A 999:155–164. https://doi.org/10.1016/S0021-9673(02)01524-8.

2. *GC × GC*

2.1. *Limitations of 1D chromatography*

Despite highly efficient, monodimensional (1D) chromatography may fail to separate highly complex samples, not presenting the peak capacity necessary to properly resolve all the compounds present.

All chromatography processes can be described by two key parameters, namely the peak capacity (n_c) and the stationary-phase selectivity. The first one corresponds to the column characteristics, such as the length, the internal diameter, the stationary-phase thickness, etc. The second one is related to the chemical composition of the stationary phase, and, consequently, with the specific kind of interactions between analytes and stationary phase.

A statistical model was created by Giddings et al. to show the practical restrictions placed on 1D chromatographic systems. The number of compounds resolved as a function of the theoretical peak capacity can be estimated using this model. From this theoretical viewpoint, they demonstrated that “no more than 37% of the peak capacity can be used to generate peak resolution”. They also mentioned that many coelutions are observable under this condition. Such a value gives a good indication of the separation power of a one-dimensional chromatography system even though it disregards stationary phase selectivity [1].

Equation (2.22) is regarded as the principal equation for resolution when two compounds are involved. It shows that the resolution (R) is affected by three parameters: efficiency (N, plate number), selectivity (α, separation factor) and retention factors (k).

$$R = \frac{1}{4}\sqrt{N}\left(\frac{\alpha-1}{\alpha}\right)\left(\frac{k}{k+1}\right) \qquad (2.22)$$

k: The benefits are very limited in terms of resolution if the column phase ratio is decreased (or a lower temperature is used), which increases the retention

factors. Only in the case of analytes with low k values (≤3), increase in k can cause a significant impact on RS.

α: The resolution significantly improves if a more selective stationary phase is used, raising the separation factor in the process. Selectivity is the factor that has the biggest impact on resolution out of the three. However, a complex mixture of compounds is not a valid application of equation (1); it only applies to a single pair of analytes. In the latter scenario, a stationary phase change frequently results in a better resolution for some analytes and a worse outcome for others. Only when a sample of low complexity is analyzed does the choice of the most selective stationary phase produce the best results.

N: The column needs to be significantly longer to generate a major increase in resolution (a four-times longer column only increases R by a factor 2). Due to the significant increase in analysis time, this type of modification is typically undesirable and obviously not a workable solution.

Therefore, using a multidimensional chromatographic system is the most efficient way to increase the separation efficiency (and selectivity) of a chromatography system.

2.2. Principle of multidimensionality

As 1D chromatography failed to completely separate complex samples, researchers began to look into the potential of multidimensional techniques. The concepts of these systems were precisely defined by Giddings et al., requiring two fundamental conditions [1]:

- Separation phenomena in each dimension must be governed by distinct physicochemical mechanisms.
- Analytes that have been resolved in the prior step should stay separated until the completion of the following separation process.

Giddings' definitions state that multidimensional systems will be significantly more advantageous if the dimensions are founded on various types of interaction mechanisms. According to Venkatramani et al.[2], separation in this situation is orthogonal. Any correlation between the dimensions, no matter how slight, will result in redundant information that will impact the global separation. Figure 2-8. depicts three degrees of correlation between two separation dimensions to demonstrate the idea of orthogonality. The peaks are spread out over the entire plane (a) in the case of completely orthogonal separation. The distribution will be more centered along the diagonal (b) the more correlated the dimensions are. The solutes will have identical retention times in the two dimensions in the most extreme case of total correlation (c), leading to the equivalent of 1D separation along the diagonal.

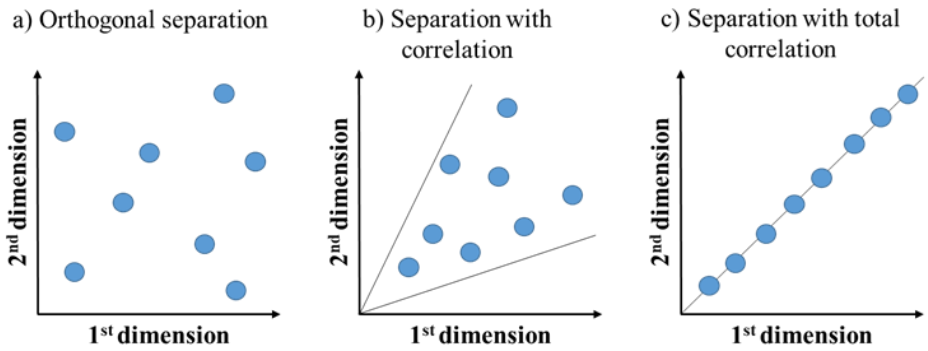

Figure 2-8: Example of various degrees of correlation between two separation dimensions. Adapted from [3].

To create effective multidimensional systems, the separation dimensions must be properly chosen, such as the choice of the two stationary phases (they have to present different selectivity), column dimensions (1D column has regular length 20-30 m for example and 2D column has to be short to have a fast separation). To achieve ordered distributions of compounds and a corresponding increase in the amount of information, a coherent choice is necessary. The term "sample dimensionality" (s) was first used by Giddings to refer to the quantity of independent variables used to describe the characteristics of the sample compounds [4]. The parameter “s” would represent a measurement of the sample complexity. It is a predictor of component peak disorder. Moreover, the disordered peak distribution in a chromatogram is not only due to s but rather the relationship between s and the separating system. The author correlates this parameter to the system dimensionality n (number of different separation steps using different mechanisms) to predict the capabilities of the system to separate the compounds from a sample. When $s > n$ the component peak distribution is predicted to be largely disordered, thus hindering separation. When $s < n$, the component distribution is ordered but the greatly enhanced peak capacity of the multidimensional system is not utilized. When the dimensionalities are equal, $s = n$, the best possibility exists to fully exploit the power of multidimensional separation without the disadvantages of disordered peak distribution.

”s” can be expressed by different physical-chemical properties: π-aromaticity interactions, chirality (host/invited interactions), hydrogen bonds, ion mobility, size or shape of molecules, chemical functions, volatility/number of carbon atoms, degree of branching, etc. A few simple example will help to explain the nature of s. If we know that our sample is entirely composed of saturated straight-chain fatty

acids, we can fully specify the components of the mixture in terms of one variable (s=1), which can be either carbon number or molecular mass.

If we now choose a fatty acid sample with variable carbon number and one double bond in the straight chain, the sample gains a second dimension: the position of the double bond.

Going a step further, a four-dimensional sample is one in which the fatty acid molecules may contain zero, one, or two double bonds on various locations. One coordinate is carbon number, another specifies the number of groups (0, 1, or 2), a third may be chosen to give the position of the group closest to the carboxyl end, and a fourth to locate the most distant group.

2.3. Comprehensive gas chromatography

In instances of comprehensive coupling, the entirety of the sample undergoes separation across each dimension. Put differently, solutes experience sequential separation across two or more dimensions. This comprehensive coupling offers a broader scope of information regarding the entire sample, making it particularly suited for characterizing highly complex matrices with limited prior knowledge. The development of comprehensive 2D chromatographic systems poses challenges, requiring synchronization between the first and second dimensions. Such systems typically comprise individual chromatographic columns for each dimension and a modulator facilitating the sequential sampling of effluents from the first column to the second [5–8].

2.3.1. Modulation

The modulator subsequently samples unmodulated peaks according to a predetermined modulation period. Each modulation cut then undergoes separation in the second dimension, resulting in chromatograms of durations corresponding to the modulation period (P_{Mod}). The alteration in signal intensity across chromatograms depends on the initial shape of the peak.

Figure 2-9 depicts the modulation phenomenon. In the shown case, two compounds co-elute. In this case, the modulation period is adjusted to split the peak into three sampling bands. Each modulation subsequently undergoes the second dimension column, effectively demonstrating the separation of the two compounds. Continuous transfer to the second column must occur rapidly to ensure that the reinjected bands are fully eluted before the next injection band arrives (avoiding wrap-around).

Consequently, the modulator's role is to periodically sample the effluents from the first separation by halting them according to a modulation period, which must be selected judiciously. Failure to completely elute the solutes before reinjection of the

subsequent sampling may result in wrap-around, wherein the compounds elute at retention times exceeding the modulation period.

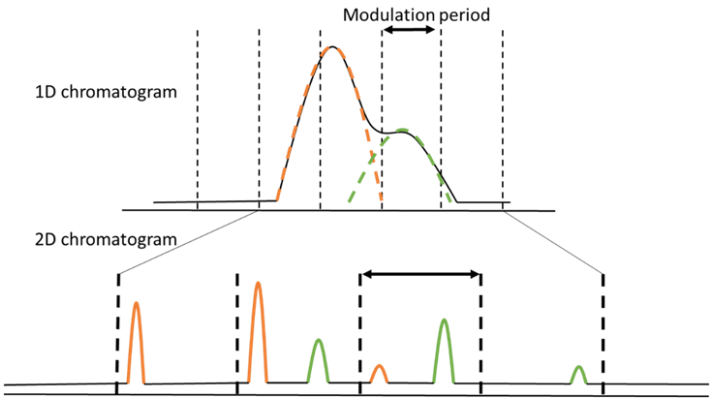

Figure 2-9: Illustration of comprehensive GC analysis.

2.3.2. Sampling frequency

The selection of sampling frequency or modulation period plays a critical role in determining separation quality, exerting a profound influence on chromatographic performance. Murphy et al. proposed the primary theory regarding the impact of modulation based on their investigations in LC×LC. Their research revealed a direct relationship between sampling frequency and the resolution of a two-dimensional chromatogram. They empirically demonstrated that shorter modulation periods lead to higher resolution in the first dimension. Additionally, they established that each peak in the first dimension should ideally be sampled at least three or four times to achieve optimal resolution, with minimal impact on the resolution in the second dimension. Consequently, Murphy's criterion, prescribing a minimum of 3 or 4 samples for each peak in the first dimension, often serves as a fundamental principle in the development of methods in two-dimensional chromatography. Stoll et al. further elaborated on this concept for two-dimensional liquid chromatography, presenting a graphical representation of the decline in resolution of the first dimension relative to the number of samples per peak [9] (Figure 2-10).

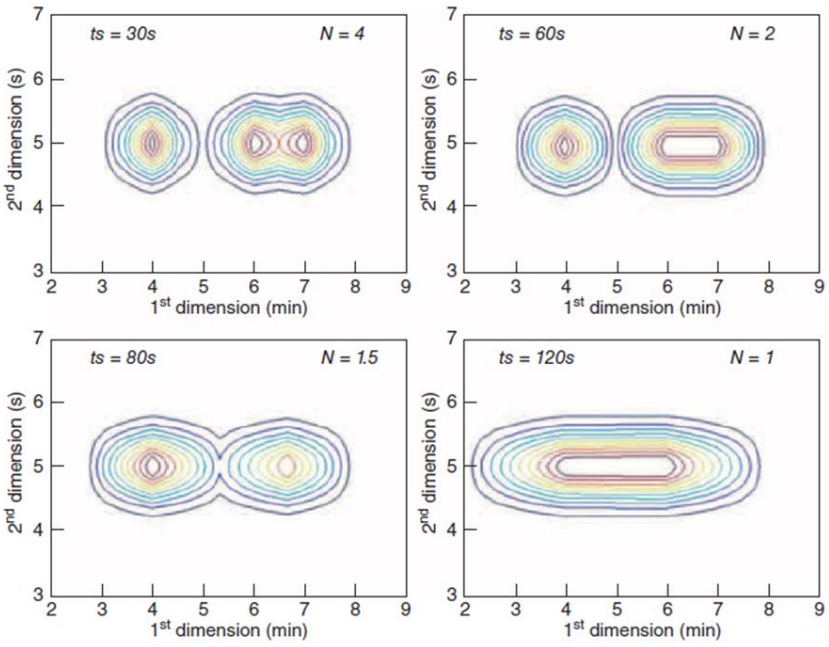

Figure 2-10: Graph of the effect of time and sampling frequency on first-dimension resolution, from [9].

2.3.3. Flow modulator

Presently, in the domain of comprehensive two-dimensional gas chromatography (GC×GC), three principal categories of modulators are utilized: thermal, valve, and flow-based. (For clarity reason, only the flow modulator will be detailed with a particular focus on the use in the thesis).

Flow-based modulators , a technology which has its origin in heart-cutting (GC-GC) initially performed using pneumatic valves, saw a significant breakthrough with the development of the Deans' switch in 1968 [10]. Recently, flow diversion modulation has gained traction as a favored approach for GC × GC modulation. Similar to valve-based modulation, flow diversion modulation employs valves (typically solenoid) to regulate gas pressures, controlling the transfer of eluate from the 1D column to the 2D column. Unlike differential flow modulation, where the two column flows are independent, flow diversion connects them, leading to communication between the columns, to varying degrees depending on system design. This adds complexity to method development and application. GC × GC utilizing flow diversion modulation gained popularity primarily due to Seeley's work in 2006, which introduced a straightforward design based on a Deans' switch, enabling 100% transfer of 1D eluate to the 2D column [11].

One challenge with many valve-based modulators, be it differential flow or flow diversion, is the high flow rates on 2D separations, often around 20 mL/min, posing compatibility issues for mass spectrometry detection due to the connection to a vacuum system. A common approach to tackle this is splitting the flow exiting the modulator prior to MS detection: either diverting part of the flow into a bleed column or splitting it to an additional detector, typically an FID. The latter permits various detector combinations to be used simultaneously with MS, tailored to specific analytical goals.

Krupcik et al. demonstrated the advantage of simultaneous detection using FID and quadrupole mass spectrometry (qMS), as the FID provides reliable quantitative analysis while the qMS spectral scan speed enables confident analyte identification [12].

Flow modulators, depending on the model and configuration, can operate in forward or reverse fill/flush mode (FFF and RFF, respectively). The difference between both modulators is the flushing direction. In case of FFF, loop is flushed in the same direction of filling. On the contrary, with RFF modulators, loop is flushed in the opposite filling direction. Both modes perform similarly at low concentrations, but at higher concentrations, RFF exhibits slightly better performance, with less broadening, improved sensitivity, and peak capacity.

Several flow diversion modulators are available on the market, they slightly different in the design but the fundamental operational process remains very similar. Figure 2-11 reports the scheme of one of the most common, as well as the one used in this thesis, implemented as a RFF modulator.

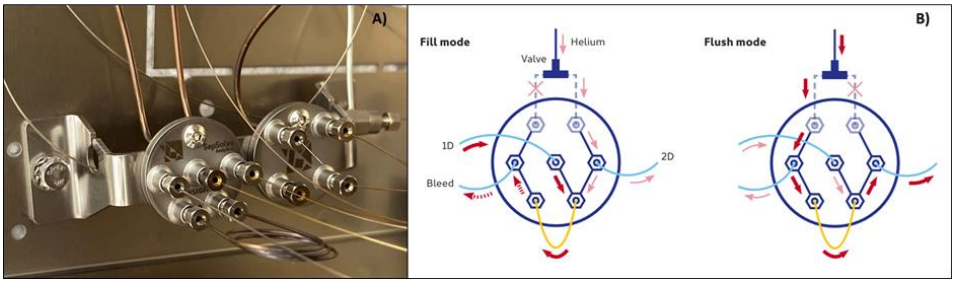

Figure 2-11: A) RFF flow modulator; B) Schematic demonstrating the operation of the reverse fill/flush modulator. During the filling step, this seven-port flow-based FM collects 1D effluent to fill the sample loop (yellow). At this time, 2D carreer gas is alimented via the valve (right side open/left side close). During flushing step, flows are reversed and the sample loop is flushed into the 2D column via the inversion of the valve (right side close/left side open).

2.4. References

[1] Giddings JC (1987) Concepts and comparisons in multidimensional separation. J High Resolut Chromatogr 10:319–323. https://doi.org/10.1002/jhrc.1240100517.

[2] Venkatramani CJ, Xu J, Phillips JB (1996) Separation orthogonality in temperature-programmed comprehensive two-dimensional gas chromatography. Anal Chem 68:1486–1492. https://doi.org/10.1021/ac951048b.

[3] Venter A (2003) Comprehensive two-dimensional supercritical fluid and gas chromatography.

[4] Giddings JC (1995) Sample dimensionality: A predictor of order-disorder in component peak distribution in multidimensional separation. J Chromatogr A 703:3–15. https://doi.org/10.1016/0021-9673(95)00249-M.

[5] Bahaghighat HD, Freye CE, Synovec RE (2019) Recent advances in modulator technology for comprehensive two dimensional gas chromatography. TrAC - Trends Anal Chem 113:379–391. https://doi.org/10.1016/j.trac.2018.04.016.

[6] Tranchida PQ, Purcaro G, Dugo P, Mondello L (2011) Modulators for comprehensive two-dimensional gas chromatography. TrAC - Trends Anal Chem 30:1437–1461. https://doi.org/10.1016/j.trac.2011.06.010.

[7] Aloisi I, Schena T, Giocastro B, Zoccali M, Tranchida PQ, Caramão EB, Mondello L (2020) Towards the determination of an equivalent standard column set between cryogenic and flow-modulated comprehensive two-dimensional gas chromatography. Anal Chim Acta 1105:231–236. https://doi.org/10.1016/j.aca.2020.01.040.

[8] Boswell H, Chow HY, Gorecki T (2020) Modulators. Elsevier

[9] Stoll DR, Li X, Wang X, Carr PW, Porter SEG, Rutan SC (2007) Fast, comprehensive two-dimensional liquid chromatography. J Chromatogr A 1168:3–43. https://doi.org/10.1016/j.chroma.2007.08.054.

[10] Deans DR (1968) A new technique for heart cutting in gas chromatography [1]Eine neue Technik des “heart cuttings” in der Gas-ChromatographieUne nouvelle technique de “Heart Cutting” dans la chromatographie en phase gazeuse. Chromatographia 1:18–22.

[11] Seeley J V, Micyus NJ, Bandurski S V, Seeley SK, McCurry JD (2007) Microfluidic deans switch for comprehensive two-dimensional gas chromatography. Anal Chem 79:1840–1847. https://doi.org/10.1021/ac061881g.

[12] Krupčík J, Gorovenko R, Špánik I, Sandra P, Armstrong DW (2013) Flow-modulated comprehensive two-dimensional gas chromatography with simultaneous flame ionization and quadrupole mass spectrometric detection. J Chromatogr A 1280:104–111. https://doi.org/10.1016/j.chroma.2013.01.015

3. SPME and chromatographic fingerprints in food analysis

Based on: S. Mascrez, D. Eggermont and G. Purcaro, SPME and chromatographic fingerprints in food analysis, The Royal Society of Chemistry, published on 24/03/2023.

3.1. Abstract

This chapter focus on the application of solid-phase microextraction in food analysis. A preliminary overview of the evolution of food analysis over the year from a technical viewpoint will be provided. This development has been followed by the evolution from more targeted towards untargeted and fingerprinting approaches. In this scenario, the coupling of SPME with gas chromatography and particularly with comprehensive multidimensional GC (GC×GC) has played a fundamental role to enhance significantly the level of information that can be extrapolated from a chromatographic fingerprint. Applications on different food commodities are discussed, emphasizing the applications that more exploited this novel approach.

3.2. Introduction

Solid-phase microextraction represents one of the most significant innovations in sample preparation. It has rapidly gained a high interest in the scientific community, particularly coupled to a gas chromatographic analysis for volatile characterization. It is interesting to highlight that in the field of GC, a groundbreaking innovation, i.e., the introduction of comprehensive multidimensional GC (GC×GC), occurred over the same years. Even more intriguing is that the scientific life of their inventors was tightly related in those years. In fact, Janusz Pawliszyn (inventor of the SPME) was the first of John Phillips (inventor of the GC×GC) ` Ph.D. students who did initial work on developing thermal modulation for multiplex GC, resulting in the work published in 1985[1]. This represents the first step towards the design of the comprehensive multidimensional GC (GC×GC) published in 1991 by Phillips and Liu [2]. The modulator Pawliszyn constructed consisted of a front of the fused silica capillary column coated with the stationary phase surrounded by the Wolfram filament from the broken light bulb, which was improved by replacing it by the resistive paint in a continuation work by Liu [3]. The operating principle is based in disturbing the sorption/desorption partitioning equilibria occurring in the column via periodic heating of the front of the column. Therefore, there is an apparent connection between the pioneering thermal modulation work, which opened the door to the design of GC×GC in 1991 and the extension of the concept to real samples rather than carrier gas which led to the development of the SPME technique introduced in 1990 [4]. In addition, it should be recognized that there is high level of compatibility between SPME as high performace sampling/extraction/GC introduction approach and high-resolution GC×GC separation as during the

desorption step no solvent is introduced into the systems simplifying comprehensive characterization of the sample and eliminating potential interferences/contaminants.

Considering such a peculiar level of human and scientific events of serendipity, it appears natural in this chapter to follow this conceptual track and provide an overview of the recent advances in food analysis that combines the use of SPME and GC×GC. A preliminary overview of the evolution of food analysis from a technical and conceptual viewpoint is provided to emphasize the fundamental role of the techniques aforementioned in the new vision of food characterization. In fact, as it will be described in more detail, the evolution of analytical chemistry and food analysis are tightly linked, allowing to move from basic wet chemistry to more advanced trace and fingerprinting approaches based mainly on chromatographic and spectrometric techniques [5–7].

The first coupling of SPME and GC×GC for food analysis occurred in 2002, when Adahchour et al., showed the potentiality of such a marriage for the characterization of garlic volatiles [8]. Since then, after a slow start of a couple of papers per year initially, the coupling gained popularity significantly from 2009 to 2010, as shown in a previous review [9]. This chapter will focus on the works carried out since 2010, and emphasis will be given to the applications that fully exploit the potentiality of the relatively new concept of the generation of food fingerprints rather than to papers related to simple characterization.

3.3. Evolution of analytical chemistry in the field of food analysis Introduction

Food is a very heterogenous matrix composed of various biochemical components. It undergoes different post-harvesting, processing, and storage steps that may alter the initial composition and structure, leading to the loss or formation of novel, desired or not, components (e.g., Maillard products or process contaminants). Food chemistry plays a major role in characterizing the final food product or following the changes over the overall process from farm to fork. No matter the specific case, the overall goals can always be reconducted to food quality, authenticity, and/or safety control.

The origin of food chemistry has not been defined rigorously due to a tight connection with agricultural chemistry, but some of the key studies that can consider marking the origin of modern food chemistry can be dated back to the end of the 18th century [5,10]. For a more comprehensive discussion of the historical overview, the readers are directed towards references [6,7,10], here, a very brief summary is reported along with a schematic overview in Figure 2-12.

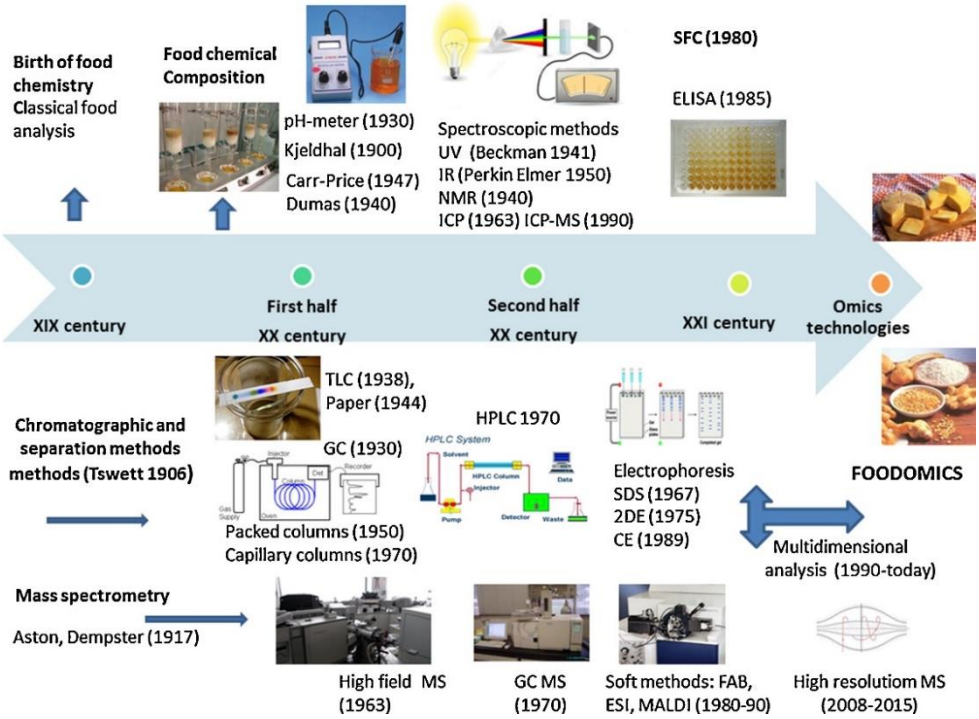

Figure 2-12: The evolution of the application of analytical chemistry methods to food analysis. Reproduced from Ref. [7] with permission from Elsevier.

The first steps in food chemistry can be reconducted back to the end of the 1700 with the discovery of the first food related components (e.g., isolation of glycerol, lactose, citric acid by C.W. Scheele; the discovery of stearic and oleic acid by M.E. Chevreul) and the introduction of the first methods to characterize foods (e.g., determination of the percentage composition of C, H, and N in dry vegetables by J.L. Gay-Lussac and L.-J. Thenard). During the same years, A. Lavoisier (1743–1794) designed a laboratory instrument (i.e., the ice calorimeter) to study what happened after the ingestion of food, proving false the phlogiston theory and showing the fundamental role of nutrition in providing energy to the human body [11].

Over the 20th century, food chemistry has undergone extensive development, from classical wet chemistry, through the development of the early analytical instruments for routine analysis, to the application of spectroscopic methods. In the early years of the 1900s (1908-1950), gravimetric, titrations, and precipitations (developed all along the 19th century) were the sole methods involved in determining the major food constituents. The milestone that started a new era for food analysis was the

introduction of the electronic pH-meter (called the “Acidimeter”) in 1934 by A.O. Beckman [12], followed shortly after by the first ultraviolet (UV) spectrophotometer in 1941 [6,12] and, the infrared (IR) spectrophotometer in 1944 [13]. The most impacting innovation in food analysis, i.e., chromatography, started with the first-ever application presented in Russian in 1901 and published in 1906 by M. Tswett [14,15]. However, the invention remained hidden since the publication was in the Russian technical literature. Thus, the creation of chromatography, as we know it today, was presented by A.J.P. Martin and R.L.M. Synge in 1941 when they showed the use of liquid-liquid partition chromatography to separate acetylated amino acids [16]. In 1952, they introduced the first gas-liquid chromatographic separation [17]. The development of chromatography will be discussed in the following paragraph in more detail.

The ultimate step into the modern era of food analysis is represented by the invention of the mass spectrometer by J.J. Thomson in 1919, which leaded to a groundbreaking advancement when coupled with GC in the 1960s. At present, GC-MS is a common and essential technique in food analysis, although the development of a more powerful generation of MS and the introduction of comprehensive multidimensional GC (GC×GC) [2] is steering food analysis into a new era.

The chromatographic and MS technology advancements have facilitated practicality of the sample preparation step. The analytical instrument, particularly the detectors, can compensate for sensitivity, thus not requiring high amounts of sample injected and thus allowing migration to more miniaturized sample preparation techniques with the inherent advantage of being also more sustainable and environmentally friendly using less amount of chemicals. At the same time, the enhanced separation power of the chromatographic techniques provides an additional purification directly into the chromatographic system, reducing preliminary sample preparation, saving time, and increasing the accuracy of the determination.

The relatively intense development on the instrumental side has led to a changing approach to problem-solving and to more articulated and variegate scientific questions. The evolution in the theoretical concept of food analysis is discussed in the following paragraph.

3.4. From basic characterization to new integrated -omics approaches

The goals in food analysis have been changing over the years following the technological advancement but at the same time also stimulating instrumental

development. At the beginning of the 1900s, the main goal was to characterize the main components of food, as the wet chemistry approaches available could not provide sufficient sensitivity or information-rich data. The instrumental era of food analysis allowed a more thoughtful investigation, extending the characterization to minor and trace components. After decades during which the general composition, the endogenous and exogenous components have been explored in-depth and decrypted, food science is now moving towards a different investigation, following the trend of biological science towards interactionism (defined below) and -omics sciences. This evolution parallels the social evolution and the consumers' awareness. In this regard, the problem has moved from guaranteeing stable and generally safe food to the necessity of high-quality food with high nutritional value and bio-active beneficial components, obviously never disregarding the safety aspects. At the same time, the assessment of food quality and authenticity has moved from detecting coarse frauds (like the addition of methanol in alcoholic beverages) to more sophisticated adulterations, such as the addition of softly refined oil in extra virgin olive oil or frauds linked to the geographical origin.

The more traditional approach to thoroughly characterize the compounds present in the sample and to reduce everything to a univariate system, where one compound corresponds to one target (also referred to as “reductionist approach”), has been proved not sufficient to answer increasingly more sophisticated questions. Therefore, food analysis is moving towards a more integrated and interactive approach. The latter, also called “interactionism”, is driven by the evolution of analytical chemistry and the evolution of the food requirements. Food analysis has thus followed the prints of biology, which has introduced and consolidated several -omics approaches (e.g., metabolomics, proteomics) [18,19]. In this regard, a landmark is the introduction of the term “foodomics” in 2009 by A. Cifuentes as “a discipline that studies the food and nutrition domains through the application and integration of advanced omics technologies to improve consumers’ well-being, health, and confidence” [20]. This definition includes a series of different and interrelated -omics sciences, such as sensomics, nutrigenomics, nutrimetabolomics, food metabolomics, etc. These define the interaction of food with a particular physiological function (e.g., sensory perception or nutritional value). Therefore the -omics sciences rely on instrumental fingerprints generated by advanced analytical instruments, aiming to gather information linked to the identity, quality, or quantitative aspects through the generation of a non-specific signal. In this context, the term fingerprint is translated from the forensic use in people identification, where specific minutiae features (i.e., ridge endings and ridge bifurcation on fingertips) are used for people identification through cross-matching with a database. The use of appropriate data mining methods, developed under the umbrella of chemometrics science, provides the extraction of useful information from the information-rich dataset. The readers are directed elsewhere for a more detailed discussion on the fundamental data mining steps [21,22]. Herein the instrumental fingerprints generation and its implication are discussed and in particular the generation of the so called “chromatographic fingerprint” [23].

An important distinction that needs to be made refers to the definition of profiling and fingerprinting [24,25]. Profiling, which can be conducted conceptually in a targeted or untargeted way, aims to obtain detailed information on the qualitative and quantitative distributions of the compounds present in the sample under study. Instead, fingerprinting relies on a high-throughput methodology capable of capturing relevant information but not necessarily achieving accurate quantitative data or identification of the entire sample composition.

Chromatographic fingerprints provide a unique situation where the data generated can be processed either following fingerprinting or profiling methodologies, providing multi-level information (as schematized in Figure 2-13). Furthermore, the resemblance with the forensic fingerprint is even more evident when considering comprehensive multidimensional chromatography, along with the quantity of information embedded in the signal [19,22]. On this perspective, the applicative papers presented in section 3.6. are selected and discussed.

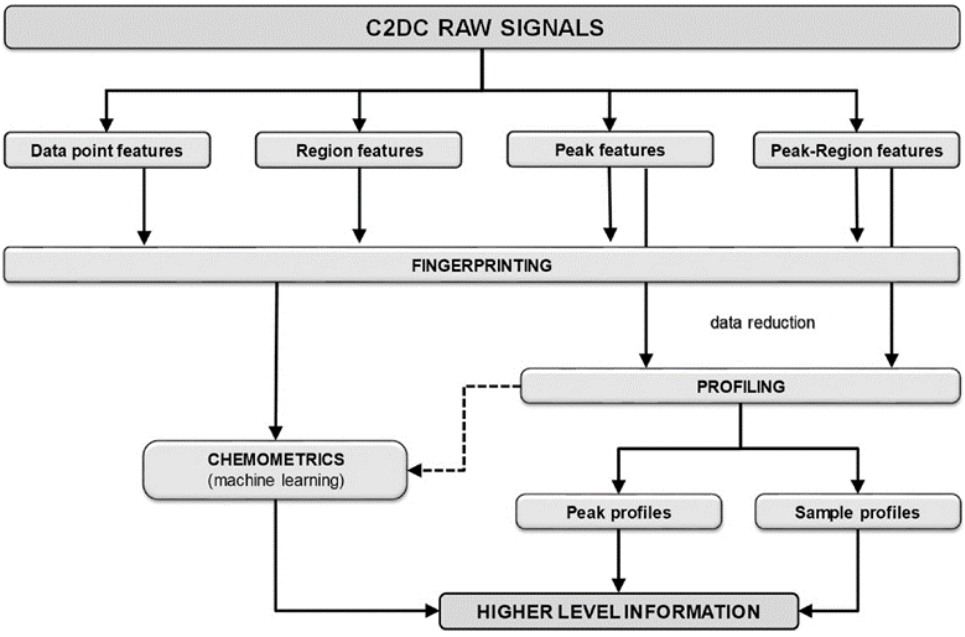

Figure 2-13: Types of features for comprehensive two dimensional chromatography (C2DC) data processing according to fingerprinting and/or profiling methodologies. Reproduced from Ref [22] with permission from Elsevier.

3.5. Evolution of gas chromatography and solid-phase microextraction in food analysis

The first headspace (HS) analysis coupled to GC was presented by Bovjin et al. in 1958[26]. During the same years, the GC technology found significant applicability

in many fields of applications, including food, and several landmark advancements were presented, including the introduction of new detectors, inlet system and the development of the column technology [27], which significantly enhance the sensitivity of the analyses. Game changers were the introduction of the capillary column by M.J.E. Golay in 1958 [28] and the coupling of GC with a mass spectrometer (MS) by R. Gohlke in 1959 [29]. Roughly 30 years after, in 1991, based on an idea of Martin present in 1944 [30], Phillips and Liu introduced comprehensive multidimensional GC (GC×GC), leading to a similar exponential increment of separation efficiency than the introduction of capillary columns [2]. GC×GC coupled two columns (based on different separation mechanisms) in series using a modulator that cuts and reinjects the eluent from the first column into the second one. The obtained separation efficiency is theoretically equal to the multiplication of the separation efficiency of the two columns. GC×GC provides higher separation power, selectivity, sensitivity, along with the formation of group type separation -patterns. For a more detailed description of the technique, the reader is directed towards the rich literature in the field [31,32]. As mentioned in the introduction, almost in parallel Pawliszyn introduced the SPME technique in 1990 [4] and in 1993 the first HS-SPME application was presented [33].

Undoubtedly the development of more powerful analytical instruments, i.e., high resolving GC and highly sensitive detectors, among which MS play an important role in the further diffusion of SPME [34–38]. A miniaturized technique that, for its intrinsic nature, do not provide exhaustive extraction yields, but rather the quantity of analytes extracted from the sample is frequently negligible. This characteristic leads to a series of advantages discussed in more detail in the theoretical chapter of this book. Despite its non-exhaustive nature, SPME provides a significant concentration factor compared to static HS extraction. Indeed, SPME has been the first high concentration capacity technique introduced, which represents a bridge between SHS and dynamic HS, being simple, fast, easy to automate, and reliable as the former but allowing a high concentration factor as DHS.

Although SPME can be applied in different modes, e.g., HS-SPME and DI-SPME, the former largely overpass the latter in terms of applications in food analysis due to scarcity of robust extraction coatings compatible with the food matrices. Despite the advantages of HS in maintaining the fiber integrity avoiding detrimental coating deterioration or instrument contamination, it limits a more balanced coverage of analytes. Indeed, analytes with good solubility into the food matrix and limited volatility are less extracted than more volatile and less soluble analytes. Therefore, the extraction of complex matrix by HS may not be representative of the chemical

composition of the sample. On the other hand, more exhaustive coverage of analytes is obtained by DI, since only the diffusion coefficient within the sample is responsible for the partition into the fiber. Moreover, HS mode is more prone to competitive adsorption than DI, especially when solid porous coatings are used [34,39]. In the direction of reducing the displacement effect, a very interesting and completely innovative approach has been recently published by Pawliszyn's group proposing a sequential extraction using thin-film SPME (TF-SPME) [40]. The authors proposed a first extraction using PDMS TF-SPME to depleting the sample of the most non-polar compounds, often responsible for displacement of the most polar one, followed by an additional extraction using HLB/PDMS TF-SPME more affine to polar compounds. This work proved as sequential extractions increased the extraction yield of the most polar compounds, avoiding displacemlent effect, thus improving linearity and quantification accuracy. Moreover, the sequential extraction can be injected separately or as a cumulative extraction increasing the overall profiling capability of the technique. We believed that this approach will open interesting perspective in the near future in food analysis.

Despite the intense research to develop new fiber with antifouling coatings to exploit the advantages of DI-SPME, this trend has not been translated into the applications developed by GC×GC yet. This is probably due to the limited number of research groups actively involved in both domains in terms of fundamental research.

This limited innovation of the use of SPME coupled to GC×GC reflects on the application of rather traditional coatings, mainly in HS mode, and limited innovation.

Nevertheless, the HS-SPME mode generally provides a rather comprehensive overview of the volatiles of the sample examined, although mediated by the specific selectivity of the polymeric coating used. Despite the evolution of the polymeric coatings [34], the triphasic fiber, i.e., divinylbenzene/carboxen/polydimethylsiloxane (DVB/CAR/PDMS) is by far the most employed one in food applications, in particular coupled to GC×GC followed by CAR/PDMS and PDMS/DVB. The trend is confirmed both in GC and GC×GC applications, as well as for different food categories (Figure 2-14).

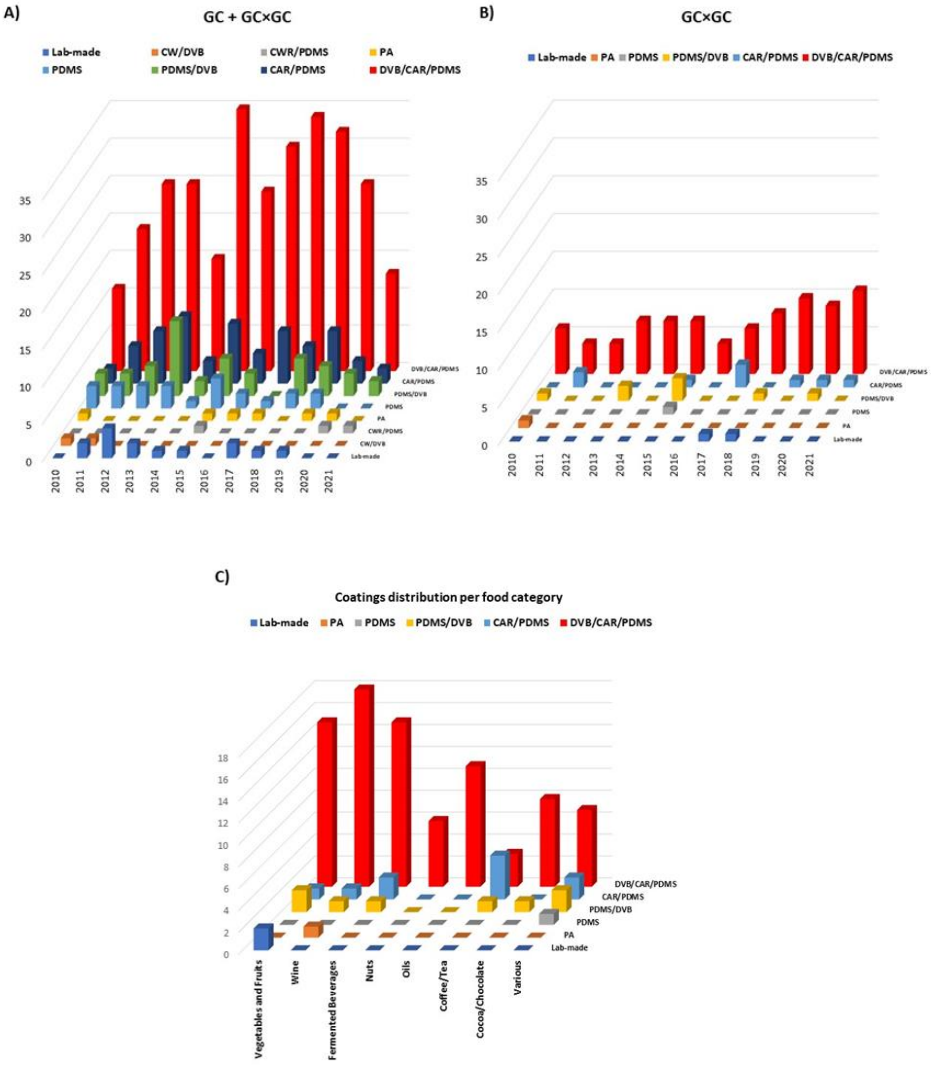

Figure 2-14: Barplot of the published food applications since 2010 A) using both SPME-GC and SPME-GC×GC; B) using only SPME-GC×GC; C) using SPME-GC×GC divided by food category.

The first used of SPME coupled to GC×GC occurred in 2002, when Adahchour et al. [8]. Few papers started to appear in the following years but mainly focused on characterization and proof-of-concept of the potentiality [9]. The first works that explored the combined techniques asking more sophisticated questions (such as geographical authenticity, process effect, etc) started to appear in 2008 [41–43].

Klimánková et al. explored the variation of basil's VOCs in relation to cultivars (five types), way of farming (organic and conventional farming), different parts of the plant (leaves, haulm, and blossom of one cultivar), and drying and freezing process (fresh, dried, frozen basil) [41]. Nevertheless, the data exploration was still limited to a univariate comparison, and the use of GC×GC was limited to confirmation of the compounds' identity. Cardeal et al. used the term fingerprints to define the 2D contour plots obtained from the SPME- GC×GC of cachaça during the distillation process and once aged in different wood barrels, but they limited their discussion to a visual comparison of the chromatograms, although suggesting the potential to apply multivariate analysis [43]. Cordero *et al.* introduced fingerprinting approaches for the analysis of food aroma in 2008 [42]. In particular, the authors discussed the application of group-type, fingerprint-type characterizations, borrow from the petrochemical field [44], and template matching for the analysis of roasted hazelnuts and coffee. The group-type approach exploited the well-structured chromatograms obtained in the 2D space when using GC×GC-MS; thus, specific classes of compounds can be visualized based on their retention time and fragmentation patterns and compared among chromatograms. The fingerprint-type comparison was presented still at its dawning based on a peer-wise differential image produced by a specific software developed shortly before [45]. This milestone paper also presented the template matching approach, which was then widely and successfully used in more sophisticated studies. This approach used a "target 2D pattern" to be matched with a "template peak pattern" created from a reference sample (arbitrarily chosen). The template pattern can be composed of all the separated compounds or a selected sub-fraction, for which the 1D and 2D retention time and the MS spectrum information are retained for subsequent matching. The template matching procedure establishes correspondences and differences among the compared samples which are then compiled in a table and made available for further classification and correlation purposes [42]. Figure 2-15 shown the three approaches presented for the characterization of coffee and hazelnut samples. Although not yet combined with chemometrics, the presented approaches constituted the methodology for the further development of chromatographic pre-processing of fingerprint data.

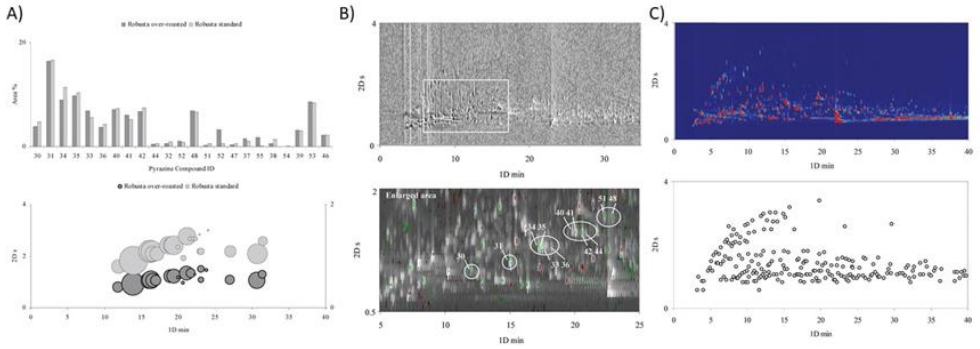

Figure 2-15: coffee samples submitted to a standard and an over-roasted thermal treatment. Histograms report the area percent of each congener, whereas bubble plot graphs describe the components' location over the 2D plane. B) Resulting 2D fingerprint, that is, differential image, produced by comparing two hazelnut samples submitted to two different thermal processes. In the enlarged area of the 2D plot in the fuzzy difference visualization, brighter/green spots correspond to those analytes that were present in larger amount in the over-roasted Piedmont hazelnut sample. Dot-plot circles indicate pyrazine ID. C) 2D plot and graphical representation of the 231 template peaks chosen from a standard roasted Roman hazelnut (i.e., arbitrarily considered as reference). Modified with from Ref [42] with permission from ACS Publications.

In 2009, Vaz-Freire et al. proposed the use of a Java-based, multithreaded, freely available, open-source, platform-independent, and public domain image processing and analysis program developed by the National Institute of Health (NIH, USA) for the fingerprinting treatment of the 2D plots obtained by the HS-SPME-GC×GC-TOFMS analysis of Portuguese olive oil samples obtained from three local cultivars (i.e., Galega vulgar, Carraquenha, and Cobrancosa) and through to different procedures (i.e., hammer-mill press line and hammer-mill integral decanter line).

In the same year, Cajka et al., presented the first large-scale study using HS-SPME-GC×GC-TOFMS to answer a relevant question on the authenticity of honey coming from the protected denomination of origin of Corsica [46]. These represent the starting works that opened the way to the application of HS-SPME-GC×GC to answer more sophisticated questions in the last decade on the quality and authenticity of food products. This is possible thanks to the unique chromatographic fingerprints provided by the 2D separation, which can be treated using either fingerprinting or profiling approach and the unique simplicity and flexibility of SPME when adequately optimized for the specific matrix. Although the scientific

production in this direction has significatively increased in the last decade, it is still rather limited and mainly applied to high-value food commodities. In fact, most of the works are still a simple characterization or with limited statistical evaluation. The use of SPME is rather standardized and usually refers to previous works. In fact, a limited number of papers presented some significant innovations or interesting SPME optimization. Nevertheless, it has been shown that the optimization of the SPME extraction, mainly in terms of coating selection and desorption parameters, may have a significant impact on the GC×GC separation performance by ruining the resolution advantage of GC×GC due to a too slow desorption process and thus causing intense tailing of the earlier eluted compounds. This apparent drawback can be turned into a benefit to efficiently evaluate the performance of new coatings in terms of desorption efficiency and stability of the extracted compounds [47]. On the other hand, the ability of GC×GC to separate the extracted compounds according to the chemical properties and the enhanced sensitivity provides the needed separation dimension to characterize the metabolomics profile of foods fully.

3.6. Applications

Herein, the applications published over the last ten years are presented divided into main food categories. The emphasis is given to works that offer a more innovative data mining approach, in line with more advanced -omics techniques. Table 2-2 summarizes the main paper published since 2010 using the combination of SPME and GC×GC.

3.6.1. Edible oil and fats, in particular olive oil

Edible oils are important components of the human diet to provide energy, nutritional components, and pleasant flavors. Among other oils, olive oil has always represented the most valuable one due to its peculiar composition, added healthier value, and economical cost. Therefore, olive oil is one of the main targets of food frauds, both regarding quality and authenticity [48]. Olive oil is divided into three commercial categories, based on a series of chemical parameters (i.e., total acidity, peroxide value, or UV absorbance on specific wavelengths) and a sensory evaluation performed by a trained panel test that evaluates codified defects and the presence of fruity aroma. The oil is thus classified as extra virgin olive oil (EVO, top quality), virgin oil (VO, slighter lower quality since presenting some sensorial defects), and lampante oil (low quality not suitable for human consumption). The latter is refined and mixed with virgin olive oil and thus sold with the label of olive oil. As this classification is ultimately mainly based on a sensory test that, for its nature, lacks objectivity, many scientists have tried to support it with more objective analytical analyses. Undoubtedly, the sensory perception is linked to the chemical compounds released by the samples and their odor potency determined by the interaction of the odorant with the human receptor. On the other hand, the relative distribution of volatiles depends on the cultivar, geographical origin, fruit ripeness, processing practices, and storage [49,50]. This means that in the

chemical fingerprints that HS-SPME-GC×GC can generate, such information is encrypted, and multiple questions can be answered [51–59].

Different fiber coatings (i.e., DVB/CAR/PDMS, PDMS/DVB, CW/DVB, PDMS) have been compared for providing comprehensive coverage of the volatile profile of olive oil, as well as different formats (SPME, HS-stir bar sorptive extraction (SBSE), monolithic material sorptive extraction) and compared to dynamic techniques [60,61]. The DVB/CAR/PDMS fiber confirmed the good quali- and quantitative coverage of the volatile profile, confirming its widespread (and almost unique) use in the analysis of olive oil.

Regarding GC×GC column selection, both configurations, i.e., apolar×polar (normal set) and polar×apolar (reverse set), has been proved effective, with generally a better distribution of the compounds all over the 2D plot (and thus higher identification capability) using the former one, but with a broadening of the most volatile and polar compounds in the second dimension [54,60] that can affect their adequate quantification.

As mentioned above, in 2009, Vaz-Freire *et al.* used an open-access image analysis software to discriminate among three Portuguese cultivars based on the image-features. Targeted profiling was used to identify the compounds within the most informative 2D region. In 2019, Lukić *et al.* used a peak-features approach, in both untargeted and targeted modes, to differentiate among different monovarietal oils obtained from five different Croatian cultivars from specific geographical area [52]. In 2014, Purcaro *et al.* combined untargeted and targeted analysis to define the blueprint of different olive oils categories (EVO, VO, and lampante oils) [54]. The volatile profile was sampled using a DVB/CAR/PDMS SPME fiber and analyzed in two different GC×GC-MS platforms equipped with complementary column (normal and reverse) sets [54]. All the data mining was carried out separately for the data obtained from the two platforms in order to cross-validate the outcomes. A first untargeted analysis was carried out using the comprehensive template matching fingerprinting approach [55]. This process does not necessarily need to identify all the features found but instead support the reliable alignment over samples [62]. The data mining was first performed in an unsupervised fashion by PCA and then refined based on the sensomics principle. The features detected in the first screening were identified and normalized based on their odour potency (based on the odour threshold) and a partial least square discriminant analysis (PLS-DA) was performed. The samples were classified into EVO and non-EVO quality. This iterative strategy combining untargeted and targeted, and profiling and fingerprinting approaches was shortly after integrated and further developed in a unique workflow named untargeted and targeted (UT) fingerprinting by Magagna *et al.* in 2016 [56]. The flowchart is based on the template matching fingerprinting, and it is composed of several steps: I) targeted analysis based on the reliably identified compounds by their MS fragmentation pattern and linear retention index (LRI); II) Untargeted analysis based on a peak-region features approach automatically performed by the software; III) Visual features fingerprinting performed as pairwise image comparison to simplify the visual comparison of the chromatograms. This approach was successfully applied to defines eight reliable chemical markers of ripening in olive

oil by combining the outcomes of the different aforementioned steps. The UT fingerprinting flowchart (Figure 2-16) was later refined to consider chromatographic misalignment and MS acquisition fluctuations for long-term studies and batch effects [57]. The effectiveness of the study was proved by intentionally causing these misalignments by changing the chromatographic setting and the MS acquisition parameters.

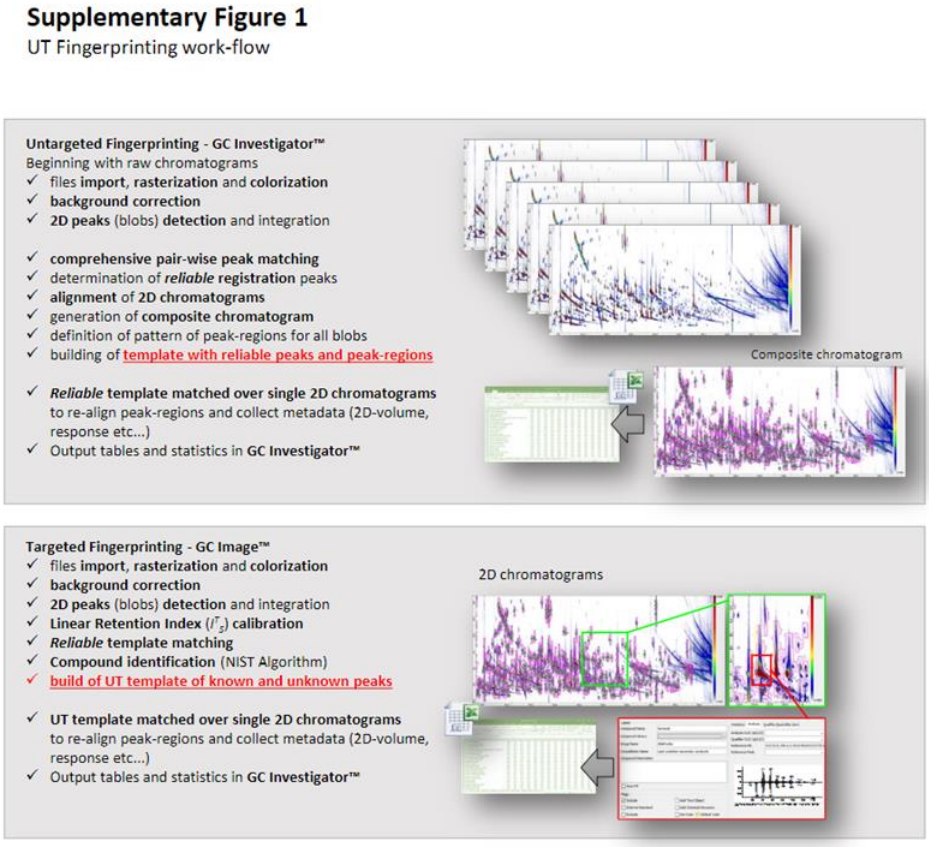

Figure 2-16: UT fingerprinting workflow. Reproduced from Ref [57] with permission from ACS Publications.

Similar approaches have been applied to the characterization of other emerging high value seeds oil, such as sesame oil, peanut, soyabean, sunflower, and virgin rapeseed oils, to detect fraudulent actions [63–65].

Despite not being performed using GC×GC separation, worth mentioning are a series of works exploring novel approach in the use of SPME, namely vacuum-

assisted SPME (Vac-SPME) [66] and multi-cumulative trapping SPME (MCT-SPME) [67–69], to enhance the level of information extractable from the HS analysis of EVO and non-EVO oils. The theoretical and practical aspects of the former approach, i.e. Vac-SPME, are detailed in the dedicated chapter authored by E. Psillakis; while a brief insight of the latter, i.e. MCT-SPME, is herein provided. MCT-SPME consists of multiple sequential extractions from the same vials (or different ones), trapping the extracted volatiles on a cryo-trap before injection into the GC system. In the works presented so far, a particular emphasis has been given to using a suitable amount of sample to not saturate the HS, thus making possible the direct correlation between the sample concentration and the extracted amount by SPME, otherwise biased by the saturation of the HS. Verifying this condition, MCT-SPME allows a higher extraction of the less volatile and more polar compounds since, as discussed for TF-SPME40, the depletion of the most volatile in the first extractions reduces the displacement effect on the following ones. This is particularly true and beneficial performing shorter repeated extraction rather than a longer single extraction (3-times 10 min were compared to a single extraction for 30 min). Furthermore, the authors showed how this approach enhances the level of information related to both the quality and authenticity of olive oil, allowing easy discrimination between EVO and non-EVO and, within the EVO samples, among the different geographical origins of the same data set [69].

3.6.2. Nuts, cocoa and chocolate

Hazelnut is among the most relevant nuts in the world for its use as an ingredient in many baked and chocolate-based products. A high-quality control is required at any level, from harvesting through drying and storage until the final use as an ingredient, to avoid rotten defects, mycotoxins formation, and guarantee stability during storage. The latter refers to lipid oxidation processes that generate off-flavours (as rancid) due to the high-fat content of these products. Moreover, hazelnuts often undergo drying and roasting processes to improve both stability and aroma, but they can generate unpleasant off-flavor if not correctly performed. Last but not least, the geographical origin also plays an important role in the overall aroma profile, creating possible standardization problems in the final product aroma. The group of prof. Cordero in Italy has intensively studied the native and process-induced volatile profile of hazelnuts over the last decade [70–75]. These works provide a very good example of the technical evolution of the chromatographic fingerprinting approach over the years in the field. In 2010, the quali-quantitative distribution of hazelnut volatiles from samples of different geographical origins and varieties (Italy, Turkey and Chile), all thermally treated with a standardized procedure, was studied [70]. Both fingerprinting (i.e., template-based fingerprinting [42,55]) and extended targeted analyses were used to extrapolate the encrypted information from the chromatographic fingerprint. The template-based

fingerprinting consists of detecting the fingerprint minutiae in each GC×GC plot by compiling a cumulative chromatogram called the "consensus template" based on many sub-parts of the main chromatogram (that may be called "tile"), which is then subsequently applied to all the chromatograms to compare, thus evaluating the features match across chromatograms and the semi-quantitative distribution of each feature. Although this approach is a good preliminary evaluation of similarities and diversity among samples, it may place two relevant peaks in the same fingerprint feature or incorrectly split a peak into two fingerprint features. The comprehensive template-matching fingerprinting represents an evolution of the previous approach, where the "consensus template" is not built on a specific sub-zone of the chromatogram but is done on peak-match based on retention times and detector response (i.e., MS fragmentation pattern). The template-matching method proved to be more sensitive and specific in detecting differences between samples compared to template-based fingerprinting. The investigation was then extended by performing a profiling of the more informative peaks to detect known markers of technological, sensorial, and botanical relevance. An effective strategy based on multiple headspace extraction was then used to quantify the key odorants in hazelnuts samples reliably [71]. The topic of quantification using HS-SPME, in particular in solid sample is of utmost importance, nevertheless it represents a chapter on its own thus it is out of the scope of the present discussion. The reader is directed towards the more theoretical chapters of this book for more information.

The comprehensive template-matching was further applied and validated to define markers of geographical origin, cultivar and variety, and thermal treatment and to follow their evolution over storage [72,73]. The workflow previously applied for olive oil [56] was used to establish reliable volatile patterns able to recognize spoiled hazelnuts [75] and to correlate the volatile profile with the primary metabolome fingerprints of hazelnuts samples [74,76].

Cocoa beans are the fundamental raw material to produce chocolate. It undergoes several pre-processes, such as fermentation, drying, roasting, and crushing to obtain the cocoa nibs, then used for producing chocolate. All these steps, along with the different geographical origins, storage, and transport conditions, play an important role in the final aroma and in avoiding spoilage, such as mold growth. Many researchers have tried to decrypt the relation between these parameters and the final volatile profile in cocoa products [77–85]. Oliveira et al. study the capability of the volatile profile sampled with a DVB/CAR/PDMS fiber to differentiate based on the geographical origin (i.e., 28 samples from Brasil and Ivory Coast) [78]. Fisher ratio was applied to select the most discriminant features, and the results were visualized using a PCA showing an explained variance of 94%. Interestingly, it has been revealed as the same varieties, harvested six months apart, generated a different volatile profile in the final chocolate produced under the same controlled conditions [82]. The multiway principal component analysis highlighted that the main class of chemical compounds that discriminate between the two harvesting periods was the hydrocarbons. The same research group investigated the volatile profile in nibs, liquor, and chocolate using a method optimized on the chocolate samples [80]. The

authors showed PCA to discriminate between the different stages of chocolate production, highlighting the characteristic compounds formed during the production steps. The different steps from the nibs to the chocolate can also cause the formation of undesired off-flavour, such as the smoky flavour, originated during the drying step when performed carelessly using burning wood or other fuels [79].

The application of the UT fingerprinting approach, already described for olive oil and hazelnut, allowed to clearly determine markers of the smoky flavour in both beans and liquors, and thus subsequently optimized a target method to quantify their presence by a more straightforward HS-SPME-GC-MS method rather than GC×GC [79]. The UT fingerprinting method was also used to effectively discriminate among cocoa nibs from different geographical origins and production steps towards chocolate, highlighting the evolution of the most significant odorants through the production chain [83]. The template-matching strategy, embedded in the UT fingerprinting method, was proved translatable among different platforms [86], and in the particular case from a thermal modulated GC×GC-MS to a flow modulated GC×2GC-MS/FID platform, proving accuracy in the classification compared to the original reference one [84]. This advancement opens perspectives of sharing templates of selected markers responding to specific questions among different laboratories for quality control purposes. Moreover, the same approach was also used to perform a data fusion between parallel chromatograms obtained by tandem ionization MS (i.e., 70 eV and 12 eV), providing a richer-data matrix for fingerprinting approach and target analysis [85]. The results were compared considering the discriminant features obtained using the UT fingerprinting method on each acquisition mode and the combined one.

Early detection of mold proliferation due to residual humidity was successfully performed by HS-SPME-GC×GC-MS, using a DVB/CAR/PDMS fiber, by detecting the presence of specific markers in the volatile profile [77].

3.6.3. Coffee and tea

Tea and coffee are stimulating beverages highly consumed worldwide. Both have beneficial effects on mood and cognitive performance, along with potential health benefits thanks to their relatively high polyphenols content. Moreover, it is undebatable that their consumption is associated with a hedonistic moment steering their market value and consumer preference. As for the other food commodities, the sensory quality passes through the volatile profile, which contains other useful information related to geographical origin, storage, and processing.

Over the last ten years, most of the works using SPME-GC×GC studied the volatile profile of tea and only one presented results on coffee [55], but the latter paper was more focused on presenting the UT fingerprinting method (already explained in more detail for other foods) rather than an application on the coffee aroma.

The majority of the research focused on tea aroma [87–93]. Magagna et al. compared the volatile profile obtained from dry tea leaves without and with the

addition of water during the extraction step using three different HS techniques, a DVB/CAR/PDMS fiber, HS sorptive extraction (HSSE) and DHS [87]. DVB/CAR/PDMS showed complementary sampling results compared to HSSE and DHS, although less effective in absolute extraction amount. The addition of water in the sampling vial significantly impacted the distribution of the analytes with the HS, enhancing the partition of less polar analytes, such as aldehyde and short-chain alcohols. Ntlholkwe et al. 88 compared the performance of six SPME coatings (i.e., PDMS, PDMS/DVB, PDMS/CAR, PDMS/CAR/DVB, CAR/PDMS, and PEG) for the analysis of honeybush tea volatiles. The author concluded that the highest extraction capability, evaluated from a visual examination of the 2D chromatograms, was obtained by PDMS/DVB and DVB/CAR/PDMS. The authors selected PDMS/DVB since, they claimed, using DVB/CAR/PDMS, too many peaks overloaded the modulator, causing streaking in the second dimension. Proper optimization of the SPME extraction condition and the GC×GC method (replacing, for instance, the highly polar secondary column with a mid-polar one) to avoid extensive tailing, as well as a proper quantitative comparison of a fair number of compounds over the chromatogram, would have most probably led to the selection of the DVB/CAR/PDMS fiber for more comprehensive coverage of the volatile profile, as proved by Zhu et al. [89]. The latter paper was wisely designed to determine the odorant responsible for the chestnut-like aroma in tea by comparing the common volatiles between teas characterized by this aroma and boiled and roasted chestnuts. The finding was then evaluated considering the odor threshold of the common analytes to evaluate their odor-activity value.

Other studies used the CAR/PDMS fiber for characterizing key odorants of the specific aroma of tea (e.g. orchid-like) but without providing any justification for the choice of the coatings [90,92,93].

3.6.4. Wine

The VOCs profile is fundamental to characterize the quality of a wine, its appreciation, and consumers' attraction. The "bouquet" of wine is composed of several hundred chemical compounds deriving from grapes (e.g., variety, pedoclimatic area, ripening), from fermentation processes (e.g., alcoholic and/or malolactic, type of yeast, conditions, etc), other production processes (e.g., maceration, maturation, microoxygention). Despite the numerous information embedded in the "bouquet" of a good glass of wine, the use of SPME-GC×GC in the field still mainly applies traditional approaches (characterization and univariate data mining) compared to the other commodities discussed. However, the chromatographic fingerprint approach has started to appear slowly. From the evaluation of the many papers published on wine in the last decade, few papers reported target analysis of wine contaminants, such as ethyl carbamate [94] and haloanisoles [95], taking advantage of the increased sensitivity and identification capability provided by GC×GC. Six papers reported a simple characterization of different wines from different production areas (i.e., Cabernet Sauvignon from

Western Australia [96], Pinotage wine from South Africa [97], Merlot [98] and Chardonnay [99] from Brasil, Marsala from Italy [100], Saperavi from Georgia [101]). More sophisticated questions related to variety, pedoclimatic and vine management impact [102–106], aging and storage of wine [107–109], and production process [110–113] have also been investigated using both univariate and multivariate data mining to extract useful information.

Vine management is the first fundamental step in the production of quality wine, Nicolli *et al.* investigate ten different vine management practices combining SPME-GC×GC data with GC-O and quantitative descriptive analysis and comparing the respective PCA built retaining the most significant features after Fisher-ratio analysis [106]. This work showed no influence of the soil type (arenosol or acrisol), irrigation practice, and distance between vines, while bud load and leaves number affected either the volatile composition and the quantitative descriptive analysis significantly, confirming how the solar exposure and the air circulation may have a fundamental role in the final wine aroma.

The volatile chromatographic fingerprint of the wine aroma has been proved successful also in providing discriminant information on the effect of the grapes harvesting day [102], on the grapes varieties [103], and the maturation-maceration optimization [110]. Robinson et al. investigated the combination of site, canopy management and yeast strains on the overall volatile profile of Australia Cabernet Sauvignon in combination with quantitative descriptive analysis [113]. Although limited to only two vineyards, the results suggested that the primary influence on the aroma profile derives from the site, followed by the canopy management, while yeast treatments had only a limited effect. Figure 2-17 shows the main outcome of this investigation.

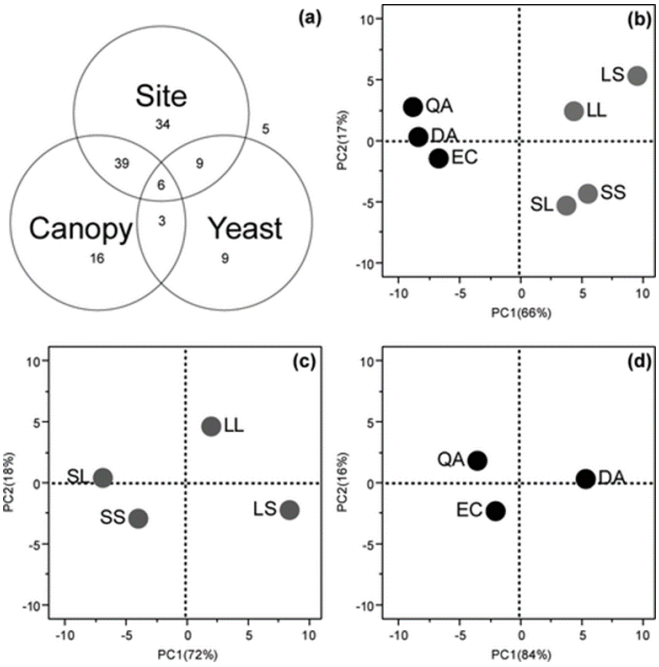

Figure 2-17: Volatile compound analysis for all seven treatments. Venn diagram (a) represents the distribution of the 121 volatile compounds that are significantly different due to treatment, score plot (b) is the PCA of volatile compounds significantly different due to site, score plot (c) is the PCA of volatile compounds significantly different due to canopy treatment at the Willyabrup site, and score plot (d) is the PCA of the volatile compounds significantly different due to yeast treatment from the Gingin site. Treatments DA, EC, QA, LL, LS, SL, and SS are labeled. Black circles are treatments from the Gingin site, and gray circles are treatments from the Willyabrup site.Reproduce from Ref [113] with permlission from ACS Publications.

On the contrary, Beckner *et al.* highlighted the significant impact in sensory perception and chemical volatiles fingerprint using six different non-Saccharomyces yeasts during Sauvignon production [111]. Schmarr *et al.* conducted a study on the effect of microoxigenation, a technological process introduced to replace the oxygenation occurring during barrel aging of wine while storing the wine in stainless steel tanks [114]. The data were unbiased treated by performing image analysis of the 2D plot allowing discrimination of the point in time and dose amount of oxygen of the microoxigenation treatments. A similar approach based on image evaluation was used to differentiate between Asti Spumante and Moscato d'Asti and monitor their evolution during storage [109].

3.6.5. Spirits, beer, and cider

Among the general category of alcoholic beverages [115–130], excluding wine, the most studied products are spirits [115–117,123–130] and, in particular, a Chinese distillate named Baijiu produced by distillation of mainly fermented sorghum [115,116,123–126]. These works used the DVB/CAR/PDMS fiber, except for the first work in 2019 that used a CAR/PDMS [115]. Most of the results were simple characterization by GC×GC of the volatile profile, combined or not with the profiling obtained with other platforms, such as GC-FID, GC-MS, GC-FPD, GC-SCD, GC-O, and sensory evaluation [115,123,125]. After alignment, identification of the relevant features, and application of a frequency of observation cutoff (80 or 50%), a correlation network was used to investigate the regional classification and the relationship between the sensory attributes and the identified aroma compounds [124]. The discrimination capability of two GC×GC column set-up, i.e., normal and reverse set, were also compared [126]. As for previous studies, both of them showed pros and contras in the orthogonality and the spatial contribution, but both of them allowed to answer the experimental questions successfully.

Only three papers investigated the aroma profile of beer, two of them were optimization and comparison of the HS sampling [118,119], while the third one was an interesting study on the effect of the yeast genetic diversity on the brewed product, and SPME-GC×GC-TOFMS was used for a basic comparison of the beer volatiles produced after fermentation with five different fully characterized yeasts [120].

An interesting paper by Zhang *et al.* compared different sample preparation techniques to characterize fermented beverages [121]. Vortex-assisted liquid-liquid microextraction, solid phase extraction (SPE), dynamic HS, multiple stir bar sorptive extraction (mSBSE) and SPME were used to characterize volatile from beer, wine and cider. The authors concluded that SPME is superior in terms of automatization and easiness of use, nevertheless they highlight as the VOCs profile is highly dependent on the sample preparation applied and that, among the one tested, a low rate of overlapping compounds was observed. For instance, in the case of beer, comparing mSBSE, SPE and SPME, only eight compounds were in common. This suggests that further development to improve the volatile coverage by a single technique would be highly desirable. In this direction the very interesting approach recently published by Pawliszyn's group using proposing a sequential TF-SPME extraction to minimize the displacement effect and increased the extraction of more polar compounds in beer.

3.6.6. Vegetables, fruits and juice

This paragraph includes many different goals and application purposes, as well rather various food classes, it is thus impossible to provide a general introduction.

Within this class of products, most of the papers performed a simple characterization [131–142], mainly using DVB/CAR/PDMS coating. Nevertheless, some interesting applications using -omics approach [47,143–147] and studies on novel SPME coatings [47,138,139] have also been published. In this regard, interesting is the paper of De Grazie et al. that evaluated the performance of a matrix-compatible coating or overcoating fiber (i.e., PDMS/DVB/PDMS) compared to the classical PDMS/DVB for extraction of target compounds from a fatty fruit as avocado [148]. This coating was developed in 2012 to overcome the deterioration and/or saturation issue of the commercial phases when exposed to contact with complex matrices, thus leading to loss of reproducibility and sensitivity [149]. The antifouling property of PDMS was exploited to increase the robustness and performance of the PDMS/DVB fiber for DI extraction of triazole in pure grape pulp [150,151]. The main issue was the presence of a high amount of carbohydrates that stick on the fiber surface and degrade during the thermal desorption. To reduce this problem, a KimWipe® cleaning procedure using methanol/water was used. Differently, when dealing with fatty matrices such as avocado, the main fatty compounds stuck on the fiber surface needed a carefully optimized mixture of water/acetone (1:9 v:v) to clean the fiber without significatively unpair the recovery of the target compounds due to back-extraction. Thus a 5 s rinsing procedure before injection and an additional post desorption cleaning in pure acetone for 30 s proved to be an optimal cleaning procedure to guarantee the stability of the fiber performance over 100 extractions (Figure 2-18). The application was associated with the use of GC×GC to investigate better the degree of matrix accumulation and artifact formation that can affect the determination of the target compounds.

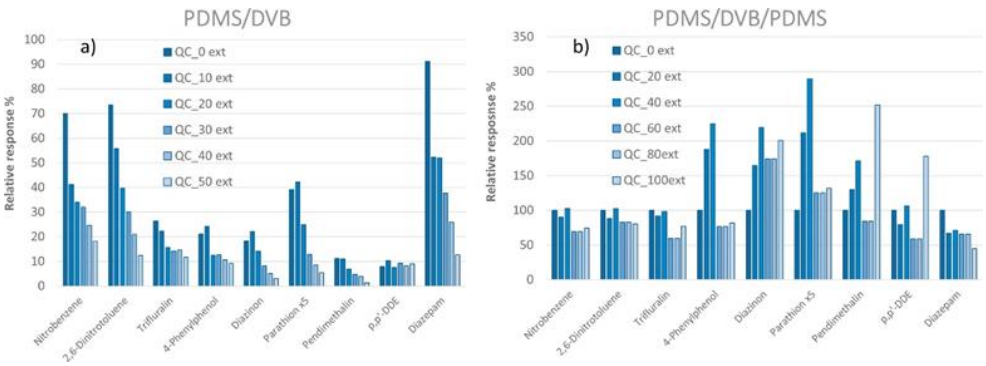

Figure 2-18: Extraction efficiency of a) PDMS/DVB coating and b) PDMS/DVB/PDMS coating towards a series of extractions. The QC extractions were performed in pure water; results are expressed as relative responses in respect to the QC performed before extractions in avocado matrix. Reproduce from Ref [148] with permission from Elsevier.

The same group also evaluated the use of polymeric ionic liquid-based (PIL) coatings in comparison to PA and PDMS for the extraction of organophosphorus pesticides in grapes [152]. In particular two PIL coatings, i.e., poly(1–4-vinylbenzyl-3-hexadecylimidazolium) bis[(trifluoromethyl)sulfonyl] imide (poly([ViBHDIM][NTf2]), PIL 1, and N,N-didecyl-N-methyl- d-glucaminium poly(2-methyl-acrylic acid 2-[1-(3-{2-[2-(3-tri- fluoromethanesulfonylamino-propoxy)-ethoxy]-ethoxy}-propylamino)-vinylamino]-ethyl ester) (Poly([DDMGlu][MTFSI]), PIL 2, were evaluated. PIL 1 showed comparable LOD than PA and better than PIL 2 and PDMS, with a broader linear range and very good repeatability (i.e., in the 0.3-13.6% range). PIL 1 also provided an interesting broad coverage in terms of extracted compounds evaluated with the support of a GC×GC-TOFMS system, showing great potential for future untargeted applications.

A fingerprinting data elaboration for the analysis of the 2D plot as images was reported for apples, quinces, pears, and pineapples [47,143,147]. The first full exploitation of the powerful coupling of SPME with GC×GC-TOFMS was presented by Pawliszyn`s group in 2012 [47]. PDMS, PA, CW, PDM/DVB, CAR/PDMS, DVB/CAR/PDMS, Carbopack Z/PDMS fibers were tested by HS- and DI-SPME for the analysis of apples carefully homogenized and diluted in NaCl saturated water. The extraction was performed for 60 min at 30 °C followed by 10 min immersion in ultra-pure water when DI-SPME was performed. The 2D separation, using a 5% column in the first dimension and a wax column in the second dimension, was exploited to evaluate the coverage of metabolites by evaluating the 2D structure. As expected, the 2D plot obtained using PDMS coating in the HS extraction showed a poor coverage of the most retained compounds in the second dimension (i.e., polar compounds), whereas PA and CW significantly improved the coverage of the more polar volatiles. The adsorption coating, i.e., DVB/CAR/PDMS, PDMS/DVB, CAR/PDMS, showed selectivity coverage across the boiling point scale independently from the polarity. The latter provided a superior extraction of the most volatile ones thanks to the microporous structure. The overall higher number of compounds were extracted by DVB/CAR/PDMS, followed by CAR/PDMS and PDMS/DVB, while the least was PDMS. Nevertheless, the plot obtained using CAR/PDMS coating was characterized by

tailing of the higher volatile compounds due to the slow desorption from the sorbent, thus impairing the precision and accuracy of the overall method. Based on the less discriminant coverage and the largest number of compounds extracted DVB/CAR/PDMS was used for further investigation on the effect of extraction time and mode (i.e., HS or DI). Increased extraction time led to better extraction of hydrophobic metabolites and extremely polar ones; while the use of DI-SPME provided a clear enhanced coverage towards the higher molecular weight and polar metabolites, as shown in Figure 2-19.

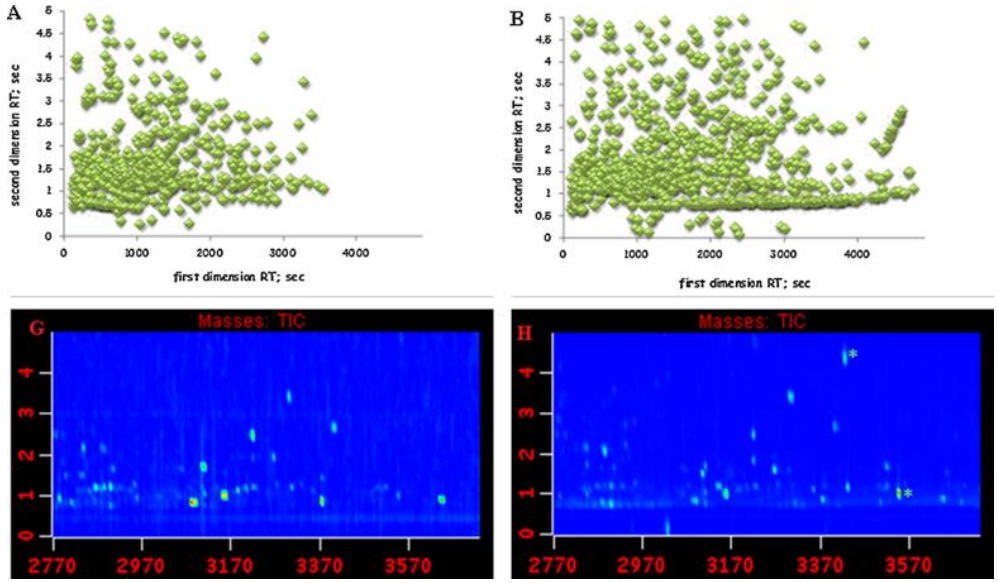

Figure 2-19: Comparison between HS-SPME (plots to the left (A, G)) and DI-SPME (plots to the right (B, H)) extraction modes for metabolite profiling in apples. Peak apex plots (plot A and B) demonstrate retention time coordinates on two-dimensional retention time plane for 555 and 906 captured metabolites found by ChromaTOF software above S/N threshold of 200 for HS- and DI-SPME modes, respectively. G and H, TIC chromatograms corresponding to HS and DI-SPME extracts, respectively. Adapted from Ref [47] with permission from Elsevier.

Finally, the thoughtfully optimized method was used to create a metabolites database of 399 apple metabolites.

Further studies were carried out to maximize the information obtained from chromatographic fingerprints generated by the powerful coupling of SPME and GC×GC. HS-SPME-GC×GC-qMS data were exported, evaluated using an image processing technique and then further elaborated by multivariate statistical analysis

to predict sample origin or ripening status [143,147]. Authentication studies of orange juice [144] and Malaysian soursop [146] samples were also conducted using a similar chemometric approach but a not clearly reported approach for data pretreatment

Johanningsmeier *et al.* investigated the changes in the volatile profile induced by *Lactobacillus buchneri* activity compared to spoilage in fermented cucumbers [145]. The untargeted profiling of the volatile profile combined with the chemical composition evolution allowed the identification of biochemical changes not considered before.

3.6.7. Various

Many other food commodities were investigated in the last ten years using SPME-GC×GC, which are grouped within a general class called "various" due to the limited number for each food kind. As for other sections in the chapter, a large number of works consisted in a detailed characterization of the food sample under study, exploiting the enhanced selectivity and separation capability of the two techniques [153–161]. An application worth a particular mention is the study devoted to improving the aroma of gluten-free bread published in 2015 by Pacyńsky *et al.* [162]. The aroma profile of wheat and wheat-rye bread was characterized and compared with a bread made from a commercial gluten-free bread mix. The latter was deficient in highly aromatic and characteristic compounds, namely pyrazines and 2-acetyl-1-pyrroline. To compensate for the lack of this compounds, different aroma precursors (i.e., cysteine/glucose, cysteine/rhamnose, cysteine/ribose, ornithine/fructose, proline/glucose, proline/ornithine, proline/rhamnose) were added to the formulation and the volatile profile, the sensory evaluation and the consumer acceptance data were compared with the reference gluten-based bread. The gluten-free bread added of proline and glucose provided the results more similar to the wheat and wheat-rye bread with an overall higher consumer acceptance (Figure 2-20).

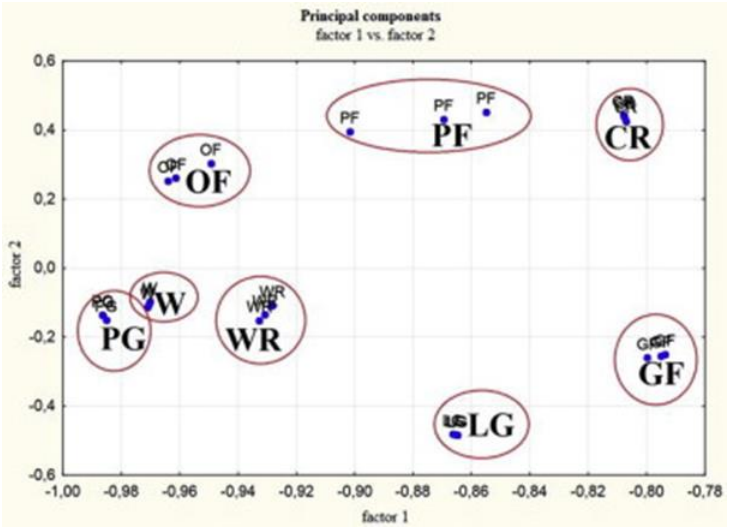

Figure 2-20: PCA plots of quantitative volatile analysis data for bread samples: wheat bread (W), wheat–rye bread (WR), gluten-free bread with no additions (GF), gluten-free breads with proline and glucose (PG), ornithine and fructose (OF), proline and fructose (PF), cysteine and rhamnose (CR), leucine and glucose (LG); factor 1 (PC1 81.25%), factor 2 (PC2 9.90%). Reproduced from Ref [162] with permission from Elsevier.

Cordero *et al.* applied the previously extensively discussed comprehensive template matching fingerprinting method to compare different high concentration capacity sample preparation techniques (i.e., SPME, SBSE, HSSE, and DHS) for the characterization of milk samples and to correlate the volatile profile with the sensory perception performed by GC-olfactometric detector [163].

The study of honey authenticity published by Cajka *et al.*, represented a milestone in the coupling of HS-SPME-GC×GC-TOFMS to answer a relevant question [46]. A total of 374 honey samples were collected over two years (2006 and 2007) from Corsica (n=219) and other European countries (n=155, including France, Italy, Austria, Ireland, and Germany). A targeted profiling approach was applied and a total of 26 targeted analytes were used for extracting further information through the use of unsupervised and supervised pattern recognition chemometrics techniques, i.e., principal component analysis (PCA) and artificial neural network (ANN). The latter proved a high ability to predict samples from Corsica based on the other year collection: i.e., 81.3% when the model was created in the 2006 set of samples and the 2007 samples were used as test set, while 81.9% was obtained the other way around. A better prediction ability (i.e., 94.6%) was obtained using a sub-set of

samples from both years to build the model. The volatile profile of honey was also successfully used to characterize the geographical origin of 347 samples from different European regions (i.e., French, Italy, Austria, Ireland, Germany, and Corsica [164].

Honey samples were also investigated to evaluate the formation of artifacts due to possible hydrolysis and thermolysis during the extraction process, particularly related to time and temperature [165]. To investigate this aspect, different pre-equilibration times and temperatures were applied, ranging between 0 and 4 h and 45 and 60 °C. The formation of several artifacts (such as hydroxymethylfurfural, 5-methyl-furfural, and furfural) was detected thanks to the increased sensitivity provided by the GC×GC.

Fang *et al.* investigated the metabolite profile of five foodborne pathogens (i.e., *Shigella sonnei*, *Escherichia coli*, *Salmonella typhimurium*, *Vibrio parahaemolyticus* and *Staphylococcus aureus*) from which a sub-group of 11 common markers were extrapolated using multivariate statistical analysis [166]. The evolution of this sub-group of markers was then investigated in contaminated food (i.e., shrimp, beef, and pork) as a proof-of-concept of the potentiality of volatile markers in the early detection of foodborne pathogens.

Table 2-2: SPME- GC×GC applications published in 2010-2021 (September).

	Sample Matrix	DI/HS	Coatings (chosen one in bold and italic)	GC×GC Column configuration		Detector	Year	Ref
				1D	2D			
cocoa/chocolate and Nuts	Chocolate	HS	DVB/CAR/PDMS	HP-5 (30 m x 0.25 mm x 0.25 µm)	SolGel-Wax (0.80 m x 0.1 mm x 0.1 µm)	qMS	2014	74
	Chocolate	HS	DVB/CAR/PDMS	HP-5 (30 m x 0.25 mm x 0.25 µm)	SolGel-Wax (0.80 m x 0.1 mm x 0.1 µm)	qMS	2019	75
	Cacao bean	HS	PDMS/DVB	RTX-5MS (20 m x 0.25 mm x 0.5 µm)	RTX-200MS (2 m x 0.18 mm x 0.2 µm)	ToFMS	2010	70
	Cocoa	HS	DVB/CAR/PDMS	HP-5 (30 m x 0.25 mm x 0.25 µm)	Solgel Wax (0.80 m x 0.1 mm x 0.1 µm)	qMS; FID	2016	71

	Cocoa	HS	DVB/CAR/PDMS	SolGel-Wax (30 m x 0.25 mm x 0.25 µm)	OV1701 (1 m x 0.1 mm x 0.1 µm)	qMS	2017	76
	Cocoa	HS	DVB/CAR/PDMS	SolGel-Wax (30 m x 0.25 mm x 0.25 µm)	OV1701 (1 m x 0.1 mm x 0.1 µm)	qMS; FID	2018	77
	Cocoa	HS	DVB/CAR/PDMS	HP-5 (30 m x 0.25 mm x 0.25 µm)	SolGel-Wax (0.80 m x 0.1 mm x 0.1 µm)	qMS	2018	73
	Cocoa	HS	DVB/CAR/PDMS	SolGel-Wax (30 m x 0.25 mm x 0.25 µm)	OV1701 (2 m x 0.1 mm x 0.1 µm)	ToFMS	2019	78
	Cocoa	HS	DVB/CAR/PDMS	SolGel-Wax (30 m x 0.25 mm x 0.25 µm)	OV1701 (2 m x 0.1 mm x 0.1 µm)	ToFMS	2020	72
	Hazelnuts	HS	DVB/CAR/PDMS	CW20 M (30 m x 0.25 mm x 0.25 µm)	OV1701 (1 m x 0.1 mm x 0.1 µm)	qMS	2010	63
	Hazelnuts	HS	DVB/CAR/PDMS	CW20 M (30 m x 0.25 mm x 0.25 µm)	OV1701 (1 m x 0.1 mm x 0.1 µm)	qMS	2012	65
	Hazelnuts	HS	DVB/CAR/PDMS	SolGel-Wax (30 m x 0.25 mm x 0.25 µm)	OV1701 (1 m x 0.1 mm x 0.1 µm)	qMS	2013	64
	Hazelnuts	HS	DVB/CAR/PDMS	DB-5 (30 m x 0.25 mm x 0.25 µm)	OV1701 (2 m x 0.1 mm x 0.1 µm)	ToFMS	2020	67
	Hazelnuts	HS	DVB/CAR/PDMS	SolGel-Wax (30 m x 0.25 mm x 0.25 µm)	OV1701 (1 m x 0.1 mm x 0.1 µm)	ToFMS	2021	68
	Groundnut	HS	DVB/CAR/PDMS	Rxi-5Sil MS (30 m x 0.25 mm x 0.25 µm)	Rxi-17Sil (0.97 m x 0.25 mm x 0.25 µm)	ToFMS	2018	149
Coffee/Tea	Tea	HS	DVB/CAR/PDMS	DB-5MS (30 m x 0.25 mm x 0.25 µm)	DB-17HT (1.9 m x 0.1 mm x 0.1 µm)	ToFMS	2018	82

	Coffee/ Juniper	HS	DVB/CAR/PDMS	SE52 (30 m x 0.25 mm x 0.25 μm)	OV1701 (1 m x 0.1 mm x 0.1 μm)	qMS	2010	55
	Tea	HS	PDMS ; PDMS/DVB; ***PDMS/CAR*** ; DVB/CAR/PDMS ; CAR/PDMS ; PA ; PEG	**HP-5 (30 m x 0.25 mm x 0.5 μm)** DB-WAXETR (30 m x 0.25 mm x 0.25 μm)	**Stabilwax (0.6 m x 0.15 mm x 0.15 μm)** Rxi-5ms (0.6 m x 0.15 mm x 0.15 μm)	FID	2017	81
	Tea	HS	DVB/CAR/PDMS	SE52 (30 m x 0.25 mm x 0.25 μm)	OV1701 (1 m x 0.1 mm x 0.1 μm)	qMS	2017	80
	Tea	HS	PDMS/DVB	Rxi-5Sil MS (30 m x 0.25 mm x 0.25 μm)	Stabilwax (0.8 m x 0.25 mm x 0.25 μm)	ToFMS	2018	84
	Tea	HS	CAR/PDMS	Rxi-5Sil MS (30 m x 0.25 mm x 0.25 μm)	Rxi-17 (1.69 m x 0.15 mm x 0.15 μm)	ToFMS	2020	85
	Tea	HS	CAR/PDMS	HP-Innowax (60 m x 0.25 mm x 0.25 μm)	BPX-1 (2 m x 0.1 mm x 0.1 μm)	qMS	2021	86
	Tea	HS	CAR/PDMS	Rtx-5 (30 m x 0.2 mm x 0.25 μm)	Rtx-200 (1.79 m x 0.15 mm x 0.15 μm)	ToFMS	2020	83
Beer, Spirits, and Cider	Beer	HS	CAR/PDMS	Stabilwax (30 m x 0.25 mm x 0.25 μm)	Rtx-200 (1 m x 0.15 mm x 0.15 μm)	ToFMS	2017	120
	Cider	HS/DI	PDMS ; CAR/PDMS ; DVB/CAR/PDMS	DB-Wax (30 m x 0.25 mm x 0.5 μm)	DB-5MS (2 m x 0.25 mm x 0.25 μm)	ToFMS	2012	123
	fermented bevarages	HS	DVB/CAR/PDMS	VF-Wax (30 m x 0.25 mm x 0.25 μm)	Rxi-17SilMS (1.5 m x 0.15 mm x 0.15 μm)	ToFMS	2020	122
	Plum brandy	HS	PDMS ; DVB/PDMS; PA; CAR/PDMS	**DB-FFAP (30 m x 0.25 mm x 0.25 μm)** HP-5 (30 m	BPX-50 (1.5 m x 0.1 mm x 0.1 μm)	ToFMS	2017	116

			x 0.25 mm x 0.25 μm)				
Liquor (Baijiu)	HS	CAR/PDMS	DB-Wax (30 m x 0.25 mm x 0.25 μm)	DB-5 (2 m x 0.15 mm x 0.15 μm)	SCD	2019	108
Liquor (Baijiu)	HS	DVB/CAR/PDMS	DB-FFAP (60 m x 0.25 mm x 0.25 μm)	Rxi-17Sil MS (1.5 m x 0.25 mm x 0.25 μm)	ToFMS	2020	110
Liquor (Baijiu)	HS	DVB/CAR/PDMS	DB-FFAP (60 m x 0.25 mm x 0.25 μm)	Rxi-17Sil MS (1.5 m x 0.25 mm x 0.25 μm)	ToFMS	2020	109
Liquor (Baijiu)	HS	DVB/CAR/PDMS	DB-FFAP (60 m x 0.25 mm x 0.25 μm)	Rxi-17Sil MS (1.5 m x 0.25 mm x 0.25 μm)	ToFMS	2020	111
Liquor (Baijiu)	HS	DVB/CAR/PDMS	SLB-5 (30 m x 0.25 mm x 0.5 μm) Supelcowax -10 (30 m x 0.25 mm x 0.5 μm)	Supelcowax-10 (0.2 m x 0.18 mm x 0.2 μm) Rtx-5 (0.9 m x 0.18 mm x 0.2 μm)	ToFMS	2021	113
Spirit banana	HS	DVB/CAR/PDMS	HP-FFAP (30 m x 0.25 mm x 0.25 μm)	Rxi-5Sil MS (1 m x 0.18 mm x 0.18 μm)	FID	2015	115
Olive oil	HS	CAR/PDMS ; PDMS/DVB ; **DVB/CAR/PDMS**	DB-5 (25 m x 0.2 mm x 0.33 μm)	Supelcowax-10 (1.2 m x 0.1 mm x 0.1 μm)	ToFMS	2013	55
Beer	HS	DVB/CAR/PDMS	VF-Wax (30 m x 0.25 mm x 0.25 μm)	Rtx-200-MS (1.5 m x 0.25 mm x 0.25 μm)	ToFMS	2021	121
Liquor (Baijiu)	HS	DVB/CAR/PDMS	DB-FFAP (60 m x 0.25 mm x 0.25 μm)	Rxi-17Sil MS (1.5 m x 0.25 mm x 0.25 μm)	ToFMS	2021	112
Liquor	HS	DVB/CAR/PDMS	HP-5MS (25 m x 0.25 mm x 0.25 μm)	Supelcowax-10 (1 m x 0.1 mm x 0.1 μm)	ToFMS	2018	117

	Beverage (huangjiu)	HS	DVB/CAR/PDMS	TG-5MS (30 m x 0.25 mm x 0.25 μm) **HP-Innowax (30 m x 0.25 mm x 0.25 μm)**	Rtx-17 (2 m x 0.1 mm x 0.1 μm) **Rtx-5MS (1.9 m x 0.1 mm x 0.1 μm)**	ToFMS	2019	118
	Beer	HS	DVB/CAR/PDMS ; ***PDMS/DVB***; PDMS; PA	Equity-5 (30 m x 0.32 mm x 0.25 μm)	DB-FFAP (0.79 m x 0.25 mm x 0.25 μm)	ToFMS	2015	119
	Liquor	HS	DVB/CAR/PDMS	DB-5MS (30 m x 0.25 mm x 0.25 μm)	DB-17HT (1.64 m x 0.1 mm x 0.1 μm)	ToFMS	2015	114
Edible oils	Olive oil	HS	DVB/CAR/PDMS	HP-Innowax (30 m x 0.25 mm x 0.25 μm)	BPX-50 (1.25 m x 0.1 mm x 0.1 μm)	ToFMS	2010	57
	Olive oil	HS	DVB/CAR/PDMS	Rxi-5MS (30 m x 0.25 mm x 0.5 m)	Supelcowax-10 (1.2 m x 0.1 mm x 0.1 μm)	qMS	2014	51
	Olive oil	HS	DVB/CAR/PDMS	SolGel-Wax (30 m x 0.25 mm x 0.25 μm)	OV1701 (1 m x 0.1 mm x 0.1 μm)	qMS	2016	53
	Olive oil	HS	DVB/CAR/PDMS	VF-Wax (30 m x 0.25 mm x 0.25 μm)	Rxi-17Sil MS (1.5 m x 0.15 mm x 0.15 μm)	ToFMS	2019	49
	Olive oil	HS	DVB/CAR/PDMS	SolGel-Wax (30 m x 0.25 mm x 0.25 μm)	OV1701 (2 m x 0.1 mm x 0.1 μm)	ToFMS	2019	58
	Olive oil	HS	DVB/CAR/PDMS	SolGel-Wax (30 m x 0.25 mm x 0.25 μm)	OV1701 (1 m x 0.1 mm x 0.1 μm)	ToFMS	2019	54
	Olive oil	HS	DVB/CAR/PDMS	HeavyWax (20 m x 0.18 mm x 0.18 μm)	DB17 (1.8 m x 0.18 mm x 0.18 μm)	qMS/FID	2021	56
	Sesame oils and soybean oils	HS	DVB/PDMS ; PDMS ; CAR/PDMS ;	DB-5MS (30 m x 0.25 mm x	Rxi-17Sil MS(1.4 m x 0.15 mm x	ToFMS	2020	60

			DVB/CAR/PDMS	0.25 µm)	0.15 µm)			
	Rapeseed oil	HS	DVB/CAR/PDMS	DB-5 (30 m x 0.25 mm x 0.1 µm)	Supelcowax-10 (0.75 m x 0.1 mm x 0.1 µm)	ToFMS	2016	61
	Rapeseed oil	HS	DVB/CAR/PDMS	DB-5 (30 m x 0.25 mm x 0.5 µm)	Supelcowax-10 (0.75 m x 0.1 mm x 0.1 µm)	ToFMS	2017	62
	Olive oil	HS	DVB/CAR/PDMS	VF-Wax (30 m x 0.25 mm x 0.25 µm)	Rtx-200MS (1.5 m x 0.25 mm x 0.25 µm)	ToFMS	2019	50
	Berries	HS	DVB/CAR/PDMS	Equity 1 (30 m x 0.25 mm x 0.25 µm)	Solgel Wax (1.6 m x 0.10 mm x 0.10 µm)	ToFMS	2015	131
	Apple/Pear	HS	DVB/CAR/PDMS	SolGel-Wax (30 m x 0.25 mm x 0.25 µm)	BPX-5 (2 m x 0.15 mm x 0.25 µm)	qMS	2010	140
	Avocado	DI	PDMS/DVB/PDMS	Rxi-5MS (30 m x 0.25 mm x 0.25 µm)	Supelcowax BP 20 (10 m x 0.1 mm x 0.1 µm)	ToFMS	2017	142
	Berries	HS	DVB/CAR/PDMS	Equity-1 (30 m x 0.25 mm x 0.25 µm)	SolGel-Wax (2 m x 0.1 mm x 0.1 µm)	ToFMS	2014	130
	Berries	HS	PDMS/DVB ; CAR/PDMS; PDMS; **DVB/CAR/PDMS**	Equity-1 (30 m x 0.25 mm x 0.25 µm)	SolGel-Wax (2 m x 0.1 mm x 0.1 µm)	ToFMS	2017	135
	Cucumber fermented	HS	DVB/CAR/PDMS	SolGel-Wax (30 m x 0.25 mm x 0.25 µm)	Rtx-17 (1 m x 0.1 mm x 0.1 µm)	ToFMS	2015	138
	Fruit (soursop)	HS	PDMS ; **CAR/PDMS** ; DVB/CAR/PDMS ; PA	DB-5 (30 m x 0.25 mm x 0.25 µm)	BPX50 (0.69 m x 0.1 mm x 0.1 µm)	ToFMS	2011	139
vegetables and fruits	Fruits	HS	DVB/CAR/PDMS	Mega CW (25 m x 0.15 mm x 0.15 µm)	OV1701 (1 m x 0.1 mm x 0.1 µm)	qMS	2017	133

	Grapes	HS	2 PIL ; PDMS ; PA	Rtx-5SilMS (30 m x 0.25 mm x 0.25 µm)	BP-20 (1 m x 0.1 mm x 0.1 µm)	qMS	2018	145
	Orange juice	HS	DVB/CAR/PDMS	SolGel-Wax (30 m x 0.25 mm x 0.25 µm)	Rxi-5Sil MS (0.8 m x 0.1 mm x 0.8 µm)	ToFMS	2015	132
	Orange juice	HS	DVB/CAR/PDMS	HP-Innowax (30 m x 0.25 mm x 0.25 µm)	BPX1 (1 m x 0.1 mm x 0.1 µm)	qMS	2020	137
	Pineapple	HS	DVB/CAR/PDMS	**HP-5 (30 m x 0.25 mm x 0.25 µm)** HP-5 (30 m x 0.25 mm x 0.25 µm) **SPWax (25 m x 0.20 mm x 0.2 µm)**	**SPWax (1 m x 0.1 mm x 0.1 µm)** HP-50 (1 m x 0.1 mm x 0.1 µm) **HP-5 (1 m x 0.1 mm x 0.1 µm)**	FID	2011	127
	Pineapple	HS	PDMS/DVB	ZB-Wax (30 m x 0.25 mm x 0.5 µm)	BPX5 (2 m x 0.15 mm x 0.25 µm)	qMS	2015	126
	Strawberry	HS	PDMS/DVB	BPX5 (30 m x 0.25 mm x 0.25 µm)	BP20 (1 m x 0.1 mm x 0.1 µm)	ToFMS	2013	129
	Truffle	HS	DVB/CAR/PDMS	SLB-5ms (30 m x 0.25 mm x 0.25 µm)	Supelcowax-10 (1.1 m x 0.1 mmx 0.1 µm)	qMS/FID	2015	134
	Apples	HS/DI	PDMS ; PA ; CW ; PDMS/DVB ; CAR/PDMS ; ***DVB/CAR/PDMS***; Carbopack Z/PDMS	Rxi-5SilMS (30 m x 0.25 mm x 0.25 µm)	Supelcowax (1.15 m x 0.1 mm x 0.1 µm) **DB-17 (1.15 m x 0.1 mm x 0.1 µm)**	ToFMS	2012	44
	Hazelnuts	HS	DVB/CAR/PDMS	SolGel-Wax (30 m x 0.25 mm x 0.25 µm)	OV1701 (1 m x 0.1 mm x 0.1 µm)	qMS	2018	66
	Watermelon juice	HS	DVB/CAR/PDMS	DB-Wax (30 m x 0.25 mm x 0.25 µm)	DB-17 (2.22 m x 0.18 mm x 0.18 µm)	O/qMS	2021	128

	Grape	HS	DVB/CAR/PDMS	DB-Wax (30 m x 0.25 mm x 0.25 µm)	Mega-17 MS (1.7 m x 0.1 mm x 0.1 µm)	ToFMS	2019	125
	Pears	HS	DVB/CAR/PDMS	Rxi-5MS (30 m x 0.25 mm x 0.25 µm)	Rxi-17Sil MS (2 m x 0.25 mm x 0.25 µm)	ToFMS	2019	124
	Wine	HS	DVB/CAR/PDMS	HP-5 (30 m x 0.32 mm x 0.25 µm)	DB-FFAP (0.79 m x 0.25 mm x 0.25 µm)	ToFMS	2010	87
	Wine	HS	PA	ZB-Wax (30 m x 0.25 mm x 0.5 µm)	BPX-5 (2 m x 0.15 mm x 0.25 µm)	qMS	2010	107
	Wine	HS	CAR/PDMS 75 um	VF-1 (30 m x 0.25 mm x 0.1 µm)	SolGel-Wax (1.5 m x 0.25 mm x 0.25 µm)	ToFMS	2011	90
	Wine	HS	DVB/CAR/PDMS	VF-5MS (30 m x 0.25 mm x 0.25 µm)	VF-17MS (1.65 m x 0.1 mm x 0.2 µm)	ToFMS	2011	89
	Wine	HS	DVB/CAR/PDMS	HP-5 (30 m x 0.32 mm x 0.25 µm)	DB-FFAP (0.79 m x 0.25 mm x 0.25 µm)	ToFMS	2011	100
	Wine	HS	DVB/CAR/PDMS	VF-5MS (30 m x 0.25 mm x 0.25 µm)	VF-17MS (1.44 m x 0.1 mm x 0.2 µm)	ToFMS	2011	106
	Wine	HS	DVB/CAR/PDMS	DB-5 (30 m x 0.25 mm x 0.25 µm) DB-Wax (30 m x 0.25 mm x 0.25 µm) **DB-Wax (30 m x 0.25 mm x 0.25 µm)**	DB-Wax (1 m x 0.1 mm x 0.1 µm) DB1ms (1.7 m x 0.1 mm x 0.1 µm) **DB17ms (1.7 m x 0.1 mm x 0.1 µm)**	ToFMS	2012	91
	Wine	HS	DVB/CAR/PDMS	Innowax (20 m x 0.18 mm x 0.2 µm)	HP-5 (5 m x 0.35 mm x 0.23 µm)	ToFMS	2021	94
Wine	Wine	HS	DVB/CAR/PDMS	DB-5 (30 m x 0.25 mm x	DB-225 (1 m x 0.1 mm	ToFMS	2013	10

			0.25 µm)	x 0.1 µm)			2
Wine	HS	DVB/CAR/PDMS	DB-Wax (30 m x mm x 0.25 µm)	DB-17ms (1.7 m x 0.18 mm x 0.18 µm)	ToFMS	2013	96
Wine	HS	PDMS ; PDMS/DVB ; CAR/PDMS ; ***DVB/CAR/PDMS***	DB-5 MS (30 m x 0.25 mm x 0.25 µm)	Supelcowax-10 (1.2 m x 0.1 mm x 0.1 µm)	ToFMS	2013	88
Wine	HS	DVB/CAR/PDMS ; PDMS; CAR/PDMS	SLB-5 ms (30 m x 0.25 mm x 0.25 µm)	Supelcowax-10 (1.2 m x 0.1 mm x 0.1 µm)	ToFMS/FID	2014	93
Wine	HS	DVB/CAR/PDMS	DB-5 (30 m x 0.25 mm x 0.25 µm)	DB-Wax (1.2 m x 0.1 mm x 0.1 µm)	ToFMS	2014	101
Wine	HS	DVB/CAR/PDMS	Carbowax (30 m x 0.25 mm x 0.25 µm)	DB-17 ms (1.7 m x 0.18 mm x 0.18 µm)	ToFMS	2014	97
Wine	HS	DVB/CAR/PDMS	Carbowax (30 m x 0.25 mm x 0.25 µm)	DB-17 ms (1.7 m x 0.18 mm x 0.18 µm)	ToFMS	2014	92
Wine	HS	Not Specified	VF-Wax MS (30 m x 0.25 mm x 0.25 µm)	Rxi-17Sil MS (1.5 m x 0.15 mm x 0.15 µm)	ToFMS	2016	104
Wine	HS	DVB/CAR/PDMS	VF-Wax MS (30 m x 0.25 mm x 0.25 µm)	Rxi-17Sil MS (1.5 m x 0.15 mm x 0.15 µm)	ToFMS	2019	95
Wine	HS	DVB/CAR/PDMS	Innowax (20 m x 0.18 mm x 0.2 µm)	HP-5 (5 m x 0.35 mm x 0.23 µm)	ToFMS	2021	94
Wine	HS	DVB/CAR/PDMS	DB-Wax (30 m x 0.25 mm x 0.25 µm)	DB-17ms (1.7 m x 0.18 mm x 0.18 µm)	ToFMS	2018	99
Wine sparkling	HS	PDMS; PDMS ; PA ; CAR/PDMS ; **PDMS/DVB** ; DVB/CAR/PDMS	DB-5 (60 m x 0.25 mm x 0.25 µm)	DB-17ms (1.7 m x 0.18 mm x 0.18 µm)	ToFMS	2015	105
Sparkling wine	HS	DVB/CAR/PDMS	VF-Wax (30 m x 0.25	Rtx-200MS (1.5 m x	ToFMS	2016	98

				mm x 0.25 µm)	0.25 mm x 0.25 µm)			
	Wine	HS	DVB/CAR/PDMS	DB-Wax (30 m x 0.25 mm x 0.25 µm)	DB-17ms (1.7 m x 0.18 mm x 0.18 µm)	ToFMS	2020	103
	Bread gluten-free	HS	CAR/PDMS	ZB-5 (30 m x 0.25 mm x 0.25 µm)	SupelcoWax (0.8 m x 0.1 mm x 0.1 µm)	ToFMS	2015	155
	Honey	HS	PDMS ; PDMS/DVB ; DVB/CAR/PDMS	HP-5 (30 m x 0.25 mm x 0.25 µm)	Supelcowax-10 (1 m x 0.1 mm x 0.1 µm)	FID	2013	157
	Rice	HS	PDMS	**HP-5 (30 m x 0.25 mm x 0.25 µm)** Solgel Wax (30 m x 0.25 mm x 0.25 µm) EtTBS-βCD (30 m x 0.25 mm x 0.25 µm)	**BP-20 (1 m x 0.1 mm x 0.1 µm)** BP-1 (1 m x 0.1 mm x 0.1 µm) BP-20 (1 m x 0.1 mm x0.1 µm)	ToFMS	2015	151
	Spice	HS	PDMS ; CAR/PDMS ; ***DVB/CAR/PDMS***	Innowax (15 m x 0.25 mm x 0.25 µm)	DB-1 (1.1 m x 0.1 mm x 0.1 µm)	FID	2013	152
	Dry milk	HS	***DVB/CAR/PDMS***; PDMS ; PA ; PEG	SolGel-Wax (30 m x 0.25 mm x 0.25 µm)	OV1701 (1 m x 0.1 mm x 0.1 µm)	qMS	2013	156
	Milk	HS	DVB/CAR/PDMS	DB-5MS (30 m x 0.25 mm x 0.25 µm)	DB-17HT (2 m x 0.1 mm x 0.15 µm)	ToFMS	2015	150
	Carp	HS	PDMS/DVB	DB-5 MS (30 m x 0.25 mm x 0.25 µm)	DB-17HT (1.64 m x 0.1 mm x 0.1 µm)	ToFMS	2020	153
	Honey	HS	DVB/CAR/PDMS	DB-5MS (30 m x 0.25 mm x 0.25 µm)	SupelcoWax -10 (1.25 m x 0.1 mm x 0.1 µm)	ToFMS	2010	158
Various	foods	HS	***DVB/CAR/PDMS*** ; PDMS/DVB ; PDMS	HP-5MS (30 m x 0.25 mm x	DB-17MS (1.1 m x 0.18 x 0.18	ToFMS	2021	159

				0.25 µm)	µm)			
	Soup	HS	DVB/CAR/PDMS	Rxi-5Sil MS (30 m x 0.25 mm x 0.25 µm)	Rxi-17Sil MS (0.95 m x 0.25 mm x 0.25 µm)	ToFMS	2018	148
	Vinegar	HS	CAR/PDMS	TG-5MS (30 m x 0.25 mm x 0.25 µm) **HP-Innowax (30 m x 0.25 mm x 0.25 µm)**	Rtx-17 (2 m x 0.1 mm x 0.1 µm) **Rtx-5MS (1.9 m x 0.1 mm x 0.1 µm)**	ToFMS	2017	147
	Cereals (sorghum)	HS	***DVB/CAR/PDMS*** ; PDMS/DVB ; PDMS ; CAR/PDMS	DB-FAP (60 m x 0.25 mm x 0.25 µm)	Rxi-17Sil MS (1.5 m x 0.25 mm x 0.25 µm)	ToFMS	2021	146
	Zaoyu (fermented fish)	HS	DVB/CAR/PDMS	Rxi-5MS (30 m x 0.25 mm x 0.25 µm)	Rtx-200 (1.79 m x 0.18 mm x 0.2 µm)	ToFMS	2021	154

3.7. References

[1] J. B. Phillips, D. Luu, J. B. Pawliszyn and G. C. Carle, Anal. Chem., 1985, 57, 2779–2787.

[2] Z. Lui and J. B. Phillips, J. Chromatogr. Sci., 1991, 29, 227–231.

[3] J. Pawliszyn and S. Liu, Anal. Bioanal. Chem., 1987, 1475–1478.

[4] C. L. Arthur and J. Pawliszyn, Anal. Chem., 1990, 62, 2145–2148.

[5] N. Stafford, Nature, 2010, 468, S16–S17.

[6] R. J. Mcgorrin, J. Agric. Food Chem., 2009, 57, 8076–8088.

[7] M. Gallo and P. Ferranti, J. Chromatogr. A, 2016, 1428, 3–15.

[8] M. Adahchour, J. Beens, R. J. J. Vreuls, A. M. Batenburg, E. A. E. Rosing and U. A. T. Brinkman, Chromatographia, 2002, 55, 361–367.

[9] P. Q. Tranchida, M. Maimone, G. Purcaro, P. Dugo and L. Mondello, TrAC - Trends Anal. Chem., 2015, 71, 74–84.

[10] O. R. Fennema, Food Chemistry, Marcel Dekker, Inc., New York, 3rd edn., 1996.

[11] C. A. Browne, A Source Book of Agricultural Chemistry, Waltham, MA, 1944.

[12] J. Ginsberg, American Chemical Society, 03/24/2004, The development of the Beckman pH meter.

[13] D. Brock, Chem. Herit., 2002, 20, 39.

[14] M. Tswett, Ber. Dtsch. Bot. Ges., 1906, 24, 316–323.
[15] L. S. Ettre, LC-GC North Am., 2003, 21, 458–467.
[16] A. J. P. Martin and R. L. M. Synge, Biochem. J., 1941, 35, 1358–1366.
[17] A. T. James and A. J. P. Martin, Biochem. J., 1952, 50, 679–690.
[18] O. Fiehn, Plant Mol. Biol., 2002, 48, 155–171.
[19] F. Stilo, C. Bicchi, S. E. Reichenbach and C. Cordero, J. Sep. Sci., 2021, 44, 1592–1611.
[20] A. Cifuentes, J. Chromatogr. A, 2009, 1216, 7109.
[21] M. Bevilacqua, R. Bro, F. Marini, Å. Rinnan, M. A. Rasmussen and T. Skov, TrAC - Trends Anal. Chem., 2017, 96, 42–51.
[22] F. Stilo, C. Bicchi, A. M. Jimenez-Carvelo, L. Cuadros-Rodriguez, S. E. Reichenbach and C. Cordero, TrAC - Trends Anal. Chem., 2021, 134, 116133.
[23] L. Cuadros-Rodríguez, C. Ruiz-Samblás, L. Valverde-Som, E. Pérez-Castaño and A. González-Casado, Anal. Chim. Acta, 2016, 909, 9–23.
[24] E. C. Horning and M. G. Horning, J. Chromatogr. Sci., 1971, 9, 129–140.
[25] O. Fiehn, Comp. Funct. Genomics, 2001, 2, 155–168.
[26] L. Bovijn, J. Pirotte and A. Berger, Gas Chromatography, London, 1958.
[27] K. D. Bartle and P. Myers, Trends Anal. Chem., 2002, 21, 547–557.
[28] M. J. E. Golay, Gas Chromatography, Butterworths, London, UK, 1958.
[29] R. S. Gohlke, Anal. Chem., 1959, 31, 535–541.
[30] R. Consden, A. H. Gordon and A. J. P. Martin, Biochem. J., 1944, 38, 224–232.
[31] P. Q. Tranchida, G. Purcaro, P. Dugo, L. Mondello and G. Purcaro, TrAC - Trends Anal. Chem., 2011, 30, 1437–1461.
[32] H. D. Bahaghighat, C. E. Freye and R. E. Synovec, TrAC - Trends Anal. Chem., 2019, 113, 379–391.
[33] Z. Zhang and J. Pawliszyn, Anal. Chem., 1993, 65, 1843–1852.
[34] N. Reyes-Garcés, E. Gionfriddo, G. A. Gómez-Ríos, M. N. Alam, E. Boyacl, B. Bojko, V. Singh, J. Grandy and J. Pawliszyn, Anal. Chem., 2018, 90, 302–360.
[35] É. A. Souza-Silva, E. Gionfriddo and J. Pawliszyn, Trends Anal. Chem., 2015, 71, 236-248.
[36] N. Reyes-Garcés and E. Gionfriddo, TrAC - Trends Anal. Chem., 2019, 113, 172–181.
[37] V. Jalili, A. Barkhordari and A. Ghiasvand, Microchem. J., 2020, 152, 104319.
[38] C. H. Xu, G. S. Chen, Z. H. Xiong, Y. X. Fan, X. C. Wang and Y. Liu, TrAC - Trends Anal. Chem., 2016, 80, 12–29.
[39] E. Gionfriddo, É. A. Souza-Silva and J. Pawliszyn, Anal. Chem., 2015, 87, 8448–8456.
[40] M. N. Wieczorek, W. Zhou and J. Pawliszyn, Food Chem., 2022, 389, 133038.

[41] E. Klimánková, K. Holadová, J. Hajšlová, T. Čajka, J. Poustka and M. Koudela, Food Chem., 2008, 107, 464–472.

[42] C. Cordero, C. Bicchi and P. Rubiolo, J. Agric. Food Chem., 2008, 56, 7655–7666.

[43] Z. L. Cardeal, P. P. de Souza, M. D. R. G. da Silva and P. J. Marriott, Talanta, 2008, 74, 793–799.

[44] W. Welthagen, J. Schnelle-Kreis and R. Zimmermann, J. Chromatogr. A, 2003, 1019, 233–249.

[45] B. V. Hollingsworth, S. E. Reichenbach, Q. Tao and A. Visvanathan, J. Chromatogr. A, 2006, 1105, 51–58.

[46] T. Cajka, J. Hajslova, F. Pudil and K. Riddellova, J. Chromatogr. A, 2009, 1216, 1458–1462.

[47] S. Risticevic, J. R. DeEll and J. Pawliszyn, J. Chromatogr. A, 2012, 1251, 208–218.

[48] L. Conte, A. Bendini, E. Valli, P. Lucci, S. Moret, A. Maquet, F. Lacoste, P. Brereton, D. L. García-González, W. Moreda and T. Gallina Toschi, Trends Food Sci. Technol., 2020, 105, 483–493.

[49] C. M. Kalua, M. S. Allen, D. R. Bedgood, A. G. Bishop, P. D. Prenzler and K. Robards, Food Chem., 2007, 100, 273–286.

[50] F. Angerosa, M. Servili, R. Selvaggini, A. Taticchi, S. Esposto and G. Montedoro, J. Chromatogr. A, 2004, 1054, 17–31.

[51] L. T. Vaz-Freire, M. D. R. G. da Silva and A. M. C. Freitas, Anal. Chim. Acta, 2009, 633, 263–270.

[52] I. Lukić, S. Carlin, I. Horvat and U. Vrhovsek, Food Chem., 2019, 270, 403–414.

[53] A. Da Ros, D. Masuero, S. Riccadonna, K. B. Bubola, N. Mulinacci, F. Mattivi, I. Lukić and U. Vrhovsek, Molecules, 2019, 24, 1–17.

[54] G. Purcaro, C. Cordero, E. Liberto, C. Bicchi and L. S. Conte, J. Chromatogr. A, 2014,1334, 101-111.

[55] C. Cordero, E. Liberto, C. Bicchi, P. Rubiolo, S. E. Reichenbach, X. Tian and Q. Tao, J. Chromatogr. Sci., 2010, 48, 251–261.

[56] F. Magagna, L. Valverde-Som, C. Ruíz-Samblás, L. Cuadros-Rodríguez, S. E. Reichenbach, C. Bicchi and C. Cordero, Anal. Chim. Acta, 2016, 936, 245–258.

[57] F. Stilo, E. Liberto, S. E. Reichenbach, Q. Tao, C. Bicchi and C. Cordero, J. Agric. Food Chem., 2019, 67, 5289–5302.

[58] F. Peres, H. H. Jeleń, M. M. Majcher, M. Arraias, L. L. Martins and S. Ferreira-Dias, Food Res. Int., 2013, 54, 1979–1986.

[59] F. Stilo, M. del P. Segura Borrego, C. Bicchi, S. Battaglino, R. M. Callejon Fernadez, M. L. Morales, S. E. Reichenbach, J. Mccurry, D. Peroni and C. Cordero, J. Chromatogr. A, 2021, 1650, 462232.

[60] T. Cajka, K. Riddellova, E. Klimankova, M. Cerna, F. Pudil and J. Hajslova, Food Chem., 2010, 121, 282–289.

[61] F. Stilo, C. Cordero, B. Sgorbini, C. Bicchi and E. Liberto, Separations, 2019, 6, 34.

[62] S. E. Reichenbach, P. W. Carr, D. R. Stoll and Q. Tao, J. Chromatogr. A, 2009, 1216, 3458–3466.

[63] Y. Sun, X. Dou, X. Yue, L. Yu, L. Zhang, J. Li and P. Li, Food Anal. Methods, 2020, 13, 1328–1336.

[64] A. Gracka, H. H. Jeleń, M. Majcher, A. Siger and A. Kaczmarek, J. Chromatogr. A, 2016, 1428, 292–304.

[65] A. Gracka, M. Raczyk, J. Hradecký, J. Hajslova, S. Jeziorski, G. Karlovits, B. Michalak, N. Bąkowska and H. Jeleń, Eur. J. Lipid Sci. Technol., 2017, 119, 1–9.

[66] S. Mascrez, E. Psillakis and G. Purcaro, Anal. Chim. Acta, 2020, 1103, 106-114.

[67] S. Mascrez and G. Purcaro, J. Sep. Sci., 2020, 43, 1934-1941.

[68] S. Mascrez and G. Purcaro, Anal. Chim. Acta, 2020, 1122, 89–96.

[69] N. D. Spadafora, S. Mascrez, L. McGregor and G. Purcaro, Food Chem., 2022, 383, 132438.

[70] C. Cordero, E. Liberto, C. Bicchi, P. Rubiolo, P. Schieberle, S. E. Reichenbach and Q. Tao, J. Chromatogr. A, 2010, 1217, 5848–5858.

[71] L. Nicolotti, C. Cordero, C. Cagliero, E. Liberto, B. Sgorbini, P. Rubiolo and C. Bicchi, Anal. Chim. Acta, 2013, 798, 115–125.

[72] J. Kiefl, C. Cordero, L. Nicolotti, P. Schieberle, S. E. Reichenbach and C. Bicchi, J. Chromatogr. A, 2012, 1243, 81–90.

[73] M. Cialiè Rosso, E. Liberto, N. Spigolon, M. Fontana, M. Somenzi, C. Bicchi and C. Cordero, Anal. Bioanal. Chem., 2018, 410, 3491–3506.

[74] M. Cialiè Rosso, M. Mazzucotelli, C. Bicchi, M. Charron, F. Manini, R. Menta, M. Fontana, S. E. Reichenbach and C. Cordero, J. Chromatogr. A, , DOI:10.1016/j.chroma.2019.460739.

[75] F. Stilo, E. Liberto, N. Spigolon, G. Genova, G. Rosso, M. Fontana, S. E. Reichenbach, C. Bicchi and C. Cordero, Food Chem., 2021, 340, 128135.

[76] M. Cialiè Rosso, F. Stilo, C. Bicchi, M. Charron, G. Rosso, R. Menta, S. E. Reichenbach, C. H. Weinert, C. I. Mack, S. E. Kulling and C. Cordero, Appl. Sci., 2021, 11, 1–18.

[77] E. M. Humston, J. D. Knowles, A. McShea and R. E. Synovec, J. Chromatogr. A, 2010, 1217, 1963–1970.

[78] L. F. Oliveira, S. C. G. N. Braga, F. Augusto, J. C. Hashimoto, P. Efraim and R. J. Poppi, Food Res. Int., 2016, 90, 133–138.

[79] P. Perotti, C. Cordero, C. Bortolini, P. Rubiolo, C. Bicchi and E. Liberto, Food Chem., 2020, 309, 125561.

[80] S. C. G. N. Braga, L. F. Oliveira, J. C. Hashimoto, M. R. Gama, P. Efraim, R. J. Poppi and F. Augusto, Microchem. J., 2018, 141, 353–361.

[81] L. F. Oliveira, S. C. G. N. Braga, P. R. Filgueiras, F. Augusto and R. J. Poppi, Talanta, 2014, 129, 303–308.

[82] S. C. G. N. Braga, L. F. Oliveira, A. R. D. A. Silva, P. Efraim, R. D. J. Poppi and F. Augusto, Brazilian J. Anal. Chem., 2019, 6, 16–26.

[83] F. Magagna, A. Guglielmetti, E. Liberto, S. E. Reichenbach, E. Allegrucci, G. Gobino, C. Bicchi and C. Cordero, J. Agric. Food Chem., 2017, 65, 6329–6341.

[84] F. Magagna, E. Liberto, S. E. Reichenbach, Q. Tao, A. Carretta, L. Cobelli, M. Giardina, C. Bicchi and C. Cordero, J. Chromatogr. A, 2018, 1536, 122–136.

[85] C. Cordero, A. Guglielmetti, C. Bicchi, E. Liberto, L. Baroux, P. Merle, Q. Tao and S. E. Reichenbach, J. Chromatogr. A, 2019, 1597, 132–141.

[86] C. Cordero, P. Rubiolo, S. E. Reichenbach, A. Carretta, L. Cobelli, M. Giardina and C. Bicchi, J. Chromatogr. A, 2017, 1480, 70–82.

[87] F. Magagna, C. Cordero, C. Cagliero, E. Liberto, P. Rubiolo, B. Sgorbini and C. Bicchi, Food Chem., 2017, 225, 276–287.

[88] G. Ntlhokwe, A. G. J. Tredoux, T. Górecki, M. Edwards, J. Vestner, M. Muller, L. Erasmus, E. Joubert, J. Christel Cronje and A. de Villiers, Anal. Bioanal. Chem., 2017, 409, 4127–4138.

[89] Y. Zhu, H. P. Lv, C. Y. Shao, S. Kang, Y. Zhang, L. Guo, W. D. Dai, J. F. Tan, Q. H. Peng and Z. Lin, Food Res. Int., 2018, 108, 74–82.

[90] C. Qi, G. Tianyang, W. Qiong, Y. Jian, L. Renyi, W. Peng, J. Shaotong and D. Yiyang, J. AOAC Int., 2021, 103, 433–438.

[91] G. Ntlhokwe, M. Muller, E. Joubert, A. G. J. Tredoux and A. de Villiers, J. Chromatogr. A, 2018, 1536, 137–150.

[92] Y. Yang, J. Hua, Y. Deng, Y. Jiang, M. C. Qian, J. Wang, J. Li, M. Zhang, C. Dong and H. Yuan, Food Res. Int., 2020, 137, 109656.

[93] J. C. Zhu, Y. Niu and Z. B. Xiao, Food Chem., 2021, 339, 128136.

[94] R. Perestrelo, S. Petronilho, J. S. Câmara and S. M. Rocha, J. Chromatogr. A, 2010, 1217, 3441–3445.

[95] H. H. Jeleń, M. Dziadas and M. Majcher, J. Chromatogr. A, 2013, 1313, 185–193.

[96] A. L. Robinson, P. K. Boss, H. Heymann, P. S. Solomon and R. D. Trengove, J. Chromatogr. A, 2011, 1218, 504–517.

[97] B. T. Weldegergis, A. De Villiers, C. McNeish, S. Seethapathy, A. Mostafa, T. Górecki and A. M. Crouch, Food Chem., 2011, 129, 188–199.

[98] J. E. Welke, V. Manfroi, M. Zanus, M. Lazarotto and C. Alcaraz Zini, J. Chromatogr. A, 2012, 1226, 124–139.

[99] J. E. Welke, M. Zanus, M. Lazzarotto and C. Alcaraz Zini, Food Res. Int., 2014, 59, 85–99.

[100] G. Dugo, F. A. Franchina, M. R. Scandinaro, I. Bonaccorsi, N. Cicero, P. Q. Tranchida and L. Mondello, Food Chem., 2014, 142, 262–268.

[101] F. Ieri, M. Campo, C. Cassiani, S. Urciuoli, K. Jurkhadze and A. Romani, Food Sci. Nutr., 2021, 9, 6492–6500.

[102] K. Šuklje, S. Carlin, J. Stanstrup, G. Antalick, J. W. Blackman, C. Meeks, A. Deloire, L. M. Schmidtke and U. Vrhovsek, Food Chem., 2019, 277, 753–765.

[103] J. E. Welke, V. Manfroi, M. Zanus, M. Lazzarotto and C. A. Zini, Food Chem., 2013, 141, 3897–3905.

[104] J. E. Welke, M. Zanus, M. Lazzarotto, F. H. Pulgati and C. A. Zini, Food Chem., 2014, 164, 427–437.

[105] S. Carlin, U. Vrhovsek, P. Franceschi, C. Lotti, L. Bontempo, F. Camin, D. Toubiana, F. Zottele, G. Toller, A. Fait and F. Mattivi, Food Chem., 2016, 208, 68–80.

[106] K. P. Nicolli, A. C. T. Biasoto, É. A. Souza-Silva, C. C. Guerra, H. P. dos Santos, J. E. Welke and C. A. Zini, Food Chem., 2018, 243, 103–117.

[107] R. Perestrelo, A. S. Barros, J. S. Câmara and S. M. Rocha, J. Agric. Food Chem., 2011, 59, 3186–3204.

[108] M. Bordiga, G. Piana, J. D. Coïsson, F. Travaglia and M. Arlorio, Int. J. Food Sci. Technol., 2014, 49, 787–796.

[109] M. Bordiga, M. Rinaldi, M. Locatelli, G. Piana, F. Travaglia, J. D. Coïsson and M. Arlorio, Food Chem., 2013, 140, 57–67.

[110] J. Aith Barbará, K. Primieri Nicolli, É. A. Souza-Silva, A. Camarão Telles Biasoto, J. E. Welke and C. Alcaraz Zini, Food Chem., 2020, 308, 125552.

[111] M. E. Beckner Whitener, J. Stanstrup, V. Panzeri, S. Carlin, B. Divol, M. Du Toit and U. Vrhovsek, Metabolomics, 2016, 12, 1–25.

[112] R. D. Soares, J. E. Welke, K. P. Nicolli, M. Zanus, E. B. Caramão, V. Manfroi and C. A. Zini, Food Chem., 2015, 183, 291–304.

[113] A. L. Robinson, P. K. Boss, H. Heymann, P. S. Solomon and R. D. Trengove, J. Agric. Food Chem., 2011, 59, 3273–3284.

[114] H. G. Schmarr, J. Bernhardt, U. Fischer, A. Stephan, P. Müller and D. Durner, Anal. Chim. Acta, 2010, 672, 114–123.

[115] X. Song, L. Zhu, X. Wang, F. Zheng, M. Zhao, Y. Liu, H. Li, F. Zhang, Y. Zhang and F. Chen, Food Chem., 2019, 297, 124959.

[116] Y. Yan, S. Chen, Y. Nie and Y. Xu, Food Res. Int., 2020, 131, 109043.

[117] Z. Zhou, Z. Ji, S. Liu, X. Han, F. Zheng and J. Mao, J. Food Process. Preserv., 2019, 43, 1–10.

[118] C. Martins, T. Brandao, A. Almeida and S. M. Rocha, J. Sep. Sc, 2015, 38, 2140–2148.

[119] P. H. Stefanuto, K. A. Perrault, L. M. Dubois, B. L'Homme, C. Allen, C. Loughnane, N. Ochiai and J. F. Focant, J. Chromatogr. A, 2017, 1507, 45–52.

[120] K. Giannakou, F. Visinoni, P. Zhang, N. Nathoo, P. Jones, M. Cotterrell, U. Vrhovsek and D. Delneri, Food Microbiol., 2021, 100, 103838.

[121] P. Zhang, S. Carlin, C. Lotti, F. Mattivi and U. Vrhovsek, Metabolomics, 2020, 16, 1–10.

[122] A. Villière, G. Arvisenet, L. Lethuaut, C. Prost and T. Sérot, Food Chem., 2012, 131, 1561–1568.

[123] L. Wang, S. Fan, Y. Yan, L. Yang, S. Chen and Y. Xu, J. Agric. Food Chem., 2020, 68, 1666–1677.

[124] Y. He, Z. Liu, M. Qian, X. Yu, Y. Xu and S. Chen, Food Chem., 2020, 331, 127335.

[125] X. Mu, J. Lu, M. Gao, C. Li and S. Chen, Molecules, 2021, 26, 6910.

[126] X. He and H. H. Jeleń, J. Chromatogr. A, , DOI:10.1016/j.chroma.2020.461774.

[127] F. Yao, B. Yi, C. Shen, F. Tao, Y. Liu, Z. Lin and P. Xu, Sci. Rep., 2015, 5, 1–6.

[128] M. Capobiango, R. B. Mastello, S. T. Chin, E. de S. Oliveira, Z. de L. Cardeal and P. J. Marriott, J. Chromatogr. A, 2015, 1388, 227–235.

[129] O. Vyviurska, F. Matura, K. Furdíková and I. Špánik, J. Food Sci. Technol., 2017, 54, 4284–4301.

[130] N. G. S. Mogollón, G. L. Alexandrino, J. R. de Almeida, Z. Niño-Ruiz, J. G. Peña-Delgado, R. Torres-Gutiérrez and F. Augusto, Chem. Cent. J., 2018, 12, 1–10.

[131] C. Wang, W. Zhang, H. Li, J. Mao, C. Guo, R. Ding, Y. Wang, L. Fang, Z. Chen and G. Yang, Molecules, 2019, 24, 1–10.

[132] P. P. Könen and M. Wüst, Beilstein J. Org. Chem., 2019, 15, 1945–1961.

[133] C. B. Steingass, R. Carle and H. G. Schmarr, Anal. Bioanal. Chem., 2015, 407, 2591–2608.

[134] M. P. Pedroso, E. C. Ferreira, L. W. Hantao, S. Bogusz and F. Augusto, J. Sep. Sci., 2011, 34, 1547–1554.

[135] F. Yang, Y. Liu, B. Wang, H. Song and T. Zou, Lwt, 2021, 137, 110478.

[136] K. Samykanno, E. Pang and P. J. Marriott, Food Chem., 2013, 141, 1997–2005.

[137] M. Kupska, T. Chmiel, R. Jędrkiewicz, W. Wardencki and J. Namieśnik, Food Chem., 2014, 152, 88–93.

[138] T. Dymerski, J. Namieśnik, K. Vearasilp, P. Arancibia-Avila, F. Toledo, M. Weisz, E. Katrich and S. Gorinstein, Talanta, 2015, 134, 460–467.

[139] R. B. Mastello, M. Capobiango, S. T. Chin, M. Monteiro and P. J. Marriott, Food Res. Int., 2015, 75, 281–288.

[140] T. M. Uekane, L. Nicolotti, A. Griglione, H. R. Bizzo, P. Rubiolo, C. Bicchi, M. H. M. Rocha-Leão and C. M. Rezende, Food Chem., 2017, 219, 13–22.

[141] R. Costa, C. Fanali, G. Pennazza, L. Tedone, L. Dugo, M. Santonico, D. Sciarrone, F. Cacciola, L. Cucchiarini, M. Dachà and L. Mondello, Lwt, 2015, 60, 905–913.

[142] T. Chmiel, M. Kupska, W. Wardencki and J. Namieśnik, Food Chem., 2017, 221, 1041–1056.

[143] C. B. Steingass, M. Jutzi, J. Müller, R. Carle and H. G. Schmarr, Anal. Bioanal. Chem., 2015, 407, 2609–2624.

[144] S. Li, Y. Hu, W. Liu, Y. Chen, F. Wang, X. Lu and W. Zheng, Talanta, 2020, 217, 121038.

[145] S. D. Johanningsmeier and R. F. McFeeters, Int. J. Food Microbiol., 2015, 215, 40–48.

[146] K. W. Cheong, C. P. Tan, H. Mirhosseini, S. T. Chin, Y. B. Che Man, N. S. A. Hamid, A. Osman and M. Basri, Food Chem., 2011, 125, 1481–1489.

[147] H. G. Schmarr and J. Bernhardt, J. Chromatogr. A, 2010, 1217, 565–574.

[148] S. De Grazia, E. Gionfriddo and J. Pawliszyn, Talanta, 2017, 167, 754–760.

[149] É. A. Souza Silva and J. Pawliszyn, Anal. Chem., 2012, 84, 6933–6938.

[150] É. A. Souza-Silva, V. Lopez-Avila and J. Pawliszyn, J. Chromatogr. A, 2013, 1313, 139–146.

[151] É. A. Souza-Silva, E. Gionfriddo, R. Shirey, L. Sidisky and J. Pawliszyn, Anal. Chim. Acta, 2016, 920, 54–62.

[152] E. Gionfriddo, É. A. Souza-Silva, T. D. Ho, J. L. Anderson and J. Pawliszyn, Talanta, 2018, 188, 522–530.

[153] S. Chen, L. Wang, D. Ni, L. Lin, H. Wang and Y. Xu, Molecules, , DOI:10.3390/molecules26164796.

[154] Z. Zhou, S. Liu, X. Kong, Z. Ji, X. Han, J. Wu and J. Mao, J. Chromatogr. A, 2017, 1487, 218–226.

[155] O. A. Adebo, P. B. Njobeh, S. C. Z. Desobgo, M. Pieterse, E. Kayitesi and D. T. Ndinteh, Food Sci. Nutr., 2018, 6, 2028–2035.

[156] G. B. Akanni, H. L. De Kock, Y. Naudé and E. M. Buys, Int. J. Food Prop., 2018, 21, 929–941.

[157] J. Yue, Y. Zheng, Z. Liu, Y. Deng, Y. Jing, Y. Luo, W. Yu and Y. Zhao, Int. J. Food Prop., 2015, 18, 2193–2212.

[158] W. Chumpolsri, N. Wijit, P. Boontakham, P. Nimmanpipug, P. Sookwong, S. Luangkamin and S. Wongpornchai, J. Food Nutr. Res., 2015, 3, 114–120.

[159] B. Maikhunthod and P. J. Marriott, Food Chem., 2013, 141, 4324–4332.

[160] H. Wang, Y. Zhu, J. Zhang, X. Wang and W. Shi, Int. J. Food Prop., 2020, 23, 777–796.

[161] Z. Chen, H. Tang, C. Ou, C. Xie, J. Cao and X. Zhang, J. Food Process. Preserv., 2021, 45, 1–27.

[162] M. Pacyński, R. Z. Wojtasiak and S. Mildner-Szkudlarz, Lwt, 2015, 63, 706–713.

[163] C. Cordero, C. Cagliero, E. Liberto, L. Nicolotti, P. Rubiolo, B. Sgorbini and C. Bicchi, J. Chromatogr. A, 2013, 1318, 1–11.

[164] I. Stanimirova, B. Üstün, T. Cajka, K. Riddelova, J. Hajslova, L. M. C. Buydens and B. Walczak, Food Chem., 2010, 118, 171–176.

[165] S. R. Rivellino, L. W. Hantao, S. Risticevic, E. Carasek, J. Pawliszyn and F. Augusto, Food Chem., 2013, 141, 1828–1833.

[166] S. Fang, S. Liu, J. Song, Q. Huang and Z. Xiang, Food Res. Int., 2021, 142, 110213.

Chapter 3

Objectives of the thesis

The purpose of this thesis was to increase the extraction yield (especially of semi-volatiles), but more importantly, to increase the level of information that can be described through the HS analysis of specific samples. The analysis of semi-volatile organic compounds (SVOCs) can elicit diverse interests depending on the specific field of application. For instance, in environmental monitoring, it serves to identify sources of pollution, such as emissions from industrial processes or vehicles. In the realm of health, SVOC analysis extends to breath analysis, offering insights into physiological conditions.

In the assessment of olive oil quality, various factors, including agronomical and technological considerations, can influence the composition of the oil. For instance, pedoclimatic conditions, encompassing weather patterns and soil characteristics, exert a direct influence on secondary metabolites like sesquiterpenes. These compounds, regarded as semi-volatiles, hold significance in the identification of origin markers, thus warranting consideration in quality assessment protocols.

To reach these goals, novel SPME methods were investigated, namely vacuum-assisted Vac-HS-SPME and multiple cumulative trapping (MCT)-HS-SPME.

Vac-HS-SPME had been widely applied for water-based samples, proving significant improvement in the extraction of semi-volatiles at milder temperatures. At increased temperature, the impact of using reduced pressure was reduced, if not nullified, due to a change in water presence in the HS affecting the fiber trapping ability. The goal of this thesis was though to investigate the effect of reduced pressure on fatty (olive oil) and solid (fish) fatty matrices. The choice of these two matrices allowed us to investigate the combination of Vac-HS-SPME in relation to higher and lower temperature in the context of a meaningful food-related application where not only the extraction yield but also the level of information extracted is driving the optimization process. In this context, the olive oil aroma fingerprint, which can be directly correlated to the commercial category of the olive oil products (i.e., extra virgin, virgin, and lampante oil) was investigated. In a first study (Chapter 4, section 1) the use of Vac-HS-SPME was compared to normal pressure HS-SPME. It has already been demonstrated (ref) that lowering the sampling pressure effectively reduced gas-side limitations while accelerating extraction kinetics. However, for viscous samples like olive oils, liquid-phase resistance played a significant role in delaying extraction. Generally, the best analytical HS-SPME strategy for obtaining a rich volatile profile from oily samples more quickly is to apply mild heating (i.e., decreasing the viscosity of the oily sample and increasing headspace concentrations reducing the uncertainty of the measurement) in conjunction with lowering the headspace's overall pressure.

From the previous studies it was evident that the lower the temperature, the greater the vacuum effect. This is why the second study seeks to demonstrate the viability of vacuum-assisted extraction at sub-ambient temperatures. In this context, the relevance of using olive oil was questionable due to its tendency to solidify at sub-ambient temperatures. This solidification process leads to a significant increase in the inhomogeneity of the matrix, resulting in partial solidification. The degree of crystallization varies from one olive oil to another depending on the proportion of

saturated fatty acids in triglycerides, which can also differ among different olive oils. Moreover, there is no practical goal of analysing olive oil at lower temperature. Therefore, in order to develop a useful “more general” application including headspace samplings at sub-ambiant temperatures, the investigation of fish spoilage with the help of selected markers was decided (Chapter 4, section 2). This matrix has been selected because fish is a highly perishable product for which sub-ambient temperatures are the norm for conservation. The spoilage markers (generated through a series of degradation pathways) have been targeted over time. Taking into account that the diffusion of compounds within a solid (or highly viscous) sample is notably slower compared to the random motion observed in a liquid sample, the diffusion of molecules into the headspace is predominantly confined to the interface between the sample and the headspace under classical extraction conditions. Therefore, in addition to the original purpose, the study has been designed to evaluate the effects of an increase in extraction yield while using vacuum assisted extraction on non-liquid fatty samples.

The second approach investigated a modification of MHE, known as multiple cumulative trapping extraction (MCT)-HS-SPME. Unlike classical MHE, MCT requires only one injection instead of multiple injections (n = number of extractions). The initial phase of the study focused on evaluating the technical potentialities: reducing the duration of each extraction cycle, minimizing the displacement effect between compounds and enhancing sensitivity. However, similar to MHE, avoiding saturation of the headspace is crucial, although this variable is often overlooked in literature. Therefore, the impact on extraction yield and the relevance of information was evaluated (Chapter 5, section 1).

Subsequent investigation revealed that using saturated headspace increases the extraction of volatiles at the expense of semi-volatiles compared to non-saturated headspace. Specifically, utilizing MCT under non-saturating conditions led to a greater extraction of semi-volatiles over volatiles (Chapter 5, section 2).

A broader cross-sample comparison study of virgin olive oil was then conducted to showcase MCT's potential in real-world scenarios. The optimized method was applied to assess the feasibility of distinguishing olive oils based on commercial categories and geographical origin (Chapter 5, section 3).

Lastly, according to the results of the two investigated methods, they were directly compared and combined to evaluate potential synergistic effects (Chapter 6). Olive oil quality markers were selected based on validated criteria from literature, facilitating comparison of the developed method with existing other analytical protocol. Additionally, a non-targeted approach was employed to identify the most significant features maximizing clustering of commercial categories under various conditions examined.

Chapter 4

Vacuum assisted HS-SPME

1. A multifaceted investigation of the effect vacuum on the headspace solid-phase microextraction of extra-virgin olive oil

Based on: S. Mascrez, E. Psillakis and G. Purcaro, *A multifaceted investigation of the effect vacuum on the headspace solid-phase microextraction of extrac-virgin olive oil*, Analytica Chimica Acta, 1103 (2020) 106-114.

1.1. Abstract

Headspace solid-phase microextraction (HS-SPME) is an easy, effective, and selective technique for the extraction of volatiles and semi-volatiles compounds. For the latter, longer equilibration times are needed, which are typically shortened by applying agitation or heating the sample. A less explored way to improve the extraction kinetics of analytes with a low-affinity for the headspace is to sample under vacuum conditions. The methodology that evolved from this approach was termed "vacuum-assisted HS-SPME" (Vac-HS-SPME) and was mainly used for water- and solid-based samples.

The aim of this work was to investigate the effect of vacuum when dealing with non-aqueous liquid samples. For this purpose, the volatile profile of extra virgin olive oil was analyzed using a divinylbenzene/carboxen/polydimethylsiloxane fiber followed by gas chromatography-mass spectrometry. The effects of extraction temperature and sampling time were investigated using traditional one-variable at a time approach and a two-variable central component design for both Vac-HS-SPME and regular HS-SPME. The results showed an important enhancement in the extraction of semi-volatile compounds when using Vac-HS-SPME, and improved the information gained for the olive oil aroma fingerprint. A theoretical formulation of the underlying process was proposed, providing new insights into the SPME extraction theory. Lowering the sampling pressure effectively reduced gas-sided limitations and accelerated extraction kinetics. However, for viscous samples such as olive oils, the liquid-phase resistance played an important role and delayed extraction. Overall, applying heating (i.e. reducing the viscosity of the oily sample and increasing headspace concentrations) next to reducing the total pressure in the headspace is the best analytical HS-SPME strategy for obtaining fast a rich volatile profile from the olive oil samples.

1.2. Introduction

As longly discussed in the introduction, when using SPME often a compromise between sensitivity and extraction time is necessary when targeting a wide variety of compounds (volatile and semi-volatile), as in the case of fingerprinting food aroma. Different strategies can be applied to improve the kinetics and maximize the number of extracted compounds, such as stirring the sample and increasing the temperature, although the latter may create undesired artifacts, especially when dealing with food samples [1,2].

An alternative and less explored and exploited way to improve extraction kinetics is the application of reduced pressure conditions during sampling. The positive effect of vacuum on HS-SPME was presented for the first time in 2001 by Brunton *et al*. for the extraction of volatiles from raw turkey meat homogenated with water [3]. In 2005, Darrouzès *et al*. proposed the use of the vacuum to enhance the HS-SPME sampling of organotin compounds from aqueous solutions [4]. The effect of reduced pressure conditions on HS-SPME (method termed vacuum-assisted HS-SPME; Vac-HS-SPME) started to be more rigorously and systematically investigated after the theoretical formulation of the underlying processes by Psillakis *et al*. in 2012 [5-13]. Ever since, Vac-HS-SPME has been successfully applied to aqueous and solid samples, resulting in high extraction efficiencies and excellent sensitivities within shorter sampling times compared to regular HS-SPME (at 1 atm). Vac-HS-SPME also displayed high performance at milder temperatures, thus preserving the sample volatile profile and avoiding possible decomposition, reactions, or artifacts formation. Few works deal with the application of Vac-HS-SPME on more complex samples. Vakinti *et al.* used Vac-HS-SPME for the determination of haloanisoles in wine samples. Although ethanol (acting as a co-solvent) affected the solubilities of target analytes and reduced their headspace abundance, the positive effect of vacuum on HS-SPME sampling remained important. In fact, for 30 min sampling, the performance of Vac-HS-SPME at 25 ºC was superior to that with regular HS-SPME sampling at 55 ºC [14]. Trujillo-Rodríguez *et al.* applied Vac-HS-SPME to the analysis of a multi-component system, namely milk and dairy products [11]. The optimization and the comparison with regular HS-SPME were carried out on a water simulant and focused on studying competitive adsorption phenomena taking place on adsorbent-type SPME fibers, rather than investigating the effect of high-fat content in the matrix.

The present work investigates for the first time the use of Vac-HS-SPME to characterize the aroma profiling of an entirely lipidic matrix, namely olive oil. Olive oil, and in particular extra virgin olive oil, is an important ingredient of the Mediterranean diet with well-known health benefits and sensory quality. The latter is correlated to a complex aroma profile, which depends on several parameters (i.e., cultivar, geographical origin, fruit ripeness, processing practices, and storage). Researchers have been dedicating strong efforts to unravel the composition of this informative fraction to understand correlations with quality attributes [15,16]. In this regard, the most widely-applied sampling technique is HS-SPME, and optimum extraction conditions report sampling temperatures ranging from room temperature up to ~80 ° C (for volatile characterization) with sampling times generally shortened when higher temperatures were applied [17]. However, olive oil degradation is accelerated when heating the samples, and at the same time, extended sampling times promote competitive displacement on the adsorbent-type SPME fibers [11,18], typically used for aroma profiling [17]. Therefore, HS-SPME sampling under reduced pressure has the potential to overcome these analytical challenges as it can yield higher extraction efficiencies at mild sampling temperatures [12].

The extraction temperature and time profile under reduced and normal pressure conditions were investigated (both using traditional one-variable at a time approach and a two-variable central component design (CCD)). Theoretical considerations on non-equilibrium HS-SPME sampling from olive oil samples are herein reported for the first time. Based on these considerations, we provide some new insights on the HS-SPME mechanism. A divinylbenzene / carboxen / polydimethylsiloxane (DVB/CAR/PDMS) fiber was used in this investigation as the most applied one for the analysis of volatile compounds in edible oils [17].

1.3. Theoretical considerations on the effect of vaccum on HS-SPME sampling from olive oil

During HS-SPME sampling, analytes transfer in the three phases involved (oil, headspace and fiber) and across two interfaces (oil/headspace and headspace/fiber). Mass transfer in the headspace/SPME polymer interface is considered a relatively fast process [18-20], while, depending on the properties of the analyte, volatilization from the liquid sample can be rate-controling, i.e. a slow equilibration process. [20,21]. For this reason, only the pressure dependence of analyte mass transfer from the liquid sample to the headpace has been formulated in the past [19,21]. It is acknowledged however that mass transfer accelerations at the headspace/SPME fiber interface may also occur when sampling under vaccum. Nonetheless, this type of non-equilibrium accelerations is difficult to monitor experimentally taken that the headspace/SPME fiber equilibration times are short anyway. It is noted that the pressure dependence of the process of analyte uptake by high capacity sorbents (stir bar coated with polydimethylsiloxane [22] or a liquid microdrop [23]) was recenty formulated and experimentaly verified. In these systems, the uptake of analytes from the gas-phase is slow and as such, accelerations under vaccum conditions could be experimentally recorded.

In general, Tthe classic two-film theory is usually used to describe the mass transfer of solutes between liquid and gas-phasesat the liquid/headspace system. This model assumes that the bulk of each phase is well mixed so that only the two thin layers at the interface are characterized by a concentration gradient. Therefore, the primary resistance to mass transfer lies in these stagnant films, across which solutes transfer by molecular diffusion. The two-film theory has been extensively applied to the problem of volatilization of chemicals from natural waters bodies, [24-26], and proved successful in describing the pressure dependence of HS-SPME sampling from water samples under non-equilibrium conditions. [12,19]. In the past, the liquid phases considered for the two-film theory were not necessarily aqueous, and the model was also used to simulate the process from non-aqueous phases, e.g., the gas leakage process from transformer oil. [27]. According to the two-film approach, the overall mass transfer coefficient, k_O, controlling volatilization of a solute from olive oil can be modeled as follows:

$$\frac{1}{k_0} = \frac{1}{k_L} + \frac{1}{k_{GL} k_G} \qquad (1)$$

where, k_G and k_L are the mass transfer coefficients for the gas and olive oil boundary layers and K_{GL} (=C_G/C_L; where C_G: concentration in the gas phase; C_L: concentration in the sample) is the gas phase-olive oil partition coefficient representing the ratio of the equilibrium concentrations in the gas phase over that in the liquid sample. and k_G and k_L are the mass transfer coefficients for the gas- and olive oil boundary layers. According to Eq. (1) for a given solute, the overall resistance to transfer from olive oil to the gas phase ($1/k_O$) can be considered as two diffusional resistances in series; namely the sum of the gas-phase resistance (1/(KGL kG) and the olive oil resistance (1/kL)).

In general, both the liquid-film and gas-film coefficients are assumed directly dependent on the diffusion coefficient in the corresponding phase (i.e., DL or DG for the liquid and gas-phases, respectively) raised to some power, which lies between 0.5 and 1 depending on the model used. [28-30].

The estimation of diffusivity in liquids is far more complicated than in gases. Among the different equation proposed, the following Wilke-Chang [31] formula has been used for solvents of high viscosity such as oils: [32,33]:

$$D_L = 7.4 \times 10^{-8} \frac{TM^{1/2}}{\eta V^{0.6}} \qquad (2)$$

with M indicating the molecular weight of the solvent; V the molar volume of the solute; η the viscosity of the solvent; and T the temperature. Eq. (2) shows that in highly viscous solvents like olive oil, diffusion coefficients will be smaller than those in water, [32] and should account for additional resistance in the liquid-film compared to an aqueous phase.

The diffusion coefficient in the gas-phase, D_G, can be estimated using different equations, all of which show an inverse proportionality to the total pressure in the system. [19]. Therefore, reduction of the total pressure during HS-SPME will increase D_G, and consequently k_G, leading to a reduced gas-phase resistance (expressed as $1/(K_{GL}\ k_G)$ in Eq. (1)). [19,21]. Accordingly, loweringreduction of the total pressure will improve the overall mass transfer coefficient for analytes where gas-phase resistance controls their volatilization rate; thus resulting in faster HS-SPME extraction kinetics and shorter equilibration times. For the rest, applying a low sampling pressure should not affect their HS-SPME extraction kinetics since the liquid-phase resistance that controls their volatilization rate is independent of the total pressure in the sample container.

According to Eq. (1), acceleration in extraction kinetics will be recorded for those analytes whose K_{GL} is sufficiently small to render the $1/(K_{GL}\ k_G)$ term comparable or superior to the liquid-phase resistance ($1/k_L$ term). K_{GL} values for solutes in olive oil as a solvent are substantially different from those with water as a solvent, due to the differences in solute-solvent and solvent-solvent molecular interactions [34].

Unfortunately, data on solute partitioning between olive oil and air are sparse and predictive theoretical models are mostly used. [35-37]. For example, linear free energy equation relationships (LFER) exist for certain homologues or families of compounds (e.g. ethers, esters, ketones) that correlate partition coefficients in air-olive oil to those in air-octanol system, with octanol representing a solvent that may participate in various combinations of dispersive, polar dipole-dipole, H-acceptor, and H-donor interactions with solutes of diverse structures [34]. However, olive oil is a mixture of compounds that may vary in composition depending on the origin of the olives. For this reason, reference is made to air-olive oil partition coefficients rather than constants. [34]. The limited access to air-olive oil partitioning data (i.e. K_{GL} values) and the complex interactions of solutes with olive oil, obstructs the establishment of a criterion that can be used for predicting the positive effect of vacuum on any compound present in olive oil. Nonetheless, the theory predicts that sampling under vacuum will accelerate extraction kinetics for those analytes where gas-phase limitations play a majot major role.

1.4. Materials and methods

1.4.1. Chemicals

Hexane was HPLC grade (MilliporeSigma®, USA). The mixture of normal alkanes (C7-C30), used for calculating the linear retention index (LRI) for confirming peak identity, was from Supelco (Bellefonte, PA, USA).

A DVB/CAR/PDMS df 50/30 μm/ 1 cm length fiber was used (kindly offered by Millipore Sigma, Bellefonte, PA, USA).

Extra-virgin olive was purchased in a local supermarket (Gembloux, Belgium).

1.4.2. Vac-HS-SPME and regular HS-SPME procedures

A custom-made closure designed and constructed at the Laboratory of Aquatic Chemistry (School of Environmental Engineering, Technical University of Crete) was used for all experiments [22]. Alternatively, the previously reported modified crimp-top Mininert®valve (Sigma-Aldrich) can be used to ensure gastight conditions inside the sampler during automation [38]. The closure was equipped with a cylindrical Thermogreen®LB-1 septum (Supelco) with half-hole (6 mm diameter × 9 mm length) and could fit a 20 mL screw top vial (Restek, Bellefonte, USA).

For Vac-HS-SPME, the air inside the sampling device was evacuated for 1 min prior to introducing the oil sample, using a MD 4C diaphragm vacuum pump (7 mbar = 0.007 atm ultimate vacuum without gas ballast) manufactured by Vacuubrand GmbH & Co. KZ (Wertheim, Germany). A 5 mL gastight syringe (SGE, Australia) was used to introduce 1.5 g of oil samples in the sample container. The sample was allowed to equilibrate with the headspace for 5 min at the temperature set for extraction. Then, the SPME fiber was exposed to headspace and

sampling was performed under agitation (250 rpm) at the selected sampling temperature.

For regular HS-SPME the air-evacuation step was omitted. A 20 mL screw top vials, metallic caps with a hole and polytetrafluoroethylene (PTFE)/silicone septa (Restek, Bellefonte, USA) were used.

Two extraction temperatures were tested, namely 30 °C and 43 °C, at different extraction times (10, 20, 30 and 40 min).

Upon completion of the sampling procedure, the fiber was retracted and transferred for thermal desorption (250 °C for 2 min, split 1:5) and analysis to a GC-MS. All experiments were run in triplicate.

Prior to starting any analytical sequence, the SPME fiber was conditioned for 20 min in the GC injector. Blanks were run periodically to ensure the absence of carryover between runs. All extractions were run in triplicate.

1.4.3. Solid-phase microextraction optimization: Central Composite Design

A two-variable (k=2) inscribed rotatable ($\alpha=1/\sqrt{k}$) central composite experimental design (CCD) was used to optimise the sampling conditions, namely extraction temperature and time. These two variables were selected based on previous works. [39,40]. The extraction temperature was tested between 30 °C and 55 °C, and the exposition time from 10 to 30 min. Temperatures higher than 55 °C were not tested to avoid the possible formation of artifacts due to oxidation and degradation products. Nine different sampling conditions were included in the design, consisting of a central point, four axial and four factorial points. The experimental runs were randomized to minimize the effect of unexpected variability. The central point was repeated three times to evaluate the repeatability of the method. The extracted-ion peak areas obtained by GC-MS were used to evaluate the extraction efficiency using the response surface plot methodology.

All samples were agitated at 250 rpm and incubated for 5 min before fiber exposure at the corresponding extraction temperature. The entire CCD was repeated under normal pressure conditions (regular HS-SPME) and under vacuum (Vac-HS-SPME).

In all the experiments, the fiber was thermally desorbed in the GC injector for 2 min at 250 °C in split mode (1:5).

1.4.4. GC-MS analysis

An Agilent 7890B GC coupled to a 5977 MSD was used for all analyses. Helium (5.0 provided by Airliquid, Belgium) was used as carrier gas at 1 mL/min flow rate. Separation was performed on a 30 m x 0.25 mm i.d. x 0.5 μm df SLB-5ms capillary column [(silphenylene polymer, practically equivalent in polarity to poly(5%diphenyl/95% methylsiloxane)] kindly obtained from MilliporeSigma (Bellefonte, PA, USA). The GC oven temperature program was as follows: 35 °C for 2 min, programmed to 250 °C at a rate of 3 °C/min and then increased to 300 °C at a rate of 25 °C/min. The MS was operating in EI at 70 eV, the source temperature was 230 °C and the quadrupole temperature was 150 °C. The results were recorded in the full scan mode in the 35-500 m/z range. Data were acquired by MassHunter GC/MS Acquisition software B.07.06.2704 (Agilent, USA), converted into AIA by MSD ChemStation F.001.03.2357 (Agilent) and processed using Shimadzu GCMSolution ver 4.45 (Shimadzu, Japan).

1.4.5. Data elaboration and statistical analysis

Chromatographic data were processed using GCMSsolution (Shimadzu). Putative identification was based on the combination of a dual filter, namely: 1) the MS similarity with the NIST17 library and the FFNSC library (Shimadzu) (≥80%) and, 2) the experimental linear retention index (LRI) within a ±10 range. A total of 33 compounds (Table 4-1) were selected over the entire chromatogram. Several rationales guided the selection: i) differences in physico-chemical properties, such as polarity and volatility; ii) previously reported as important compounds for the extra virgin olive oil aroma characterization [41-44], iii) no or limited coelution. All the chemical-physical properties of the 33 compounds selected (reported in Table 4-1) were obtained from the ChemSpider website (http://www.chemspider.com/).

All statistical analyses were performed using R v3.3.2 (R Foundation for Statistical Computing, Vienna, Austria) and Minitab 19 (https://www.minitab.com/en-us/).

1.5. Results and discussion

The aroma of extra virgin olive oil is reflected in a complex volatile components profile. Based on previous experience [16], a non-polar column (5% phenyl) was used, along with a rather slow oven temperature program (3 $^{o}C.min^{-1}$) to minimize coelution at this preliminary investigation stage.

Despite a careful selection of the 33 compounds considered, it was not possible to completely avoid the partial coelution of some compounds, especially in the case of the richer profile obtained with Vac-HS-SPME. The partial coelution with other compounds is one of the reasons for some of the rather high relative standard deviations (RSDs %) that were found for some compounds (>15%), as well as some strange behavior in the surface response of the experimental design. In some cases, a low absolute signal was recorded in one of the two sampling conditions affecting

repeatability, but a general trend was observed overall. Finally, such higher RSDs compared to previous Vac-HS-SPME experiments can also be explained by the properties and complexity of the matrix, as discussed in more detail in the next section.

Table 4-1: List of the selected compounds together with their Chemical Abstracts Service (CAS) number, boiling point (B_p), Henry's constant (K_H , atm.m3.mol-1), octanol-air partition constant (K_{oa}, atm.m^3.mol^{-1}), octanol-water partition constant (K_{ow}, atm.m^3.mol^{-1}), Vapour pressure (Vp, mmHg at 25 °C), Molecular weight (M_W, g.mol^{-1}) and Molecular volume (M_V, cm^3) , and linear retention index (IT) experimentally calculated and reported in the literature.

#	Compound Name	CAS	M_W (g mol^{-1})	V_M (cm^3)	B_P (°C)	Log K_H (atm m3 mol^{-1})	log K_{oa} (atm m^3 mol^{-1})	log K_{ow} (atm m^3 mol^{-1})	V_p (mmHg at 25°C)	*m/z*	I^T_{ex}	I^T_{Lib}
v1	Ethanol	64-17-5	46.1	59.1	72.6	-5.33	3.379	-0.14	82.8	45	601	552
v2	Acetic acid	64-19-7	60.1	56.2	117.1	-5.54	5.218	0.09	13.9	60	634	641
v3	Ethyl Acetate	141-78-6	88.1	98.0	73.9	-3.42	2.991	0.86	111.7	43	648	630
v4	1-Penten-3-ol	616-25-1	86.1	104.0	112.5	-4.64	4.514	1.12	11.2	57	690	685
v5	Penten-3-one	1629-58-9	84.1	103.3	104.3	-3.71	3.748	0.90	31.1	55	691	683
v6	Pentan-3-one	96-22-0	86.1	108.2	101.0	-3.60	3.43	0.75	35.8	57	700	697
v7	2(E)-Pentenal	1576-87-0	84.1	102.0	126.8	-3.86	3.607	1.09	11.5	55	760	751
v8	1-pentanol	71-41-0	88.1	108.6	138,5	4.83	4.785	1.33	2.8	42	772	761
v9	*n*-octane	111-65-9	114.2	160.6	126.4	0.29	3.062	4.27	14.2	43	800	800
v10	Hexanal	66-25-1	100.2	124.9	127.0	-3.45	3.84	1.80	10.9	56	801	801
v11	2(E)-Hexenal	6728-26-3	98.1	118.5	146.5	-3.94	4.279	1.58	4.6	69	852	850
v12	1-Hexanol	111-27-3	102.2	125.0	158.2	-4.76	5.185	1.82	0.9	56	872	867
v13	Pentanoic acid	109-52-4	102.1	105.7	185.3	-5.29	6.105	1.56	0.5	60	881	893
v14	Heptanal	111-71-7	114.2	141.4	150.4	-3.34	4.247	2.29	3.9	70	903	906
v15	2(E)-Heptenal	18829-55-5	112.1	135.0	166.0	-3.81	4.341	2.07	1.8	83	960	956
v16	Benzaldehyde	100-52-7	106.1	101.1	178.7	-4.64	4.442	1.71	1.0	106	965	960
v17	Hexanoic acid	142-62-1	116.1	122.2	204.6	-5.14	6.429	2.05	0.2	60	978	979
v18	6-methylhept-5-en-2-one	110-93-0	126.2	151.1	173.3	-3.75	4.122	2.06	1.3	43	987	986
v19	Octanal	124-13-0	128.2	157.9	163.4	-3.20	4.457	2.78	2.1	84	1004	1006

v20	Hex-(3Z)-enyl acetate	3681-71-8	14 2.2	15 7.7	17 5.2	- 3.35	4. 195	2. 61	1.4	67	10 05	1 008
v21	Acetic acid, hexyl ester	142-92-7	14 4.2	16 4.1	17 1.5	- 3.05	4. 494	2. 83	1.4	43	10 13	1 012
v22	ß-Ocimene,(E)	13877-91-3	13 6.2	17 5.5	17 5.2	- 0.62	3. 398	4. 80	1.6	93	10 47	1 046
v23	Oct-(2E)-enal	2548-87-0	12 6.2	15 1.5	19 0.1	- 3.63	5. 093	2. 57	0.6	70	10 60	1 059
v24	*n*-octanol	111-87-5	13 0.2	15 8.1	19 4.7	- 4.68	5. 999	2. 81	0.1	56	10 74	1 076
v25	2-Nonanone	821-55-6	14 2.2	17 4.2	19 3.5	- 3.15	4. 496	2. 71	0.6	58	10 92	1 093
v26	Nonanal	124.19-6	14 2.2	17 4.4	19 0.8	- 3.10	4. 793	3. 27	0.5	57	11 05	1 107
v27	Octanoic acid	124-07-2	14 4.2	15 5.2	23 9.3	- 4.73	7. 488	3. 03	0.1	60	11 70	1 192
v28	Methyl salicylate	119-36-8	15 2.1	12 5.8	22 2.0	- 5.24	4. 947	2. 60	0.1	12 0	11 97	1 192
v29	Decanal	112-31-2	15 6.3	19 0.9	20 9.0	- 2.95	4. 893	3. 76	0.2	57	12 07	1 208
v30	Dec-(2E)-enal	3913-81-3	15 4.2	18 4.5	23 0.0	- 3.63	5. 451	3. 55	0.1	70	12 64	1 265
v31	Nonanoic acid	112-05-0	15 8.2	17 1.7	25 4.9	- 4.67	7. 748	3. 52	0.0	60	12 67	1 275
v32	Undec-(8Z)-enal	58296-81-4	16 8.3	20 1.0	24 2.8	- 3.35	5. 545	4. 04	0.0	70	13 66	1 365
v33	α-Farnesene, (E,E)	502-61-4	20 4.3	25 1.5	27 9.6	- 0.19	5. 067	7. 10	0.0	93	15 06	1 504

Figure 4-1 reports the chromatograms obtained using regular and Vac-HS-SPME sampling at 30 °C for 20 min, the compounds selected for comparison purposes are highlighted as well.

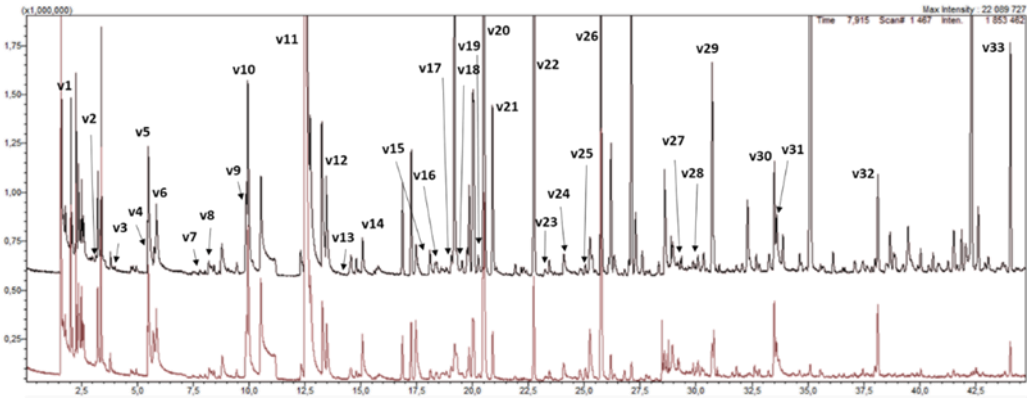

Figure 4-1: Comparison of the total ion chromatogram obtained using regular (brown, bottom chromatogram) and Vac-HS-SPME (black, upper chromatogram) sampling. Compounds identification refers to Table 4-1.

1.5.1. Insights on the experimental data obtained under vacuum and regular pressure conditions

Figure 42A shows the Vac-HS-SPME/HS-SPME peak area ratios obtained at 30 °C for each sampling time tested. Ratio values sufficiently larger than 1 indicate accelerations in the extraction rates with Vac-HS-SPME compared to regular HS-SPME [12]; while ratio values close to 1 indicate that Vac-HS-SPME and HS-SPME perform similarly and that the equilibrium is reached [12]. It is ackowledged that the use of a porous SPME fiber may result in competitive adsorption phenomena, and conferring about reaching equilibrium may not be appropriate [45]. Nonetheless, the word equilibrium is used here and denotes similar performances of Vac-HS-SPME and HS-SPME. Figure 4-2A shows that compounds characterized by lower molecular weight and higher volatility [ethanol (v1), acetic acid (v2), ethyl acetate (v3), 1-penten-3-ol (v4), penten-3-one (v5), and possibly pentan-3-one (v6)] reached equilibrium, under both pressure conditions, close to 10 min of extraction as the corresponding peak area ratios took values close to 1 at each sampling time tested (Figure 6.2A). (E)-pentenal (v7), 2(E)-hexenal (v11), and 1-hexanol (v12) reached the equilibrium around 20 min as the Vac-HS-SPME/HS-SPME peak area ratios leveled off after this sampling time. For isopentyl alcohol (v8), octane (v9), and hexanal (v10) a higher uptake under vacuum conditions was observed up to 30 min. For the majority of the rest, the positive effect of vacuum insisted even after 30 min of sampling. For some of these analytes the response of the instrument was low and resulted in some inconsistencies in the sampling time trends recorded.

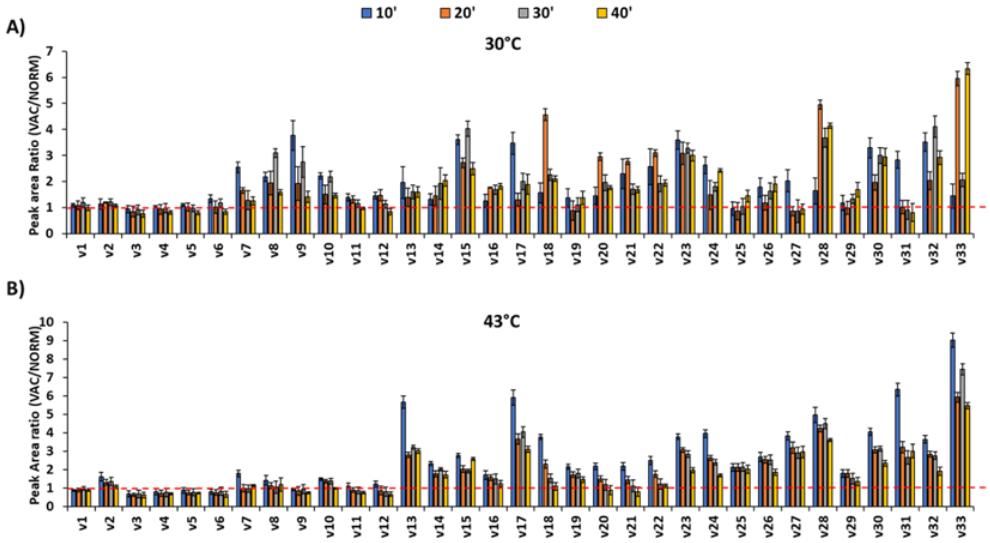

Figure 4-2: Changes in extraction efficiency for each sampling time at A) 30 °C and B) 43 °C upon reducing the total pressure expressed as Vac-HS-SPME/HS-SPME peak area ratios. The red dashed line highlights the threshold 1 above which accelerations in extraction kinetics are recorded with Vac-HS-SPME.

Figure 4-2B gives the corresponding Vac-HS-SPME/HS-SPME peak area ratios obtained at 43 °C. The increased temperature impacted the volatilization rates of smaller and more volatile analytes to the extent that the first 12 eluting analytes (ethanol (v1) up to 1- hexanol (v12)) reached the equilibrium faster under regular conditions as well. Note that extraction kinetics were accelerated by the increased temperature, but the final amount of analyte extracted at equilibrium was not affected (Figure 4-3). For the vast majority of the remaining compounds, the effects of higher temperature and low pressure were effectively combined and, compared to 30 °C, resulted in a higher improvement in extraction efficiencies at earlier sampling times. The Vac-HS-SPME/HS-SPME peak area ratios decreased with increasing sampling time, indicating that the equilibrium was approached.

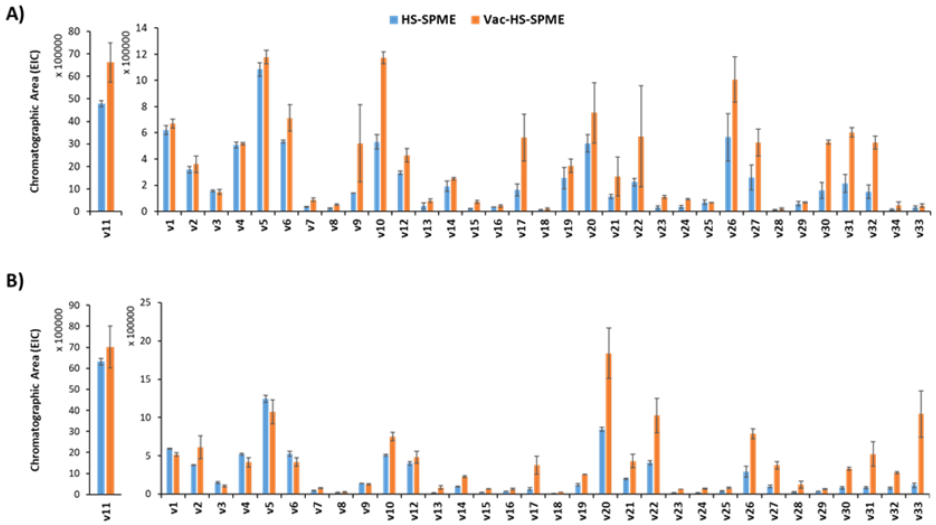

Figure 4-3: Extraction yield using HS-SPME and Vac-HS-SPME sampling conditions. Extraction time 10 minutes at A) 30 °C and B) 43 °C. Compounds name code as for Table 4-1.

When sampling from water or water-containing solutions, heating the sample under reduced pressure conditions was not always successful [12]. The adverse effect of temperature on Vac-HS-SPME was primarily due to the increased humidity in the headspace, which altered the pressure in the vial. Moreover, it was noticed that the increased humidity affected more the absorbent-type compared to adsorbent-type SPME fibers [21]. Here, the use of olive oil samples excluded the presence of an excessive amount of water molecules in the headspace and allowed studying the synergistic effect of temperature and low-pressure conditions. Nonetheless, the presence of high amounts of water-immiscible hydrocarbons in the headspace and the use of a solid sorbent accelerated swelling of the fiber with a consequently increased presence of siloxane on the GC trace [46].

Cavalli et al. reported the extraction time profiles at 25 °C of some olive oil (Sabine variety) volatile compounds using a DVB/CAR/PDMS fiber [47]. In their report, the individual curves obtained for some compounds common to the present study, namely octane (v9), β-ocimene (v22), nonanal (v26) and α-farnesene (v33), were far from equilibrium after sampling the headspace for 40 min and the response of the instrument was particularly low for the sesquiterpene α-farnesene (v33). Matich et al. studied a model system consisting of four butanoate esters and α-farnesene dissolved in squalane [48]. The HS-SPME extraction time profiles at 20 °C showed that the two lowest molecular weight volatiles equilibrated between the squalane solution, the atmosphere, and the fiber in 5-10 min, whereas α-farnesene was far from equilibrium even after sampling the headspace for 90 min. Although not directly related to the present studies, the authors also investigated α-farnesene uptake as a function of air movement in the headspace above the sampled fruits. A strong dependency was reported, which pointed to the slow evaporation rate of this analyte as well as the relative importance of the gas-phase resistance during the volatilization process. Here, the extraction of α-farnesene (v33) was largely improved when adopting the Vac-HS-SPME. The present results on α-farnesene are of importance since this compound was often reported to be the most representative terpenic hydrocarbon in extra virgin olive oils from different geographical regions [49,50].

At 30 °C, the results obtained with Vac- and regular HS-SPME showed relatively high variability, especially for analytes not having attained an equilibrium within the sampling times tested, and the effect was more pronounced with Vac-HS-SPME (almost all analytes under non-equilibrium conditions were affected). Heating the sample from 30 °C to 43 °C decreased the error associated with measurements under each sampling pressure tested even for compounds for which an equilibrium was not

reached over the tested conditions. The high variability obtained at 30 °C was a rather unexpected finding, especially because Vac-HS-SPME was previously found to improve repeatability when sampling water samples at milder sampling temperatures [11]. A possible explanation may lie in the high viscosity of the olive oil matrix. At 30 °C, a ~49 mPa s viscosity value was measured for the olive oil tested here (Table 4-2), being approximately 60 times larger than that of water at the same temperature. This high viscosity value increased liquid-phase resistance and "delayed" analyte diffusion through the liquid boundary layer of the olive oil matrix. This is particularly important when targeting analytes with a small affinity for the headspace, regardless of the pressure conditions inside the sample vial [20]. For these analytes, HS-SPME is considered a multi-stage process with analyte molecules being transferred from the liquid sample to the gas phase every time the headspace concentrations fall below equilibrium levels [19,20]. This "replenishment" depends on the resistance in the liquid phase, which is particularly relevant for viscous liquid samples such as olive oil. Although not dependent on pressure conditions, this process is more critical for Vac-HS-SPME due to the intensification of the sampling process under reduced pressure conditions [45,51] and may account for the higher variability at 30 °C. Heating the sample from 30 °C to 43 °C decreased the olive oil viscosity by around 40 % (i.e., ~30 mPa.s) and improved the liquid-phase diffusivity. At this temperature, the olive oil sample could replenish headspace analyte concentrations faster, and the error associated with the measurements was improved compared to 30 °C.

Table 4-2: Viscosity of the olive oil sample at different temperature.

T	**mPa.s**		
30 °C	49.43	±	0.05
35 °C	40.50	±	0.02
43 °C	30.70	±	0.02
50 °C	24.60	±	0.00
55 °C	21.20	±	0.00

1.5.2. Insights on the results obtained using the two-variable CCD: a study of the response surfaces

Usually, the use of univariate design for SPME optimization might overlook possible variable interaction, limiting the understanding of the phenomena occurring using vacuum conditions compared to classical SPME. In 2008, Pawliszyn *et al.* pioneered the use of a design-of-experiments (DOE) for HS-SPME optimization in coffee samples investigating five independent parameters: the amount of sample, incubation time, extraction time, incubation/extraction temperature, and agitation speed [39]. It was shown that extraction time and temperature are the two main variables affecting the performance of HS-SPME. In 2018, Borget *et al.* confirmed the main significance of these two parameters in extra virgin olive oil samples, after applying a full factorial CCD with three independent factors (time, temperature, and sample quantity) [40].

Based on these previous findings, a two-variables (k=2; temperature and time) CCD, as described in section 1.4.3., was applied to support the understanding of the vacuum effect on the temperature-time interaction.

The overall effect of the vacuum was evaluated by comparing the total number of peaks and the total peak area. For counting, compounds present in the fiber blank were removed (e.g. siloxanes). The total number of peaks did not change much over the different conditions of the CCD; it increased by about 14% using Vac-HS-SPME (~180 peaks, S/N= 50). The total peak area, instead, showed an important improvement. As expected from the theory [12], the maximum was reached at milder temperature and shorter time when Vac-HS-SPME sampling were used, namely ~45 °C for ~25 min (Figure 4-4b), while within the ranges tested the regular pressure conditions were still far from a local maximum even at the highest temperature and the longest extraction time tested (Figure 4-4a). Moreover, the maximum obtained using Vac-HS-SPME showed about a 40% higher intensity compared to the highest uptake observed in regular HS-SPME.

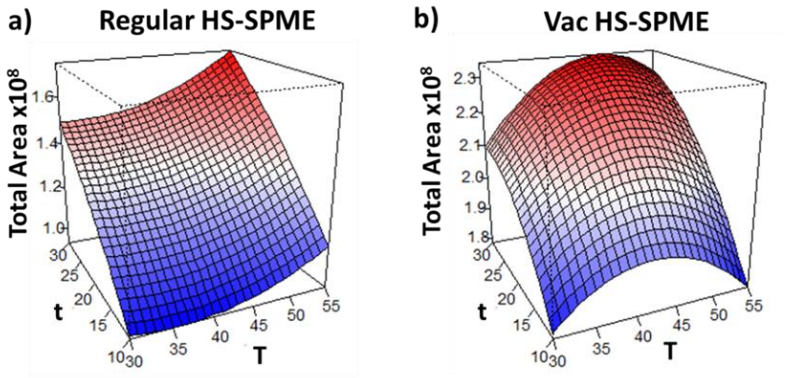

Figure 4-4: Response surface for the total chromatographic area for a) regular HS-SPME and b) Vac-HS-SPME sampling.

Interestingly comparing the Pareto charts of the standardized effects obtained using Regular HS-SPME and Vac-HS-SPME on the total chromatographic area, the statistical significance of each factor and their interaction changed, especially in terms of absolute effect (Figure 4-5). Under regular sampling, both temperature and time had a significant impact on the overall extraction yield, with time playing a more significant role (~3 times higher), as also previously reported in the literature [39]. When Vac-HS-SPME sampling was performed, the standardized effects were largely reduced below the significant level, but time remained the prominent factor. Although the effect of reduced pressure sampling was highly compound-dependent (as aforementioned), the selection of the optimal sampling conditions in complex untargeted applications, like the present one, is usually based on an overall compromise. Further evaluation of every single compound was carried out to support the previous observation on the use of sampling under vacuum (The results are not all reported hereto keep spare space. Readers can find the supplementary figures in the corresponding articles) , while here the general trends are summarized.

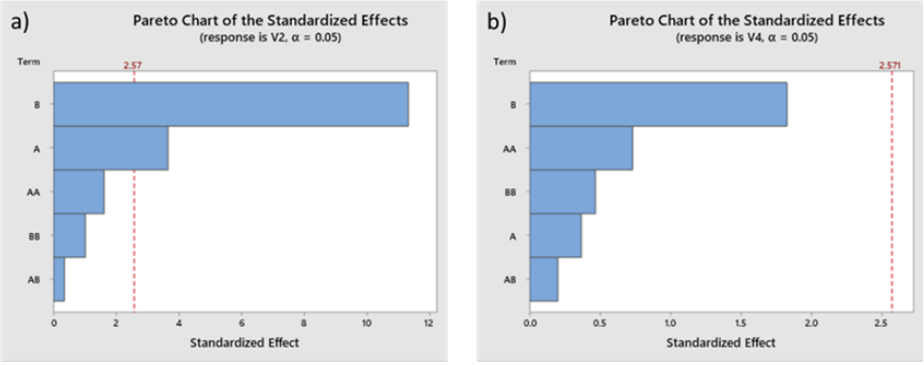

Figure 4-5: *Pareto chart of the standardized effects for the total chromatographic area under a) regular HS-SPME and b) Vac-HS-SPME sampling. A: Temperature; B: time.*

For the earlier eluted compounds (v1-v10), the more volatile ones, the surface response recorded under regular condition was generally very similar to the one recorded under Vac-HS-SPME sampling. The higher response was generally obtained at 30 °C for 30 min, although not a maximum, and the response surface showed a descending trend towards higher temperatures. For these compounds, the effect of vacuum was limited, as also previously observed.

The majority of the remaining compounds showed a similar trend under regular HS-SPME extraction, with a local maximum at 55 °C for 30 min of extraction but still not a plateau. For a few compounds, the equilibrium was reached at this point [showing a plateau, as for benzaldehyde (v16), 6-methylhept-5-en-2-one (v18), decanal (v29)]; for these compounds the response surfaces obtained using Vac-HS-SPME extraction showed different behaviors. The appearance of a plateau at the

highest/longest conditions (55 °C and 30 min) or at a shorter time and milder conditions was observed for v13, v14, v16, v17, v18, v23, v24, v25, v26, v28, v30, v33. The response surfaces of oct-(2E)-nal (v23) is reported in Figure 6.6. as an example of this ideal behaviour.

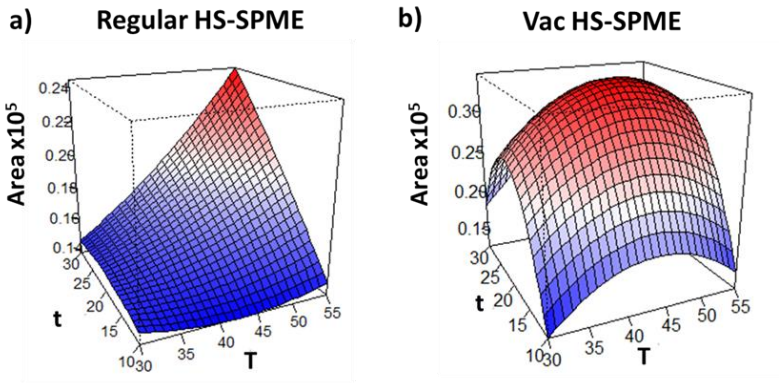

Figure 4-6: *Response surface for oct-(2E)-nal (v23) under a) regular HS-SPME and b) Vac-HS-SPME conditions.*

For all the other cases, the temperature-time interaction was compound dependent and changed in some unexpected way. For instance, for 1-hexanol (v12) the maximum was maintained over the different time tested (10-30 min) when Vac-HS-SPME extraction was performed. Observing the standard effects (Pareto chart reported in Figure 4-7) only temperature (and its quadratic relationship) remained significant under vacuum conditions.

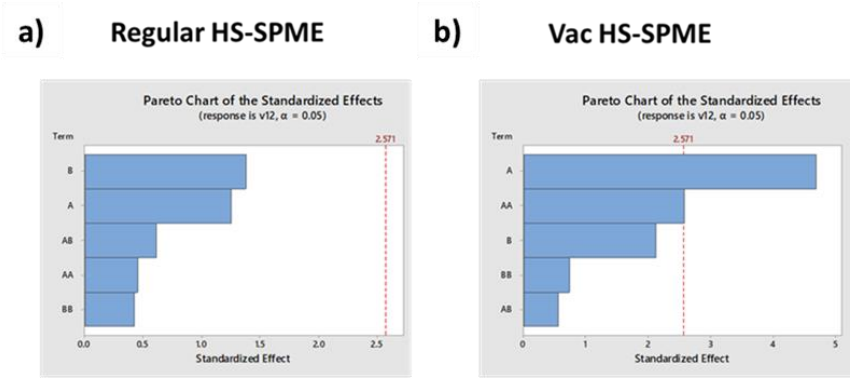

Figure 4-7: *Pareto chart of the standardized effects for v12 under a) regular HS-SPME and b) Vac-HS-SPME sampling. A: Temperature; B: time.*

Indeed, the optimum was obtained at about 35 °C (almost no difference at different extraction times), while higher extraction temperature led to a lower uptake independently from the extraction time, probably due to a displacement effect (Figure 4-8).

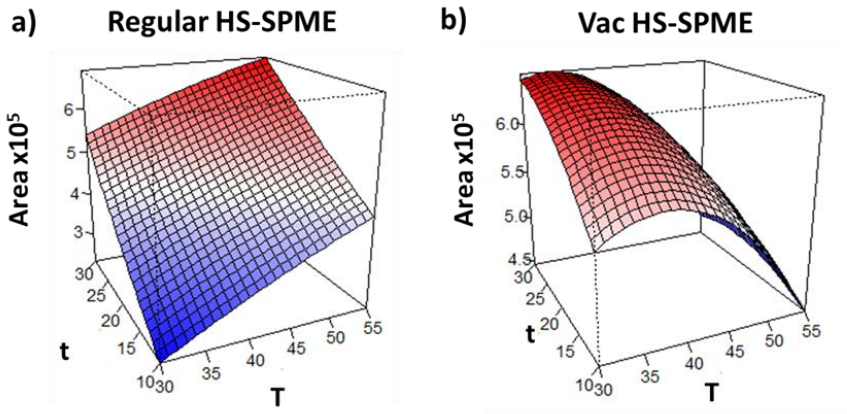

Figure 4-8: *Response surface for 1-hexanol (v12) under a) regular HS-SPME and b) Vac-HS-SPME conditions.*

A similar behavior but independent from the temperature was observed for octanal (v19), where the optimum extraction time was at 25 min independently of the temperature used. However, the increase of the peak that was partially coeluted with octanal, namely hex-(3Z)-enyl acetate (v20), was observed, affecting a proper quantification of octanal.

1.6. Conclusion

This work investigated, for the first time, the application of Vac-HS-SPME to oily samples. The positive effect of vacuum on HS-SPME sampling was shown and discussed thoroughly both using a univariate approach and a CCD. The limited access to air-olive partitioning data and the complex interactions of solutes with olive oil limited the formulation of a definitive criterion for predicting the positive effect of vaccum on HS-SPME. It was observed and postulated that the extraction process can be limited not only by the gas-phase resistance but also by the diffusion coefficient of the analyte in the highly-viscous oily phase. The absence of water in the sample allowed applying heating without a detrimental effect on the Vac-HS-SPME sampling, an effect commonly reported in aqueous samples. It was clearly shown that for highly viscous liquids, the effect of temperature remains important as it increases the diffusivity through the liquid thin film adjacent to the interface and facilitates mass transfer. It was concluded that applying heating next to reducing the total pressure in the headspace is the best analytical HS-SPME strategy for obtaining fast a rich volatile profile from the olive oil samples.

Such a powerful approach can provide a more detailed insight on the volatile fraction of olive oil, supporting the identification of characteristic pattern or specific markers able to discriminate between the different commercial category of olive oil, namely virgin, extra-virgin and lampante oil.

Further investigations are ongoing using a simplify model to reduce possible confounding effects, such as chromatographic coelution and displacement effects on the fiber. Moreover, Vac-HS-SPME will be used to explore the fingerprinting of different oils and evaluate its capability to enhance the extractable information for pattern recognition purposes.

1.7. References

[1] J. Pawliszyn, Theory of Solid-Phase Microextraction, 38 (2000) 270–278.

[2] Z. Zhang, J. Pawliszyn, Headspace Solid-Phase Microextraction, Anal. Chem. 65 (1993) 1843–1852. http://doi:10.1021/ac00062a008.

[3] N.P. Brunton, D.A. Cronin, F.J. Monahan, The effects of temperature and pressure on the performance of Carboxen/PDMS fibres during solid phase microextraction (SPME) of headspace volatiles fro m cooked and raw turkey breast, Flavour Fragr. J. 16 (2001) 294–302. http://doi:10.1002/ffj.1000.

[4] J. Darrouzès, M. Bueno, C. Pécheyran, M. Holeman, M. Potin-Gautier, New approach of solid-phase microextraction improving the extraction yield of butyl and phenyltin compounds by combining the effects of pressure and type of agitation, J. Chromatogr. A. 1072 (2005) 19–27. http://doi:10.1016/j.chroma.2005.02.026.

[5] E. Psillakis, E. Yiantzi, L. Sanchez-Prado, N. Kalogerakis, Vacuum-assisted headspace solid phase microextraction: Improved extraction of semivolatiles by non-equilibrium headspace sampling under reduced pressure conditions, Anal. Chim. Acta. 742 (2012) 30–36. http://doi:10.1016/j.aca.2012.01.019.

[6] E. Psillakis, A. Mousouraki, E. Yiantzi, N. Kalogerakis, Effect of Henry's law constant and operating parameters on vacuum-assisted headspace solid phase microextraction, J. Chromatogr. A. 1244 (2012) 55–60. http://doi:10.1016/j.chroma.2012.05.006.

[7] E. Psillakis, E. Yiantzi, N. Kalogerakis, Downsizing vacuum-assisted headspace solid phase microextraction, J. Chromatogr. A. 1300 (2013) 119–126. http://doi:10.1016/j.chroma.2013.02.009.

[8] E. Yiantzi, N. Kalogerakis, E. Psillakis, Vacuum-assisted headspace solid phase microextraction of polycyclic aromatic hydrocarbons in solid samples, Anal. Chim. Acta. 890 (2015) 108–116. http://doi:10.1016/j.aca.2015.05.047.

[9] E. Yiantzi, N. Kalogerakis, E. Psillakis, Design and testing of a new sampler for simplified vacuum-assisted headspace solid-phase microextraction, Anal. Chim. Acta. 927 (2016) 46–54. http://doi:10.1016/j.aca.2016.05.001.

[10] M.L. Glykioti, E. Yiantzi, E. Psillakis, Room temperature determination of earthy-musty odor compounds in water using vacuum-assisted headspace solid-

phase microextraction, Anal. Methods. 8 (2016) 8065–8071. http://doi:10.1039/c6ay02210c.

[11] M.J. Trujillo-Rodríguez, V. Pino, E. Psillakis, J.L. Anderson, J.H. Ayala, E. Yiantzi, A.M. Afonso, Vacuum-assisted headspace-solid phase microextraction for determining volatile free fatty acids and phenols. Investigations on the effect of pressure on competitive adsorption phenomena in a multicomponent system, Anal. Chim. Acta. 962 (2017) 41–51. http://doi:10.1016/j.aca.2017.01.056.

[12] E. Psillakis, Vacuum-assisted headspace solid-phase microextraction: A tutorial review, Anal. Chim. Acta. 986 (2017) 12–24. http://doi:10.1016/j.aca.2017.06.033.

[13] D. Orazbayeva, B. Kenessov, E. Psillakis, D. Nassyrova, M. Bektassov, Determination of transformation products of unsymmetrical dimethylhydrazine in water using vacuum-assisted headspace solid-phase microextraction, J. Chromatogr. A. 1555 (2018) 30–36. http://doi:10.1016/j.chroma.2018.04.048.

[14] M. Vakinti, S.M. Mela, E. Fernández, E. Psillakis, Room temperature and sensitive determination of haloanisoles in wine using vacuum-assisted headspace solid-phase microextraction, J. Chromatogr. A. 1602 (2019) 142–149. http://doi:10.1016/j.chroma.2019.03.047.

[15] F. Angerosa, M. Servili, R. Selvaggini, A. Taticchi, S. Esposto, G. Montedoro, Volatile compounds in virgin olive oil: Occurrence and their relationship with the quality, J. Chromatogr. A. 1054 (2004) 17–31. http://doi:10.1016/j.chroma.2004.07.093.

[16] G. Purcaro, C. Cordero, E. Liberto, C. Bicchi, L.S. Conte, Toward a definition of blueprint of virgin olive oil by comprehensive two-dimensional gas chromatography, J. Chromatogr. A. 1334 (2014) 101–111. http://doi:10.1016/j.chroma.2014.01.067.

[17] L. Sghaier, J. Vial, P. Sassiat, D. Thiebaut, M. Watiez, S. Breton, D.N. Rutledge, C.B.Y. Cordella, An overview of recent developments in volatile compounds analysis from edible oils: Technique-oriented perspectives, Eur. J. Lipid Sci. Technol. 118 (2016) 1853–1879. http://doi:10.1002/ejlt.201500508.

[18] J. Koziel, M. Jia, J. Pawliszyn, Air sampling with porous solid-phase microextraction fibers, Anal. Chem. 72 (2000) 5178–86. http://www.ncbi.nlm.nih.gov/pubmed/11080861.

[19] E. Psillakis, E. Yiantzi, L. Sanchez-Prado, N. Kalogerakis, Vacuum-assisted headspace solid phase microextraction: Improved extraction of semivolatiles by non-equilibrium headspace sampling under reduced pressure conditions, Anal. Chim. Acta. 742 (2012) 30–36. http://doi:10.1016/j.aca.2012.01.019.

[20] T. Górecki, J. Pawliszyn, Effect of Sample Volume on Quantitative Analysis by Solid-phase MicroextractionPart 1. Theoretical Considerations, Analyst. 122 (1997) 1079–1086. http://doi:10.1039/a701303e.

[21] E. Psillakis, Vacuum-assisted headspace solid-phase microextraction: A tutorial review, Anal. Chim. Acta. 986 (2017) 12–24. http://doi:10.1016/j.aca.2017.06.033.

[22] N. Solomou, C. Bicchi, B. Sgorbini, E. Psillakis, Vacuum-assisted headspace sorptive extraction: Theoretical considerations and proof-of-concept extraction of polycyclic aromatic hydrocarbons from water samples, Anal. Chim. Acta. (2019). http://doi:10.1016/j.aca.2019.10.050.

[23] E. Psillakis, N. Koutela, A.J. Colussi, Vacuum-assisted headspace single-drop microextraction: eliminating interfacial gas-phase limitations, Anal. Chim. Acta. (2019) In press. http://doi:10.1016/j.aca.2019.09.056.

[24] H.-P. Chao, Volatilization characteristics of organic solutes in stirred solution., J. Environ. Manage. 90 (2009) 3422–8. http://doi:10.1016/j.jenvman.2009.05.022.

[25] D. Mackay, A.W. Wolkoff, Rate of evaporation of low-solubility contaminants from water bodies to atmosphere, Environ. Sci. Technol. 7 (1973) 611–614. http://doi:10.1021/es60079a001.

[26] D. Mackay, T.K. Yuen, Volatilization Rates of Organic Contaminants from Rivers, Water Qual. Res. J. 15 (1980) 83–201. http://doi:10.2166/wqrj.1980.006.

[27] X.F. Wang, Z.D. Wang, Q. Liu, G. Wilson, P. Jarman, D. Walker, Evaluation of mass transfer rate of dissolved gases in transformer oils, in: 2016 Int. Conf. Cond. Monit. Diagnosis, IEEE, 2016: pp. 477–480. http://doi:10.1109/CMD.2016.7757865.

[28] R.E. Rathbun, D.. Tai, Application of the Two-Film Model to the Volatilization of Acetone and t-Butyl Alcohol from Water as a Function of Temperature, (1988).

[29] D. Mackay, Effects of Surface Films on Air-Water Exchange Rates, J. Great Lakes Res. 8 (1982) 299–306. http://doi:10.1016/S0380-1330(82)71968-9.

[30] A. Tamir, J.C. Merchuk, Effect of diffusivity on gas-side mass transfer coefficient, Chem. Eng. Sci. 33 (1978) 1371–1374. http://doi:10.1016/0009-2509(78)85119-7.

[31] C.R. Wilke, P. Chang, Correlation of diffusion coefficients in dilute solutions, AIChE J. 1 (1955) 264–270. http://doi:10.1002/aic.690010222.

[32] B.C.H. Warren, R.E. Pattle, Determination and correlation of diffusion coefficients of some dyes in organic solvents of high viscosity, J. Appl. Chem. Biotechnol. 27 (2007) 533–538. http://doi:10.1002/jctb.5020270406.

[33] M.H. Hilder, M. van den Tempe, Diffusivity of water in groundnut oil and paraffi oil, J. Appl. Chem. Biotechnol. 21 (2007) 176–178. http://doi:10.1002/jctb.5020210608.

[34] R.P. Schwarzenbach, P.M. Gschwend, D.M. Imboden, Environmental Organic Chemistry, Second Edition, John Wiley & Sons Inc, Hoboken, New Jersey, 2003.

[35] A.C. Chamberlin, D.G. Levitt, C.J. Cramer, D.G. Truhlar, Modeling free energies of solvation in olive oil, Mol. Pharm. 5 (2008) 1064–1079. https://www.ncbi.nlm.nih.gov/pubmed/19434923.

[36] M.H. Abraham, P.L. Grellier, R.A. McGill, Determination of olive oil–gas and hexadecane–gas partition coefficients, and calculation of the corresponding

olive oil–water and hexadecane–water partition coefficients, J. Chem. Soc., Perkin Trans. 2. (1987) 797–803. http://doi:10.1039/P29870000797.

[37] M.H. Abraham, A. Ibrahim, Gas to olive oil partition coefficients: A linear free energy analysis, J. Chem. Inf. Model. 46 (2006) 1735–1741. http://doi:10.1021/ci060047p.

[38] D. Orazbayeva, B. Kenessov, E. Psillakis, D. Nassyrova, M. Bektassov, Determination of transformation products of unsymmetrical dimethylhydrazine in water using vacuum-assisted headspace solid-phase microextraction, J. Chromatogr. A. 1555 (2018) 30–36. http://doi:10.1016/j.chroma.2018.04.048.

[39] S. Risticevic, E. Carasek, J. Pawliszyn, Headspace solid-phase microextraction-gas chromatographic-time-of-flight mass spectrometric methodology for geographical origin verification of coffee, Anal. Chim. Acta. 617 (2008) 72–84. http://doi:10.1016/j.aca.2008.04.009.

[40] T.H. Borges, E. Ramalhosa, I. Seiquer, J.A. Pereira, Use of response surface methodology (Rsm) for the identification of the best extraction conditions for headspace solid-phase micro extraction (hs-spme) of the volatile profile of cv. arbequina extra-virgin olive oil, Eur. J. Lipid Sci. Technol. 120 (2018). http://doi:10.1002/ejlt.201700356.

[41] F. Stilo, E. Liberto, S.E. Reichenbach, Q. Tao, C. Bicchi, C. Cordero, Untargeted and Targeted Fingerprinting of Extra Virgin Olive Oil Volatiles by Comprehensive Two-Dimensional Gas Chromatography with Mass Spectrometry: Challenges in Long-Term Studies, J. Agric. Food Chem. 67 (2019) 5289–5302. http://doi:10.1021/acs.jafc.9b01661.

[42] C. Oliver-Pozo, R. Aparicio-Ruiz, I. Romero, D.L. García-González, Analysis of Volatile Markers for Virgin Olive Oil Aroma Defects by SPME-GC/FID: Possible Sources of Incorrect Data, J. Agric. Food Chem. 63 (2015) 10477–10483. http://doi:10.1021/acs.jafc.5b03986.

[43] C. Oliver-Pozo, D. Trypidis, R. Aparicio, D.L. Garciá-González, R. Aparicio-Ruiz, Implementing Dynamic Headspace with SPME Sampling of Virgin Olive Oil Volatiles: Optimization, Quality Analytical Study, and Performance Testing, J. Agric. Food Chem. 67 (2019) 2086–2097. http://doi:10.1021/acs.jafc.9b00477.

[44] G. Purcaro, C. Cordero, E. Liberto, C. Bicchi, L.S. Conte, Toward a definition of blueprint of virgin olive oil by comprehensive two-dimensional gas chromatography, J. Chromatogr. A. 1334 (2014) 101–111. http://doi:10.1016/j.chroma.2014.01.067.

[45] M.J. Trujillo-Rodríguez, V. Pino, E. Psillakis, J.L. Anderson, J.H. Ayala, E. Yiantzi, A.M. Afonso, Vacuum-assisted headspace-solid phase microextraction for determining volatile free fatty acids and phenols. Investigations on the effect of pressure on competitive adsorption phenomena in a multicomponent system, Anal. Chim. Acta. 962 (2017) 41–51. http://doi:10.1016/j.aca.2017.01.056.

[46] J. Pawliszyn, Handbook of Solid Phase Microextraction, First, Elsevier Inc., London, 2012.

[47] J.F. Cavalli, X. Fernandez, L. Lizzani-Cuvelier, A.M. Loiseau, Comparison of Static Headspace, Headspace Solid Phase Microextraction, Headspace Sorptive Extraction, and Direct Thermal Desorption Techniques on Chemical Composition of French Olive Oils, J. Agric. Food Chem. 51 (2003) 7709–7716. http://doi:10.1021/jf034834n.

[48] A.J. Matich, D.D. Rowan, N.H. Banks, Solid Phase Microextraction for Quantitative Headspace Sampling of Apple Volatiles, Anal. Chem. 68 (1996) 4114–4118. http://doi:10.1021/ac9604548.

[49] L. Cerretani, M.D. Salvador, A. Bendini, G. Fregapane, Relationship between sensory evaluation performed by Italian and spanish official panels and volatile and phenolic profiles of virgin olive oils, Chemosens. Percept. 1 (2008) 258–267. doi:10.1007/s12078-008-9031-3.

[50] S. Ben Temime, E. Campeol, P.L. Cioni, D. Daoud, M. Zarrouk, Volatile compounds from Chétoui olive oil and variations induced by growing area, Food Chem. 99 (2006) 315–325. http://doi:10.1016/J.FOODCHEM.2005.07.046.

[51] E. Psillakis, E. Yiantzi, N. Kalogerakis, Downsizing vacuum-assisted headspace solid phase microextraction, J. Chromatogr. A. 1300 (2013) 119–126. http://doi:10.1016/j.chroma.2013.02.009.

2. Sub-ambient temperature sampling of fish volatiles using vacuum-assisted headspace solid phase microextraction: Theoretical considerations and proof of concept

Based on: N. Delbecque, S. Mascrez, E. Psillakis and G. Purcaro, *Sub-ambient temperature sampling of fish volatiles using vacuum-assisted headspace solid phase microextraction: Theoretical considerations and proof of concept*, Analytica Chimica Acta, 1192 (2022) 339365.

2.1. Abstract

The extraction of volatiles from perishable food at a sub-ambient temperature using headspace solid-phase microextraction (HS-SPME) was never considered due to the corresponding loss in sensitivity. We propose HS-SPME sampling under vacuum (Vac-HS-SPME) to compensate problems of sensitivity loss and achieve substantial improvement in extraction efficiencies whilst sampling at temperatures as low as 5 ºC. The approach was applied to fish samples, representing a highly vulnerable perishable food sample. The theoretical considerations explaining the performance of Vac-HS-SPME at sub-ambient temperatures are discussed and related to the increase in gas diffusivities when sampling under vacuum. A comparative study between Vac- and regular HS-SPME for the extraction of 18 compounds from salmon was carried out at different temperatures (5, 30 and 40 °C) and sampling times (10-60 min). For the majority of the compounds, Vac-HS-SPME at 5 °C yielded similar or superior extraction efficiencies than regular HS-SPME even when sampling at 40 °C. However, four compounds were better extracted at 1 atm presumably due to the intensification of competitive adsorption of analytes on the SPME fiber under vacuum or the partial losses of more volatile analytes during air-evacuation in the presence of the frozen samples. Sub-ambient temperature sampling (5 °C) combined with Vac-HS-SPME was also applied to monitor the changes in the volatile profile of salmon, redfish, and cod refrigerated for up to five days. The results were compared and discussed to those obtained with regular HS-SPME at 40 °C. Overall, this contribution opens the door to a new and more powerful approach for the analysis of volatiles in refrigerated foods and has a great potential for quality control and freshness assessment.

2.2. Introduction

Fish represents a valuable diet component and at the same time, a highly vulnerable and perishable food that suffers rapid quality deterioration from harvesting to retailing when not properly handled and stored [1]. The decline in sensory quality generally results from different chemical, enzymatic autolytic and microbial processes, and it is perceived as the loss of freshness and spoilage

development [2–5], the rates of which, depend on many factors such as kind of fish species, storage time, and temperature [6].

The high demand for fresh fish highlighted the necessity for effective methods to assess its quality and freshness. To this end, several methods have been used to monitor fish quality, including sensory, microbiological, physical, and chemical analysis [7]. Regarding the latter, sample preconcentration followed by gas chromatography (GC) is a widespread approach to analyze low concentrations of fish volatiles [2,3]. Among the different sample preparation methods, dynamic headspace extraction is the preferred technique, offering good sensitivity and efficacy [3]. In an attempt to simplify the sample preparation step, solid-phase microextraction (SPME) was previously proposed for sampling fish volatiles [2,3,7–9]. For complex samples, such as fish, the headspace SPME (HS-SPME) sampling mode is adopted where the SPME fiber is placed in the headspace above the sample [10,11]. HS-SPME equilibration times span from a few minutes to several hours, depending on many variables, such as the sample type and properties of the target analytes [12]. Stirring the sample and increasing the temperature are the most exploited strategies to improve analyte volatilization from the sample and accelerate extraction kinetics [11]. However, stirring is not always possible (e.g., in the case of solid samples), and the use of high temperatures may reduce the affinity of analytes for the SPME fiber and as such, result in sensitivity losses [11]. For fish samples, HS-SPME sampling temperatures usually range from mild (e.g., 30 min sampling 40 ºC [3]) to high temperatures (e.g., 90 min sampling 60 ºC or 2 h at 50 ºC [7,13]). However, even at mild sampling temperatures, the volatile profile of the originally refrigerated fish sample may be altered.

An alternative and less explored strategy to improve HS-SPME extraction kinetics is sampling under reduced pressure conditions, in a method termed vacuum-assisted HS-SPME (Vac-HS-SPME). Vac-HS-SPME has been successfully applied to various analytes and matrices, including water, solids, and complex food matrices like wine, dairy products, and extra virgin olive oil [12,14,15]. Translated in practice, Vac-HS-SPME was found to accelerate extraction kinetics and resulted in improved extraction efficiencies even at mild sampling temperatures and/or short sampling times.

The use of HS-SPME sampling from perishable food at a sub-ambient temperature was never considered due to the substantial loss in sensitivity. The aim of this work was to investigate for the first time the potential of Vac-HS-SPME for sampling volatiles at a temperature well below that of room temperature (i.e., 5 °C representing refrigerator temperature). The theoretical considerations explaining the superior performance of Vac-HS-SPME at sub-ambient temperatures are discussed. To demonstrate the benefits of adopting the vacuum approach, a comparative study between Vac-HS-SPME and regular HS-SPME sampling was carried out at different sampling temperatures and times. Raw fish was chosen as a case study being an excellent example of a sample that would benefit from the sub-ambient temperature sampling. Finally, changes in the volatile profiles from three types of raw refrigerated fish samples were monitored on a daily basis and for up to five days

using Vac-HS-SPME at 5 °C, and the results were compared to those obtained with regular HS-SPME at 40 °C.

2.3. Theoritical considerations

Temperature significantly effects analyte's partitioning properties, with partition coefficients and vapor pressures being more sensitive to temperature variations because of the large enthalpy change associated with transfer to the vapor phase [16]. The simplest general correlation for expressing the effect of temperature on equilibrium constants is the integrated van't Hoff correlation [16], which assumes a constant change in enthalpy over the narrow environmental temperature range [17]. The magnitude of the temperature effect will depend on the properties of the compounds and phases involved and it is expected to be more significant if the gas phase is involved [17]. It should be noted here that the van't Hoff correlation also assumes partitioning between homogenous phases, which is not valid for the partitioning between an SPME fiber and a multi-component sample. Nonetheless, it can be used to estimate the effect [11]. The van't Hoff correlation predicts that setting the sampling temperature at a value below that of room temperature during HS-SPME will reduce the partition coefficient between the headspace and the sample. At the same time, the SPME fiber coating/headspace partition coefficient will increase when decreasing the sampling temperature; an effect also recorded during partitioning equilibria between water, air and octanol [18]. However, this increased affinity for the SPME fiber will have a limited impact on extraction efficiencies, given that at sub-ambient sampling temperatures, vapor pressures and, as such, analyte headspace concentrations are decreased, as predicted by the Clapeyron equation [16]. It should be noted here that SPME fiber coating/headspace partition coefficients were also reported to increase with the cold-fiber SPME approach [19], where the sample matrix is heated at an elevated temperature whilst maintaining the fiber at a cool temperature. Cold-fiber SPME facilitates the mass transfer and the release of analytes into the headspace but also creates a temperature gap between the cold fiber coating and the hot headspace. Since absorption is an exothermic process, this temperature gap significantly increases the partition coefficients of analytes and improves extraction efficiencies [19,20]. Based on the above considerations, the cold-fiber SPME system is different from the one investigated here, where the sample, headspace, and fiber are all maintained at the same temperature, and as such, there is no temperature gap.

In general, lowering the total pressure can only affect the extraction efficiency of analytes at a pre-equilibrium stage [17]. During HS-SPME and assuming fast equilibration between the headspace/SPME fiber coating, sampling under vacuum will improve mass transfer rates from the sample to the headspace [12]. For liquid samples, the pressure dependence of pre-equilibrium HS-SPME sampling was explained using the classic two-film theory whereby reducing the total pressure was found to reduce gas-phase resistance due to the corresponding increase in gas-phase diffusion coefficients, Dg [14]. A modified form of Fick's law of diffusion was used

for solid samples to describe the vapor flux assumed to diffuse through a stagnant boundary layer located between the solid and the air [21]. This relationship showed that the vapor flux of chemicals at the soil surface would increase when lowering the sampling pressure due to the simultaneous increase in Dg. It should be noted here that the improvement in Dg values under vacuum will also result in faster transport of analytes in the bulk gas phase; though this does not represent a rate-limiting step [22].

The gas-phase diffusion coefficient of a trace compound A is often given by the Fuller-Schettler-Giddings correlation [14]:

$$D_g = \frac{0.001 \times T^{1.75} \sqrt{\frac{1}{M_{air}} + \frac{1}{M_A}}}{P[(\sum V_{air})^{\frac{1}{3}} + (\sum V_A)^{\frac{1}{3}}]^2} \quad (1)$$

where P, is the total pressure, Mair and MA respectively the molecular weights of air and the analyte, and Vair and VA the molar volumes of air and the analyte. Eq. (1) reveals the temperature and pressure dependencies of D_g and predicts improvements in D_g, and as such, in the overall HS-SPME extraction kinetics, when increasing the sampling temperature and/or decreasing the total pressure. The combined effects of lowering the sampling temperature and the total pressure were never considered in the past. To this end, providing calculations on D_g as a function of these two parameters can give some important insights taken that D_g is directly related to the effect of vacuum on HS-SPME regardless of the sample matrix. Accordingly, at any given temperature, reducing the sampling pressure from 1 to 0.04 atm (typical value considered in Vac-HS-PME for water-containing samples [23]) will improve D_g values more than 25 times for any given analyte [23]) This relative improvement in D_g will be the same regardless of the chosen temperature since the effects of other components in Eq. (1) cancel each other out. The effect of vacuum on D_g is significantly larger than that of decreasing the temperature from e.g., 30 ºC to 5 ºC at a constant total pressure. In this case, and assuming a small effect of temperature on molar volumes for the temperature range considered [17], D_g values will be reduced by only 14%. The strong effect of total pressure on diffusivities is further demonstrated when calculating the combined effects of lowering the total pressure and temperature on D_g values, where moving from 30 ºC and 1 atm to 5 ºC and 0.04 atm yields a 22-fold improvement in D_g. The above calculations imply that sampling under vacuum and at a sub-ambient temperature may improve HS-SPME extraction kinetics, since D_g improvements will remain significant. The only limitation to this effect can be the negative effect of temperature on headspace analyte concentrations and partition constants between the headspace and sample. However, the faster mass transfer rates at a reduced total pressure may actually result in faster replenishment of the analytes' headspace concentrations, leading to faster overall HS-SPME extraction kinetics.

2.4. Materials and methods

2.4.1. Chemicals and materials

Normal alkanes (C7-C30), CAR/PDMS, PDMS/DVB and DVB/CAR/PDMS (df 50/30 µm/ 2 cm length) fibers were kindly provided by MilliporeSigma, the life science business of Merck KGaA (Darmstadt, Germany). Each SPME fiber was conditioned as recommended by the manufacturer. Prior to use, vials and caps were kept at 65 °C to remove any contaminants. Fish fillets were purchased from a local supermarket (Gembloux, Belgium) and consisted of salmon fillet (Oncorhynchus sp.), cod (Gadus sp.), and redfish (Sebastes norvegicus (Ascanius, 1772)).

2.4.2. Preparation of fish samples

During preliminary studies and investigations on the effects of sampling temperature and time, a freshly bought salmon fillet was left for 24 h at room temperature to intensify the presence of volatiles. Then the fish was homogenized in a blender (VEO Home, KWG-130B, France), portioned, weighted to 5.0 ± 0.5 g, placed in 20-mL vials (Restek, Bellefonte, USA), capped with metallic screw caps with a hole and polytetrafluoroethylene (PTFE)/silicone septa (Restek), and stored in a freezer (-18 °C) until analysis. The same salmon fillet sample was used for the entire set of these studies.

For the spoilage assessment, salmon, cod, and redfish were bought fresh early in the morning and directly homogenized and portioned (5.0 ± 0.5 g) in 20-mL vials, capped and stored aerobically at 4 °C until analysis.

2.4.3. Vac- and regular HS-SPME extraction procedures

The specially designed vial closures used for Vac-HS-SPME sampling were provided by Prof. Elefteria Psillakis [24]. Each closure was equipped with a cylindrical Thermogreen®LB-1 septum (Supelco) with half-hole (6 mm diameter × 9 mm length) and could provide gastight fit to the 20 mL screw top vials as well as allow automation of the method. The samples were removed from the freezer, the metallic screw caps were replaced by the special vial closures, and the air inside the vial was evacuated for 1 min using a MD 4C diaphragm vacuum pump (7 mbar = 0.007 atm ultimate vacuum without gas ballast, Vacuubrand GmbH & Co. KZ, Wertheim, Germany). The samples were then defrosted for 10 minutes at room temperature before analysis. For regular HS-SPME the air-evacuation step was omitted and the metallic screw caps and vials containing the fish sample were used as stored. The capped vials containing the fish sample were placed in the autosampler when extraction was done at temperatures above 30 °C. Extractions at 5 °C were carried out manually using an iced water bath. In all cases, fish smples were left to equilibrate for 10 min with the headspace at a preset extraction temperature (5, 30 or 40 °C) before Vac-HS-SPME or regular HS-SPME at the preset sampling time (ranging from 10–60 min) as discussed in the text. All experiments were run in triplicate.

For the fish spoilage investigations, the changes on the volatile profile of the three studied fish samples during storage in the refrigerator were monitored by analyzing the samples in triplicate every day and for up to 5 days (d0-d4) using regular HS-SPME at 40 °C and Vac-HS-SPME at 5 °C. The sampling time for this set of studies was 30 min.

2.4.4. GC-MS analysis

An Agilent 7890B GC coupled to a 5977 mass spectrometer detector (for this detector the acronym MS instead of MSD is used in the text) was used for all analyses. Helium was used as carrier gas at 1 mL/min flow rate. Cooling the column below ambient temperature was not possible and to avoid excessive broadening in time of the early eluting compounds, the SPME fiber was desorbed in the GC inlet at 250 °C for 2 min with a 1:5 split ratio in order to accelerate the transfer of compounds from the injector into the GC column [25]. Separation was performed on a 30 m × 0.25 mm i.d. × 0.5 μm df SLB-5ms capillary column [(silphenylene polymer, practically equivalent in polarity to poly(5%diphenyl/95% methylsiloxane)] kindly provided from MilliporeSigma (Bellefonte, PA, USA). The GC oven temperature program was as follows: 35 °C for 2 min, programmed to 250 °C at a rate of 12 °C/min and then increased to 300 °C at a rate of 25 °C/min. The MS was operating in EI at 70 eV, the source and quadrupole temperatures were set at 250 °C and 150 °C, respectively. The results were recorded in the full scan mode in the 35-500 m/z range. Data were acquired by MassHunter GC/MS Acquisition software B.07.06.2704 (Agilent, USA), converted into AIA by MSD ChemStation F.001.03.2357 (Agilent) and processed using Shimadzu GCMSolution ver 4.45 (Shimadzu, Japan). Putative identification was based on the combination of a dual filter, namely: (i) the MS similarity with the NIST17 library and the FFNSC library (Shimadzu) (≥80%) and, (ii) the experimental linear retention index (LRI) within a ±10 range compared to the one reported in the FFNSC library for the same column stationary phase and geometry.

The SPME fiber was conditioned for 20 min in the GC injector before starting any analytical sequence. Blanks were run periodically to ensure the absence of carry-over between runs.

2.5. Results and discussion

2.5.1. Preliminary experiments

In a preliminary set of experiments, the entire fish volatile profile of the salmon fillet was investigated at 30 °C and for 30 min of sampling using three different SPME fibers (namely: PDMS/DVB, CAR/PDMS and DVB/CAR/PDMS) with Vac- and regular HS-SPME. From the resulting spectra, 18 compounds were selected and tentatively identified based on the similarity match with commercial databases (NIST and FFNSC) and an experimental LRI having ± 10 units compared to the LRI reported in the commercial databases. The selected compounds, shown in Table 4-3,

covered the volatility range of different chemical classes (alkanes, aldehydes, alcohols) and were previously reported as markers for fish [26-32]. One of the selected compounds consisted of butylated hydroxytoluene (BHT), an antioxidant often added to food and animal feed, including farmed fish feed [33]. Monitoring BHT was of interest, taken that this compound is subject to regulation, and an acceptable daily intake (ADI) of 0 - 0.3 mg/kg body-weight was recommended by the World Health Organization [34].

Table 4-3: List of the 18 selected compounds together with their Chemical Abstracts Service (CAS) number, molecular weight (M_W), boiling point (B_p), octanol-air partition coefficients (logKoa), linear retention index experimentally calculated (LRI_{exp}) and reported in the literature (LRI_{lib}), mass spectra similarity (MS%) and the ion used for area determination (Quantifier).

n°	NAME	CAS	M_W (g mol^{-1})	B_p (°C)	logK_{oa}	LRI_{exp}	LRI_{lib}	MS%	Quantifier (*m/z*)
1	Butanal, 2-methyl-	96-17-3	86.132	94	3.417	658	662	98	44
2	Butanal, 3-methyl-	590-86-3	86.132	92	3.011	665	676	96	57
3	2,4-dimethyl-heptane	2213-23-2	128.255	115	2.396	792	788	92	43
4	Styrene	100-42-5	104.149	145	3.899	891	891	90	104
5	Heptanal	111-71-7	114.185	153	4.247	901	906	87	70
6	2,6-Dimethyl-4-heptanol	108-82-7	144.254	178	5.358	949	950	85	43
7	Octanal	124-13-0	128.212	171	4.457	1003	1006	89	43
8	Benzeneacetaldehyde	122-78-1	120.148	195	5.43	1048	1045	97	91
9	Nonanal	124-19-6	142.239	214	4.793	1104	1107	93	57
10	Dodecane	112-40-3	170.335	216	3.573	1199	1200	93	57
11	Decanal	112-31-2	156.265	208	4.893	1206	1208	88	57
12	Tridecane	629-50-5	184.361	235	4.659	1299	1300	88	57
13	Tetradecane	629-59-4	198.388	253	4.625	1399	1400	94	57
14	Pentadecane	629-62-9	212.415	269	4.998	1499	1500	95	57
15	BHT	128-37-0	220.35	265	8.874	1507	1503	92	205
16	Hexadecane	544-76-3	220.35	287	6.914	1598	1600	90	57
17	Heptadecane	629-78-7	240.468	302	5.493	1699	1700	95	57
18	Octadecane	593-45-3	254.494	317	5.859	1798	1800	90	57

The extraction efficiencies obtained for the 18 selected compounds when using each of the three tested SPME fibers are given in Figure 4-9.

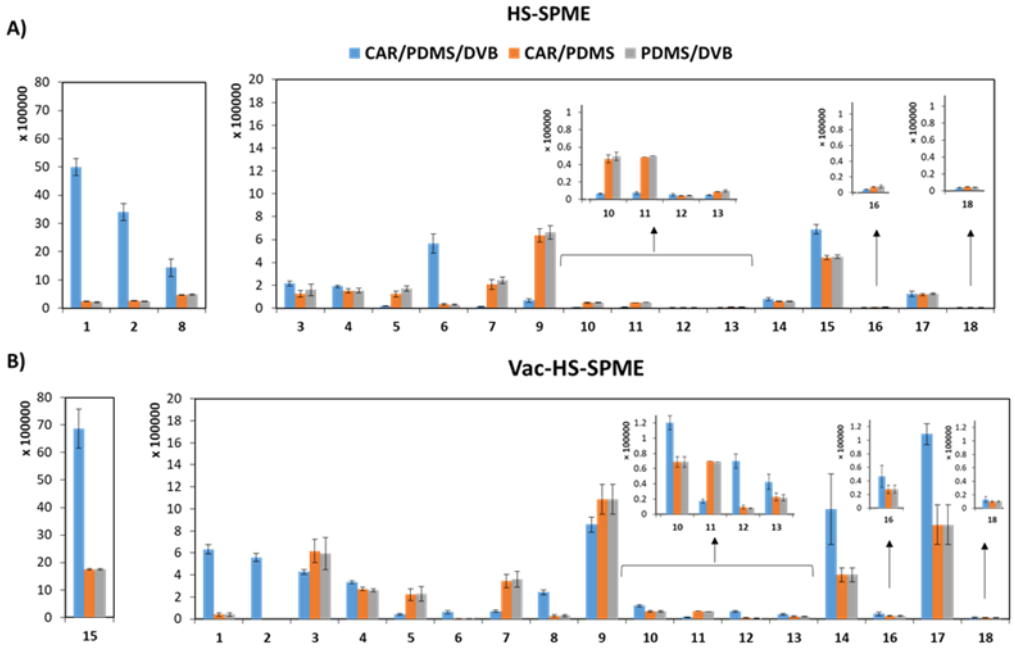

Figure 4-9: *Response surface for 1-hexanol (v12) under a) regular HS-SPME and b) Vac-HS-SPME.*

Figure 4-9 shows that during regular HS-SPME, the DVB/CAR/PDMS fiber showed the highest extraction yield for eight out of the 18 selected markers (2-methyl-butanal (1), 3-methyl-butanal (2), 2,4-dimethyl-heptane (3), styrene (4), 2,6-dimethyl-4-heptanol (6), benzeneacetaldehyde (8), pentadecane (14), and BHT(15)). Heptanal (5), octanal (7), nonanal (9) and dodecane (10) were better extracted at 1 atm with CAR/PDMS or PDMS/DVB fibers (comparable results, $p > 0.05$). These two fibers showed very similar extraction yields for most selected markers, with the exception of tridecane (12), heptanal (5) and octadecane (18). Tridecane and heptanal were better extracted with PDMS/DVB and octadecane with CAR/PDMS ($p < 0.05$).

With Vac-HS-SPME, the DVB/Car/PDMS fiber yielded higher extraction yields for 12 compounds out of 18 selected markers ($p < 0.05$). Only heptanal (5), octanal (7), were significantly better extracted using either CAR/PDMS or PDMS/DVB, while hexadecane (16) and octadecane (18) gave comparable results among the three different fibers ($p > 0.05$).

In accordance with a past report [3], DVB/CAR/PDMS fiber showed the highest extraction yield for most markers under each pressure condition, and for this reason, it was selected for further experiments. Moreover, increased extraction efficiencies were obtained with Vac-HS-SPME compared to HS-SPME and the only exceptions were (1) 2-methyl-butanal, (2) 3-methyl-butanal, (6) 2,6-dimethyl-4-heptanol and

(8) benzeneacetaldehyde that were better extracted under regular pressure conditions. During the present studies, air evacuation proceeded in the presence of the frozen samples and for a short period of time (1 min). Although these conditions were chosen so as to minimize the aspiration of volatile analytes [35], the partial loss of the more volatiles target analytes (especially (1) 2-methyl-butanal, (2) 3-methyl-butanal) cannot be excluded. Another possible explanation for the low extraction efficiencies of these four analytes when sampling under vacuum, may be competitive adsorption onto the SPME fiber. Indeed, in complex samples, such as the fish samples investigated here, competition for space onto the adsorbent DVB/CAR/PDMS fiber can be more intense, as the higher headspace concentrations compared to 1 atm can displace minor components or compounds with less affinity for the adsorbent [11,36].

In general, Vac-HS-SPME sampling resulted in richer GC traces compared to the one obtained when sampling at 1 atm. Eluting compounds that were not included in Table 4-3 consisted of secondary metabolites and siloxanes. As reported in the past, the presence of high amounts of water-immiscible hydrocarbons in the headspace and the use of a solid sorbent accelerated swelling of the fiber and increased the presence of siloxanes [25]. During this initial set of investigations, attempts were also made to avoid coelution. However, it was not possible to completely prevent partial coelution of some compounds under any conditions, especially with Vac-HS-SPME. For this reason, some rather high relative standard deviations (RSD %) were recorded for some compounds (>20%).

2.5.2. Effects of temperature and sampling time

The extraction time profiles of the 18 selected compounds were obtained under reduced and atmospheric pressure conditions at three different sampling temperatures, with 5 °C representing the refrigerator temperature, 30 °C being close to room temperature and the lowest value that could be set at the autosampler, and 40 °C representing a commonly applied temperature for sampling fish samples [3]. Richer profiles and enhanced extraction efficiencies were recorded with Vac-HS-SPME, even when sampling at a temperature as low as 5 °C. Figure 4-10 shows a comparison between the chromatograms obtained at 5 °C with Vac- and regular HS-SPME.

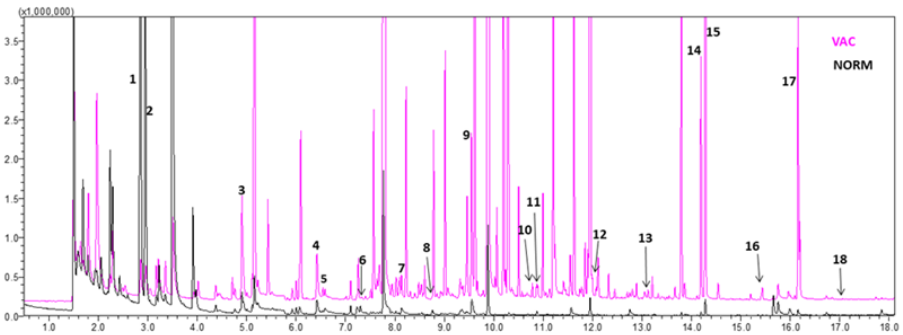

Figure 4-10: *Comparison of the total ion chromatograms obtained using regular HS-SPME (black, bottom chromatogram) and Vac-HS-SPME (fuchsia, upper chromatogram) for sampling the volatile profile of salmon fillet. Coding of compounds as in Table 4-3. Other experimental parameters: DVB/CAR/PDMS fiber, 30 min of sampling at 5 °C.*

Figure 4-11 summarizes the results obtained at the different temperatures and times tested under the two pressure conditions. The complete information on average peak area and RSD values obtained from the present studies is given in Table 4-4. As expected, extraction efficiencies increased with increasing sampling temperature and time. Figure 4-11 also illustrates the positive effect of vacuum at each sampling time and temperature for the majority of the selected compounds. For reasons discussed earlier, the only compounds that were not efficiently extracted under vacuum compared to atmospheric pressure were compounds (1), (2), (6) and (8).

Table 4-4: Average peak areas obtained with regular HS-SPME and Vac-HS-SPME at different sampling times (10, 20, 30, 40, 60 min) and temperatures (T: 5 °C, 30 °C, and 40 °C) tested. The relative standard deviations (RSD) from the triplicate runs are also given. Coding of compounds (#) as in Table 4-3.

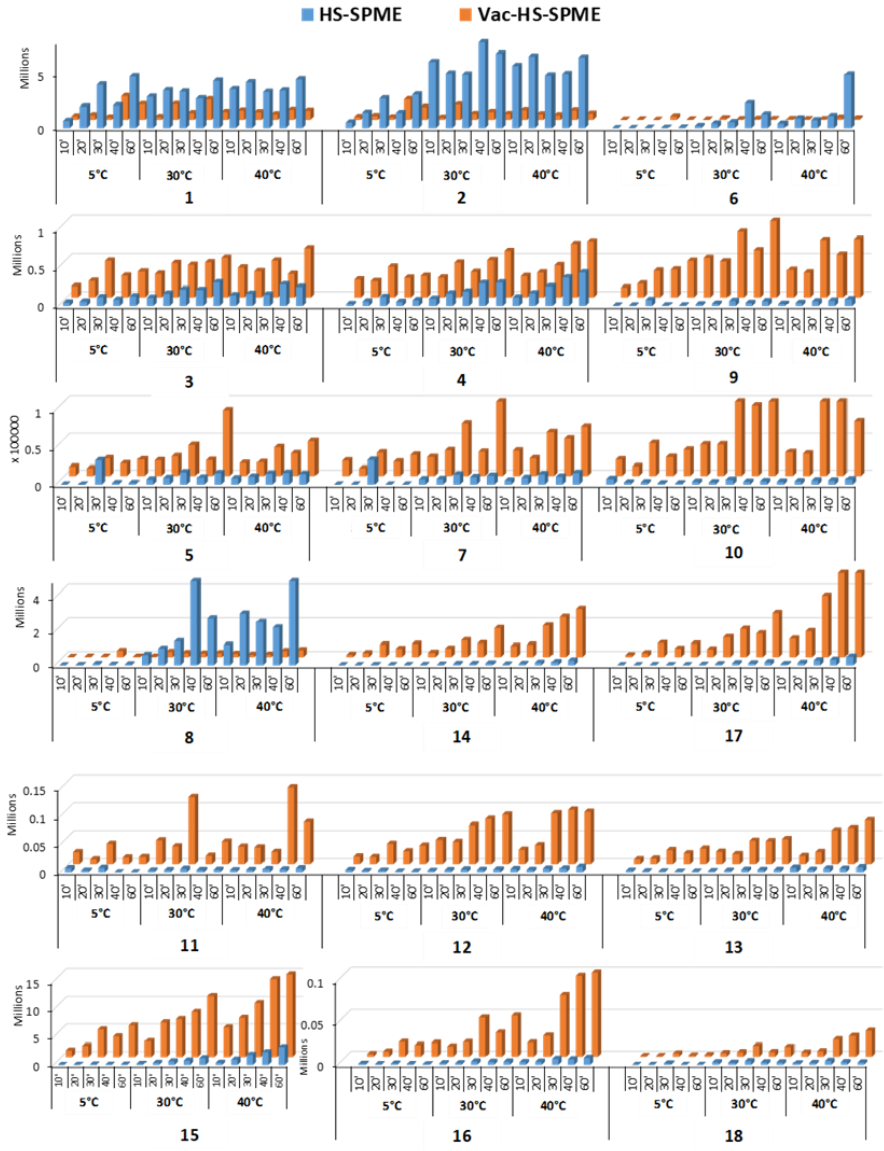

Figure 4-11: *Extraction time profiles (10-60 min of sampling) of the selected compounds in salmon obtained under regular (HS-SPME; blue bars) and reduced total pressure (Vac-HS-SPME; orange bars) at different sampling temperatures (5, 30 and 40 °C). Coding of compounds as in Table 4-3. Analytes are grouped based on analytical signals rather than shown in increasing coding numbers. Error bars cannot be reported with this visualization and this information is given in Table 4-4.*

Table 4-4: Average peak areas obtained with regular HS-SPME and Vac-HS-SPME at different sampling times (10, 20, 30, 40, 60 min) and temperatures (T: 5 °C, 30 °C, and 40 °C) tested. The relative standard deviations (RSD) from the triplicate runs are also given. Coding of compounds (#) as in Table 6.3.

			Average		**RSD**	
#	**T**	**Time**	**HS-SPME**	**Vac-HS-SPME**	**HS-SPME**	**Vac-HS-SPME**
1	**5 °C**	**10'**	775230	321449	14	12
		20'	2011721	425461	21	12
		30'	4078668	222189	5	16
		40'	2121856	2202200	23	0
		60'	4499914	1508193	16	17
	30 °C	**10'**	3090262	255545	13	18
		20'	3529624	1457939	19	16
		30'	3398490	633554	9	7
		40'	2758616	1896628	15	17
		60'	4431872	740861	13	15
	40 °C	**10'**	3624713	902729	8	14
		20'	4275533	723857	16	19
		30'	3132497	511404	21	17
		40'	3501463	966816	9	8
		60'	4556706	862526	27	25
2	**5 °C**	**10'**	608135	259947	11	9
		20'	1461657	351669	23	12
		30'	2763051	227631	7	11
		40'	1426440	1902655	8	9
		60'	3026970	1122160	18	16
	30 °C	**10'**	6176267	192659	23	20
		20'	5082921	1396284	16	18
		30'	4988272	558377	14	7
		40'	8129255	747838	22	18
		60'	6946970	558503	17	8
	40 °C	**10'**	5790331	928040	13	20
		20'	6688638	531593	12	19
		30'	4568889	393719	21	23
		40'	5037640	966815	6	8
		60'	6600202	597351	17	10
3	**5 °C**	**10'**	45638	148464	19	18
		20'	57224	216974	12	2
		30'	114206	481936	12	9

		40'	81836	285760	22	12
		60'	125226	338715	20	19
	30 °C	**10'**	108271	310665	7	22
		20'	162800	452277	23	21
		30'	216928	427387	9	5
		40'	209667	465422	8	14
		60'	295503	486702	18	17
	40 °C	**10'**	132558	419640	18	13
		20'	160310	344328	22	20
		30'	148959	461843	10	20
		40'	281231	308015	8	5
		60'	249728	643661	2	11
4	**5 °C**	**10'**	24805	234380	14	3
		20'	59001	213642	8	9
		30'	118463	403296	5	5
		40'	54990	257145	17	19
		60'	75020	281240	28	11
	30 °C	**10'**	94801	259242	14	5
		20'	165725	456679	21	18
		30'	190485	333798	6	5
		40'	298162	489141	8	7
		60'	305227	608753	11	22
	40 °C	**10'**	111153	279558	13	7
		20'	167005	326810	13	3
		30'	256558	423111	25	5
		40'	372265	700873	2	17
		60'	437990	735615	13	8
5	**5 °C**	**10'**	0			18
		20'	0	10493		13
		30'	33746	23880	15	3
		40'	2024	17038	23	19
		60'	1977	22342	40	12
	30 °C	**10'**	7041	21143	22	24
		20'	9141	26293	11	14
		30'	16857	41947	14	23
		40'	9640	21538	11	8
		60'	15666	87858	19	5
	40 °C	**10'**	8617	17709	6	20
		20'	10262	19895	18	16
		30'	14957	39814	18	20

		40'	15992	30648	23	8
		60'	14442	47206	23	6
6	**5 °C**	**10'**	0	16122		3
		20'	7415	31929	31	6
		30'	31594	4904	2	9
		40'	23858	325952	6	25
		60'	56273	31751	10	10
	30 °C	**10'**	195761	17494	10	21
		20'	436647	136200	19	6
		30'	564727	64065	15	21
		40'	2307550	95061	15	6
		60'	1301307	82117	20	19
	40 °C	**10'**	425511	80741	17	11
		20'	907158	59555	9	8
		30'	752497	66007	15	14
		40'	1131818	204631	28	13
		60'	4994881	139094	24	19
7	**5 °C**	**10'**	0	20754		11
		20'	0	10409		15
		30'	34935	31658	18	20
		40'	0	20055		19
		60'	0	28537		15
	30 °C	**10'**	7360	25493	11	11
		20'	7658	34751	13	23
		30'	13741	71216	9	12
		40'	10301	32630	13	11
		60'	12208	156099	18	12
	40 °C	**10'**	5658	34316	18	20
		20'	9367	23889	2	11
		30'	14004	59308	13	23
		40'	10875	50803	6	16
		60'	15920	66594	26	1
8	**5 °C**	**10'**	0	18449		16
		20'	12450	29251	15	0
		30'	78891	36787	20	14
		40'	34362	376079	23	22
		60'	53496	34673	15	12
	30 °C	**10'**	613317	30193	24	19
		20'	1001213	317184	2	11

		30'	1428171	241811	3	8
		40'	6090115	208475	13	16
		60'	2789496	232009	18	22
	40 °C	**10'**	1217114	220891	18	14
		20'	3072244	131009	12	16
		30'	2581531	150363	11	8
		40'	2252936	362698	10	18
		60'	6351491	422560	21	21
9	**5 °C**	**10'**	4412	116585	10	10
		20'	6041	164186	12	13
		30'	79668	351201	15	12
		40'	7285	367566	21	17
		60'	7687	480343	22	14
	30 °C	**10'**	22022	518393	19	23
		20'	29424	471908	22	16
		30'	66793	857782	21	8
		40'	39787	618329	7	19
		60'	62119	1070794	17	21
	40 °C	**10'**	27913	358187	5	9
		20'	39301	325590	5	11
		30'	60950	753735	7	14
		40'	69956	560503	8	13
		60'	87617	763998	11	27
10	**5 °C**	**10'**	7668	22238	18	18
		20'	2866	13229	18	7
		30'	3119	44481	18	3
		40'	1531	25629	11	13
		60'	1592	35561	31	9
	30 °C	**10'**	3961	42744	2	11
		20'	3156	42856	13	18
		30'	6521	120277	12	8
		40'	3971	94551	6	19
		60'	4728	178500	30	7
	40 °C	**10'**	4011	32101	6	15
		20'	4503	30283	8	6
		30'	5714	125147	3	22
		40'	5641	138142	1	5
		60'	7155	74212	16	10
11	**5 °C**	**10'**	7544	21917	16	20

		20'	3078	9150	17	16
		30'	8191	38873	22	14
		40'	0	12350		15
		60'	0	13135		20
	30 °C	**10'**	3322	43173	13	18
		20'	3858	35045	7	10
		30'	6521	120277	12	8
		40'	4059	15348	8	3
		60'	4728	40900	30	5
	40 °C	**10'**	3762	31776	7	19
		20'	4185	30283	16	6
		30'	5887	22405	7	12
		40'	5255	137948	11	6
		60'	7396	75578	12	11
12	**5 °C**	**10'**	4017	13515	31	14
		20'	2335	13216	24	2
		30'	3120	36833	22	7
		40'	1491	23495	16	12
		60'	1336	33528	15	12
	30 °C	**10'**	2423	37161	8	4
		20'	4002	40317	31	11
		30'	5343	70110	29	13
		40'	4499	84350	11	16
		60'	5136	88770	17	4
	40 °C	**10'**	5957	26164	24	17
		20'	4571	34421	10	4
		30'	6777	90924	9	12
		40'	6971	97284	12	9
		60'	10041	93626	11	17
13	**5 °C**	**10'**	3177	9241	28	22
		20'	1839	10452	11	11
		30'	1515	25709	23	16
		40'	1152	20407	20	20
		60'	1515	28171	9	10
	30 °C	**10'**	1997	22627	20	15
		20'	3077	18324	25	6
		30'	4729	42477	13	24
		40'	4098	44837	21	16
		60'	4453	48554	13	15
	40 °C	**10'**	8405	15734	20	18

		20'	4703	22089	20	4
		30'	7063	59537	5	8
		40'	6672	65518	3	24
		60'	9377	78632	11	5
14	**5 °C**	**10'**	8590	137515	20	15
		20'	8059	238135	18	11
		30'	15983	741764	6	16
		40'	11738	481181	21	18
		60'	12316	782777	16	18
	30 °C	**10'**	19732	263543	12	21
		20'	42346	511472	24	20
		30'	79646	997202	17	17
		40'	76082	850820	11	12
		60'	110909	1726071	23	16
	40 °C	**10'**	46073	654553	6	8
		20'	86029	738360	9	4
		30'	160631	1877547	5	17
		40'	192968	2402806	14	6
		60'	290432	2869801	11	10
15	**5 °C**	**10'**	17296	1198889	16	21
		20'	33323	2018961	13	11
		30'	103625	4992900	14	17
		40'	67663	3819359	17	13
		60'	83694	5712505	32	15
	30 °C	**10'**	194877	2852199	11	13
		20'	394348	6270063	13	18
		30'	689560	6865892	6	10
		40'	815164	8174033	7	19
		60'	1241476	11078653	15	16
	40 °C	**10'**	410844	5341368	3	5
		20'	980403	7095083	14	2
		30'	1836295	9803722	6	8
		40'	2339381	14014180	8	2
		60'	3255652	14881938	1	6
16	**5 °C**	**10'**	1175	3367	21	3
		20'	851	6214	37	15
		30'	1450	17502	10	12
		40'	853	13828	33	22
		60'	607	16434	27	24

	30°C	**10'**	1935	12320	29	13
		20'	1849	17408	1	16
		30'	4055	46724	7	14
		40'	3645	26932	15	19
		60'	3972	42511	19	11
	40 °C	**10'**	3338	17444	24	21
		20'	3835	24894	24	5
		30'	7086	73864	10	18
		40'	6681	95992	7	18
		60'	8367	117351	6	10
17	**5 °C**	**10'**	5133	122257	3	9
		20'	7266	230994	18	11
		30'	17154	829452	4	18
		40'	9530	520880	15	16
		60'	9054	807073	17	9
	30 °C	**10'**	34730	463393	21	12
		20'	59944	1185751	21	18
		30'	124608	1678334	19	6
		40'	119630	1407558	14	20
		60'	184617	2390179	17	15
	40 °C	**10'**	69882	1095029	4	20
		20'	149268	1539888	14	4
		30'	304163	3655265	4	18
		40'	338413	5421433	24	11
		60'	525973	6182043	5	13
18	**5 °C**	**10'**	0	922		20
		20'	0	870		18
		30'	1539	4017	15	22
		40'	0	1435		30
		60'	0	1997		22
	30 °C	**10'**	2943	4469	33	14
		20'	2478	5506	21	23
		30'	4489	12948	30	4
		40'	2932	5716	16	21
		60'	2644	10426	25	18
	40 °C	**10'**	1766	5081	14	10
		20'	2317	6610	13	13
		30'	4759	20558	9	22
		40'	3280	24618	12	3

60'	2802	30840	20	27

The variability of the results, were then calculated as RSD values and the results are given in Table 4-5. As seen, the overall median (calculated by considering all selected compounds at all sampling temperatures) was 14.0% for both regular and Vac-HS-SPME. A clear decreasing trend (median value dropped from 17.0% to 11.0%) was observed with regular HS-SPME when increasing the extraction temperature. On the contrary, the calculated variability Vac-HS-SPME at the different extraction temperatures did not show any particular trend (values between 12.7 and 14.2%).

Table 4-5: Average and median RSD obtained with regular HS-SPME and Vac-HS-SPME at the different sampling times (10, 20, 30, 40, 60 min) and temperatures (T: 5 °C, 30 °C, and 40 °C) tested, as reported in Table S1. Average and median values calculated on the RSD ratio between Vac and regular HS-SPME at the different sampling times (10, 20, 30, 40, 60 min) and temperatures (T: 5 °C, 30 °C, and 40 °C) reported in Table 4-4.

	RSD HS-SPME		**RSD Vac-HS-SPME**		**RSD ratio Vac-HS-SPME/HS-SPME**	
	Average	**Median**	**Average**	**Median**	**Average**	**Median**
5 °C	17.4	17.0	13.5	13.5	0.985	0.822
30 °C	15.6	15.0	14.2	15.0	1.321	0.947
40 °C	12.3	11.0	12.7	12.0	1.645	1.000
Total	*15.0*	*14.0*	*13.5*	*14.0*	*1.335*	*0.911*

The Vac-HS-SPME/HS-SPME peak area ratios were also calculated for each sampling time and the results are depicted in Figure 4-12. Some peak area ratios could not be calculated due to the zero absolute signal obtained under atmospheric pressure (complete data set can be found in Table 4-4). The impact of low-pressure conditions on the variability of the extraction compared to regular HS-SPME was then evaluated by considering the ratio between the RSD values calculated for Vac-HS-SPME and HS-SPME for all values reported in Table 4-4. The overall median and the median for each extraction temperature was calculated with values below 1 indicating a lower RSD when sampling under vacuum conditions. An overall slight improvement was generally obtained under vacuum (ratio = 0.911), which reflected the significant improvement observed at 5 °C (0.822 median value of the RSD ratio) when sampling under vacuum. It is noted that the same variability was observed

when sampling at 40 °C under atmospheric or low-pressure conditions (median=1.000) (Table 4-5).

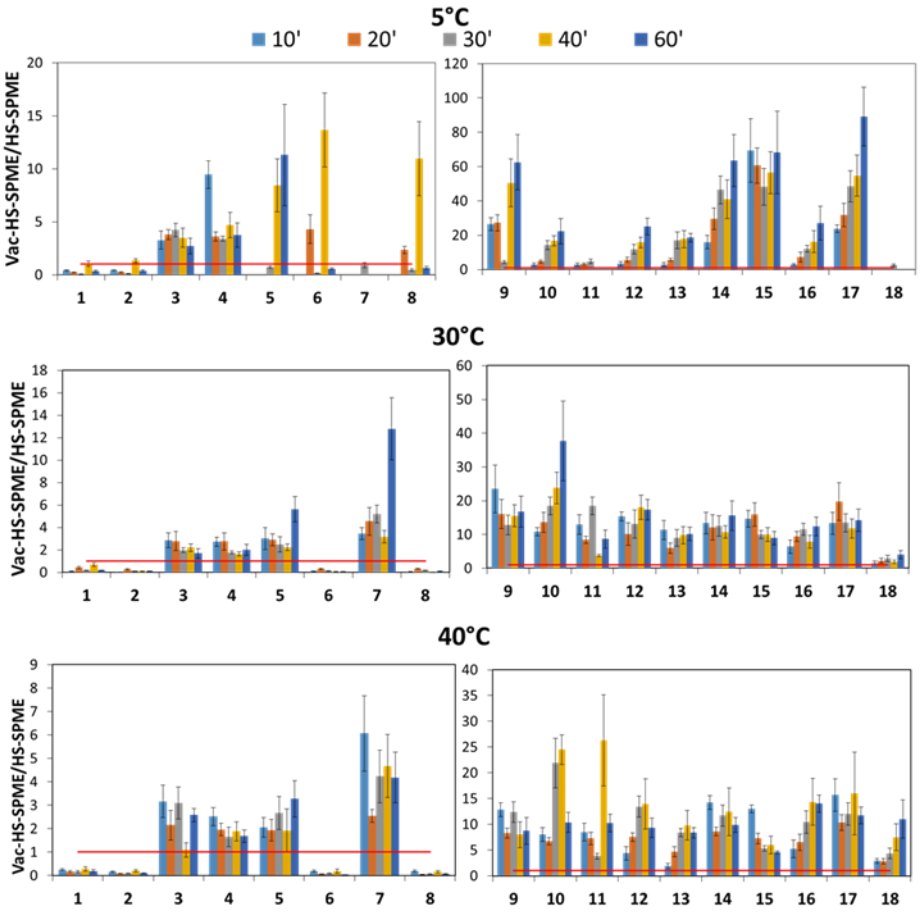

Figure 4-12: *Changes in extraction efficiency upon reducing the total pressure (expressed as Vac-HS-SPME/HS-SPME peak area ratios) at each sampling temperature and time tested here. Coding of compounds as in Table 4-3.*

The results shown in Figure 4-12 were also evaluated by considering that peak area ratios with values: >1 corresponded to improved extraction rates when sampling under vacuum; <1 corresponded to superior performance at 1 atm; and close to 1 indicated that Vac-HS-SPME and HS-SPME performed similarly i.e., equilibrium was reached under both pressure conditions [37]. Figure 4-12 shows that with the exception of the four compounds (1), (2), (6) and (8), almost all peak area ratios were >1 (with the exception of the four compounds aforementioned, i.e. (1), (2), (6) and (8)), further demonstrating the positive effect of vacuum on HS-SPME. The

largest improvements in extraction efficiencies when sampling under vacuum were obtained for later eluting compounds, corresponding to the least volatile analytes. For these analytes, very high peak area ratios were recorded especially for decreased sampling temperatures and extended sampling times, e.g., at 5 °C and 60 min of sampling, the extraction efficiency of heptadecane (17) was close to 80 times larger with Vac-HS-SPME compared to regular HS-SPME.

By far, the most important point to note was the exceptional performance of Vac-HS-SPME at 5 °C with all target compounds being detected even for sampling times as short as 10 min. The superior performance of Vac-HS-SPME merits further discussion, especially when considering that Vac-HS-SPME sampling at 5 °C generally provided similar or higher extraction efficiencies than regular HS-SPME at 30 °C or 40 °C. To better visualize the performance of Vac-HS-SPME at 5°C, the peak area ratios obtained for Vac-HS-SPME at 5 °C over regular HS-SPME at 30 °C or 40 °C were calculated at each time tested, and the results are given in Table 6.6. As seen, the more volatile markers (3), (4) and (5) gave more or less comparable results and for the majority of the compounds eluting after compound (7), higher peak area ratios were recorded under vacuum and a cool sampling temperature. The only exceptions were the four compounds (1), (2), (6), (8) discussed earlier, and compound (18).

The latter was the least volatile analyte monitored here and it was assumed that for this analyte, temperature remained a critical parameter to control for increasing headspace concentrations.

Table 4-6: Changes in extraction efficiencies at each time tested, expressed as peak area ratios of Vac-HS-SPME at 5 °C over HS-SPME at 30 °C or HS-SPME at 40 °C. To easily visualize the changes, color scales are applied with shades of red to white for peak area ratios taking values from 0 to 1 and shades of white to blue for peak area ratios from 1 to the highest value. Coding of compounds as in Table 4-3.

	5°C Vac-HS-SPME/ 30°C HS-SPME					5°C Vac-HS-SPME/ 40°C HS-SPME				
#	10'	20'	30'	40'	60'	10'	20'	30'	40'	60'
1	0.1	0.1	0.1	0.7	0.1	0.1	0.1	0.1	0.5	0.1
2	0.1	0.1	0	0.3	0.1	0.1	0.1	0	0.4	0.1
3	1.4	1.3	2.2	1.4	1.1	1.1	1.4	3.2	1	1.4
4	2.5	1.3	2.1	0.9	0.9	2.1	1.3	1.6	0.7	0.6
5	1.8	1.1	1.4	1.8	1.4	1.5	1	1.6	1.1	1.5
6	0.1	0.1	0	0.1	0	0	0	0	0.3	0
7	2.8	1.4	2.3	1.9	2.3	3.7	1.1	2.3	1.8	1.8
8	0	0	0	0.1	0	0	0	0	0.2	0
9	5.9	6.1	5.3	9.2	7.7	4.7	4.6	5.8	5.3	5.5
10	5.6	4.2	6.8	6.5	7.5	5.5	2.9	7.8	4.5	5
11	6.6	1.1	6.7	3	2.8	5.8	1	7.5	2.4	1.8
12	5.1	3.3	6.9	5.2	6.5	2.4	2.9	5.4	3.4	3.3
13	4.6	3.4	5.4	4.7	6.3	1.1	2.2	3.6	3	3
14	6.3	5.6	9.3	6.4	7.1	3	2.8	4.6	2.5	2.7
15	6.2	5.1	7.2	4.6	4.6	2.9	2.1	2.7	1.6	1.8
16	1.7	3.4	4.3	3.8	4.1	1	1.6	2.5	2.1	2
17	3.2	3.9	6.7	4.2	4.3	1.6	1.5	2.7	1.5	1.5
18	0.3	0.4	0.9	0.5	0.7	0.5	0.4	0.9	0.5	0.7

The present experimental results on regular HS-SPME confirmed our theoretical predictions and an overall negative effect of sub-ambient temperature sampling on extraction efficiencies was recorded. However, sampling at 5 °C and under reduced pressure conditions resulted in a significant improvement in analytical signals. Lowering the total pressure increased Dg values and enhanced analytes' transfer rates from the sample to the headspace. This acceleration in mass transfer, when combined with the increased affinity of analytes towards the fiber at a cool sampling temperature, resulted in extraction efficiencies for most target analytes that were similar or higher than those obtained with regular HS-SPME at 30 or 40 °C. The experimental results obtained with Vac-HS-SPME demonstrated that diffusivity is an important parameter to control for the successful extraction of volatiles and semi-volatiles at a sub-ambient temperature i.e., headspace concentrations can be replenished at a faster rate, leading to higher amounts of analytes extracted by the SPME fiber despite the unfavorable decrease in headspace/sample partition coefficients.

2.5.3. Changes in the profile of the target compounds during storage of different fish samples

In a subsequent set of experiments, the 18 selected compounds were monitored on a daily basis and for up to five days (d0-d4) using three different types of fishes (salmon, redfish, and cod) stored under refrigerated conditions. For comparison reasons, sampling proceeded using Vac-HS-SPME at 5 °C and regular HS-SPME at 40 °C, and the sampling time was set at 30 min. The result obtained for the five-day monitoring of one of the three fish samples (To keep spare space. Readers can find supplementary data in the corresponding article) and all information on average peak area values and RSD values are given in Table 6.7. It is noted that the sample of cod at day 3 (d2) and 40 °C was lost due to a technical problem. As expected, not all selected compounds could be detected in all three fish samples. Moreover, in accordance with past results [4], the detected compounds appeared sporadically or fluctuated during storage, while others exhibited a more consistent ascending or descending trend, depending on the type of spoiling bacteria and storage conditions.

Table 4-7: Peak areas of the 18 selected markers in salmon samples during five days (d0-d4) of refrigeration. Results obtained with regular HS-SPME and Vac-HS-SPME at 5 and 40°C after 30 min sampling. The RSD values from the triplicate runs are also given. Coding of compounds (#) as in Table 4-3.

		5°C		**40°C**	
		Vac-HS-SPME		**HS-SPME**	
#	**Storage Day**	**Average**	**RSD**	**Average**	**RSD**
1	**d0**	4288	28	3281	18
	d1	599836	16	443541	17
	d2	271204	32	205771	18
	d3	145023	1	151257	4
	d4	115299	22	26212	28
2	**d0**	0		0	
	d1	734826	14	306231	20
	d2	586394	2	163523	34
	d3	363838	13	289228	19
	d4	24793	23	75844	13

		1			
3	**d0**	19699	16	26482	0
	d1	48440	31	96410	24
	d2	73891	25	70115	29
	d3	68909	23	82290	5
	d4	29766	3	47688	33
4	**d0**	17533	23	53794	5
	d1	13338	12	31587	25
	d2	15266	21	27506	28
	d3	13431	16	11810	24
	d4	5381	18	6991	23
5	**d0**	0		2349	53
	d1	0		0	
	d2	0		0	
	d3	0		0	
	d4	0		0	
6	**d0**	0		0	
	d1	26104	31	0	
	d2	40621	19	18902	17
	d3	31575	25	12688	21
	d4	30169	23	24917	3
7	**d0**	0		26550	51
	d1	0		16830	13
	d2	0		14621	29
	d3	0		2175	36
	d4	0		3353	9
8	**d0**	0		0	
	d1	9 68172	23	47109	7
	d2	7 65673	28	1 29345	31
	d3	3 45312	9	6 11793	45
	d4	1 11566	10	30320	44
9	**d0**	0		8 12657	3
	d1	0		8 10328	41
	d2	0		8111	45

	d3	0		5715	20
	d4	0		11485	39
10	**d0**	0		1493	21
	d1	0		1729	24
	d2	0		1229	32
	d3	0		1223	7
	d4	0		578	9
11	**d0**	0		1236	14
	d1	0		0	
	d2	0		0	
	d3	0		0	
	d4	0		0	
12	**d0**	0		2658	29
	d1	0		0	
	d2	0		0	
	d3	0		0	
	d4	0		0	
13	**d0**	0		1501	35
	d1	0		0	
	d2	0		0	
	d3	0		0	
	d4	0		0	
14	**d0**	6641	17	22012	30
	d1	7586	15	14103	28
	d2	6361	12	6139	7
	d3	6878	16	5382	33
	d4	3931	20	3470	36
15	**d0**	14339 0	7	43091 3	39
	d1	12935 7	5	27093 8	37
	d2	11320 4	6	10563 6	2
	d3	93829	4	82980	30
	d4	55413	16	35378	34
16	**d0**	0		456	21
	d1	0		0	
	d2	0		0	

	d3	0		0	
	d4	0		0	
17	**d0**	7050	12	11258	28
	d1	5751	8	7451	26
	d2	4096	21	3148	7
	d3	5210	15	2811	20
	d4	3055	19	2130	17
18	**d0**	0		0	
	d1	0		0	
	d2	0		0	
	d3	0		0	
	d4	0		0	

It should be reminded at this point that this set of studies consisted of a proof of concept and several limitations existed for directly relating results to fish freshness and quality assessment. First, the analyzed fish samples had no indication of the storage time before purchase. In addition, the 18 compounds as selected for salmon samples were monitored in all three fish samples, and it is acknowledged that they may not be the ideal choice for freshness and quality assessment of the three different fish species tested here. In general, the volatile profile of fish has been investigated for quality control during shelf-life, and some indicators have been proposed for monitoring studies. However, assigning indicators is a complicated task, with the chemical composition of fish varying greatly among species and from an individual fish to another, depending on age, sex, environment, and season [38]. Moreover, different fish species may be spoiled by different specific spoilage organisms, and even if fish samples are stored under identical conditions (temperature and atmosphere), different metabolites may be produced, including off-odors and off-flavors associated with spoilage [5,39]. At the same time, the comparison between Vac-HS-SPME at 5 °C and regular HS-SPME at 40 °C, should be considered with caution since two different sampling temperatures were applied, and this may have contributed to the recorded deviations in extraction efficiencies and trends over time. In this connection, there were some cases where the target analyte exhibited not only different trends over time but also different extraction efficiencies with the two tested HS-SPME sampling methods (e.g., octanal (7)). Next to the different sampling temperatures used it should be always kept in mind that the headspace composition varied among the fish type tested. Target analytes were therefore expected to be present in varying multi-component mixtures and this may also have affected analyte uptake by the SPME fiber under the two different sampling conditions examined here [40].

Figure 4-13 compares the results on selected markers whilst using Vac-HS-SPME sampling at 5 °C and regular HS-SPME at 40 °C. Hydrocarbons are usually found at a low concentration level in the headspace of different fish species and are believed to contribute to the fish smell [41]. Here, different alkanes were detected in a relatively low content in all fish samples. Pentadecane (14) was previously proposed to highly correlate with standard indicators of fish quality, and in combination with a small number of carbonyls were previously proposed for assessing fish quality [2,7]. For the salmon and redfish samples, pentadecane was more effectively extracted with Vac-HS-SPME at 5 °C and generally exhibited a decreasing trend with increasing storage time (Figure 6.13.). This is in accordance with past studies on pentadecane sampled from salmon [7] and yellowfin tuna [2] samples. For cod samples the signals of pentadecane (14) remained low throughout the storage time tested.

Styrene (4) was also detected in all fish samples under each pressure condition and exhibited a decreasing trend. The origins of styrene are not well understood [7], and in some cases, its presence was assumed to be due to migration from packaging material [42].

In general, aldehydes are correlated to the oxidation of unsaturated fatty acids, such as oleic and linoleic acid [41]. Here, heptanal (5) was detected in redfish samples and exhibited an upward trend with increasing storage time up to four days and regular HS-SPME at 40 °C yielded higher analytical signals compared to Vac-HS-SPME at 5 °C (Figure 4-13). Octanal (7) was detected in salmon with Vac-HS-SPME at 5 °C after one day of incubation and, as seen in the past [7], after this time exhibited a decreasing trend with increasing chill-storage time. In redfish, regular HS-SPME at 40 °C gave a stronger signal for octanal (7) compared to Vac-HS-SPME and an upward trend over storage time. Nonanal (9) was detected in all three fish types and higher extraction efficiencies were recorded when using Vac-HS-SPME at 5 °C. Moreover, with the exception was redfish, a descending trend over storage time was recorded [7].

Compounds 2- and 3-methyl butanal ((1) and (2) respectively) were previously proposed to be products of bacterial activity and have been suggested as potential spoilage indicators [4]. In salmon samples, these two aldehydes showed remarkable evolution after one-day of incubation and trends were comparable under each pressure and temperature tested. On the contrary, in redfish samples, 3-methyl butanal (2) yielded close to similar extraction efficiencies between Vac-HS-SPME at 5 °C and HS-SPME at 40 °C and a fluctuating trend.

An important finding here was that BHT (15) was detected in all fish samples when using Vac-HS-SPME at 5 °C (Figure. 4-13.). Only in the case of salmon, regular HS-SPME sampling at 40 °C was successful in detecting this analyte, suggesting that a much higher total amount of this antioxidant was present in this specific fish sample. The above finding depicts the importance of adopting the Vac-HS-SPME approach to achieve higher sensitivity for this additive.

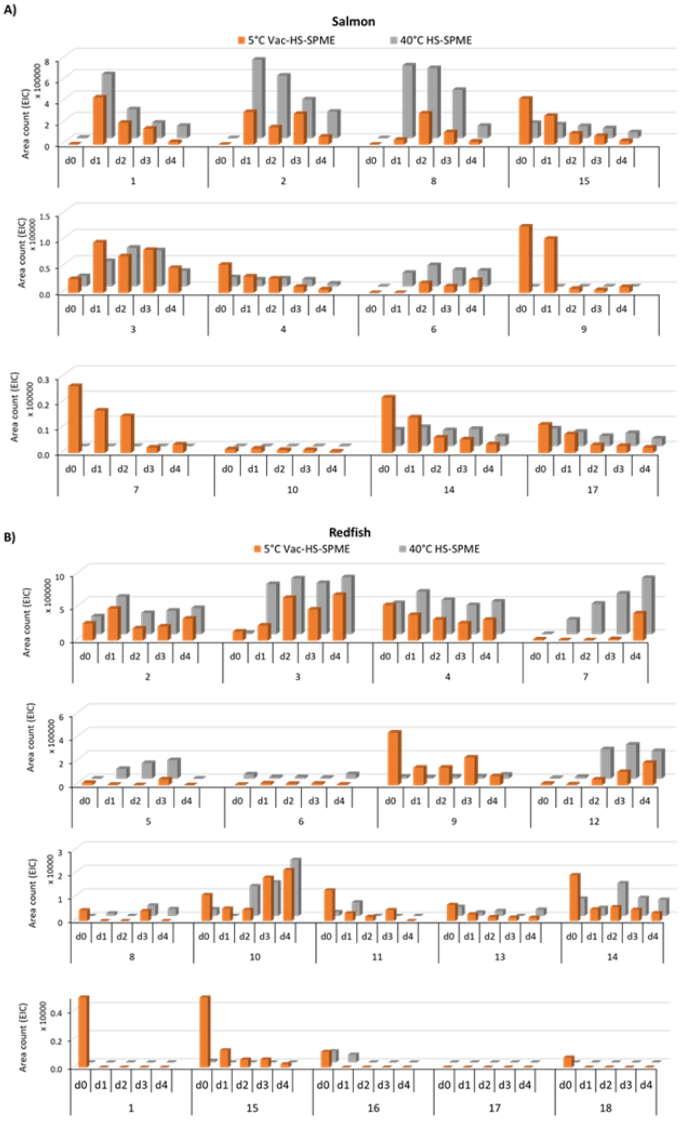
A)
Salmon
5°C Vac-HS-SPME
40°C HS-SPME
Area count (EIC) x 100000
d0 d1 d2 d3 d4
1
2
8
15
Area count (EIC) x 100000
3
4
6
9
Area count (EIC) x 100000
7
10
14
17
B)
Redfish
5°C Vac-HS-SPME
40°C HS-SPME
Area count (EIC) x 100000
2
3
4
7
Area count (EIC) x 100000
5
6
9
12
Area count (EIC) x 10000
8
10
11
13
14
Area count (EIC) x 100000
1
15
16
17
18

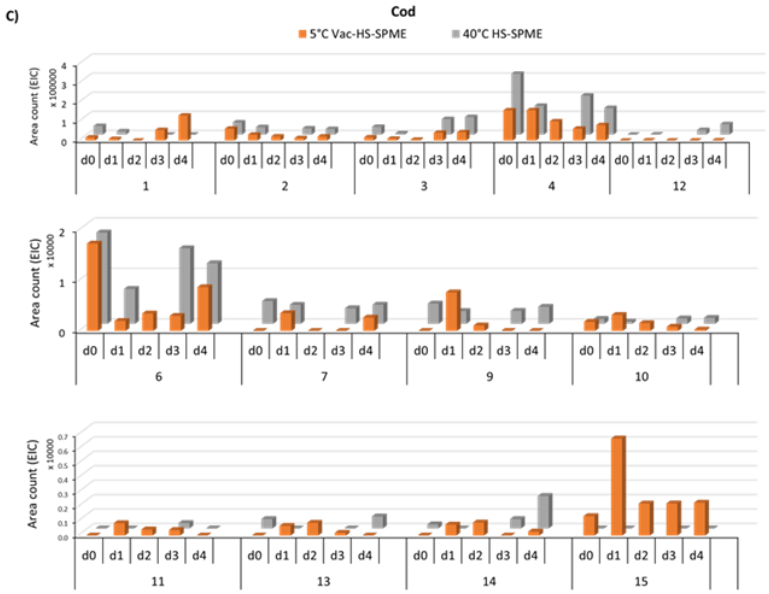

Figure 4-13: *Variation of the average peak areas of selected compounds in (A) salmon, (B) redfish, and (C) cod during five days of storage in a refrigerator (d0-d5). Results were obtained using Vac-HS-SPME at 5 °C (orange bars) and regular HS-SPME at 40 °C (grey bars) after a 30 min extraction. Coding of compounds as in Table 4-3. Error bars cannot be reported with this visualization and the full table containing this information is reported in Tables 4-7.*

2.6. Conclusion

This is the first contribution describing sub-ambient temperature (5 °C) extraction of volatile and semi-volatiles from perishable products. HS-SPME sampling under vacuum at a cool temperature proved a viable alternative to heating fish samples at 1 atm. For most selected compounds, Vac-HS-SPME at 5 °C yielded extraction efficiencies that were comparable or superior to those obtained with regular HS-SPME at 30 or 40 °C. As a proof-of-concept, three different fish samples were investigated over time and Vac-HS-SPME sampling at 5 °C resulted comparable to HS-SPME sampling at 40 °C. The superior performance of Vac-HS-SPME at sub-ambient temperatures was related to the combination of the enhanced analyte transfer rates in the headspace next to the increased affinity of analytes towards the fiber.

The present results open the way to a wide area of new studies aiming to investigate the possibility of using such a powerful approach for quality assessment and spoilage studies on delicate and perishable samples that are highly affected by changes in temperature. Vac-HS-SPME sampling at a cool temperature preserves the volatile profile of samples and rules out the initiation of enzymatic or degradation

processes triggered by heating. Sub-ambient temperature Vac-HS-SPME sampling records a more realistic “snapshot” of the compounds emitted by food samples when refrigerated. This feature may allow future studies to identify additional compounds responsible for the aroma, flavor but also off-flavors and off-odors of refrigerated food samples. Our related current and future investigations focus on the freshness/quality markers to be used for the different fish species, their quantification, as well as expand the approach to other types of perishable food.

2.7. References

[1] V.P. Lougovois, V.R. Kyrana, Freshness Quality and Spoilage of Chill-Stored Fish, 2014.

[2] R.K.B. Edirisinghe, A.J. Graffham, S.J. Taylor, Characterisation of the volatiles of yellowfin tuna (Thunnus albacares) during storage by solid phase microextraction and GC-MS and their relationship to fish quality parameters, Int. J. Food Sci. Technol. 42 (2007) 1139–1147. https://doi.org/10.1111/j.1365-2621.2006.01224.x.

[3] J. Iglesias, I. Medina, Solid-phase microextraction method for the determination of volatile compounds associated to oxidation of fish muscle, J. Chromatogr. A. 1192 (2008) 9–16. https://doi.org/10.1016/j.chroma.2008.03.028.

[4] F.F. Parlapani, A. Mallouchos, S.A. Haroutounian, I.S. Boziaris, Volatile organic compounds of microbial and non-microbial origin produced on model fish substrate un-inoculated and inoculated with gilt-head sea bream spoilage bacteria, LWT - Food Sci. Technol. 78 (2017) 54–62. https://doi.org/10.1016/j.lwt.2016.12.020.

[5] A. Kritikos, I. Aska, S. Ekonomou, A. Mallouchos, F.F. Parlapani, S.A. Haroutounian, I.S. Boziaris, Volatilome of Chill-Stored European Seabass (Dicentrarchus labrax) Fillets and Atlantic Salmon (Salmo salar) Slices under Modified Atmosphere Packaging, Molecules. 25 (2020) 1981. https://doi.org/10.3390/molecules25081981.

[6] P.K. Prabhakar, S. Vatsa, P.P. Srivastav, S.S. Pathak, A comprehensive review on freshness of fish and assessment: Analytical methods and recent innovations, Food Res. Int. 133 (2020) 109157. https://doi.org/10.1016/j.foodres.2020.109157.

[7] R.L. Wierda, G. Fletcher, L. Xu, J.-P. Dufour, Analysis of Volatile Compounds as Spoilage Indicators in Fresh King Salmon (Oncorhynchus tshawytscha) During Storage Using SPME−GC−MS, J. Agric. Food Chem. 54 (2006) 8480–8490. https://doi.org/10.1021/jf061377c.

[8] C.C. Grimm, S.W. Lloyd, R. Batista, P. V. Zimba, Using microwave distillation-solid-phase microextraction-gas chromatography-mass spectrometry for analyzing fish tissue, J. Chromatogr. Sci. 38 (2000) 289–296. https://doi.org/10.1093/chromsci/38.7.289.

[9] G. Duflos, F. Moine, V.M. Coin, P. Malle, Determination of volatile compounds in whiting (Merlangius merlangus) using headspace-solid-phase microextraction-gas chromatography-mass spectrometry, J. Chromatogr. Sci. 43 (2005) 304–312. https://doi.org/10.1093/chromsci/43.6.304.
[10] É.A. Souza-Silva, E. Gionfriddo, J. Pawliszyn, A critical review of the state of the art of solid-phase microextraction of complex matrices II. Food analysis, TrAC Trends Anal. Chem. 71 (2015) 236–248. https://doi.org/10.1016/j.trac.2015.04.018.
[11] J. Pawliszyn, Handbook of Solid Phase Microextraction, First, Elsevier Inc., London, 2012.
[12] E. Psillakis, The effect of vacuum: an emerging experimental parameter to consider during headspace microextraction sampling, Anal. Bioanal. Chem. (2020). https://doi.org/10.1007/s00216-020-02738-x.
[13] G. Duflos, V.M. Coin, M. Cornu, J.-F. Antinelli, P. Malle, Determination of volatile compounds to characterize fish spoilage using headspace/mass spectrometry and solid-phase microextraction/gas chromatography/mass spectrometry, J. Sci. Food Agric. 86 (2006) 600–611. https://doi.org/10.1002/jsfa.2386.
[14] E. Psillakis, E. Yiantzi, L. Sanchez-Prado, N. Kalogerakis, Vacuum-assisted headspace solid phase microextraction: Improved extraction of semivolatiles by non-equilibrium headspace sampling under reduced pressure conditions, Anal. Chim. Acta. 742 (2012) 30–36. https://doi.org/10.1016/j.aca.2012.01.019.
[15] E. Psillakis, Vacuum-assisted headspace solid-phase microextraction: A tutorial review, Anal. Chim. Acta. 986 (2017) 12–24. https://doi.org/10.1016/j.aca.2017.06.033.
[16] D. Mackay, W.Y. Shiu, K. Ma, S.C. Lee, Properties and Environmental Fate Second Edition Introduction and Hydrocarbons, 2006. http://www.crcnetbase.com/doi/book/10.1201/9781420044393.
[17] R.P. Schwarzenbach, P.M. Gschwend, D.M. Imboden, Environmental Organic Chemistry, Second Edition, John Wiley & Sons Inc, Hoboken, New Jersey, 2003.
[18] S. Xu, B. Kropscott, Evaluation of the three-phase equilibrium method for measuring temperature dependence of internally consistent partition coefficients (KOW, KOA, and KAW) for volatile methylsiloxanes and trimethylsilanol, Environ. Toxicol. Chem. 33 (2014) 2702–2710. https://doi.org/10.1002/etc.2754.
[19] Z. Zhang, J. Pawliszyn, Quantitative Extraction Using an Internally Cooled Solid Phase Microextraction Device, Anal. Chem. 67 (1995) 34–43. https://doi.org/10.1021/ac00097a007.
[20] A.R. Ghiasvand, S. Hosseinzadeh, J. Pawliszyn, New cold-fiber headspace solid-phase microextraction device for quantitative extraction of polycyclic aromatic hydrocarbons in sediment, J. Chromatogr. A. 1124 (2006) 35–42. https://doi.org/10.1016/j.chroma.2006.04.088.

[21] E. Yiantzi, N. Kalogerakis, E. Psillakis, Vacuum-assisted headspace solid phase microextraction of polycyclic aromatic hydrocarbons in solid samples, Anal. Chim. Acta. 890 (2015) 108–116. https://doi.org/10.1016/j.aca.2015.05.047.
[22] A. Zhakupbekova, N. Baimatova, B. Kenessov, A critical review of vacuum-assisted headspace solid-phase microextraction for environmental analysis, Trends Environ. Anal. Chem. 22 (2019) e00065. https://doi.org/10.1016/j.teac.2019.e00065.
[23] E. Psillakis, N. Koutela, A.J. Colussi, Vacuum-assisted headspace single-drop microextraction: Eliminating interfacial gas-phase limitations, Anal. Chim. Acta. 1092 (2019) 9–16. https://doi.org/10.1016/j.aca.2019.09.056.
[24] E. Psyllaki, Methods and vial closures for headspace extraction under vacuum, 2020, USA non-provisional patent application No. 17/100,070; PCT International Application No. PCT/IB2020/060957, n.d.
[25] S. Mascrez, E. Psillakis, G. Purcaro, A multifaceted investigation on the effect of vacuum on the headspace solid-phase microextraction of extra-virgin olive oil, Anal. Chim. Acta. 1103 (2020). https://doi.org/10.1016/j.aca.2019.12.053.
[26] G. Duflos, F. Leduc, A. N'Guessan, F. Krzewinski, O. Kol, P. Malle, Freshness characterisation of whiting (Merlangius merlangus) using an SPME/GC/MS method and a statistical multivariate approach, J. Sci. Food Agric. 90 (2010) 2568–2575. https://doi.org/10.1002/jsfa.4122.
[27] R.I. Pratama, I. Rostini, E. Lviawaty, Volatile components of raw Patin Catfish (Pangasius hypophthalmus) and Nile Tilapia (Oreochromis niloticus), IOP Conf. Ser. Earth Environ. Sci. 176 (2018). https://doi.org/10.1088/1755-1315/176/1/012040.
[28] R. Triqui, N. Bouchriti, Freshness Assessments of Moroccan Sardine (Sardina pilchardus): Comparison of Overall Sensory Changes to Instrumentally Determined Volatiles, J. Agric. Food Chem. 51 (2003) 7540–7546. https://doi.org/10.1021/jf0348166.
[29] J. Iglesias, I. Medina, F. Bianchi, M. Careri, A. Mangia, M. Musci, Study of the volatile compounds useful for the characterisation of fresh and frozen-thawed cultured gilthead sea bream fish by solid-phase microextraction gas chromatography-mass spectrometry, Food Chem. 115 (2009) 1473–1478. https://doi.org/10.1016/j.foodchem.2009.01.076.
[30] T. Miyasaki, M. Hamaguchi, S. Yokoyama, Change of Volatile Compounds in Fresh Fish Meat during Ice Storage, J. Food Sci. 76 (2011). https://doi.org/10.1111/j.1750-3841.2011.02388.x.
[31] G. Duflos, V.M. Coin, M. Cornu, J.F. Antinelli, P. Malle, Determination of volatile compounds to characterize fish spoilage using headspace/mass spectrometry and solid-phase microextraction/gas chromatography/mass spectrometry, J. Sci. Food Agric. 86 (2006) 600–611. https://doi.org/10.1002/jsfa.2386.
[32] D. Li, J. Zhang, S. Song, L. Feng, Y. Luo, Influence of heat processing on the volatile organic compounds and microbial diversity of salted and vacuum-

packaged silver carp (Hypophthalmichthys molitrix) fillets during storage, Food Microbiol. 72 (2018) 73–81. https://doi.org/10.1016/j.fm.2017.11.009.
[33] A.-K. Lundebye, H. Hove, A. Måge, V.J.B. Bohne, K. Hamre, Levels of synthetic antioxidants (ethoxyquin, butylated hydroxytoluene and butylated hydroxyanisole) in fish feed and commercially farmed fish, Food Addit. Contam. Part A. 27 (2010) 1652–1657. https://doi.org/10.1080/19440049.2010.508195.
[34] U.S. Environmental Protection Agency (EPA), Provisional Peer-Reviewed Toxicity Values for Butylated Hydroxytoluene (BHT), (2013).
[35] F. Capetti, P. Rubiolo, C. Bicchi, A. Marengo, B. Sgorbini, C. Cagliero, Exploiting the versatility of vacuum-assisted headspace solid-phase microextraction in combination with the selectivity of ionic liquid-based GC stationary phases to discriminate Boswellia spp. resins through their volatile and semivolatile fractions, J. Sep. Sci. (2020) 1–11. https://doi.org/10.1002/jssc.202000084.
[36] M.J. Trujillo-Rodríguez, V. Pino, E. Psillakis, J.L. Anderson, J.H. Ayala, E. Yiantzi, A.M. Afonso, Vacuum-assisted headspace-solid phase microextraction for determining volatile free fatty acids and phenols. Investigations on the effect of pressure on competitive adsorption phenomena in a multicomponent system, Anal. Chim. Acta. 962 (2017) 41–51. https://doi.org/10.1016/j.aca.2017.01.056.
[37] E. Psillakis, Vacuum-assisted headspace solid-phase microextraction: A tutorial review, Anal. Chim. Acta. 986 (2017) 12–24. https://doi.org/10.1016/j.aca.2017.06.033.
[38] Z.C. Petricorena, Chemical Composition of Fish and Fishery Products, in: P.C.K. Cheung (Ed.), Handb. Food Chem., Springer Berlin Heidelberg, Berlin, Heidelberg, 2015: pp. 1–28. https://doi.org/10.1007/978-3-642-41609-5_12-1.
[39] A.R. Davies, Modified-atmosphere packaging of fish and fish products, Fish Process. Technol. 605 (1997) 200–223. https://doi.org/10.1007/978-1-4613-1113-3_7.
[40] E. Gionfriddo, É. A. Souza-Silva, J. Pawliszyn, Headspace versus Direct Immersion Solid Phase Microextraction in Complex Matrixes: Investigation of Analyte Behavior in Multicomponent Mixtures, Anal. Chem. 87 (2015) 8448–8456. https://doi.org/10.1021/acs.analchem.5b01850.
[41] W. Hou, Q. Han, H. Gong, W. Liu, H. Wang, M. Zhou, T. Min, S. Pan, Analysis of volatile compounds in fresh sturgeon with different preservation methods using electronic nose and gas chromatography/mass spectrometry, RSC Adv. 9 (2019) 39090–39099. https://doi.org/10.1039/c9ra06287d.
[42] S.E. Pinches, P. Apps, Production in food of 1,3-pentadiene and styrene by Trichoderma species, Int. J. Food Microbiol. 116 (2007) 182–185. https://doi.org/10.1016/j.ijfoodmicro.2006.12.001.

Chapter 5

Multiple-cumulative trapping HS-SPME

Exploring multiple-cumulative trapping solid-phase microextraction for olive oil aroma profiling

Based on: S. Mascrez and G. Purcaro, *Exploring multiple-cumulative trapping solid-phase microextraction for olive oil aroma profiling*, Journal of Separation Science, 43 (2020) 1934-1941.

1.1. Abstract

Headspace solid-phase microextraction is a solvent-free sample preparation technique that is based on the equilibrium among a three-phase system, i.e., sample-headspace-fiber. A compromise between sensitivity and extraction time is usually needed to optimize the sample throughput, especially when a large number of samples are analyzed, as usually the case in cross-samples studies. This work explores the capability of multiple-cumulative solid-phase microextraction on the characterization of the aroma profiling of olive oils, exploiting the automation capability of a novel headspace autosampler. It was shown as multiple-cumulative-solid-phase microextraction has the potential to improve the overall sensitivity and burst the level of information for cross-sample studies by using cumulative shorter extraction times.

1.2. Introduction

The combination of two related but distinct equilibria, namely the sample/HS equilibrium (measured by its distribution coefficient K_{hs}) and the HS/fiber equilibrium (measured by K_{fh}), determines the magnitude of extraction. Sampling can be carried out under equilibrium or non-equilibrium conditions. In the former case, the extraction yield is theoretically maximized. This is true for liquid coatings, which extract analytes via absorption mechanism, while it is not always the case for coatings exploiting adsorption mechanisms, where competition may occur, reducing the extraction yield [1,2]. Nevertheless, the amount extracted by SPME (n) is proportional to the initial concentration (C0) in the sample both under equilibrium and non-equilibrium conditions, according to equation (1):

$$n = \frac{K_{hs}\ K_{fh}\ V_f\ V_s\ C_0}{K_{hs}\ K_{fh}\ V_f + K_{hs}\ V_h + V_s} \qquad (1)$$

where, C_0: initial concentration; K_{hs} and K_{fh}: distribution coefficient sample/HS and fiber/HS, respectively; V_s, V_h, V_f: volume of the samples, the HS and the fiber coating, respectively.

At present, most of the applications involving HS-SPME are aiming to fingerprinting and profiling the HS of the samples for cross-sample comparison, pattern recognition, or biomarkers extrapolation [3-7]. Samples are usually characterized by a complex HS profile containing hundreds of compounds, each one

characterized by its own K_{hs} and K_{fh}. The most volatile compounds usually reach equilibrium rather quickly, while semi-volatiles require longer time. Therefore, a compromise between sensitivity and extraction time is usually needed to optimize the sample throughput, especially when a large number of samples are analyzed, as usually the case in cross-samples studies. Moreover, the additional diversion from the theory, observed when adsorption-type fibers are used (as the most employed divinylbenzene/carboxen/polydimethylsiloxane (DVB/CAR/PDMS) [8]) complicates even more the scenario.

Different strategies have been applied to maximize the extraction yields and, at the same time, improving the kinetics and thus the sample throughput. Apart from stirring and increasing the temperature (the latter has to be used with care to avoid artifacts formation), a powerful approach is the used of reduced pressure condition inside the sampling vial, a technique termed Vac-HS-SPME by Psillakis *et al*., who systematically investigated it and formulated the underlying principle [9-13]. But other approaches have been proposed over the time, although not systematically investigated. Oliver-Pozo *et al.* [14] develop a dynamic HS sampling system to facilitate analytes accumulation into the SPME fiber. Another interesting alternative was presented by Lipinski in 2000 [15] using multiple cumulative direct immersion-SPME to enhance the sensitivity for analysis of pesticides in water; a stop-flow approach was used to focalize the compounds at the front of the cool GC column (40 °C) before the GC separation. The same idea was exploited by Chin *et al*. in 2012 [16] to maximize the odor detection limit in GC-olfactometry screenings of wine aroma. The HS-SPME mode was used, and the compounds were focalized using a cold trap at the head of the column. Different fiber-coating combinations were tested, providing a more comprehensive fingerprinting and higher sensitivity. The work was mainly focused on the optimization of the trapping condition at the head of the column, while little attention was devoted on the SPME sampling potentiality.

This work aims to explore the capability of multiple-cumulative trapping SPME (from now on, MCT-SPME) on the characterization of the aroma profile of olive oils, exploiting the automation capability of a novel HS autosampler.

The fingerprinting of olive oil is a challenging task of interest for quality and authenticity assessment. Investigation of the volatile fraction is an informative and diagnostic tool for olive oil characterization and sensory evaluation [3,17-19]; thus, the possibility to enhance the extractable information gaining a higher level of understanding is highly desirable. As a first investigation of the MC-SPME mode, the DVB/CAR/PDMS fiber was used as the most common fiber for the analysis of volatile in edible oils [8].

1.3. Materials and methods

1.3.1. Chemicals and reagents

Hexane GC grade (MilliporeSigma®, USA) was used to dilute normal alkanes (C7-C30) mixture (Supelco, PA, USA) used for calculating the linear retention index (LRI) for confirming peak identity.

The divinylbenzene/carboxen/polydimethylsiloxane (DVB/CAR/PDMS) df 50/30 µm/ 1 cm length fiber was kindly provided by MilliporeSigma (Bellefonte, PA, USA).

1.3.2. Olive oil samples

An extra-virgin olive oil sample was purchased at a local supermarket (Gembloux, Belgium) for the first part of the investigation regarding the profile using one single extraction or multiple-cumulative extractions.

Extra-virgin (EVO), virgin (VO), and lampante (LO) olive oils characterized by their sensory evaluation (internal panel) [20] and of certain cultivar and geographical origin were kindly provided by Carapelli Firenze SpA - Italy (Deoleo group). A detailed list of samples is reported in Table 5-1.

Table 5-1: . List of samples analyzed, along with cultivars, year of harvesting, geographical origin and sensory panel evaluation according to [29].

				Positive attributes			Negative attributes			
Code	**Geograph. origin**	**Cultivar**	**Harvesting**	**Fruity**	**Bitter**	**Pungent**	**Fusty**	**Musty**	**Winey**	**Rancid**
EVO_01	Spain	Picual, Hojiblanca, Picudo, Manzanilla, Morisca, Carrasquena	2018/19	4.3	4.6	5	0	0	0	0
EVO_02	Italy	Leccino, Moraiolo, Frantoio	2018/19	3.8	3.8	4.3	0	0	0	0
EVO_03	Spain	Picual, Hojiblanca, Picudo	2018/19	2.9	2	3.2	0	0	0	0
EVO_05	Italy	Frantoio	2018/19	4	3.6	3.8	0	0	0	0
EVO	Italy	Morai	2018/19	4	3.5	3.8	0	0	0	0

_06		olo								
VO_01	Spain	Picual	2018/19	2.6	3.8	2.9	0	0.5	0	0.8
VO_02	Italy	Coratina	2018/19	1.6	1.3	2	1.8	0.5	0	1
LO_01				0	0	0	4	0	0	3
LO_02				0.9	1	1	1	1.9	0.5	1.1
LO_03				1.1	1	1	0	0.6	0	2.5
LO_04				1	0.6	0.8	1.7	1	0	1

1.3.3. Headspace solid-phase microextraction procedure

Samples (1.50 ± 0.05 g) were weighed in a 20 mL screw top vials, metallic caps with a hole and polytetrafluoroethylene (PTFE)/silicone septa (Restek, USA). The SPME extraction was automated in a Centri Autosampler (Markes International Ltd, UK). The sample, under agitation (300 rpm), was equilibrated for 5 min at 43 °C before exposing the fiber for 10 or 30 min. The fiber was conditioned as suggested by the provider prior to the first use.

The fiber was then thermally desorbed at 250 °C for 2 min in split mode with a trap flow of 50 mL/min. The trap (U-T12ME-2S, Markes International, general purpose in the C4-C32 volatile range) was cooled at 0 °C during desorption of the fiber in the injector, then 1 min purge at 50 mL/min was performed before heating the trap to 300 °C. A 1:5 split was applied after the trap to facilitate the transfer of the analytes into the head of the GC column. When MC-SPME were performed, a 5 min enrichment delay was allowed before the following extraction. Three and six cumulative extractions were performed from the same vial. All experiments for investigating the trend of the MC-SPME were run in triplicate. Real-word samples were analyzed in single. Before starting any samples batch, an SPME fiber blank was performed, as well as periodically to ensure the absence of carryover between runs.

1.3.4. GC-MS analysis

Injections were performed using a Centri autosampler (Markes International) integrated to a Shimadzu GCMS-TQ8050 NX (Japan), consisting of a GC2030 coupled to triple-quadrupole mass spectrometer detector (TQ-MS) (Shimadzu, Germany). The separation was performed on a 30 m × 0.25 mm i.d. × 0.5 μm df SLB-5ms capillary column [(silphenylene polymer, practically equivalent in polarity to poly(5%diphenyl/95% methylsiloxane)] kindly obtained from MilliporeSigma (USA). GC oven temperature program: 30 °C for 5.5 min to 310 °C at 10 °C/min. Elution was performed using helium in constant linear velocity mode at 35.9 cm/s,

corresponding to an initial inlet over-pressure of 45.6 kPa. The MS was operated in single-quadrupole mode, in EI mode at 70 eV. The ion source and transfer line temperatures were 200 °C and 280 °C, respectively. The scan range was set to 50-450 m/z with an acquisition frequency of 10 Hz. Data were acquired using Shimadzu GCMSolution ver 4.45 (Shimadzu, Japan). NIST17s and FFNSC 3.0 MS commercial libraries were used for identification. Putative identification was based on the combination of a dual filter, namely: 1) the MS similarity with the NIST17 library and the FFNSC library (Shimadzu) (≥80%) and, 2) the experimental LRI within a ±15 units range.

1.3.5. Data elaboration and statistical analysis

The data matrix resulting from the olive oil samples analysis was first normalized using Probabilistic Quotient Normalization. The data underwent a logarithmic transformation to stabilize the variance and making the distribution of the variables closer to normal [21].

The number of features still outweighed the number of samples; therefore, to overcome this limitation, a machine learning algorithm was applied to build a three-class model and select the most discriminatory core volatile analytes. The Random Forest algorithm was used for this purpose as it can deal with highly collinear data, and the effect of outliers is kept under control [22]. The algorithm provides a ranking of the features, expressed as mean decrease accuracy, based on the influence of each feature, after permutation, on the overall accuracy of the model obtained averaging the prediction from a multitude of de-correlated decision trees.

The separation performances of the different conditions were evaluated, measuring the inter-group Euclidean distance [21].

All statistical analyses were performed using R v3.6.1 (R Foundation for Statistical Computing, Vienna, Austria), Excel® (Microsoft Office, version 2016), and Morpheus® (https://software.broadinstitute.org/morpheus/).

1.4. Results and discussion

The novel autosampler employed in this study allows, after desorption of the SPME fiber into the inlet, to either direct the compounds into the column (called “direct mode”), or trapping the compounds on a cooled trap before rapidly desorbing and injecting them into the analytical column (called “trapping mode”). In the former case, the trap is bypassed with a system of valves. A slight improvement was observed in terms of peak focalization, shape, and resolution (Figure 5-1). Therefore, the entire experimental design was carried out using the trapping option, also when a single extraction was performed.

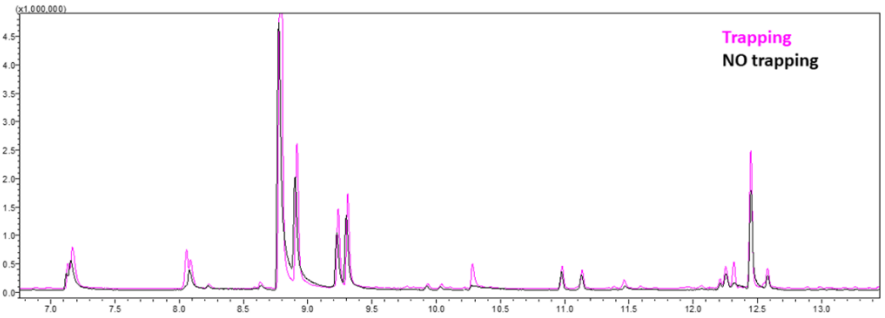

Figure 5-1: *Expansion of overlay of the GC traces acquired using "Direct mode" (black trace) and "Trapping mode" (pink trace).*

Forty-nine compounds were selected over the entire chromatogram covering a wide range of polarity and volatility, focusing mainly (but not exclusively) on previously reported compounds in extra-virgin olive oil aroma characterization [3,14,23-25].

The list of the 49 selected compounds is reported in Table 5-2, along with their LRI (experimental and reported in the literature), CAS number, and similarity match (MS%).

Table 5-2: List of selected analytes along with CAS register number, experimental and literature linear retention index (LRI), and similarity match of the mass spectrum with the commercial libraries (MS%).

#	Name	CAS	LRI_{exp}	LRI_{lib}	MS%
1	2-methyl- Butanal	96 - 17 - 3	658	662	96
2	1-Penten-3-ol	616 - 25 - 1	670	671	98
3	1-Penten-3-one	1629 - 58 - 9	672	677	95
4	1-Butanol, 2-methyl	123 - 51 - 3	719	723	96
5	1-Butanol, 3-methyl-	137 - 32 - 6	723	729	89
6	Pent-(2E)-enal	1576 - 87 - 0	743	751	95
7	Toluene	108 - 88 - 3	755	763	96

8	Pent-(2Z)-enol	1576 - 95 - 0	764	767	89
9	Pent-(2E)-enol	1576 - 96 - 1	767	769	97
10	Hexanal <n->	66 - 25 - 1	798	801	94
11	Hex-(2Z)-enal	16635-54-4	849	850	93
12	Hex-(2E)-enal	6728 - 26 - 3	856	857	98
13	Hex-(3E)-enol	928 - 97 - 2	860	867	98
14	Hex-(2E)-enol	928 - 95 - 0	871	868	98
15	Hexanol	111 - 27 - 3	874	867	99
16	Styrene	100 - 42 - 5	889	891	88
17	$C_6H_{12}O$ (cyclic alcohol)	3524 - 75 - 2	895	903	85
18	Cyclopentanemethanol	3524 - 75 - 2	899	903	85
19	2,4-Hexadienal, (2E,4E)-	142 - 83 - 6	909	914	97
20	Citronellyl formate	105 - 85 - 1	940	953	82
21	γ-Pentalactone	108 - 29 - 2	953	955	94
22	1-Heptanol	111 - 70 - 6	973	970	83
23	3-Methoxytoluene	100 - 84 - 5	989	983	80
24	Hex-(3Z)-enyl acetate	3681 - 71 - 8	1007	1008	99
25	Benzyl alcohol	100 - 51 - 6	1036	1040	97
26	Hexalactone <gamma->	695 - 06 - 7	1055	1056	94
27	Acetophenone	98 - 86 - 2	1068	1069	92
28	Benzene, 1-ethenyl-4-ethyl-	3454 - 07 - 7	1087	1096	89
29	Nonanal	124 - 19 - 6	1104	1104	97
30	(3E)-4,8-Dimethyl-1,3,7-nonatriene	19945 - 61 - 0	1118	1113	92

31	ε-Hexalactone	502 - 44 - 3	1143	1137	89
32	Cinnamaldehyde, (E)-	14371 - 10 - 9	1186	1189	90
33	δ-Propylvalerolactone	698 - 76 - 0	1191	1205	82
34	Cinnamaldehyde, (Z)-	57194 - 69 - 1	1203	1218	90
35	1-Dodecene	112 - 41 - 4	1206	1204	92
36	γ-Octalactone	104 - 50 - 7	1262	1263	82
37	Undecan-2-one	112 - 12 - 9	1295	1294	80
38	Tridecane	629 - 50 - 5	1300	1300	84
39	Undecanal	112 - 44 - 7	1312	1309	93
40	α-Copaene	138874 - 68 - 7	1389	1375	95
41	Tetradecane	629 - 50 - 5	1400	1400	86
42	Dodecanal	112 - 54 - 9	1411	1410	95
43	γ-Undecalactone	104 - 67 - 6	1475	1483	82
44	Tetradecanal	124 - 25 - 4	1615	1619	91
45	2-Pentadecanone	2345 - 28 - 0	1701	1697	92
46	Dibutyl adipate	105 - 99 - 7	1767	1747	94
47	n-Butylbenzenesulfonamide	3622 - 84 - 2	1797	1802	96
48	Hexadecanal	629 - 80 - 1	1819	1823	92
49	1-Hexadecanol	36653 - 82 - 4	1878	1884	98

1.4.1. Study of the multiple-cumulative trapping solid-phase microextraction conditions

The same EVO collected from the market was extracted multiple times (i.e., three and six times), maintaining the cold trap between the injector and the analytical column cold for the duration of all the multiple extractions. The cold trap was then rapidly heated to release all the retained analytes into the analytical column. The MCT-HS-SPME mode was compared with the data obtained with a traditional single

extraction. An amount of 1.5 g of the sample was used, as previously reported in similar studies, as well as 43 °C as the extraction temperature [3,13,26]. When porous fibers are used (as DVB/CAR/PDMS), shorter extraction time is suggested to reduce the competitive adsorption [2,27]. Therefore, different extraction times were tested, namely 10 and 30 min.

The extraction profile obtained for the 49 selected compounds is shown in Figure 5-3.

The trends of each targeted analyte at different repeated MCT-HS-SPME (1, 3, and 6), at both 10 and 30 min, are reported in the bar plots in Figure 5-2. As expected, the increment was proportional to the number of extractions at both times. The gain in sensitivity using MCT-HS-SPME was evaluated by normalizing the results to the amount obtained after a single extraction. Theoretically, a linear cumulative increment (i.e., 3 and 6 times higher signal when 3 and 6 extractions are performed, respectively) can be observed when the HS is saturated with the analyte of interest, which means that the quantity extracted is depending on K_{fh} and that it is easily replenished in the subsequent equilibration time.

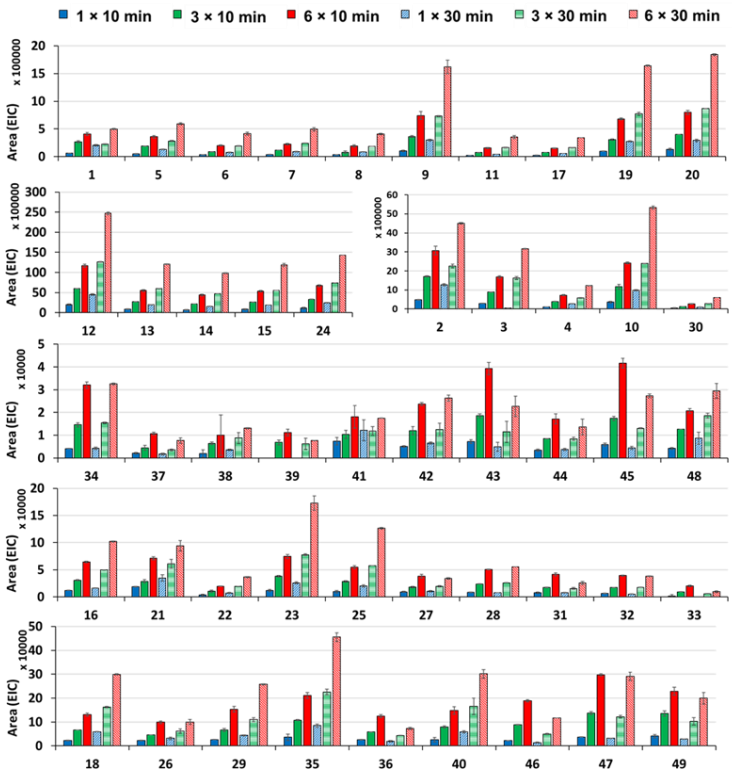

Figure 5-2: *Extraction yield for multiple (1, 3, and 6) HS-SPME using 10 and 30 min extraction time. Compounds grouped according to comparable absolute intensity. Compounds name code as for Table 5-2.*

Considering the overall trend, extracting for 10 min 3- and 6-times, an average of 3.0- and 6.0- folds (median of 3.0 and 5.9, respectively) increment compared to the single extraction was recorded, respectively; while a decrease in the cumulative uptake was observed when extracting 30 min with an average of 2.6 and 5.4 (median of 2.7 and 5.4, respectively) when trapping 3 and 6 times, respectively. These results indicate that the HS is most probably saturated and that when extracting only 10 min, the HS is quickly replenished in the subsequent equilibrations with the compounds coming from the matrix. On the other hand, exposing the fiber to the HS for 30-min removed a higher amount of compounds at each extraction, leading to a decrease in the cumulative response. Most probably, this indicates that after a certain number of extractions, the HS is not saturated anymore and an exponential decrease of the response occurs, as expected from the theory [28], which translated in a non-linear cumulative increment.

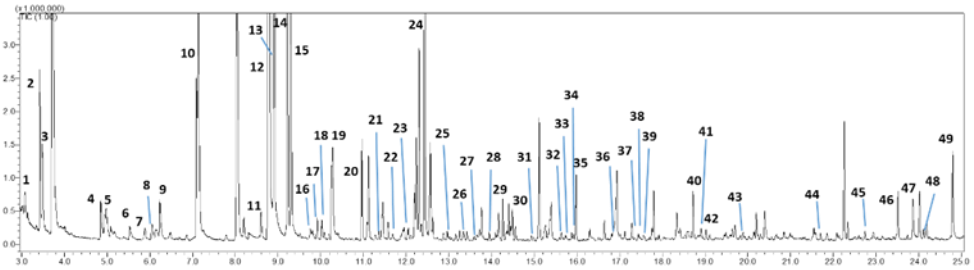

Figure 5-3: *Total ion chromatogram of an EVO sample (1.5 g in a 20 mL vial, extracted for 10 min at 43 °C). Compounds name code as for Table 5-2.*

It is also interesting to notice that extended extraction time (30 min) did not necessarily provide better results than shorter extraction time (10 min). This is more evident for the semi-volatile compounds, for which, in some cases, 10 min extraction provided a higher extraction yield, as for instance for compounds 43, 44 and 45 (Figure 5-5). Comparing the ratio between the amount extracted in 10 min and 30 min at a single extraction, 3- and 6-cumulative extractions, a clear trend was observed despite the number of extractions performed. In fact, the early eluted compounds showed a higher uptake when sampling for 30 min (ratio>1,

generally~2.0-2.5), while for less volatile compounds a ratio ≤ 1 was recorded (blueish color in the heat map of Figure 7.6.; the lowest was 0.5 for #33).

This means, contrarily to what is reported in the literature (extraction time usually in the 30-60 min range [7,13]), that sampling for a shorter time allows providing a better fingerprint of the volatile profile of extra virgin olive oil, covering a more comprehensive range of compounds, although at the expense of a lower sensitivity for the most volatile compounds. Moreover, it is important to notice that comparing the response obtained with 3-cumulative extraction for 10 min and a single extraction for 30 min (which means the same overall extraction time), a higher signal was obtained for the 3-cumulative extractions for all the compounds (ratio>1; median: 1.5; min: 0.8; max: 6.3), except for compound #8, #21, and #41 with a 0.9, 0.8, and 0.9 ratio, respectively (Figure 5-5). This was also observed in cumulative DI-SPME by Lipinski [15], concluding that for the same overall extraction time, MCT-SPME is preferable for gaining in sensitivity.

It is important to highlight that the sampling strategy is the first important step in the analytical flowchart that may alter the fingerprint profile based on one or more specific characteristics of the compounds (such as polarity or volatility) altering the final potential results. This is particularly true when SPME is used; in fact, the fiber represents a first selective filter towards molecules affine to the fiber sorbent phase rather than giving a real image of the HS content. Moreover, the profile is altered even more when competitive adsorption processes occur, which are strictly related to the extraction time (i.e., longer extraction time facilitates the occurrence of the displacement effect) [2,27,29]. This means that sampling is a fundamental step for ameliorating or weakening the level of information and that there is still a broad space for improvement.

1.4.2. Application of multiple-cumulative trapping solid-phase microextraction for pattern recognition

In the context of cross-sample comparison and pattern recognition analysis, the GC-MS peak area information is usually treated as a concentration indicator for the compound of interest in the sample (for a batch of homogenous samples where the same matrix effect occurs) [5]. This generally accepted approach can be misleading, in particular when the quantification of compounds is less straightforward as in SPME. When working with SPME, two equilibria are involved, as mentioned in the introduction. For the same compound, the K_{fh} determines the maximum fiber capacity, while K_{hs} guides the difference in the HS concentration when the amount of the compounds between two samples is different. When the HS is saturated, differences in C_0 are hindered by the maximum capacity of the HS. This means that

when working under HS saturated condition, the information obtainable are flawed. The most frequent amount of sample used in the literature is 1.5 g (or more) [3,24,26,30,31], which saturates the HS (as shown before) for most of the compounds. The use of MCT-SPME should improve the cross-sample comparison amplifying the differences and maximizing the signal of the analytes of interest, thus simultaneously improving the sensitivity and the level of information obtainable. In fact, when the HS is not saturated, an exponential decrease in the signal is expected. Therefore, it is expected that while some compounds will saturate the HS for all the 6 extractions leading to a linear increment of their signal; other will not saturate the HS for all the 6 extractions performed (some not even during the first extraction), thus amplifying the differences in the overall profile after MCT-HS-SPME.

As a proof-of-concept, 11 samples of olive oils (5 extra-virgins, 2 virgins, and 4 lampante oils) (Table 5-1) were analyzed. A single trapping extraction was compared with 6-multiple SPME performed for 10 min. In this context, the use of shorter extraction time (10 min rather than 30 min), allows improving the response of the analytes limiting the loss of information due to competitive effects, as highlighted before.

The results were aligned, obtaining 183 analytes in total. The two data matrices obtained were cleaned independently to remove siloxane. Further reduction was based on a frequency of observation cutoffs of 50% within at least a group. The final data matrices contained 115 and 148 features for the samples undergone to one single trapping extraction and 6-multiple SPME, respectively.

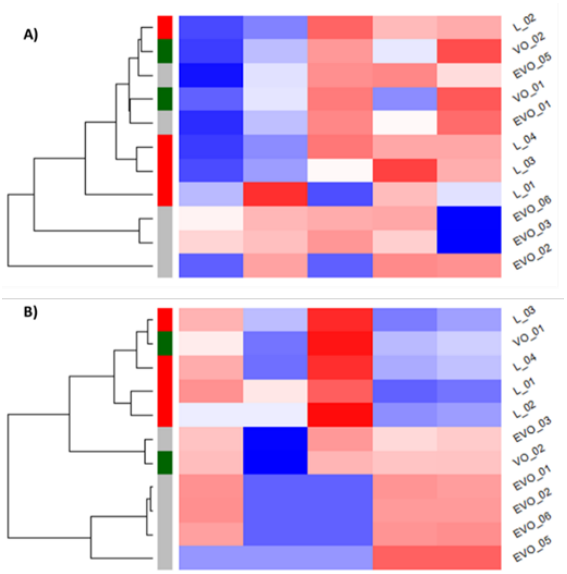

Figure 5-4: *Heat-maps and hierarchical clustering analysis of olive oil samples using the RF selected features for A) single extraction and B) 6-cumulative extractions. Data were normalized by PQN and log transformed.*

The choice of the further data mining approach was based on the results previously reported by Purcaro *et al.* [4]. Unpredictable systematic variation was minimized by performing PQN normalization. Logarithmic transformation was applied to stabilize the variance, normalized the distribution of the variables, and reduce the weight of very intense compounds over much lower ones. A first comparison was carried out at this stage, but also an additional feature reduction was applied to avoid that features outweighed the number of samples. RF was chosen over other feature reduction methods as proved very consistent in several works reported in the literature, despite the previous data treatment [4,22]. The features were selected according to the mean decrease accuracy values obtained from the RF algorithm. Heat maps with hierarchical clustering analysis were used to visualize the pattern obtained after feature reduction (Figure 5-4). Although the numerousness of the sampling is limited, some trends can be discussed. EVOs were well separated from LOs only when MCT-HS-SPME was used, while, in both cases, VOs are confused either with EVOs or LOs, as for their same definition. In fact, VOs are samples that, differently from EVO, present some defects, but not as strong as LOs and still maintaining important positive attributes.

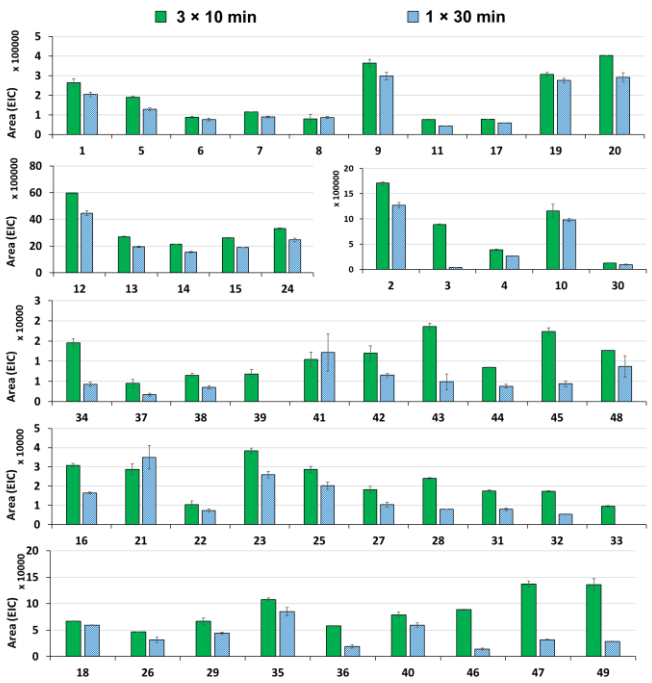

Figure 5-5: *Extraction yield for 3×10min-MCT-HS-SPME 30 min single extraction time. Compounds grouped according to comparable absolute intensity. Compounds name code as for Table 5-2.*

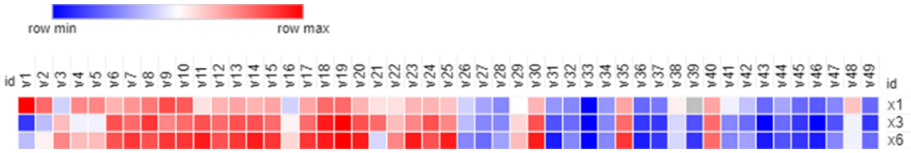

Figure 5-6: *Normalized response ratio (30 min/10 min) for single (x1) and normalized response ratio for MCT-HS-SPME [×3-(30 min/10 min) and ×6-(30 min/10 min)]. Compounds name code as for Table 5-2.*

For a more numerical comparison, the pair-wise Euclidean distance between groups was calculated (Table 5-3).

Table 5-3: Normalized response ratio (30 min/10 min) for single (x1) and normalized response ratio.

N trapping extraction	**Feature selection**	**Euclidean distance**		
		EVO-VO	**EVO-LO**	**VO-LO**
1	**NO**	17.7	18.3	17.3
1	**Yes**	3.2	3.7	1.5
6	**NO**	21.9	24.0	20.9
6	**Yes**	4.7	6.8	3.1

Using a 6-cumulative extraction, the Euclidean distances between groups increased, either applying or not the additional features selection step, for all the three distances considered, namely EVO-VO, EVO-LO, and VO-LO. The features selected using the RF algorithm were different for the two datasets, except for one common compound, namely undecan-2-one. Two compounds were not detected when a single extraction was performed, namely cyclododecanol and octacosane, two later eluted compounds. The list of the selected features is reported in Table 5-4. Although a larger number of samples is needed for a proper statistical elaboration, it can be hypothesized that the role of semi-volatile compounds is highly important for pattern recognition purposes.

Table 5-4: . Identification of the selected features using the random forest algorithm for each conditions (single and 6-cumulative extractions).

Compound	CAS	LRI_{exp}	LRI_{Lib}	MS %	N extractions
n-Butyl aldehyde	123 - 72 - 8	635	644	92	6
(Z)-Hex-2-ene, 5-methyl-	13151 - 17 - 2	676	661	90	6
Hept-(2E)-enal	18829-55-5	941	956	97	1
1-Octen-3-ol	3391 - 86 - 4	966	969	91	1
Undecan-2-one	112 - 12 - 9	978	972	85	1/6
Octanal	124 - 13 - 0	990	1005	97	1
Nonanoic acid	112 - 05 - 0	1265	1272	93	1
Cyclododecanol	1724 - 39 - 6	1638	1627	80	6
Octacosane	630 - 02 - 4	2212	2207	80	6

1.5. Conclusion

This work investigated the potential of MCT-HS-SPME for the characterization of the olive oil aroma profile. It was shown as MCT-SPME has the potential to improve the overall sensitivity and burst the level of information for cross-sample studies. The use of MCT-HS-SPME using shorter extraction time is preferable compared to equivalent single extraction time, both in terms of overall signal and for limiting the competitive mechanism that occurs when adsorption-type fibers are used. It was shown as the cumulative increment is linearly proportional to the number of extraction when the HS is saturated. Although this is a general limitation for "semi-quantitative" cross-sample analysis [5], it was here shown that can be overcome by MCT-HS-SPME leading to a higher overall signal meanwhile amplifying the differences among samples.

Further studies are ongoing to investigate the impact of MCT-HS-SPME when the HS is not saturated.

1.6. References

[1] Pawliszyn, J., Theory of Solid-Phase Microextraction. 2000, 38, 270–278.

[2] Górecki, T., Yu, X., Pawliszyn, J., Theory of analyte extraction by selected porous polymer SPME fibres. Analyst 1999, 124, 643–649.

[3] Purcaro, G., Cordero, C., Liberto, E., Bicchi, C., Conte, L. S., Toward a definition of blueprint of virgin olive oil by comprehensive two-dimensional gas chromatography. J. Chromatogr. A 2014, 1334, 101–111.

[42] Purcaro, G., Stefanuto, P. H., Franchina, F. A., Beccaria, M., Wieland-Alter, W. F., Wright, P. F., Hill, J. E., SPME-GC×GC-TOF MS fingerprint of virally-infected cell culture: Sample preparation optimization and data processing evaluation. Anal. Chim. Acta 2018, 1027, 158–167.

[5] Stilo, F., Cordero, C., Sgorbini, B., Bicchi, C., Liberto, E., Highly informative fingerprinting of extra-virgin olive oil volatiles: The role of high concentration-capacity sampling in combination with comprehensive two-dimensional gas chromatography. Separations 2019, 6, 34.

[6] Purcaro, G., Rees, C. A., Wieland-alter, W. F., Schneider, M. J., Wang, X., Stefanuto, P., Wright, P. F., Enelow, R. I., Hill, J. E., States, U., States, U., Volatile fingerprinting of human respiratory viruses. J. Breath Res. 2017, 12, 026015.

[7] Purcaro, G., Rees, C. A., Melvin, J. A., Bomberger, J. M., Hill, J. E., Volatile fingerprinting of Pseudomonas aeruginosa and respiratory syncytial virus infection in an in vitro cystic fibrosis co-infection model. J. Breath Res. 2018, 12, 046001.

[8] Sghaier, L., Vial, J., Sassiat, P., Thiebaut, D., Watiez, M., Breton, S., Rutledge, D. N., Cordella, C. B. Y., An overview of recent developments in volatile compounds analysis from edible oils: Technique-oriented perspectives. Eur. J. Lipid Sci. Technol. 2016, 118, 1853–1879.

[9] Psillakis, E., Yiantzi, E., Sanchez-Prado, L., Kalogerakis, N., Vacuum-assisted headspace solid phase microextraction: Improved extraction of semivolatiles by non-equilibrium headspace sampling under reduced pressure conditions. Anal. Chim. Acta 2012, 742, 30–36.

[10] Psillakis, E., Mousouraki, A., Yiantzi, E., Kalogerakis, N., Effect of Henry's law constant and operating parameters on vacuum-assisted headspace solid phase microextraction. J. Chromatogr. A 2012, 1244, 55–60.

[11] Yiantzi, E., Kalogerakis, N., Psillakis, E., Design and testing of a new sampler for simplified vacuum-assisted headspace solid-phase microextraction. Anal. Chim. Acta 2016, 927, 46–54.

[12] Psillakis, E., Vacuum-assisted headspace solid-phase microextraction: A tutorial review. Anal. Chim. Acta 2017, 986, 12–24.

[13] Mascrez, S., Psillakis, E., Purcaro, G., A multifaceted investigation on the effect of vacuum on the headspace solid-phase microextraction of extra-virgin olive oil. Anal. Chim. Acta 2020, 1103, 106–114.

[14] Oliver-Pozo, C., Trypidis, D., Aparicio, R., Garciá-González, D. L., Aparicio-Ruiz, R., Implementing Dynamic Headspace with SPME Sampling of Virgin Olive Oil Volatiles: Optimization, Quality Analytical Study, and Performance Testing. J. Agric. Food Chem. 2019, 67, 2086–2097.

[15] Lipinski, J., Automated multiple solid phase micro extraction. An approach to enhance the limit of detection for the determination of pesticides in water. Fresenius. J. Anal. Chem. 2000, 367, 445–449.

[16] Chin, S. T., Eyres, G. T., Marriott, P. J., Cumulative solid phase microextraction sampling for gas chromatography-olfactometry of Shiraz wine. J. Chromatogr. A 2012, 1255, 221–227.

[17] Angerosa, F., Servili, M., Selvaggini, R., Taticchi, A., Esposto, S., Montedoro, G., Volatile compounds in virgin olive oil: Occurrence and their relationship with the quality. J. Chromatogr. A 2004, 1054, 17–31.

[18] Romero, I., García-González, D. L., Aparicio-Ruiz, R., Morales, M. T., Validation of SPME-GCMS method for the analysis of virgin olive oil volatiles responsible for sensory defects. Talanta 2015, 134, 394–401.

[19] Aparicio, R., Morales, M. T., Aparicio-Ruiz, R., Tena, N., García-González, D. L., Authenticity of olive oil: Mapping and comparing official methods and promising alternatives. Food Res. Int. 2013, 54, 2025–2038.

[20] IOC, Sensory Analysis of Olive Oil - Method for the Organoleptic Assessment of Virgin Olive Oil. Int. Olive Counc. 2018.

[21] Massart, D., Chemometrics : A Textbook. Elsevier Science Ltd., New York 1988.

[22] Smolinska, A., Hauschild, A.-C., Fijten, R. R. R., Dallinga, J. W., Baumbach, J., van Schooten, F. J., Current breathomics—a review on data pre-processing techniques and machine learning in metabolomics breath analysis. J. Breath Res. 2014, 8, 027105.

[23] Stilo, F., Liberto, E., Reichenbach, S. E., Tao, Q., Bicchi, C., Cordero, C., Untargeted and Targeted Fingerprinting of Extra Virgin Olive Oil Volatiles by Comprehensive Two-Dimensional Gas Chromatography with Mass Spectrometry: Challenges in Long-Term Studies. J. Agric. Food Chem. 2019, 67, 5289–5302.

[24] Oliver-Pozo, C., Aparicio-Ruiz, R., Romero, I., García-González, D. L., Analysis of Volatile Markers for Virgin Olive Oil Aroma Defects by SPME-GC/FID: Possible Sources of Incorrect Data. J. Agric. Food Chem. 2015, 63, 10477–10483.

[25] Mascrez, S., Psillakis, E., Purcaro, G., A multifaceted investigation on the effect of vacuum on the headspace solid-phase microextraction of extra-virgin olive oil. Anal. Chim. Acta 2019, DOI: 10.1016/j.aca.2019.12.053.

[26] Magagna, F., Valverde-Som, L., Ruíz-Samblás, C., Cuadros-Rodríguez, L., Reichenbach, S. E., Bicchi, C., Cordero, C., Combined untargeted and targeted fingerprinting with comprehensive two-dimensional chromatography for volatiles and ripening indicators in olive oil. Anal. Chim. Acta 2016, 936, 245–258.

[27] Trujillo-Rodríguez, M. J., Pino, V., Psillakis, E., Anderson, J. L., Ayala, J. H., Yiantzi, E., Afonso, A. M., Vacuum-assisted headspace-solid phase microextraction for determining volatile free fatty acids and phenols. Investigations on the effect of pressure on competitive adsorption phenomena in a multicomponent system. Anal. Chim. Acta 2017, 962, 41–51.

[28] Kolb, B., Ettre, L. E., Static Headspace-Gas Chromatography: Theory and Practice. Wiley-VHC, New York 2006.

[29] Zhang, Z., Pawliszyn, J., Headspace Solid-Phase Microextraction. Anal. Chem. 1993, 65, 1843–1852.

[30] Cerretani, L., Salvador, M. D., Bendini, A., Fregapane, G., Relationship between sensory evaluation performed by Italian and spanish official panels and volatile and phenolic profiles of virgin olive oils. Chemosens. Percept. 2008, 1, 258–267.

[31] Cavalli, J. F., Fernandez, X., Lizzani-Cuvelier, L., Loiseau, A. M., Comparison of Static Headspace, Headspace Solid Phase Microextraction, Headspace Sorptive Extraction, and Direct Thermal Desorption Techniques on Chemical Composition of French Olive Oils. J. Agric. Food Chem. 2003, 51, 7709–7716.

2. Enhancement of volatile profiling using multiple-cumulative trapping solid-phase microextraction. Consideration on sample volume

Based on: S. Mascrez and G. Purcaro, *Enhancement of volatile profiling using multiple-cumulative trapping solid-phase microextraction. Consideration on sample volume*, Analytica Chimica Acta, 1122 (2020) 89-96.

2.1. Abstract

In the present work, the performance of the multiple-cumulative trapping headspace solid-phase microextraction technique used in the headspace linearity range and saturated headspace was investigated and compared, with the ultimate goal of maximizing the fingerprinting information extractable using a cross-sample comparison algorithm for olive oil quality assessment. It was highlighted as the use of 0.1 g of olive oil provides comparable or even better profiling than 1.5 g at a little expense of sensitivity. However, the use of multiple-cumulative-solid-phase microextraction, along with the correct sample volume, improved not only the overall sensitivity but significantly burst the level of information for cross-sample studies.

2.2. Introduction

Among the different techniques for volatiles profiling of foods, headspace solid-phase microextraction is probably the most widely applied. The main advantages of HS-SPME are easy automation, solvent-free applications, and flexibility due to the different sorbents commercially available [1]. This easy-to-use technique has its theoretical basis on the combination of two equilibria between three-phases [2]. The first equilibrium occurs between the sample and the HS (measured by its distribution constant, K_{hs}), and the second one is between the HS and the fiber (K_{fh}). Both equilibrium or non-equilibrium extractions can be performed; in the former case, the

extraction yield is theoretically maximized, but only when liquid-fiber coatings are used (alias when analytes are extracted via absorption mechanism). The situation is more complicated when sorbent coatings exploiting adsorption mechanisms are used. In the latter case, competition may occur, reducing the extraction yield [3,4]. Nevertheless, the amount extracted by SPME (n) is theoretically proportional to the initial concentration (C_0) in the sample both under equilibrium and non-equilibrium conditions, according to equation (1):

$$n = \frac{K_{hs}\ K_{fh}\ V_f\ V_s\ C_0}{K_{hs}\ K_{fh}\ V_f + K_{hs}\ V_h + V_s} \qquad (1)$$

where C_0: initial concentration; K_{hs} and K_{fh}: distribution coefficient HS/sample and fiber/HS [5], respectively; V_s, V_h, V_f: volume of the samples, the HS, and the fiber coating, respectively.

This proportionality can also be expressed as:

$$A = \frac{C_0}{K_{hs} + ß} \qquad (2)$$

Where A is the chromatographic area, and ß the phase ratio ($ß = V_h/V_s$); when not considering the additional effect of the fiber selectivity and the partition coefficient between the HS and the fiber (K_{fh}) [6]. However, the direct proportionality between the chromatographic area and C_0 is verified only when working in the HS linearity condition, avoiding HS saturation. Verification of the HS linearity is highly mandatory when accurate quantification through calibration is the goal [6]. The calibration procedure then adjusts for other factors, such as matrix effect and response mediated by the fiber. However, verification of HS linearity should not be neglected either when the area intensity of different samples (without calibration) is used as an indicator of absolute concentration, as done when large studies of cross-sample comparisons are performed [7]. The HS linearity range depends on K_{hs} and the activity coefficients of each component. It is generally in the 0.1-1% range of the actual concentration in the sample. It is affected by the sampling temperature, time, and ß. Besides, there are the effects related to the specific sorbent extraction, such as the absorption or adsorption extraction mechanisms (which may lead, in the latter case, to displacement effects), sorbent amount, and sampling temperature and time, which determine the extent of compounds extracted by the fiber as well [6,7]. When multi-component analysis of complex volatile fractions is performed, linearity conditions are a compromise to accommodate both trace and major compounds.

At present, most of the applications involving HS-SPME use adsorption-type fiber, i.e., divinylbenzene/carboxen/polydimethylsiloxane (DVB/CAR/PDMS) [8] with the goal to cover the broaden possible volatility and polarity range of volatiles and to maximize the area response. Moreover, to increase the sensitivity, the trend is the increase of the sample volume, without verifying the HS linearity condition. In this study, olive oil was used as an example matrix. The fingerprinting and profiling

of olive oil volatiles have been extensively studied for quality and authenticity assessment, with the ultimate goal to support the sensory evaluation and discovery of frauds [9–14]. The typical amount of sample used (i.e., ~1.5 g) [10,15,16] leads to HS saturation, as recently showed [7,17]. Sampling from a saturated HS may reduce the information derivable from the volatile fingerprint, regardless the chemometrics tool applied (e.g., hierarchical cluster analysis, random forest, etc). This limitation can be circumvent using multiple-cumulative SPME (MCT-HS-SPME), exploiting the trapping technology. This technique improved the overall sensitivity, amplifying the difference among sample classes, turning the saturation of the HS into an advantage [17]. However, the potentiality of MCT-HS-SPME, when working in the HS linearity condition, has never been investigated.

In the present work, the performance of the MCT-HS-SPME technique used in the HS linearity range and saturated HS was investigated and compared, with the ultimate goal of maximizing the fingerprinting information extractable using a cross-sample comparison algorithm for olive oil quality assessment.

2.3. Materials and methods

2.3.1. Chemicals and reagents

Hexane GC grade (MilliporeSigma®, USA) was used to dilute normal alkanes (C7-C30) mixture (Supelco, PA, USA) used for calculating the linear retention index (LRI) for confirming peak identity.

The divinylbenzene/carboxen/polydimethylsiloxane (DVB/CAR/PDMS) df 50/30 µm 1 cm length fiber was kindly provided by Millipore Sigma (USA).

2.3.2. Olive oil samples

An extra-virgin olive oil sample was purchased at a local supermarket (Gembloux, Belgium).

Twelve samples of olive oil belonging to different quality categories, namely 6 extra-virgin (EVO), 2 virgin (VO), and 4 lampante (LO) olive oils were kindly provided by Carapelli Firenze SpA - Italy (Deoleo group). The samples were of verified geographical and botanical origin and the data of the sensory evaluation carried out according to the International Olive Oil Council protocol [18] were provided as well (Table 5-5).

Table 5-5: List of samples analyzed, along with cultivars, year of harvesting, geographical origin and sensory panel data.

SAMPLE CODE	ORIGIN	CULTIVAR*	YEAR	SENSORY EVALUATION	
				POSITIVE	*NEGATIVE*

					Fruity	Bitter	Pungent	Fusty	Musty	Winey	Rancid
1	**EVO_06**	Spain	*P, H, Pi, Ma, Mo, Ca*	18/19	4.3	4.6	5	0	0	0	0
2	**EVO_06**	Italy	*Le, Mor, Fr*	18/19	3.8	3.8	4.3	0	0	0	0
3	**EVO_06**	Spain	*P, H, Pi*	18/19	2.9	2	3.2	0	0	0	0
4	**EVO_06**	Spain	*P, H, Ar*	18/19	4	3.5	3.8	0	0	0	0
5	**EVO_06**	Italy	*Fr*	18/19	4	3.6	3.8	0	0	0	0
6	**EVO_06**	Italy	*Mor*	18/19	4	3.5	3.8	0	0	0	0
	VO_01	Spain	*P*	18/19	2.6	3.8	2.9	0	0.5	0	0.8
	VO_02	Italy	*Cor*	18/19	1.6	1.3	2	1.8	0.5	0	1
	LO_01				0	0	0	4	0	0	3
	LO_02				0.9	1	1	1	1.9	0.5	1.1
	LO_03				1.1	1	1	0	0.6	0	2.5
	LO_04				1	0.6	0.8	1.7	1	0	1

* P: Picual; H: Hojiblanca; Pi: Picudo; Ma: Manzanilla; Mo: Morisca; Ca: Carrasquena; Le: Leccino; Mor: Moraiolo; Fr: Frantoio; A: Arbequina; Cor: Coratina

2.3.3. HS-SPME procedure

Different amounts of EVO (0.1, 0.25, 0.5, 1.0, and 1.5 g) were weighed in a 20 mL screw top vials, metallic caps with a central hole and polytetrafluoroethylene (PTFE)/silicone septa (Restek, USA).

Before the first use, the SPME fiber was properly conditioned, as suggested by the provider. Centri Autosampler (Markes International Ltd, UK) was used to automate the sample extraction. The sample was agitated at 300 rpm and heated at 43 °C, after 5 min of equilibration, the fiber was exposed to the HS for 10 or 30 min.

The fiber was then thermally desorbed at 250 °C for 2 min. The trap (U-T12ME-2S, Markes International, general-purpose in the C4-C32 volatile range) was cooled at 0 °C during desorption of the fiber in the injector, then 1 min purge at 50 mL/min was performed before heating the trap to 300 °C (hold 10 min) at the maximum ramp temperature allowed by the system. A 1:5 split was applied after the trap. MCT-HS-SPME was carried out with a 5 min enrichment delay (at 43 °C) before the following extraction. Three and six cumulative extractions were performed from the same vial. Specific conditions were then selected for the real-world samples analyzed for cross-sample comparison. The complete sampling design is reported in Table 5-6.

Table 5-6: List of samples analyzed, along with cultivars, year of harvesting, geographical origin.

Sample amount (g)	Extraction time (min)	N cumulative extraction		
0.1	*10*	*1*	*3*	*6*
	30	*1*	3	6
0.25	10	1	3	6
	30	1	3	6
0.5	10	1	3	6
	30	1	3	6
1.0	10	1	3	6
	30	1	3	6
1.5	*10*	*1*	3	*6*
	30	1	3	6

All experiments for investigating the trend of the MCT-HS-SPME were run in triplicate. Real-word samples were analyzed in single. Before starting any samples batch, an SPME fiber blank was performed, as well as periodically to ensure the absence of carryover between runs.

2.3.4. GC-MS analysis

All analyses were performed on a Shimadzu GCMS-TQ8050 NX (Japan), consisting of a GC2030 coupled to a triple-quadrupole mass spectrometer detector (TQ-MS) (Shimadzu, Germany), equipped with a Centri autosampler (Markes International). The chromatographic column was a 30 m × 0.25 mm i.d. × 0.5 μm df SLB-5ms capillary column [(silphenylene polymer, practically equivalent in polarity to poly(5%diphenyl/95% methylsiloxane)] kindly obtained from MilliporeSigma (USA). GC oven temperature program: 30 °C for 5.5 min to 310 °C at 10 °C/min. Carrier gas: helium in constant linear velocity mode at 35.9 cm/s, corresponding to an initial inlet over-pressure of 45.6 kPa. The MS was operated in single-quadrupole mode, in EI mode at 70 eV. The ion source and transfer line temperatures were 200 °C and 280 °C, respectively. The scan mass range was set to 50-450 m/z, with an acquisition frequency of 10 Hz. Data were acquired using Shimadzu GCMSolution ver 4.45 (Shimadzu, Japan). NIST17s and FFNSC 3.0 MS commercial libraries were used for identification. Putative identification was based on the combination of the MS similarity with the NIST17 library and the FFNSC library (Shimadzu) (≥80%) with the confirmation using experimental linear retention index (LRI) within a ±15 range.

2.3.5. Data elaboration and statistical analysis

The data matrix resulting from the olive oil samples analysis was first normalized using Probabilistic Quotient Normalization (PQN) [19]. The data underwent a logarithmic transformation to stabilize the variance and making the distribution of the variables closer to normal [20].

The number of features still outweighed the number of samples; therefore, to overcome this limitation, a machine learning algorithm, namely the random forest (RF) was applied to build a three-class model and select the most discriminatory core volatile analytes [21].

The separation performances of the different conditions were evaluated, measuring the inter-group Euclidean distance [20].

All statistical analyses were performed using R v3.6.1 (R Foundation for Statistical Computing, Vienna, Austria), Excel® (Microsoft Office, version 2016), and Morpheus® (https://software.broadinstitute.org/morpheus/).

2.4. Results and discussion

The HS-SPME extraction from the sample vial was performed multiple times, the fiber was then desorbed into the injector inlet and the compounds released were trapped into a cold trap located between the heated inlet and the head of the analytical column. When the multiple extractions (3 or 6) were completed, the trap was rapidly heated to release the compounds into the analytical column. The use of MCT-HS-SPME was explored using decreasing sample volume to define the sample amount that did not cause saturation of the HS. Moreover, the difference in the overall gain of information on the volatile profile in single extraction or MCT-HS-SPME was evaluated when working in the HS linear range or with HS saturation.

For the first comparison study, 49 compounds were selected, covering a wide range of polarity and volatility [10,11,13,17,22,23] (Table 5-7).

Table 5-7: List of selected analytes along with CAS register number, similarity match of the mass spectrum with the commercial libraries (MS%), experimental and literature linear retention index (LRI), boiling point (B_p), and logarithmic octanol-air partition coefficient (log K_{oa}).

#	CAS	Name	MS%	LRI_{exp}	LRI_{Lib}	Bp	log K_{oa}
1	96 - 17 - 3	2-Methylbutanal	96	658	662	93.57	3.414
2	616 - 25 - 1	1-Penten-3-ol	98	670	671	112.5	4.514
3	1629 - 58 - 9	1-Penten-3-one	95	672	677	104.3	3.748
4	137 - 32 - 6	2-Methylbutan-1-ol	96	719	723	128.7	4.529

5	123 - 51 - 3	3-Methylbutan-1-ol	89	723	729	131.2	4.39
6	1576 - 87 - 0	Pent-(2E)-enal	95	743	751	126.8	3.60
7	108 - 88 - 3	Toluene	96	755	763	110.6	3.29
8	1576 - 95 - 0	Pent-(2Z)-enol	89	764	767	141.3	4.44
9	1576 - 96 - 1	Pent-(2E)-enol	97	767	769	141.3	4.44
10	66 - 25 - 1	n-Hexanal	94	798	801	127.9	3.84
11	16635-54-4	Hex-(2Z)-enal	93	849	850	146.5	4.27
12	6728 - 26 - 3	Hex-(2E)-enal	98	856	857	146.5	4.27
13	928 - 97 - 2	Hex-(3E)-enol	98	860	867	159.6	4.80
14	928 - 95 - 0	Hex-(2E)-enol	98	871	868	159.6	4.80
15	111 - 27 - 3	Hexanol	99	874	867	158.2	5.18
16	100 - 42 - 5	Styrene	88	889	891	145.2	3.89
17	3524 - 75 - 2	$C_6H_{12}O$ (cyclic alcohol)	85	895	903	125.9	3.09
18	3524 - 75 - 2	Cyclopentanemethanol	85	899	903	125.9	3.09
19	142 - 83 - 6	2,4-Hexadienal, (2E,4E)-	97	909	914	155.9	4.76
20	105 - 85 - 1	Citronellyl formate	82	940	953	244.7	-
21	108 - 29 - 2	γ-Pentalactone	94	953	955	206.6	2.36
22	111 - 70 - 6	1-Heptanol	83	973	970	176.9	5.73
23	100 - 84 - 5	3-Methoxytoluene	80	989	983	172.2	-
24	3681 - 71 - 8	Hex-(3Z)-enyl acetate	99	1007	1008	174.2	4.19
25	100 - 51 - 6	Benzyl alcohol	97	1036	1040	204.7	5.96
26	695 - 06 - 7	Hexalactone <gamma->	94	1055	1056	214.9	2.73
27	98 - 86 - 2	Acetophenone	92	1068	1069	202	4.95
28	07/07/3454	Benzene, 1-ethenyl-4-ethyl-	89	1087	1096	192.3	4.97
29	124 - 19 - 6	Nonanal	97	1104	1104	190.8	4.79
30	19945 - 61	(3E)-4,8-Dimethyl-1,3,7-	92	1118	111	195.	3.76

	- 0	nonatriene			3	6	5	
31	502 - 44 - 3	ε-Hexalactone	89	1143	1137	225.4	2.811	
32	14371 - 10 - 9	Cinnamaldehyde, (E)-	90	1186	1189	246.8	6.084	
33	698 - 76 - 0	δ-Propylvalerolactone	82	1191	1205	239.8	3.475	
34	57194 - 69 - 1	Cinnamaldehyde, (Z)-	90	1203	1218	246.8	6.084	
35	112 - 41 - 4	1-Dodecene	92	1206	1204	213.9	4.196	
36	104 - 50 - 7	γ-Octalactone	82	1262	1263	239.1	3.475	
37	112 - 12 - 9	Undecan-2-one	80	1295	1294	230.8	6.675	
38	629 - 50 - 5	Tridecane	84	1300	1300	234.5	4.659	
39	112 - 44 - 7	Undecanal	93	1312	1309	226.1	5.699	
40	138874 - 68 - 7	α-Copaene	95	1389	1375	248.5	4.458	
41	629 - 50 - 5	Tetradecane	86	1400	1400	253.9	4.625	
42	112 - 54 - 9	Dodecanal	95	1411	1410	242.2	6.078	
43	104 - 67 - 6	γ-Undecalactone	82	1475	1483	286	4.576	
44	124 - 25 - 4	Tetradecanal	91	1615	1619	271.6	6.811	
45	2345 - 28 - 0	2-Pentadecanone	92	1701	1697	293.3	6.878	
46	105 - 99 - 7	Dibutyl adipate	94	1767	1747	300.9	7.99	
47	3622 - 84 - 2	N-Butylbenzenesulfonamide	96	1797	1802	326.7	6.362	
48	629 - 80 - 1	Hexadecanal	92	1819	1823	297.8	7.545	
49	36653 - 82 - 4	1-Hexadecanol	98	1878	1884	310.9	9.256	

All the data were acquired in triplicate; the average was considered for comparison purposes. Very good repeatability was obtained at each condition tested with an average relative standard deviation percentage (RSD %) of 8.5 [median 8.5; min: 3.8% and max: 30% (for the less intense compounds)].

2.4.1. Effect of different sample amount on the volatile profile using MCT-HS-SPME

As mentioned in the introduction, to use the area intensity as an indicator of the absolute concentration in the sample, the HS linearity condition should be verified

[6,7]. Therefore, the sample volume to be used needs to be appropriately optimized. According to the theory, when the HS linearity condition is verified, multiple headspace extractions (MHE) from the same vial determine an exponential decline of the chromatographic area recorded, according to equation 3:

$$A_i = A_1 e^{-q(i-1)} \quad (3)$$

Where A is the chromatographic area; i indicates the number of extraction steps; q is a constant.

To determine q, equation (3) is transformed into a linear equation in the following form:

$$\ln Ai = -q(i-1) + \ln A1 \quad (4)$$

For an analogy, the application of MCT-HS-SPME generates a cumulative curve described by a logarithmic equation as (5):

$$Ai = A1 \times \ln[q(i-1)] \quad (5)$$

Which is transformed into a linear curve to determine q according to the exponential equation (6):

$$e^{A_i} = q(i-1) + e^{A^1} \quad (6)$$

Thus, when the HS linearity condition is verified, the exponential model should give a better coefficient of determination (R^2 ~1), while when the HS is saturated, the same amount is extracted each time, thus obtaining a linear model. The R^2 obtained with the two different models (i.e. linear and exponential), extracting for 10- or 30-min different sample volumes (i.e., 0.1, 0.25, 0.5, 1.0, and 1.5 g) are plot in heat-maps depicted in Figure 5-7.

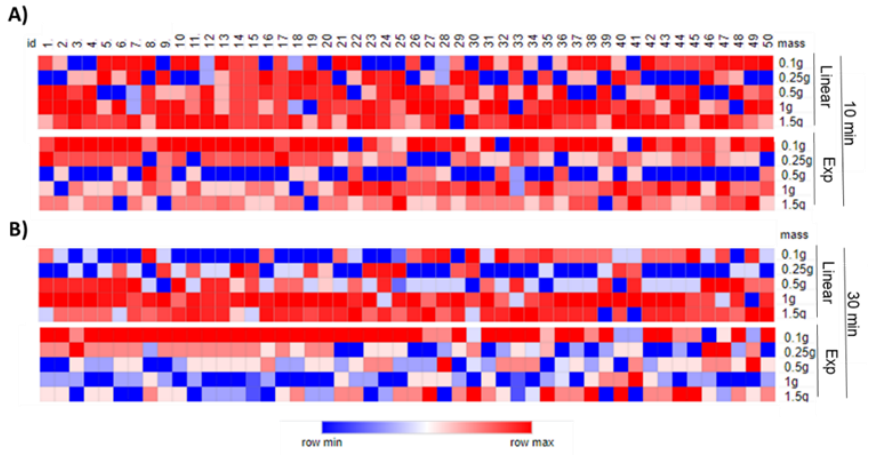

Figure 5-7: *Heat-maps representing the distribution of the coefficients of determination (R^2) obtained applying a linear or an exponential model on the MCT-HS-SPME extraction of different amounts of sample (0.1, 0.25, 0.5, 1.0, 1.5 g) extracting for A) 10 min or B) 30 min. Data were column scaled.*

Reddish color in the heat-maps represents an R^2 closer to 1, while more blueish colors mean values progressively farther from 1. Applying the linear model R2 closer to 1 were obtained for the majority of the compounds when higher amounts of sample (i.e., 1 and 1.5 g) were extracted (both at 10- and 30-min extraction time); while, the linear model was less suitable when lower amounts of sample were extracted (i.e., 0.1 g). As aforementioned, the linear model fits better the cumulative curve when the HS was saturated with the compound of interest. On the other hand, when transforming the variables according to the exponential model, R^2 was maximized when 0.1 g of sample volume was extracted. This behavior denoted that a much lower amount of sample allowed to verify the HS linearity condition for most of the compounds considered, at both 10 or 30 min of extraction.

However, the sample volume impacts the sensitivity differently according to the partition coefficient of the analyte. The increase of the sample volume improved the extraction of compounds characterized by high volatility; contrarily, low volatile compounds are almost not affected [6]. Unfortunately, data on solute partitioning between olive oil and air are sparse. Predictive theoretical models have been proposed correlating partition coefficients in the air-olive oil to those in the air-octanol (K_{oa}) system [24–26]. However, olive oil is far to be a homogenous and reproducible product since its composition is highly cultivar, year of harvesting, and geographical origin dependent. Therefore, in this context, the impacts of the sample

volume on the sensitivity was evaluated by correlating the area response with Koa (Figure 5-8). Precisely, the ratio between the chromatographic peak area obtained extracting 1.5 g and 0.1 g was plotted against K_{oa} (visualize against log K_{oa} for scaling reason). It has to be specified, as showed above, that when 1.5 g of sample is analyzed, the HS of most of the compounds resulted saturated; thus, the chromatographic area recorded is a function of the K_{fh} rather than K_{hs}, mainly when a single extraction is performed. However, it was observed that even in this extreme case, the improvement in sensitivity was limited showing a median over the 49 compounds of 1.3 (min: 0.4; max: 1.8) and 1.5 (min: 0.1; max: 2.3) extracting for 10 and 30 min, respectively. However, no trend in relation to K_{oa} was clearly observed when a single extraction was performed. Different was the situation when 6-MCT-HS-SPME were performed. In the latter case, we can assume that, when starting from saturated HS, after a certain number of extractions a decrease in the HS concetration might occur, at least for some compounds, resembling more the ideal situation of HS linearity. Indeed, after 6-MCT-HS-SPME, a clear trend was observed, especially when 30 min extraction was performed (Figure 5-8). Here the theory was confirmed with a not significant increment towards higher K_{oa}. A similar trend, although less evident, was observed when extracting multiple times for 10 min (median: 1.2; min: 0.7; max: 2.9).

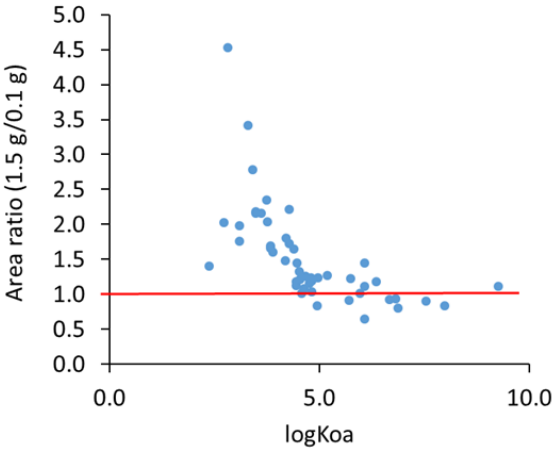

Figure 5-8: *Change in extraction efficiency as a function of the log K_{oa} when extracting for 30 min at 43 °C. The red line highlight the threshold of 1 above which increase in the sensitivity is recorded for extraction of 1.5 g.*

Finally, the extraction efficiency was compared at 10 and 30 min of extraction for both 0.1 g and 1.5 g. When porous fibers are used (as DVB/CAR/PDMS), shorter extraction time is suggested to reduce the competitive adsorption [3,27]. This means that, for most of the compounds, the possibility of sampling not at the equilibrium is increased (as also shown in the surface responses reported in our previous work [15]), which reflects in a lower sensitivity. To evaluate the potential loss of sensitivity, the ratio between the chromatographic area obtained extracting 30 and 10 min was calculated. Independently from the number of multiple extractions, as well as from the sample volume, the ratios of the targeted analytes showed medians in the 1.5-2.1 range, with a maximum 3.3-fold increase at 30 min. A slight decreasing trend of the increment can also be observed towards less volatile compounds. This means that while longer extraction times are beneficial for more volatile compounds, shorter times increase the uptake of the less volatile ones. This is even more evident when MCT-HS-SPME is performed. The same total extraction time was compared when performed as a single extraction or multiple shorter one. Therefore, a 30 min single extraction was compared with 3 × 10 min MCT-SPME. A significant increment was observed, both for 0.1 g and 1.5 g of sample volume, ranging between almost no-increment (ratio=1) and ~4-fold. Figure 5-9 depicted the overall trend in the sensitivity increment when 0.1 g of sample was extracted.

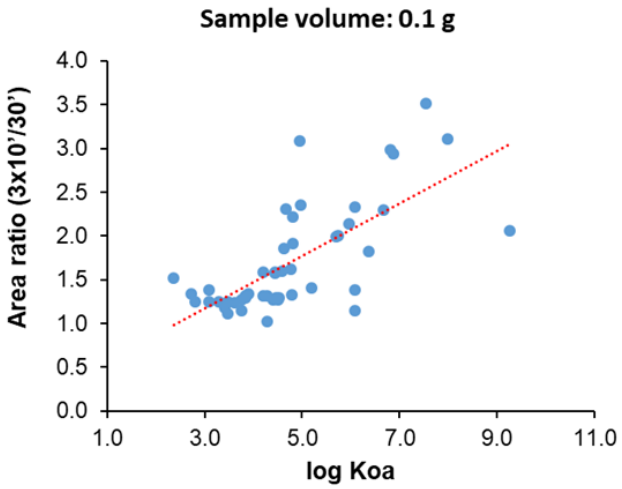

Figure 5-9: *Chromatographic peak area ratio between performing 3-times 10-min-MCT-HS-SPME and a single 30-min extraction versus log K_{oa}. The dotted red line highlights the general trend.*

It can be concluded that sampling for a multiple-short sampling time provides a better overview of the volatile and semi-volatile profile of extra virgin olive oil, covering a more comprehensive range of compounds. The application of MCT-HS-SPME may be beneficial to enhance even more the overall information extractable from HS profiling, with the main advantage of not impacting the sample throughput.

Figure 5-10 reports the comparison among the chromatographic traces obtained by performing single or MCT-HS-SPME at 10 or 30 min with 0.1 g sample volume. In the box, an expanded area to emphasize the gain in sensitivity obtained by performing 3-time 10 min-MCT-HS-SPME.

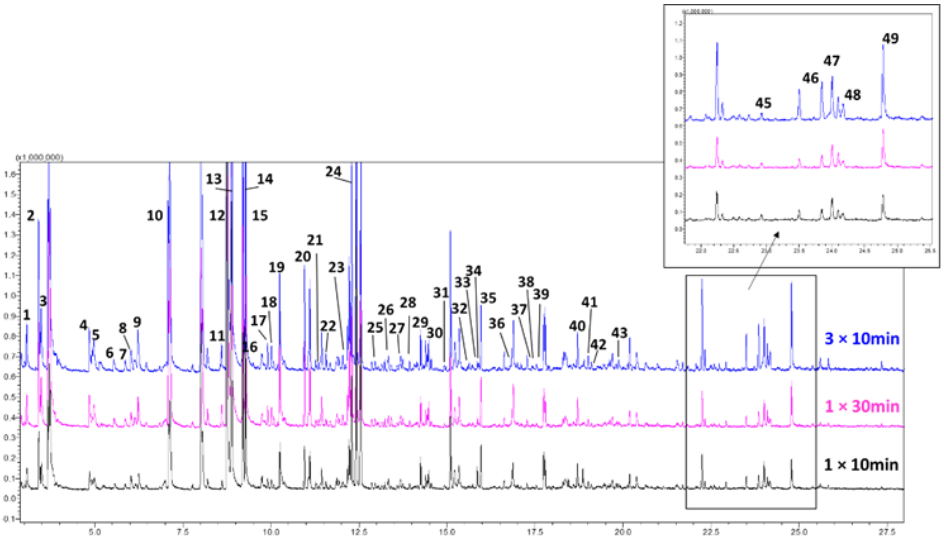

Figure 5-10: *Total ion chromatogram of an EVO sample (0.1 g in a 20 mL vial at 43 °C) extracted 1-time for 10 min, 1 time for 30 min or 3-time for 10 min using MCT-HS-SPME. In the box expansion of the chromatographic area within the box.*

2.4.2. Cross-sample comparison using MCT-HS-SPME

To evaluate the enhancement in the overall information extractable using the MCT-HS-SPME, a cross-sample comparison was performed based on pattern recognition technique. As it has been discussed, the generally accepted approach to treat the GC-MS peak area information as a concentration indicator can be misleading [7], especially when working outside the HS linear range, alias in HS saturation condition. Under the latter conditions, differences in the total concentration among samples are hindered by the maximum capacity of the HS, leading to a less informative fingerprint. Such a situation is very commonly encountered in the literature, where the usual sample volume for EVO analysis is ~1.5 g or more

[10,13,16,28,29]. However, due to the high complexity of the EVO volatile profile and the wide dynamic range of its components, the use of lower sample volume, although beneficial for the most abundant constituent, can be detrimental for the sensitivity of important trace components. In light of this, we hypothesized that the use of the MCT-HS-SPME approach improves the cross-sample comparison amplifying the differences and enhancing the sensitivity, in particular, when working in the HS linear range.

Twelve samples of olive oils (6 EVO, 2 VO, and 4 LO) (Table 5-5) were selected as a proof-of-concept. The experimental design is highlighted in italic in Table 5-6. Two different sample amounts were tested, namely 1.5 and 0.1 g. Single extraction and 6-MCT-HS-SPME were performed, exposing the fiber to the HS for 10 min. When using 0.1 g of the sample, also 3-MCT-HS-SPME (10 min of extraction) and a single 30-min extraction were tested.

The data obtained from each condition was treated separately to maximize the final results. The manual pre-processing of each batch of samples included: chromatograms alignment and cleaning of the data matrix to remove siloxane. Further reduction was based on a frequency of observation cutoffs of 50% within at least a group (i.e., EVO, VO, or LO). The data matrices pre-processed were then normalized and log-transformed. An additional feature reduction step was applied using the random forest (RF) algorithm. A permutation test evaluates the importance of each feature and an averaged value, called mean decrease accuracy, is returned [21,30]. Features are then ranked according to a decreasing mean decrease accuracy value and the most significative ones are chosen based on the cutoff depicted by the 'elbow' of the graph [31].

Heat maps with hierarchical clustering analysis were used to visualize the pattern and the pair-wise Euclidean distances between groups were calculated (Table 5-8.). Figure 5-11 shows the heat-maps obtained after feature selection for all the conditions tested.

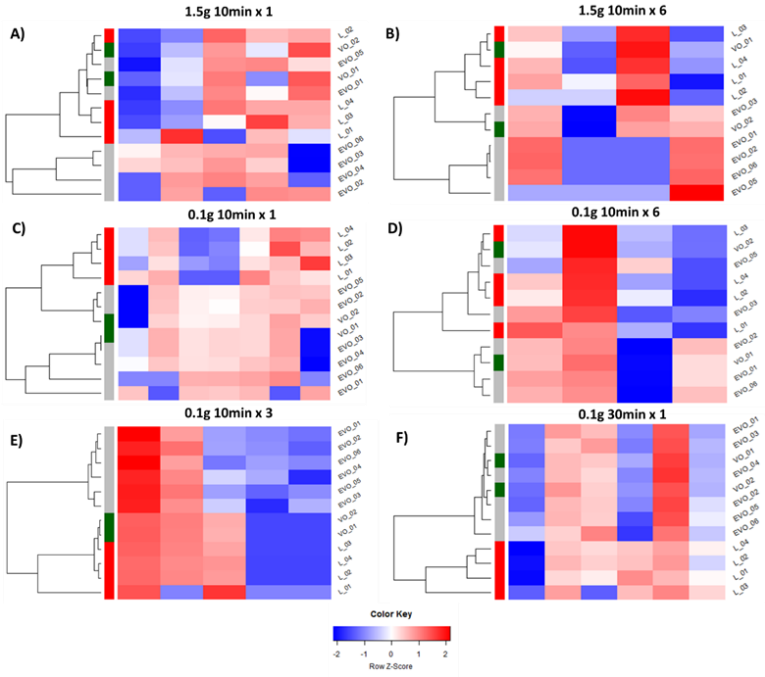

Figure 5-11: *Heat-maps and hierarchical clustering analysis of olive oil samples using the RF selected features for A) single extraction for 10 min with 1.5 g of sample; B) 6-cumulative 10 min-extractions with 1.5 g of sample; C) single extraction for 10 min with 0.1 g of sample; D) 6-cumulative 10 min-extractions with 0.1 g of sample; E) 3-cumulative 10 min-extractions with 0.1 g of sample; F) single extraction for 30 min with 0.1 g of sample. Data were normalized by PQN and log transformed.*

Although the number of samples is limited, some important outcomes can be discussed. The first relevant comparison is between the saturated and non-saturated HS conditions (alias 1.5 g and 0.1 g of sample volume, respectively) performing a single extraction. Figures 7.11A and B show as the three groups, namely EVO, VO, and LO, are better clustered using 0.1 g of sample volume, also reflected in a higher Euclidean distance reported in Table 5-8.

The MCT-SPME improved the clustering both using 1.5 g or 0.1 g of samples (Figure 5-11B, D, and E), but for different reasons. In the case of 1.5 g, where the HS is saturated, the improvement is related to the amplification of the difference in the volatile profile obtained performing multiple extractions, as discussed in details in [17]; while in the case of 0.1 g, where the HS linearity is verified, it is most

possibly related to an increase of sensitivity, especially for trace compounds. However, it is noteworthy that the trend of improvement when working in the HS linearity range is not proportional. In fact, the Euclidean distance is maximized performing 3-MCT-HS-SPME (Table 5-8., Figure 5-11E), both without and with feature selection, although particularly true when data selection was applied. The decrease of the performance performing 6-MCT-HS-SPME (Figure 5-11D) can be related to an adverse alteration in the actual profiling of the HS of the samples. The sensory perception is correlated to the relative distribution of the overall volatiles rather than to the absolute intensity of specific compounds. Therefore, it can be hypothesized that excessive multiple extractions alter the odorant profile, impacting the samples classification.

Finally, performing the HS-SPME for a longer time, i.e., 30 min, the clustering capability was significantly reduced, especially for the most critical discrimination between EVO and VO (Figure 5-11F and Table 5-8.).

Table 5-8: Pair-wise Euclidean distances with and without features selection at the different conditions tested as for Table 5-6.

Extraction time	**Sample volume**	**N° Extr.**	**Feature selection**	**Euclidean distance**		
				EVO-VO	**EVO-L**	**VO-L**
10 min	**1.5 g**	**1**	**No**	17.7	18.7	17.3
		1	**Yes**	3.6	4.1	1.5
		6	**No**	21.9	24.0	20.9
		6	**Yes**	4.7	6.8	3.1
	0.1 g	**1**	**No**	13.5	17.2	16.0
		1	**Yes**	3.6	5.1	4.4
		3	**No**	19.3	21.4	19.3
		3	**Yes**	6.0	7.8	4.5
		6	**No**	20.4	20.4	19.9
		6	**Yes**	2.2	3.1	2.6
30 min		**1**	**No**	18.1	20.9	20.1

	1	**Yes**	0.5	4.2	4.0

It is noteworthy to mention that VOs are the most critical samples to discriminate because, differently from EVO, they present some sensory defects, but not as strong as LOs and still maintaining important positive attributes. The use of 3-MCT-HS-SPME for 10 min was the only condition that allowed to clearly discriminate not only EVO and LO, but also VO without any misclassification, which is a highly significant outcome. It can be hypothesized that a major role in this positive result is played by less volatile components, which are enhanced when multiple-short sampling time are performed.

2.5. Conclusion

In this work, different aspects of the use of HS-SPME were highlighted. The use of short extraction time is highly beneficial when adsorption-type fibers, as DVB/CAR/PDMS, are used. Moreover, the selection of a proper sample volume, avoiding saturation of the HS, provides a more informative HS fingerprinting at a little expense of sensitivity.

In this context, the use of MCT-HS-SPME allowed to boost both aspects, i.e., increasing the sensitivity of the less volatile compounds and maximizing the level of information. It has been shown as the use of multiple-short sampling time (3×10 min) improved the overall results of the cross-sample comparisons applying pattern recognition algorithms. The efficient discrimination between EVO, VO and LO is of high importance for quality and authenticity studies.

On the other side, an excessive number of cumulative extractions led to a negative impact on the actual HS profile and thus samples classification performance, probably due to the response enhancment of less informative and confounding components.

2.6. References

[1] Z. Zhang, J. Pawliszyn, Headspace Solid-Phase Microextraction, Anal. Chem. 65 (1993) 1843–1852. http://doi:10.1021/ac00062a008.

[2] J. Pawliszyn, Theory of Solid-Phase Microextraction, 38 (2000) 270–278.

[3] T. Górecki, X. Yu, J. Pawliszyn, Theory of analyte extraction by selected porous polymer SPME fibres, Analyst. 124 (1999) 643–649. http://doi:10.1039/a808487d.

[4] E. Gionfriddo, É.A. Souza-Silva, J. Pawliszyn, Headspace versus Direct Immersion Solid Phase Microextraction in Complex Matrixes: Investigation of Analyte Behavior in Multicomponent Mixtures, Anal. Chem. 87 (2015) 8448–8456. http://doi:10.1021/acs.analchem.5b01850.

[5] J. Pawliszyn, Handbook of Solid Phase Microextraction, First, Elsevier Inc., London, 2012.

[6] B. Kolb, L.E. Ettre, Static headspace-gas chromatography: theory and practice, Wiley-VHC, New York, 2006. http://doi:10.5860/choice.44-1529.

[7] F. Stilo, C. Cordero, B. Sgorbini, C. Bicchi, E. Liberto, Highly informative fingerprinting of extra-virgin olive oil volatiles: The role of high concentration-capacity sampling in combination with comprehensive two-dimensional gas chromatography, Separations. 6 (2019) 34. http://doi:10.3390/separations6030034.

[8] L. Sghaier, J. Vial, P. Sassiat, D. Thiebaut, M. Watiez, S. Breton, D.N. Rutledge, C.B.Y. Cordella, An overview of recent developments in volatile compounds analysis from edible oils: Technique-oriented perspectives, Eur. J. Lipid Sci. Technol. 118 (2016) 1853–1879. http://doi:10.1002/ejlt.201500508.

[9] F. Angerosa, M. Servili, R. Selvaggini, A. Taticchi, S. Esposto, G. Montedoro, Volatile compounds in virgin olive oil: Occurrence and their relationship with the quality, J. Chromatogr. A. 1054 (2004) 17–31. http://doi:10.1016/j.chroma.2004.07.093.

[10] G. Purcaro, C. Cordero, E. Liberto, C. Bicchi, L.S. Conte, Toward a definition of blueprint of virgin olive oil by comprehensive two-dimensional gas chromatography, J. Chromatogr. A. 1334 (2014) 101–111. http://doi:10.1016/j.chroma.2014.01.067.

[11] F. Stilo, E. Liberto, S.E. Reichenbach, Q. Tao, C. Bicchi, C. Cordero, Untargeted and Targeted Fingerprinting of Extra Virgin Olive Oil Volatiles by Comprehensive Two-Dimensional Gas Chromatography with Mass Spectrometry: Challenges in Long-Term Studies, J. Agric. Food Chem. 67 (2019) 5289–5302. http://doi:10.1021/acs.jafc.9b01661.

[12] I. Romero, D.L. García-González, R. Aparicio-Ruiz, M.T. Morales, Validation of SPME-GCMS method for the analysis of virgin olive oil volatiles responsible for sensory defects, Talanta. 134 (2015) 394–401. http://doi:10.1016/j.talanta.2014.11.032.

[13] C. Oliver-Pozo, R. Aparicio-Ruiz, I. Romero, D.L. García-González, Analysis of Volatile Markers for Virgin Olive Oil Aroma Defects by SPME-GC/FID: Possible Sources of Incorrect Data, J. Agric. Food Chem. 63 (2015) 10477–10483. http://doi:10.1021/acs.jafc.5b03986.

[14] R. Aparicio, M.T. Morales, R. Aparicio-Ruiz, N. Tena, D.L. García-González, Authenticity of olive oil: Mapping and comparing official methods and promising alternatives, Food Res. Int. 54 (2013) 2025–2038. http://doi:10.1016/j.foodres.2013.07.039.

[15] S. Mascrez, E. Psillakis, G. Purcaro, A multifaceted investigation on the effect of vacuum on the headspace solid-phase microextraction of extra-virgin olive oil, Anal. Chim. Acta. 1103 (2020) 106–114. http://doi:10.1016/j.aca.2019.12.053.

[16] F. Magagna, L. Valverde-Som, C. Ruíz-Samblás, L. Cuadros-Rodríguez, S.E. Reichenbach, C. Bicchi, C. Cordero, Combined untargeted and targeted fingerprinting with comprehensive two-dimensional chromatography for volatiles

and ripening indicators in olive oil, Anal. Chim. Acta. 936 (2016) 245–258. http://doi:10.1016/j.aca.2016.07.005.

[17] S. Mascrez, G. Purcaro, Exploring multiple-cumulative solid-phase microextraction for olive oil aroma profiling, J. Sep. Sci. (2020) , 43 (2020) 1934-1941. https://doi.org/10.1002/jssc.20200098.

[18] IOC, Sensory Analysis of Olive Oil - Method for the Organoleptic Assessment of Virgin Olive Oil, Int. Olive Counc. (2018). http://www.internationaloliveoil.org/estaticos/view/224-testing-methods.

[19] F. Dieterle, A. Ross, G. Schlotterbeck, H. Senn, Probabilistic quotient normalization as robust method to account for dilution of complex biological mixtures. Application in1H NMR metabonomics, Anal. Chem. 78 (2006) 4281–4290. http://doi:10.1021/ac051632c.

[20] D. Massart, Chemometrics : a textbook, Elsevier Science Ltd., New York, 1988.

[21] A. Smolinska, A.-C. Hauschild, R.R.R. Fijten, J.W. Dallinga, J. Baumbach, F.J. van Schooten, Current breathomics—a review on data pre-processing techniques and machine learning in metabolomics breath analysis, J. Breath Res. 8 (2014) 027105. http://doi:10.1088/1752-7155/8/2/027105.

[22] S. Mascrez, E. Psillakis, G. Purcaro, A multifaceted investigation on the effect of vacuum on the headspace solid-phase microextraction of extra-virgin olive oil, Anal. Chim. Acta. (2019). http://doi:10.1016/j.aca.2019.12.053.

[23] C. Oliver-Pozo, D. Trypidis, R. Aparicio, D.L. Garciá-González, R. Aparicio-Ruiz, Implementing Dynamic Headspace with SPME Sampling of Virgin Olive Oil Volatiles: Optimization, Quality Analytical Study, and Performance Testing, J. Agric. Food Chem. 67 (2019) 2086–2097. http://doi:10.1021/acs.jafc.9b00477.

[24] A.C. Chamberlin, D.G. Levitt, C.J. Cramer, D.G. Truhlar, Modeling free energies of solvation in olive oil, Mol. Pharm. 5 (2008) 1064–1079.

[25] M.H. Abraham, P.L. Grellier, R.A. McGill, Determination of olive oil–gas and hexadecane–gas partition coefficients, and calculation of the corresponding olive oil–water and hexadecane–water partition coefficients, J. Chem. Soc., Perkin Trans. 2. (1987) 797–803. http://doi:10.1039/P29870000797.

[26] M.H. Abraham, A. Ibrahim, Gas to olive oil partition coefficients: A linear free energy analysis, J. Chem. Inf. Model. 46 (2006) 1735–1741. http://doi:10.1021/ci060047p.

[27] M.J. Trujillo-Rodríguez, V. Pino, E. Psillakis, J.L. Anderson, J.H. Ayala, E. Yiantzi, A.M. Afonso, Vacuum-assisted headspace-solid phase microextraction for determining volatile free fatty acids and phenols. Investigations on the effect of pressure on competitive adsorption phenomena in a multicomponent system, Anal. Chim. Acta. 962 (2017) 41–51. http://doi:10.1016/j.aca.2017.01.056.

[28] L. Cerretani, M.D. Salvador, A. Bendini, G. Fregapane, Relationship between sensory evaluation performed by Italian and spanish official panels and

volatile and phenolic profiles of virgin olive oils, Chemosens. Percept. 1 (2008) 258–267. http://doi:10.1007/s12078-008-9031-3.

[29] J.F. Cavalli, X. Fernandez, L. Lizzani-Cuvelier, A.M. Loiseau, Comparison of Static Headspace, Headspace Solid Phase Microextraction, Headspace Sorptive Extraction, and Direct Thermal Desorption Techniques on Chemical Composition of French Olive Oils, J. Agric. Food Chem. 51 (2003) 7709–7716. http://doi:10.1021/jf034834n.

[30] G. Purcaro, P.H. Stefanuto, F.A. Franchina, M. Beccaria, W.F. Wieland-Alter, P.F. Wright, J.E. Hill, SPME-GC×GC-TOF MS fingerprint of virally-infected cell culture: Sample preparation optimization and data processing evaluation, Anal. Chim. Acta. 1027 (2018) 158–167. http://doi:10.1016/j.aca.2018.03.037.

[31] P.W.T. Krooshof, B. Üstün, G.J. Postma, L.M.C. Buydens, Visualization and recovery of the (Bio)chemical interesting variables in data analysis with support vector machine classification, Anal. Chem. 82 (2010) 7000–7007. http://doi:10.1021/ac101338y.

3. Exploring multiple-cumulative trapping solid-phase microextraction coupled to gas chromatography-mass spectrometry for quality and authenticity assessment of olive oil

Based on: N. Spadafora, S. Mascrez, L. McGregor and G. Purcaro, *Exploring multiple-cumulative trapping solid-phase microextraction coupled to gas chromatography-mass spectrometry for quality and authenticity assessment of olive oil*, Food Chemistry, 383 (**2022**) 132438.

3.1. Abstract

This study explores the potential of an innovative multi-cumulative trapping headspace-solid-phase microextraction approach coupled with untargeted data analysis to enhance the information provided by aroma profiling of virgin olive oil. Sixty-nine samples of different olive oil commercial categories (extra-virgin, virgin and lampante oil) and different geographical origins were analysed using this novel workflow. The results from each sample were aligned and compared using for the first time a tile-based approach to enable the mining of all of the raw data within the chemometrics platform without any pre-processing methods. The data matrix obtained allowed the extraction of multiple-level information from the volatile profile of the samples. Not only was it possible to classify the samples within the

commercial category they belong to; but the same data also provided interesting information regarding the geographical origin of the extra-virgin olive oil.

3.2. Introduction

Virgin olive oil is a high-value food commodity and an important ingredient of the Mediterranean diet with characteristic health benefits and sensory quality. According to European Regulation No 2568/1991 and following modifications [1], physically extracted olive oil is classified into different commercial categories (i.e., extra virgin oil (EVO), virgin oil (VO), and lampante oil (LO)) based on physicochemical and sensory parameters. The sensory evaluation is based on highly standardized procedures following the European and the International Olive Council (IOC) methods [1,2]. Nevertheless, it still poses several trading problems due to the inherent difficulty of the sensory evaluation to guarantee robustness and reproducibility of the results. The evaluation procedure is tedious, time-consuming (4 samples can be assessed per session, with a maximum of 3 sessions per day), and costly, and considering the high number of samples that must be evaluated, may easily fail in consistency and robustness [3].The need to support the organoleptic analysis has been officially highlighted during the Horizon 2020 EU program (H2020-SFS-14a-2014) and it is one of the goals of the OLEUM European Project (Horizon 2020; Grant Agreement No. 635690).

The sensory perception is tightly correlated to the complex aroma profile of olive oil, which reflects several biological, geographical, and technological aspects (i.e., cultivar, geographical origin, fruit ripeness, processing practices, and storage). A strong effort has been dedicated to characterize and correlate the volatile profiles to the quality and authenticity attributes of the olive oil [4-11].

From the analytical viewpoint, different techniques have been used to profile the volatiles, but headspace solid-phase microextraction coupled with gas chromatography-mass spectrometry is by far the most widely applied [6]. The amount extracted by SPME (n) is theoretically proportional to the initial concentration (C_0) in the sample both under equilibrium and non-equilibrium conditions, but the direct proportionality between the chromatographic area and the C_0 is verified only when working in the HS linearity condition, alias avoiding saturation of the HS [12]. Therefore, verification of HS linearity should not be neglected either when the area intensity of different samples is used as an indicator of absolute concentration, as usually done when untargeted studies of cross-sample comparisons are performed [13]. The HS linearity range depends on the distribution coefficient HS/sample (K_{hs}) and the activity coefficients of the analytes, but it is generally in the 0.1-1% range of the sample concentration. Most of the applications for characterizing the volatile profile of olive oil have used a sample quantity in the 1.0-6.0 g range for a 10- or 20-mL vial [6] However, it has been shown (also in the previous chapter) as these quantities largely saturate the HS hindering the ability to perform effective cross-sample comparison by diminishing the differences and weakening the capability to discriminate among different olive oil quality categories

[11,13-15]. The use of a lower amount of sample is recommended to resolve this issue (i.e., 0.1 g in a 20 mL vial), while it does not significantly impair the sensitivity. The same authors propose the use of a multiple-cumulative trapping SPME approach, to improve the overall sensitivity (in particular for the semi-volatiles) meanwhile amplifying the difference among classes by using shorter multiple extraction time rather than a single longer extraction.

In this study, the MCT-HS-SPME-GC-MS technique using the reduced amount of sample discussed previously was validated using 69 samples (34 of EVO, 22 VO, and 13 LO). Moreover, a novel post-analysis data mining platform was utilised, incorporating tile-based data analysis to reduce the complexity of the data and find class-differentiating chemical features. Tile-based fisher ratio approaches have previously been applied to two-dimensional GC [16], but to the authors' knowledge, this is the first reported application for monodimensional GC-MS. The combination of the entire analytical flowchart from MCT-HS-SPME to the data mining platform was explored for the first time in its capability to extract information at multi-levels, not only limited to the commercial class but extended to the geographical origin.

3.3. Materials and methods

3.3.1. Chemicals and reagents

A normal alkane (C7-C30) mixture (MilliporeSigma®, USA) was used to calculate the linear retention index (LRI) and confirm peak identity. The divinylbenzene/carboxen/polydimethylsiloxane (DVB/CAR/PDMS) df 50/30 µm/ 1 cm length fiber was kindly provided by Millipore Sigma (USA).

3.3.2. Olive oil samples

Samples of olive oil from different categories (i.e., EVO, VO, and LO) were kindly provided by Carapelli Firenze SpA - Italy (Deoleo group) along with the sensory evaluation, carried out by the internal recognized official panel following the IOC protocol [17], and additional chemical analyses carried out according to the official method reported in the Reg 2568/91 and following modifications (i.e., acidity, peroxide values, UV measurements, fatty acids profile, ethyl esters, and waxes). All the information are reported in the Table 7.9. A total of 69 samples of olive oil were analyzed, belonging to different quality categories according to the requirements of the EU Reg 2568/91 [1], namely 34 EVO, 22 VO, and 13 LO. The EVO and VO samples were of verified geographical and botanical origin.

Table 5-9: List of samples analyzed, along with cultivars, year of harvesting, geographical origin and sensory panel data (according to (IOC, 2018)). (Cultivars: Ar: Arbequina; Ho: Hojiblanca; Pl: Picual; Po: Picudo; Co: Coratina; Ko: Koreiniki; Ct: Chetui; Cl: Chemlali; NdB: Nocellara del Belice; Mo: Moraiolo; Fr: Frantoio; Og: Ogliarola; Le: Leccino; Mz: Manzanilla; Mr: Morisca; Ca:

Carrasquena; Cb: Cornicabra; Md: Maduval; Ve: Verdial; Cz: Cobranzosa; LdG: Lechin de Granada; Cr:Cerasuola)

Sample code	Geographical origin	Blend (%)					Cultivar	Harve
		Spain (%)	Portugal (%)	Tunisia (%)	Italy (%)	Greece (%)		
S8	Spain, Portugal	55.65	44.35				Ar, Ho, Pl, Po	18/1
S9	Spain	100					Ar, Cb, Pl	18/1
S10	Spain, Tunisia	90		10			Cb, Pl, Ct, Cl	18/1
S11	Spain, Portugal	85.71	14.29				Pl, Ho, Po	18/1
S12	Spain, Tunisia	97.8		2.2			Ar, Pl, Ho, Po, Cl	18/1
S13	Spain	100					Ar, Cb	18/1
S14	Spain	100					Ar, Pl, Ho, Po	18/1
S15	Spain	100					Ar, Pl, Ho, Po	18/1
S16	Spain, Portugal	85	15				Pl, Ho, Po, Md, Ve, Cz	18/1
S17	Italy				100		Co, Og, Cr	17/18-1
S18	Spain	100					Ar, Cb, Pl	18/1
S19	Spain	100					Ar, Cb, Pl	18/1
S20	Spain, Portugal	82.32	17.68				Pl, Ho, Po, Md, Ve, Cz	18/1
S21	Spain, Portugal, Tunisia	75.85	23.09	1.06			Ar, Pl, Ho, Po, Mz, Mr, Ca, Ct, Cl	18/1
S22	Spain, Tunisia	85.1		14.9			Pl, Ar, Ho, Mz, LdG, Ct, Cl	18/1
S23	Spain, Tunisia	96.67		3.33			Pl, Ar, Ho, Ct, Cl	18/1
S24	Spain	100					Pl, Ar, Ho, Mz, LdG	18/1
S25	Spain, Tunisia	90		10			Pl, Ar, Ho, Mz, LdG, Ct, Cl	18/1
S26	Spain	100					Pl, Ho, Po, Mz, Mr, Ca	18/1
S7	Italy				100		Le, Mo, Fr	18/1
S38	Spain	100					Pl, Ho, Po	18/1
S54	Spain	100					Pl, Ho, Ar	18/1
S53	Tunisia			100			Ar, Cl	18/1
S65	Italy				100		Co	17/18-1

S66	Spain	100		Ar	18/1
S67	Italy		100	Co	17/18-1
S28	Italy		100	Fr	18/1
S29	Italy		100	Mo	18/1
S30	Italy		100	Mo	18/1
S6	Italy		100	Co	18/1
S39	Italy		100	NdB	18/1

3.3.3. HS-SPME procedure

A quantity of 0.1 g of oil was weighed in 20 mL screw top vials, metallic caps with a central hole and polytetrafluoroethylene (PTFE)/silicone septa (Restek, USA).

The DVB/CAR/PDMS SPME fiber was conditioned at the first use, as suggested by the manufacturer. A SPME fiber blank was performed at the start of the sampling batch and at set points during the sequence ensuring absence of carryover. The Centri® sample extraction and enrichment platform (Markes International Ltd, UK) was used to perform all the MCT-HS-SPME extraction according to the conditions previously optimized [14]. Briefly, the sample was equilibrated for 5 minutes at 43 °C before 10 min extraction in stirring condition at 300 rpm. The fiber was then thermally desorbed at 250 °C for 2 min in split mode with a trap flow of 50 mL/min. The trap (U-T12ME-2S, Markes International, general-purpose in the C4-C32 volatile range) was cooled at 0 °C during desorption of the fiber in the injector. The HS-SPME extraction was performed three times, with a 5 min enrichment delay (at 43 °C), maintaining the trap at 0 °C during the three extractions. Then the trap was purged for 1 min at 50 mL/min and heated to 300 °C at the maximum ramp rate allowed by the system.

All the samples were injected once as the robustness of the method was supported by previous data on optimization showing an average relative standard deviation (RSD) of 8.5% over a broad range of analytes [14].

3.3.4. GC-MS analysis

A Shimadzu GCMS-TQ8050 NX (Shimadzu, Germany), consisting of a GC2030 and triple-quadrupole mass spectrometer detector (TQ-MS), coupled to the Centri platform (Markes International, UK) was used to perform all analyses. The chromatographic column was a 30 m × 0.25 mm i.d. × 0.5 μm df SLB-5ms capillary column [(silphenylene polymer, practically equivalent in polarity to poly(5%diphenyl/95% methylsiloxane)] kindly obtained from MilliporeSigma (USA). GC oven temperature program: 30 °C for 3.5 min to 310 °C at 5 °C/min. Helium was used as carrier gas in constant linear velocity mode at 30 cm/s, corresponding to an initial inlet over-pressure of 21.6 kPa. The MS was operated in single-quadrupole mode, in EI mode at 70 eV. The ion source and transfer line temperatures were 200 °C and 280 °C, respectively. The scan range was set to 50-

450 m/z, with an acquisition frequency of 10 Hz. Data were acquired using Shimadzu GCMSolution ver 4.45 (Shimadzu, Japan). NIST17 and FFNSC 3.0 MS commercial libraries were used for identification. Putative identification was based on the combination of the MS similarity with the NIST17 library and the FFNSC library (Shimadzu) (≥80%) with the confirmation using experimental linear retention index (LRI) within a ±15 range referring to the LRI reported in the databases using the same 5% stationary phase as reference.

The data acquired with GCMSolution were exported in .cdf and imported in ChromCompare+ (SepSolve Analytical, UK) for post-acquisition data elaboration.

3.3.5. Data elaboration

5.3.3.5.1. Data alignment

The 69 chromatograms were firstly aligned to one user-selected reference chromatogram in ChromCompare+ software (SepSolve Analytical). The alignment algorithm was used to overcome retention time drift observed across the dataset (Figure 5-12.). The algorithm used the available spectral information to automatically align each chromatogram in the dataset to a single 'reference' chromatogram. No further data pre-treatment was required.

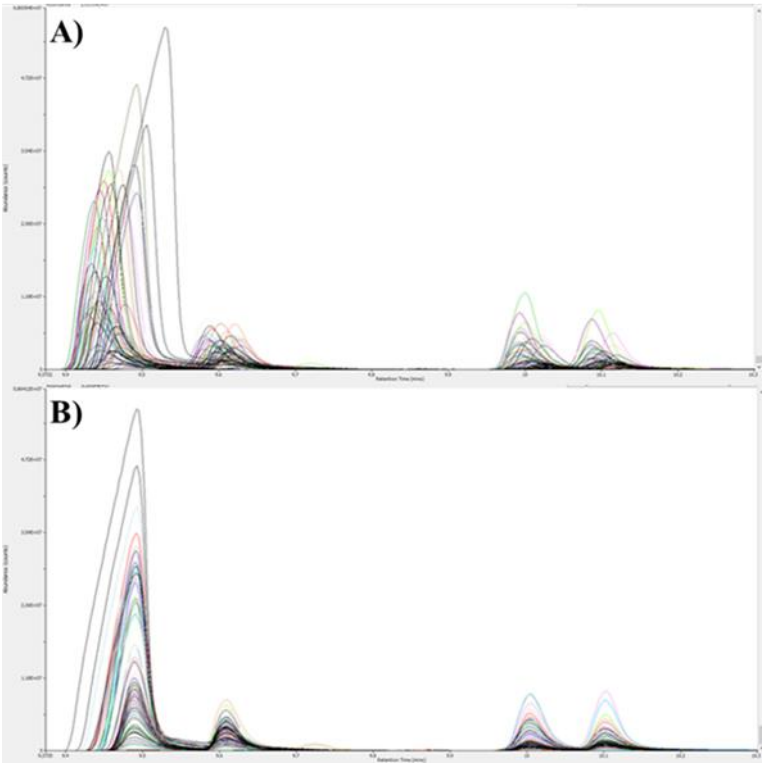

Figure 5-12: *Overlaid TIC chromatograms for all olive oil samples analysed in this study. A small region of the chromatogram is shown A) before alignment and B) after alignment.*

5.3.3.5.2. Untargeted tile-based approach

A tile-based approach was applied to the aligned chromatograms to enable the raw data to be imported into the chemometrics platform directly, without the application of any pre-processing methods, such as integration and identification. Each chromatogram was divided into small sections or 'tiles' (in this case, 5 second windows with a 20% overlap), and the signal for every individual m/z channel was summed for each tile, for comparison across every chromatogram in the dataset. This resulted in thousands of analytical features, labelled according to the retention time of the tile they were located in and the specific m/z channel.

The data matrix resulting from the olive oil samples analysis was first normalized using the grand total abundance. The data underwent a square root transformation to stabilize the variance and making the distribution of the variables closer to normal [18].

Data reduction was then performed using the proprietary feature selection algorithm in ChromCompare+ software (SepSolve Analytical). The algorithm uses a multivariate method to consider the covariance between features. This enabled the top 100 most significant differentiators of the known sample classes (e.g. EVO versus non-EVO) to be found.

The tile-based software enables data reduction and preliminary statistical evaluation to be performed independently from the identification of each feature, significantly simplifying the overall flowchart of data elaboration. However, each feature is correlated with a specific tile, thus the retention time and m/z information is retained, allowing identificaton of the most significanly contributing peaks from the original chromatogram.

The number of features still outweighed the number of samples; therefore, a machine learning algorithm, namely random forest was applied to build models and select the most discriminatory core volatile analytes [19].

5.3.3.5.3. Further statistical analysis

Hierachical clustering was performed with the hclust function in package stat using MetaboAnalyst 5.0 [20]. The heatmap was column normalized and each feature underwent a square root transformation to make features intensity more comparable.

Weighted correlation network analysis (WCNA) was used to correlate sensory descriptors with the top 20 discriminatory VOCs profile with a soft-power setting of 4 using 'flashClust' and 'WGCNA' in R software v.3.6.2 [21,22].

3.4. Results and discussions

Most untargeted studies use the response of the instrument as a correlation of the concentration amount of the specific compound in the sample; therefore, despite the fact that no absolute quantification is generally performed, it is implicit and thus needs to be taken into account during method optimization. This assumption works well unless saturation of the extraction media occurs. This is true also for HS-SPME analysis, where saturation may occurs in the fiber or in the HS. The latter, is often overlooked, while it is highly important to meet the HS linearity condition to validate the instrumental response/concentration correlation and to maximize the information extractable [12-14]. Therefore, the sample volume to be used must be appropriately optimized. In this work, we used the conditions we previously proved optimal to maximize the level of cross-sample comparison information in terms of sample volume and number of multiple trapping [14]. It is worth stressing that it was observed that the use of lower sample volume affected the signal differently depending on the K_{hs} of the analytes. Higher volatile compounds (low K_{hs}) showed an increased signal with higher sample volume, while less volatile compounds (high K_{hs}) were almost not affected. Moreover, it has been shown that longer extraction time increased the extraction yield of the most volatile compounds at the expense of the less volatile. This is likely due to a displacement effect which can occur when using porous fibers [23,24] such as the DVB/CAR/PDMS fiber used in this study. Performing MCT-HS-SPME for a shorter extraction time enhanced the sensitivity significantly for the less volatile compounds (up to ~4-folds), similarly to the effect obtained applying vacuum-assisted extraction [23,24],but with no additional manipulation compared to traditional HS-SPME.

In this work, the enhanced level of information obtainable with the MCT-HS-SPME approach was investigated in a larger number of samples (69 vs the 12 used as a proof of concept in [14]) and multiple questions were investigated to extract not only the information regarding the quality category (i.e., EVO, VO, or LO) but also the geographical origin and the capability to distinguish blends of different origins.

3.4.1. Profiling of olive oils for quality assessment

The set of samples were examined within the post-processing platform using the entire raw data, investigating all the m/z as different channels, and finally visualizing the data by means of a PCA (Figure 5-13). A data reduction step was applied to minimize noise and reduce redundancy, before multivariate feature discovery to rank the features based on their significance, with the 50 most discriminatory features selected for further elaboration. The overall fingerprint of the volatile profile allowed separation of the EVO samples from the non-EVO ones mainly towards the PC1 with 54.5% of variance explained; while VO and LO resulted still partially overlapped. For definition, the EVO samples present only positive sensory attributes since any negative attributes would declassify the sample to VO. On the other hand, VO and LO oils may present both positive and negative

attributes at different intensities, thus are less well-defined which is reflected by the partial overlap of the two clusters, as also reported previously [9].

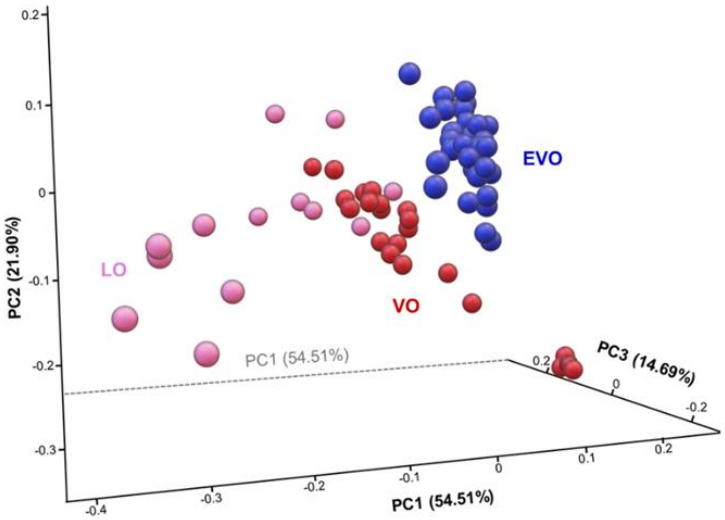

Figure 5-13: *Untargeted Principal Component Analysis of the entire set of samples analyzed by MCT-HS-SPME-GC-MS.*

The non-parametric random forest approach was applied as it has proven to be robust to highly collinear data and resistant to different outliers [25,26]. Based on the preliminary data exploration, the samples were separated into two classes, namely EVO and non-EVO. Figure 5-14 shows the PCA obtained using the top 20 most discriminatory features that were selected using Random Forest. The list of the selected features is reported in Table 5-10 along with the MS similarity match, the linear retention index (LRI) experimentally calculated and compared with the literature, and the indication of the group where each feature is more abundant. More detailed visualization of the relative abundance of each feature between the two groups (i.e., EVO and non-EVO, i.e. LO and VO) is reported in Figure 5-15. Except for F18 and F20 for which no significant difference ($p>0.05$) was highlighted between the EVO and non-EVO group, all the other features were significantly ($p<0.05$) different. In Figure 5-15, the significance among the three groups (i.e., EVO, VO and LO) is reported.

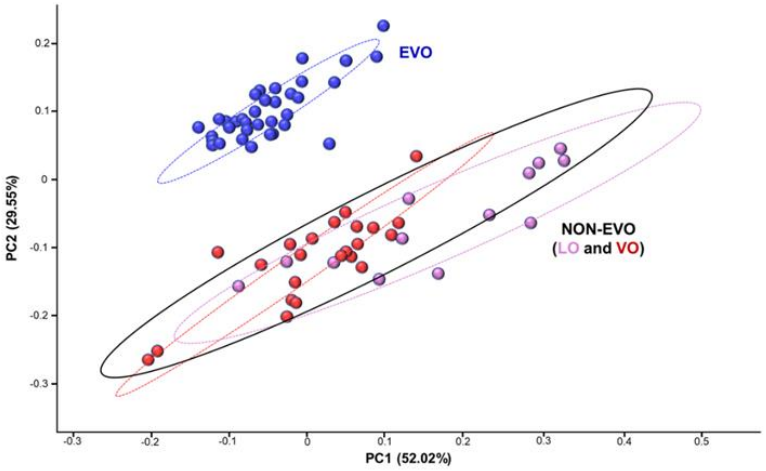

Figure 5-14: *Principal Component Analysis obtained using the 20 top discriminatory features obtained with random forest of the entire set of samples analyzed by MCT-HS-SPME-GC-MS.*

Table 5-10: List of the top discriminatory features extrapolated after three-groups (EVO, VO, and LO) random forest analysis, reported in order of elution, along with the CAS number, their octanol air partition (K_{oa}), mass similarity match (MS%), linear retention index (LRI) experimentally calculated and reported in the literature (LRI_{lib}).

Feature code		Compound	PubChem CID	CAS	K_{oa}	MS %	* LRI	LRI_{lib}	Relative intensity#
1	F9	Unknown					693		↑ EVO
2	F17	(*E*)-2-Penten-1-ol	5364920	1576 - 96 - 1	4.44	85	748	769	↑ EVO
3	F18	Hexanal	6184	66 - 25 - 1	3.84	97	818	806	↑ LO
4	F19	2-Octene	5364448	13389 - 42 - 9	3.02 6	84	831	824	↑ LO
5	F20	(*E*)-2-Hexenal	5281168	6728 - 26 - 3	4.27 9	88	850	857	↑ VO
6	F1	2-Heptanone	8051	110 - 43 - 0	4.14 1	82	893	898	↑ LO
7	F2	(*E*)-2-Heptenal	5283316	18829 - 55 - 5	4.34 1	95	957	956	↑ LO
8	F3	Oct-1-en-3-ol	18827	3391 - 86 - 4	5.62 5	86	981	978	↑ LO
9	F4	Octanal	454	124 - 13 - 0	4.45 7	92	1003	1005	↑ LO
10	F5	(*E*)-2-Octen-1-al	5283324	2548 - 87 - 0	5.09 3	85	1059	1053	↑ LO
11	F6	cis-3-Nonen-1-ol	5364631	10340-23-5	5.91	81	1072	1077	↑ LO
12	F7	Methyl nonyl ether	522469	7289 - 51 - 2		83	1092	1091	↑ LO

13	F8	Phenol, 4-ethyl-	31242	123 - 07 - 9	7.08	91	1165	1166	↓EVO
14	F10	Pulegone	442495	89 - 82 - 7	5.45	92	1240	1241	↓EVO
15	F11	Carvone	7439	99 - 49 - 0	5.21	95	1244	1246	↓EVO
16	F12	α-Terpinyl Acetate	111037	80 - 26 - 2	5.33	84	1350	1349	↓EVO
17	F13	Unknown lactone	-	-	-	-	1363	-	↑ LO
18	F14	Tetradecane	12389	629 - 59 - 4	4.62	92	1398	1400	↓EVO
19	F15	Unknown alkane	-	-	-	-	1406	-	↓EVO
20	F16	Hexadecanol	2682	36653 - 82 - 4	9.25	84	1882	1884	↓EVO

* calculated using the normal alkanes (C7-C30) mixture from MilliporeSigma®(, USA) on the 30 m × 0.25 mm i.d. × 0.5 µm df SLB-5ms capillary column [(silphenylene polymer, practically equivalent in polarity to poly(5%diphenyl/95% methylsiloxane)].

Boxplots of the relative abundance of each feature within the groups, (i.e., EVO , VO and LO) are reported in Figure 5-15.

Seventeen out of the 20 selected features were tentatively identified based on the MS similarity match over 80% and the LRI match with data reported in the commercial libraries used (i.e., NIST17 and FFNSC 3.0). All the compounds showed an LRI difference < ±15 compared to the LRI reported in the databases for the same column stationary phase, except for the earliest eluting component, for which the LRI was extrapolated as eluted before the first eluting alkane, showing a higher discrepancy (i.e., F17 -21).

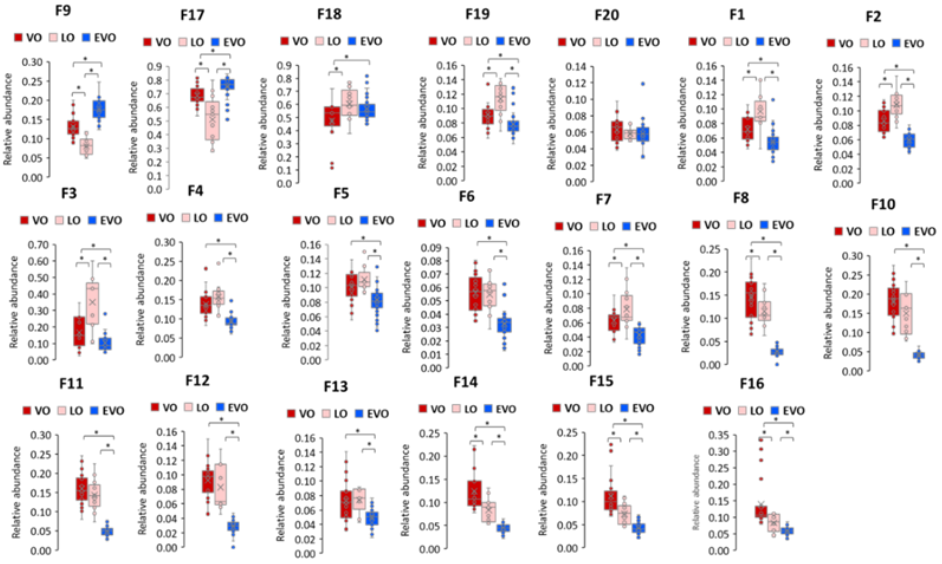

Figure 5-15: *Boxplot of volatiles reported in Table 5-10 discriminating between EVO and non-EVO (LO and VO). The lower, middle and upper lines of the box correspond to the first, second and third quartiles (the 25th, 50th, and 75th percentiles, respectively). The upper whisker extends from the upper line to the largest value no further than 1.5 × IQR from the line (where IQR is the inter-quartile range). The lower whisker extends from the bottom line to the smallest value at most 1.5 × IQR of the range. Data beyond the end of the whiskers are called "outlying" points and are plotted individually. * : p<0.05.*

The sub-group of non-EVO samples, namely VO and LO were then treated separately since the highly significant difference of this group of samples from the EVO masked the difference between VO and LO. A hierarchical cluster (HC) analysis was performed based on the top 20 features (VOCs), discriminating the different classes of oil samples and considering the similarity measure based on Pearson's correlation and the average linkage where the clustering uses the centroids of the observations. The HM, along with the dendrogram reported in Figure 5-16 provides visualization of the data. Each colored cell on the map corresponds to the relative abundance of each feature after square root transformation to make features intensity more comparable. The HM on the right side shows results from WCNA analysis based on the Pearson's correlation of each compound with the sensory descriptor. A negative correlation is shown in blue, while a positive correlation is shown in red. The sensory evaluation score is reported in Table 5-9 and it was provided by an official/recognized panel following the exact procedure elucidated in the IOC Guidelines [17].

Three main hierarchical clusters among features are visible. The first one includes from F5 [(E)-2-octen-1-al] to F19 (2-octene) where higher relative abundance (reddish color on the cells) is shown in most of the LO samples. These compounds show a negative correlation with fruitiness, spiciness, and bitterness while are positively correlated to the negative attributes. Indeed their odor quality is generally referred to as fat, grassy, nut, mouldy, earthy [7, 27]. In particular, F2 [(E)-2-heptanal], F5 [(E)-2-octen-1-al] and F18 (hexanal) have been reported in the literature as correlated to the rancid attributes [4,7].

The second cluster includes features from F13 (unknown lactone) to F15 (unknown alkane) in Figure 5-16, these compounds are mostly low in LO samples, and generally show a higher abundance in VOs and specifically the highest relative abundance in four VOs (i.e., S3, S4, S5, S68), except for F13 (unknown lactone) that shows a fluctuating pattern. Most of the compounds of this cluster are also positively correlated to the positive sensory attributes. Among these, F20 [(E)-2-hexenal] has been largely reported as specific of EVO, thus related to positive attributes [6], F17 [(E)-2-penten-1-ol] has been reported by Cecchi and co-workers [28] has characteristic of EVO. This features cluster includes hexadecanol, long-chain alcohol reported as characterized by bivalent descriptors, such as waxy, greasy, but also floral [27].

The third cluster from F4 (octanal) to F11 in Figure 5-16 shows no significant trends across the samples. This lack of correlation is reflected in the sensory descriptors, which are only slightly more positively correlated to the positive attributes, except for octanal (F4), which shows a marked positive correlation to moldy (musty-humid earthy) and fusty/muddy as previously reported by [8, 29]. The compounds of this cluster are also relatively more intense in the LOs, which presents scores >0 on the positive attributes (Table 5-9). Moreover, in this group, carvone (F11) and pulegone (F10) are also present, which so far have been reported only in aromatized olive oils [30,31].

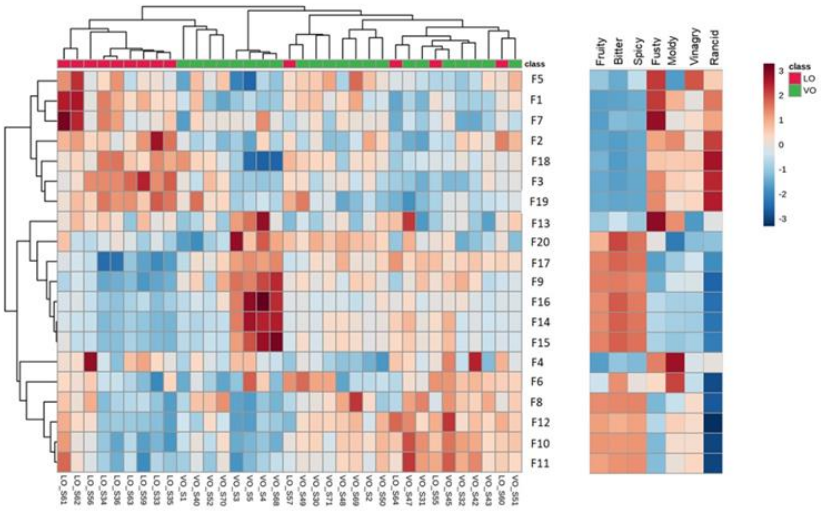

Figure 5-16: *Results of the hierarchical cluster analysis showed through a heatmap and a dendrogram. Weighted correlation network analysis (WCNA) was used to correlate sensory descriptors with the top 20 discriminatory VOCs profile with a soft-power setting of 4. Each colored cell on the map corresponds to the relative abundance of each feature (column normalized) after square root transformation to make features intensity more comparable. Red color showed higher intensity and positive correlation, while blu is lower intensity and negative correlation.*

3.4.2. Geographical origin of extra virgin olive oil

The second step of the research focused on the EVO samples and particularly on the samples with a specific geographical origin to evaluate the capability of the volatiles to discriminate and verify the authenticity information reported in the label. The geographical origin of the EVOs represents a significant added value on the final price, since consumers are willing to pay more for products from a specific known region compared to a blended EVO [32]. Therefore, it is necessary to find a reliable and robust tool to verify the absence of commercial frauds, which are common and

not yet easily detectable despite several different instrumental approaches that have been proposed over the years [33-36]. Among the different characteristics investigated, the volatile profile of olive oil has been proven highly correlated with the geographical origin [28,37,38]. Nevertheless, the volatile fingerprinting is complicated by the many factors that affect the volatile profile besides the geographical origin, such as the pedoclimatic conditions during the tree's growth, the varietal origin, the olive processing conditions, and storage [4]. In this study, the use of a properly optimized sample volume (i.e., 0.1 g) coupled with the innovative MCT-HS-SPME approach allowed to maximize the information extractable thanks to the fact that the HS was not saturated, thus guaranteeing an unbiased volatile profile. Such an approach, proven successful for quality discrimination, has never been investigated for authentication purposes. Here the subset of EVO samples (n=34) was separately analyzed to explore such a capability. In the set of 34 samples, 12 samples were from Spain, 10 samples from Italy, 2 samples from Tunisia, the remaining 10 were blends of oil of different origins in known ratios created by the company for its commercial purpose (Table 5-9). Among them only 9 were monovarietal and one of an unknown cultivar.

In this case, the datatset was split into classes based on the known origin of the sample (i.e. Spain, Italy, Tunisia, etc.) and subjected to grand total normalization and square root transformation. A three-cluster model was created based on the three geographical origins available after multivariate feature discovery. The 25 most significant features based on Random Forest selection were visualized in a three-dimensional PCA (Figure 5-18). In total, 12 compounds were identified as contributing to the top 25 differences – this is due to the nature of the tile-based approach, where overlapped sections are used (i.e. the same compound was found across multiple tiles). The list of the 12 identified compounds is reported in Table 5-11., along with the similarity match, LRI and the group where the feature is predominant among the three groups (boxplots of the relative abundance of each feature within the three geographical origins (i.e., Spain, Italy and Tunisia) are reported in Figure 5-17.).

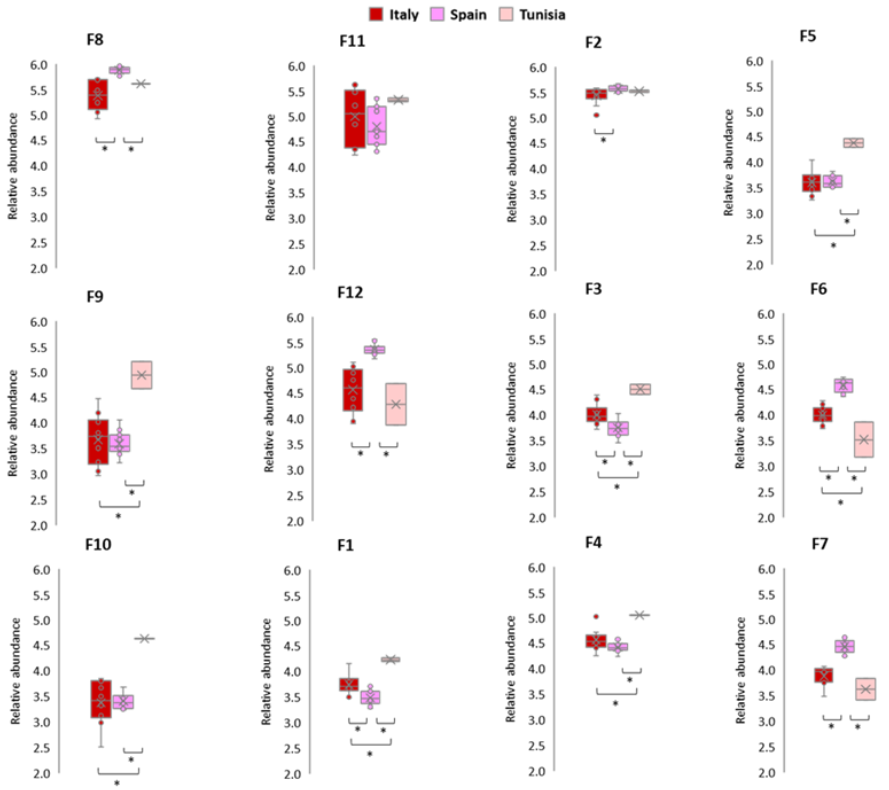

Figure 5-17: *Boxplot of volatiles reported in Table 5-11 discriminating for the geographical origin (i.e. Spain, Italy , and Tunisia). The lower, middle and upper lines of the box correspond to the first, second and third quartiles (the 25th, 50th, and 75th percentiles, respectively). The upper whisker extends from the upper line to the largest value no further than 1.5 × IQR from the line (where IQR is the inter-quartile range). The lower whisker extends from the bottom line to the smallest value at most 1.5 × IQR of the range. Data beyond the end of the whiskers are called "outlying" points and are plotted individually.*: p<0.05.*

A total explained variance of ~98% was reported by the first three PCs (PC1: 83.15%, PC2: 12.89%, and PC3: 2.96%). The three geographical regions were very well discriminated against each other, without any misassigned sample. The blended samples were plotted in the PCA obtained using the selected feature from the 3-class model. All the blended samples were clustered with the Spanish samples, indeed the most abundant origin (over 75%) for all of them. It is important to highlight that the blends were mainly composed by Spain/Tunisia and Spain/Portugal. Samples originated only from Spain were the most abundant (12 samples), while no sample originated from Portugal and only two samples from Tunisia were available. Therefore, the statistical power of the two underrepresented geographical regions was feeble (i.e., Tunisia) or null (i.e. Portugal). Nevertheless, it can be observed that

all the blends clustered with the corresponding main geographical origin (i.e., Spain) but at the edge of the cluster. The two samples that slightly moved away from the Spain cluster towards Tunisia, were S22 and S10, composed by 15% and 10% of Tunisia originated oil, respectively. Among the remaining three Spain/Tunisia blend, samples S12 and S23 were characterized by < 3.5% of Tunisian oil, while S25 had 10% of Tunisian oil but clustered close to the other two blend samples.
It can be hypothesized that with a proper sampling distribution of the different origin and a dedicated experimental design, it could be possible to create a kind of calibration to set a minimum blend addition to discriminate the presence of a different origin oil and possibly a calibration to estimate the different quantity used in the blend.

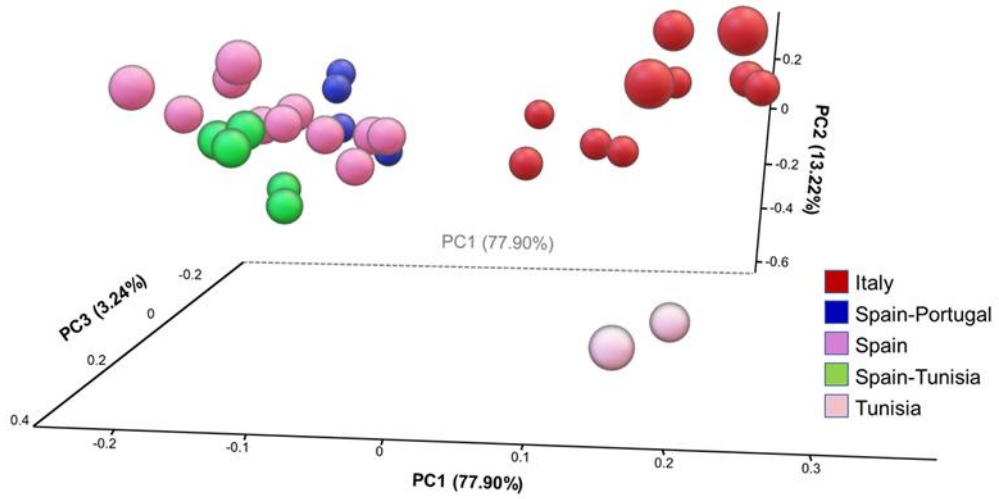

Figure 5-18: *Principal Component Analysis obtained using the 12 top discriminatory features obtained with random forest using the 34 EVO samples analyzed by MCT-HS-SPME-GC-MS. The RF algorithm was performed in a 3-class model, namely Italy, Spain and Tunisia, while the blends were later projected in the PCA.*

Table 5-11: List of the top discriminatory features extrapolated after random forest analysis to discriminate among the three different geographical regions, namely Spain, Italy and Tunisia, reported in order of elution, along with the CAS number, their octanol air partition (Koa), mass similarity match (MS%), linear retention index (LRI) experimentally calculated and reported in the literature (LRIlib).

Feature code		Compound	PubChem CID	CAS	K_{oa}	MS %	LRI*	LRI_{lib}	Relative intensity#
1	F9	Unknown					693		↑ EVO
2	F17	(*E*)-2-Penten-1-ol	5364920	1576 - 96 - 1	4.44	85	748	769	↑ EVO
3	F18	Hexanal	6184	66 - 25 - 1	3.84	97	818	806	↑ LO
4	F19	2-Octene	5364448	13389 - 42 - 9	3.026	84	831	824	↑ LO
5	F20	(*E*)-2-Hexenal	5281168	6728 - 26 - 3	4.279	88	850	857	↑ VO
6	F1	2-Heptanone	8051	110 - 43 - 0	4.141	82	893	898	↑ LO
7	F2	(*E*)-2-Heptenal	5283316	18829 - 55 - 5	4.341	95	957	956	↑ LO
8	F3	Oct-1-en-3-ol	18827	3391 - 86 - 4	5.625	86	981	978	↑ LO
9	F4	Octanal	454	124 - 13 - 0	4.457	92	1003	1005	↑ LO
10	F5	(*E*)-2-Octen-1-al	5283324	2548 - 87 - 0	5.093	85	1059	1053	↑ LO
11	F6	cis-3-Nonen-1-ol	5364631	10340-23-5	5.91	81	1072	1077	↑ LO
12	F7	Methyl nonyl ether	522469	7289 - 51 - 2		83	1092	1091	↑ LO
13	F8	Phenol, 4-ethyl-	31242	123 - 07 - 9	7.08	91	1165	1166	↓EVO
14	F10	Pulegone	442495	89 - 82 - 7	5.451	92	1240	12410	↓EVO
15	F11	Carvone	7439	99 - 49 - 0	5.21	95	1244	1246	↓EVO
16	F12	α-Terpinyl Acetate	111037	80 - 26 - 2	5.336	84	1350	1349	↓EVO
17	F13	Unknown lactone	-	-	-	-	1363	-	↑ LO
18	F14	Tetradecane	12389	629 - 59 - 4	4.625	92	1398	1400	↓EVO
19	F15	Unknown alkane	-	-	-	-	1406	-	↓EVO
20	F16	Hexadecanol	2682	36653 - 82 - 4	9.256	84	1882	1884	↓EVO

3.5. Conclusion

The present study confirmed the potential of volatiles fingerprint in supporting quality and authenticity assessment in the field of olive oil volatiles. The use of a reduced sample amount (i.e., 0.1 g) to avoid HS saturation and of the recently introduced MCT-HS-SPME approach was proven successful in answering multiple questions in the field of olive oil quality and authenticity. The generation of a more representative volatile profile as not biased by saturation and displacement effect allowed to extract a high level of information already from the untargeted cross-sample comparison, i.e. EVO vs non-EVO. The use of an integrated data elaboration platform which used a tile-based fisher ratio approach usually applied in 2D GC but here tested for the first time in 1D GC, allowed to refine the questions into the differentiation of VO and LO oil with a satisfactory degree of incertitude. Moreover, the volatile profile was clearly distinguished among different geographical regions, showing promising results on the possibility to create a “mixture scale” to highlight the presence of blended oil samples. Further devoted studies would be necessary for this direction with a much larger set of samples of each geographical area to increase the statistical power and the accuracy of the model.

3.6. References

[1] European Commission Regulation No 2568/1991. (1991). Commission Regulation (EEC) No 2568/91 of 11 July 1991 on the characteristics of olive oil and olive-residue oil and on the relevant methods of analysis. Official Journal of the European Commission.

[2] IOC. (2018a). Sensory Analysis of Olive Oil - Method for the Organoleptic Assessment of Virgin Olive Oil. International Olive Council, (15).

[3] Conte, L., Bendini, A., Valli, E., Lucci, P., Moret, S., Maquet, A., … Gallina Toschi, T. (2020). Olive oil quality and authenticity: A review of current EU legislation, standards, relevant methods of analyses, their drawbacks and recommendations for the future. Trends in Food Science and Technology, 105(February 2019), 483–493. https://doi.org/10.1016/j.tifs.2019.02.025.

[4] Angerosa, F., Servili, M., Selvaggini, R., Taticchi, A., Esposto, S., & Montedoro, G. (2004). Volatile compounds in virgin olive oil: Occurrence and their relationship with the quality. Journal of Chromatography A, 1054(1–2), 17–31. https://doi.org/10.1016/j.chroma.2004.07.093.

[5] Casadei, E., Valli, E., Aparicio-Ruiz, R., Ortiz-Romero, C., García-González, D. L., Vichi, S., … Toschi, T. G. (2021). Peer inter-laboratory validation study of a harmonized SPME-GC-FID method for the analysis of selected volatile compounds in virgin olive oils. Food Control, 123. https://doi.org/10.1016/j.foodcont.2020.107823.

[6] Cecchi, L., Migliorini, M., & Mulinacci, N. (2021). Virgin olive oil volatile compounds: Composition, sensory characteristics, analytical approaches, quality control, and authentication. Journal of Agricultural and Food Chemistry, 69(7), 2013–2040. https://doi.org/10.1021/acs.jafc.0c07744.

[7] Kalua, C. M., Allen, M. S., Bedgood, D. R., Bishop, A. G., Prenzler, P. D., & Robards, K. (2007). Olive oil volatile compounds, flavour development and quality: A critical review. Food Chemistry, 100(1), 273–286. https://doi.org/10.1016/j.foodchem.2005.09.059.

[8] Purcaro, G., Cordero, C., Liberto, E., Bicchi, C., & Conte, L. S. (2014). Toward a definition of blueprint of virgin olive oil by comprehensive two-dimensional gas chromatography. Journal of Chromatography A, 1334. https://doi.org/10.1016/j.chroma.2014.01.067.

[9] Quintanilla-Casas, B., Bustamante, J., Guardiola, F., García-González, D. L., Barbieri, S., Bendini, A., … Tres, A. (2020). Virgin olive oil volatile fingerprint and chemometrics: Towards an instrumental screening tool to grade the sensory quality. Lwt, 121(November 2019), 108936. https://doi.org/10.1016/j.lwt.2019.108936.

[10] Quintanilla-Casas, B., Marin, M., Guardiola, F., García-González, D. L., Barbieri, S., Bendini, A., … Tres, A. (2020). Supporting the sensory panel to grade virgin olive oils: an in-house-validated screening tool by volatile fingerprinting and chemometrics. Foods, 9(10), 1–14. https://doi.org/10.3390/foods9101509.

[11] Stilo, F., Liberto, E., Reichenbach, S. E., Tao, Q., Bicchi, C., & Cordero, C. (2019). Untargeted and Targeted Fingerprinting of Extra Virgin Olive Oil Volatiles by Comprehensive Two-Dimensional Gas Chromatography with Mass Spectrometry: Challenges in Long-Term Studies. Journal of Agricultural and Food Chemistry, 67(18), 5289–5302. research-article. https://doi.org/10.1021/acs.jafc.9b01661.

[12] Kolb, B., & Ettre, L. E. (2006). Static headspace-gas chromatography: theory and practice. Choice Reviews Online. New York: Wiley-VHC. https://doi.org/10.5860/choice.44-1529.

[13] Stilo, F., Cordero, C., Sgorbini, B., Bicchi, C., & Liberto, E. (2019). Highly informative fingerprinting of extra-virgin olive oil volatiles: The role of high concentration-capacity sampling in combination with comprehensive two-dimensional gas chromatography. Separations, 6(3), 34. https://doi.org/10.3390/separations6030034.

[14] Mascrez, Steven, & Purcaro, G. (2020a). Enhancement of volatile profiling using multiple-cumulative trapping solid-phase microextraction. Consideration on sample volume. Analytica Chimica Acta, 1122, 89–96. https://doi.org/10.1016/j.aca.2020.05.007.

[15] Mascrez, Steven, & Purcaro, G. (2020b). Exploring multiple-cumulative solid-phase microextraction for olive oil aroma profiling. Journal of Separation Science, , 43 (2020) 1934-1941. https://doi.org/10.1002/jssc.20200098.

[16] Freye, C. E., Moore, N. R., & Synovec, R. E. (2018). Enhancing the chemical selectivity in discovery-based analysis with tandem ionization time-of-flight mass spectrometry detection for comprehensive two-dimensional gas chromatography. Journal of Chromatography A, 1537, 99–108. https://doi.org/10.1016/j.chroma.2018.01.008.

[17] IOC. (2018b). Sensory Analysis of Olive Oil - Method for the Organoleptic Assessment of Virgin Olive Oil. International Olive Council, (15). Retrieved from http://www.internationaloliveoil.org/estaticos/view/224-testing-methods.

[18] Massart, D. (1988). Chemometrics : a textbook. Elsevier Science Ltd., New York.

[1819] Smolinska, A., Hauschild, A.-C., Fijten, R. R. R., Dallinga, J. W., Baumbach, J., & van Schooten, F. J. (2014). Current breathomics—a review on data pre-processing techniques and machine learning in metabolomics breath analysis. Journal of Breath Research, 8(2), 027105. https://doi.org/10.1088/1752-7155/8/2/027105.

[20] Pang, Z., Chong, J., Zhou, G., De Lima Morais, D. A., Chang, L., Barrette, M., … Xia, J. (2021). MetaboAnalyst 5.0: Narrowing the gap between raw spectra and functional insights. Nucleic Acids Research, 49(W1), W388–W396. https://doi.org/10.1093/nar/gkab382.

[21] Langfelder, P., & Horvath, S. (2012). Fast R functions for robust correlations and hierarchical clustering. Journal of Statistical Software, 46(11), 1–17. https://doi.org/10.18637/jss.v046.i11.

[22] Muto, A., Müller, C. T., Bruno, L., McGregor, L., Ferrante, A., Chiappetta, A. A. C., … Spadafora, N. D. (2020). Fruit volatilome profiling through GC × GC-ToF-MS and gene expression analyses reveal differences amongst peach cultivars in their response to cold storage. Scientific Reports, 10(1), 1–16. https://doi.org/10.1038/s41598-020-75322-z.

[23] Trujillo-Rodríguez, M. J., Pino, V., Psillakis, E., Anderson, J. L., Ayala, J. H., Yiantzi, E., & Afonso, A. M. (2017). Vacuum-assisted headspace-solid phase microextraction for determining volatile free fatty acids and phenols. Investigations on the effect of pressure on competitive adsorption phenomena in a multicomponent system. Analytica Chimica Acta, 962, 41–51. https://doi.org/10.1016/j.aca.2017.01.056.

[24] Górecki, T., Yu, X., & Pawliszyn, J. (1999). Theory of analyte extraction by selected porous polymer SPME fibres. Analyst, 124(5), 643–649. https://doi.org/10.1039/a808487d.

[25] Breiman, L. (2001). Random forests. Machine Learning, 45(1), 5–32. https://doi.org/10.1023/A:1010933404324.

[26] Purcaro, Giorgia, Stefanuto, P. H., Franchina, F. A., Beccaria, M., Wieland-Alter, W. F., Wright, P. F., & Hill, J. E. (2018). SPME-GC×GC-TOF MS fingerprint of virally-infected cell culture: Sample preparation optimization and data processing evaluation. Analytica Chimica Acta, 1027, 158–167. https://doi.org/10.1016/j.aca.2018.03.037.

[26] IOC. (2018b). Sensory Analysis of Olive Oil - Method for the Organoleptic Assessment of Virgin Olive Oil. International Olive Council, (15). Retrieved from http://www.internationaloliveoil.org/estaticos/view/224-testing-methods.

[27] Üçüncüoğlu, D., & Sivri-Özay, D. (2020). Geographical origin impact on volatile composition and some quality parameters of virgin olive oils extracted from the “Ayvalık” variety. Heliyon, 6(9). https://doi.org/10.1016/j.heliyon.2020.e04919.

[28] Cecchi, L., Migliorini, M., Giambanelli, E., Rossetti, A., Cane, A., Mulinacci, N., & Melani, F. (2020). Authentication of the geographical origin of virgin olive oils from the main worldwide producing countries: A new combination of HS-SPME-GC-MS analysis of volatile compounds and chemometrics applied to 1217 samples. Food Control, 112(February), 107156. https://doi.org/10.1016/j.foodcont.2020.107156.

[29] Sales, C., Portolés, T., Johnsen, L. G., Danielsen, M., & Beltran, J. (2019). Olive oil quality classification and measurement of its organoleptic attributes by untargeted GC–MS and multivariate statistical-based approach. Food Chemistry, 271(July 2018), 488–496. https://doi.org/10.1016/j.foodchem.2018.07.200.

[30] Assami, K., Chemat, S., Meklati, B. Y., & Chemat, F. (2016). Ultrasound-Assisted Aromatisation with Condiments as an Enabling Technique for Olive Oil Flavouring and Shelf Life Enhancement. Food Analytical Methods, 9(4), 982–990. https://doi.org/10.1007/s12161-015-0273-9.

[31] Kiralan, S. S., Karagoz, S. G., Ozkan, G., Kiralan, M., & Ketenoglu, O. (2021). Changes in Volatile Compounds of Virgin Olive Oil Flavored with Essential

Oils During Thermal and Photo-Oxidation. Food Analytical Methods, 883–896. https://doi.org/10.1007/s12161-020-01926-w.

[32] European Union. (2006). Council regulation (EC/510/2006) of 20 March 2006 on the protection of geographical indications and designations of origin for agricultural products and foodstuffs. Official Journal of the European Union, L93(510), 12–25.

[33] Cajka, T., Riddellova, K., Klimankova, E., Cerna, M., Pudil, F., & Hajslova, J. (2010). Traceability of olive oil based on volatiles pattern and multivariate analysis. Food Chemistry, 121(1), 282–289. https://doi.org/10.1016/j.foodchem.2009.12.011.

[34] Gumus, Z. P., Celenk, V. U., Tekin, S., Yurdakul, O., & Ertas, H. (2017). Determination of trace elements and stable carbon isotope ratios in virgin olive oils from Western Turkey to authenticate geographical origin with a chemometric approach. European Food Research and Technology, 243(10), 1719–1727. https://doi.org/10.1007/s00217-017-2876-4.

[35] Mohamed, M. Ben, Rocchetti, G., Montesano, D., Ali, S. Ben, Guasmi, F., Grati-Kamoun, N., & Lucini, L. (2018). Discrimination of Tunisian and Italian extra-virgin olive oils according to their phenolic and sterolic fingerprints. Food Research International, 106 (December 2017), 920–927. https://doi.org/10.1016/j.foodres.2018.02.010.

[36] Ruisánchez, I., Jiménez-Carvelo, A. M., & Callao, M. P. (2021). ROC curves for the optimization of one-class model parameters. A case study: Authenticating extra virgin olive oil from a Catalan protected designation of origin. Talanta, 222(June 2020). https://doi.org/10.1016/j.talanta.2020.121564.

[37] Lukić, I., Carlin, S., Horvat, I., & Vrhovsek, U. (2019). Combined targeted and untargeted profiling of volatile aroma compounds with comprehensive two-dimensional gas chromatography for differentiation of virgin olive oils according to variety and geographical origin. Food Chemistry, 270(March 2018), 403–414. https://doi.org/10.1016/j.foodchem.2018.07.133.

[38] Ouni, Y., Flamini, G., Issaoui, M., Nabil, B. Y., Cioni, P. L., Hammami, M., … Zarrouk, M. (2011). Volatile compounds and compositional quality of virgin olive oil from Oueslati variety: Influence of geographical origin. Food Chemistry, 124(4), 1770–1776. https://doi.org/10.1016/j.foodchem.2010.08.023.

Chapter 6

Combination of Vacuum-assisted and multiple-cumulative trapping HS-SPME

1. Vacuum-assisted and multi-cumulative trapping in headspace solid-phase microextraction combined with comprehensive multidimensional chromatography-mass spectrometry for profiling olive oil aroma

Based on: S. Mascrez, J. Aspromonte, N. Spadafora, and G. Purcaro, *Vacuum-assisted and multi-cumulative trapping in headspace solid-phase microextraction combined with comprehensive multidimensional chromatography-mass spectrometry for profiling olive oil aroma*, Food Chemistry, 442 (2024) 138409.

1.1. Abstract

In the present work vacuum (Vac) and multiple cumulative trapping (MCT) headspace solid phase microextraction (HS-SPME) were evaluated as alternative or combined techniques for the volatile profiling. A higher extraction performance for semi-volatiles was shown by all three techniques. Synergic combination of Vac and MCT showed up to 5-times extraction power for less volatile compounds. The hyphenation of said techniques with comprehensive two-dimensional gas chromatography (GC×GC) enabled a comprehensive analysis of the volatilome. Firstly, 18 targeted quality markers, previously defined by means of classical HS-SPME, were explored for their ability to classify commercial categories. The applicability of such markers proved to be limited with the alternative sampling techniques. An untargeted approach enables the selection of specific features for each technique showing a better classification capacity of the commercial categories. No misclassifications were observed, except for one extra virgin olive oil classified as virgin olive oil in 3 × 10 min Vac-MCT-HS-SPME.

1.2. Introduction

In 1990, Arthur and Pawliszyn developed a solvent-free sample preparation method known as solid-phase microextraction (SPME) [1]. Since its introduction, it has experienced exponential popularity and rapid diffusion in several fields of application, including pharmaceutical, environmental, and food analysis [2–4]. Thanks to its simplicity for automation, commercial availability of a fair variety of sorbent materials, and null or very limited solvent use, SPME is still one of the most applied miniaturized and green analytical techniques, especially in the analysis of volatiles and semi-volatiles [5]. Among the various formats and extraction modes, fiber and headspace (HS) extraction are still the most employed as robust and reliable methods to preconcentrate semi-volatile and volatile analytes [6]. In particular, SPME has found wide application in untargeted metabolomics studies, being highly suitable to be coupled with powerful chromatographic techniques such as multidimensional comprehensive gas chromatography (GC×GC) coupled with mass spectrometry (MS). This technique can provide highly specific chromatographic fingerprints from which different levels of information can be

extracted thanks to dedicated data handling. GC×GC allows for enhanced characterization of the broad range of compounds extracted using SPME. Nevertheless, the coverage of compounds in untargeted studies is determined by a compromise between sensitivity and sample throughput. Indeed, sensitivity is maximized when the extraction is performed under equilibrium conditions. However, attaining equilibrium can range from a few minutes to several hours, depending on the nature of the sample. Nevertheless, it should be noted that longer extraction times may hinder the extraction of some compounds due to the displacement effects [7,8]. Either when equilibrium is not reached or when displacement effects take place, the less volatile compounds are released from the fiber, thus limiting the coverage range of the extraction.

Temperature and stirring have been the most exploited parameters to improve the extraction capacity in SPME. However, other alternatives to accelerate the extraction kinetics and in-crease the yield of less volatile compounds have been investigated more recently; namely, vacuum-assisted (Vac-) and multi-cumulative trapping (MCT) HS. The former, consisting in evacuating the air from the vial before exposing the SPME fiber, was introduced by Brunton *et al.* in 2001 [9] and systematically investigated since 2012 by Psillakis et al. [10–12]. Vac-HS-SPME has proven an outstanding effect in enhancing the kinetics of extraction at milder temperatures. Since 2012, Vac-HS-SPME has been effectively used with a variety of sam-ples, both liquid and solid [13–18]. In particular, we investigated its effect in the extraction from fat samples (i.e., virgin olive oil) for the first time, proving an increment up to almost 10-fold (i.e., for α-farnesene) on the less volatile compounds. Moreover, a synergic effect with temperature that reduced the sample's viscosity and favored the HS's replenishment af-ter the rapid depletion of the most volatile into the fiber was proven [18].

Alternatively, MCT-HS-SPME has shown a similar behaviour towards the enrichment of the less volatile analytes when multiple extractions are performed from the same vial [19–21]. This technique consists in extracting multiple times from the HS of the same vial, desorbing the fiber each time in the injector, and trapping the compounds in a cold trap located between the injector and the analytical column. Once the defined number of extraction is completed, the cold trap is heated up and the trapped compounds transferred into the chromatographic column. The repeated extraction depletes the HS from the most volatile compounds, reducing displacement and favoring the mass transfer of the less volatile ones into the HS. The analytes extracted with the fiber are repeatedly trapped in a cold trap before thermal desorption into the GC system in a single run. In their initial studies, Mascrez *et al.* [19–21] showed that using MCT increased the extraction yield of SPME at a given absolute time (i.e., 3 extractions of 10 min each vs a single 30 min extraction) by a factor of 1 to 3.5. It was also shown how the number of repeated extractions is an important parameter to be optimized in order to maximize the discrimination among commercial categories in a cross-sample comparison study of virgin olive oil quality [20]. Moreover, the enhanced extraction yield led to the ability to use the same virgin olive oil study of volatiles to answer multiple questions

related to both quality (i.e., discrimination into commercial categories) and authenticity (i.e., geographical origin) [21].

The aim of the present paper is to compare Vac-HS-SPME and MCT-HS-SPME approaches and to investigate the possible synergic effect derived by the combined application of Vac-MCT-HS-SPME. The data were all acquired by exploiting the enhanced separation provided by a reversed fill/flush flow modulated GC×GC. These methods were applied to virgin olive oil samples of different commercial categories and geographical origins. The extraction responses of the studied methods were evaluated, focusing on specific quality markers high-lighted by previous studies [22–29], particularly in the context of the OLEUM European pro-ject (Horizon 2020; Grant Agreement No. 635690). The cross-sample discrimination ability was evaluated using the 18 markers validated by an inter-laboratory collaborative trial with-in the OLEUM Project [22], and independently by performing data reduction and selecting the most significant features using random forest (RF).

1.3. Materials and methods

1.3.1. Chemicals and reagents

A normal alkane (C7-C30) mixture (MilliporeSigma®, USA) was used to calculate the linear retention index (LRI) and confirm peak identity. The 2 cm length fiber coated with divinylbenzene/carboxen/polydimethylsiloxane (DVB/CAR/PDMS) was kindly provided by MilliporeSigma® (USA).

1.3.2. Olive oil samples

Twenty-four samples of olive oil belonging to different commercial categories, namely 11 extra-virgin (EVO), 8 virgin (VO), and 5 lampante (LO) olive oils, were kindly provided by Carapelli Firenze SpA - Italy (Deoleo group). The samples were of verified geographical origin and the sensory evaluation, carried out according to the International Olive Council protocol [30], was also provided by the Carapelli Firenze SpA. The trained sensory panel is officially recognized at the European level and listed by the Italian Ministry of Agriculture, Food Sovereignty and Forestry (Table 6-1).

A VO sample (VO-03) was used for the preliminary verifications and methods comparison.

Table 6-1: List of samples analyzed, along with year of harvesting, geographical origin and sensory panel data (according to [24]).

Sample code	Geographical origin	Blend (%)	Harvest year	Positive attributes	Negative attributes

		Spain (%)	Tunisia (%)	Italy (%)		Fruity	Bitter	Pungent	Fusty/Muddy sediment	Musty-humid earthy	Vinegary	Rancid
EVO-01	Tunisia		100		18/19	2.4	2.3	2.9	0	0	0	0
EVO-02	Italia			100	18/19	3.9	3.5	4	0	0	0	0
EVO-03	Italia			100	18/19	3.8	3.8	4.3	0	0	0	0
EVO-04	Spagna	100			18/19	4.5	3.9	4.1	0	0	0	0
EVO-05	Spagna	100			18/19	2.2	2.8	2.4	0	0	0	0
EVO-06	Spagna, Tunisia	96.67	3.33		18/19	2.3	2.1	2.3	0	0	0	0
EVO-07	Spagna	100			18/19	4	4.5	4.5	0	0	0	0
EVO-08	Spagna, Tunisia	90	10		18/19	4	3.5	3.9	0	0	0	0
EVO-09	Italia			100	18/19	4	3.6	3.8	0	0	0	0
EVO-10	Spagna	100			18/19	3.7	2.9	3.7	0	0	0	0
EVO-11	Tunisia		100		18/19	2.6	1.6	1.6	0	0	0	0
VO-01	Italia			100		3.3	2.8	3.5	0.5	0	0.5	0
VO-02	Italia			100		2.8	2.5	2.7	0	0	0	1
VO-03	Italia			100		2	2	2	0.5	0	0	1
VO-04	Italia			100	18/19	2.7	2.5	2.7	0	0	0	1
VO-05	Spagna	100				2	1.4	1.8	1	0.4	0	1
VO-06	Spagna	100			16/17	1.6	1.8	2	1.4	0.7	0	0.5
VO-07	Spagna	100			16/17	2	2	2	1.4	0.6	0	1
VO-08	Spagna, Tunisia					1.9	1.3	1.4	0.4	0.7	0	0
LO-01						0	0	0	3.1	1.6	0	1.6
LO-02						1	1	1.1	0.9	0.7	0	1.8
LO-03						0	0	0	0	0	0	3.8
LO-04						0	0	0	2	0	0	3.6
LO-05						0	0	0	2	0	0	3.6

1.3.3. HS-SPME procedures

All the SPME extractions were performed using a Centri® sample extraction and enrichment platform (Markes International Ltd, Bridgend, UK) equipped with a general-purpose trap (U-T12ME-2S, Markes International, general-purpose in the C4-C32 volatile range). The DVB/CAR/PDMS SPME fiber was used. It was conditioned before the first use, as suggested by the manufacturer. A blank analysis was performed at the start of the sampling batch and at different points during sequences, ensuring the absence of carry-over. Extractions in Vac-HS-SPME, MCT-HS-SPME, or the combined Vac-MCT-HS-SPME were performed as described below and in triplicate for each of the procedures for comparison purposes. While in all cases, the fiber was thermally desorbed at 250 °C for 2 min. The trap (U-T12ME-2S) was cooled at 0 °C during the desorption of the fiber in the injector. Then, 2 min of purge at 50 mL/min were performed before heating the trap at 300 °C (hold 5 min). A 1:5 split was set on the trap to facilitate the transfer of analytes into the head of the GC column in a narrow chromatographic band.

Quantities of 0.1 g of oil were weighed in 20 mL screw top vials. Metallic caps with a central hole and polytetrafluoroethylene (PTFE)/silicone septa (Restek, Bellefonte, USA) were used for MCT-HS-SPME and regular HS-SPME. In the case of Vac-HS-SPME and Vac-HS-SPME the custom-made cap, designed and constructed at the Laboratory of Aquatic Chemistry (School of Environmental Engineering, Technical University of Crete) was used. The latter cap was equipped with cylindrical Thermogreen®LB-1 septum (Supelco) with half-hole (6 mm diameter × 9 mm length) and could fit 20 mL screw top vials (Restek). These caps used to perform Vac-HS-SPME are now commercially available at ExtraTECH Analytical Solutions (Khania, Grece).

MCT-HS-SPME Procedure: The extraction was performed according to the optimized conditions reported in the previous study [21,22]. Briefly, 3-times 10-min cumulative extractions were performed at 43 °C, setting a 5 min equilibration time between extractions at the same temperature. This condition is also called 3×10 min-MCT-HS-SPME later in the text.

Vac-HS-SPME procedure: The air inside the sampling device was evacuated for 1 min using a MD4C diaphragm pump (7 mbar = 0.007 atm final vacuum without gas ballast) manufactured by Vacuubran GmbH & Co. KZ (Werthem, Germany) before introducing the oil sample. Gastight syringe was used to introduce 0.1 g of virgin olive oil into the vial. A two-variable ($k = 2$) inscribed rotatable ($\alpha = 1/\sqrt{k}$) central composite design (CCD) was used to verify the conditions previously optimized [18], where 1.5 g instead of 0.1 g of oil sample was used. The final conditions were set at 43 °C for 30 min of extraction. This condition is also called 1×30min-Vac-HS-SPME later in the text.

Vac-MCT-HS-SPME procedure: After verification that the vials under vacuum were still sealed after repeated extraction, 3-times 10-min and 2-times 15-min cumulative extractions were performed at 43 °C, setting a 5 min equilibration time between extractions at the same temperature, as done in the atmospheric pressure

MCT-HS-SPME procedure. This condition is also called 3×10min-Vac-MCT-HS-SPME later in the text.

1.3.4. GC×GC-qMS analysis

A Shimadzu GCMS-TQ8050 NX (Kyoto, Japan) was used for all analyses. The system was equipped with a reverse fill/flush (RFF) INSIGHT flow modulator (SepSolve Analytical Ltd., Peterborough, UK). An apolar Rxi-5ms (20 m × 0.18 mm × 0.18 µm) was used in the first dimension. A mid-apolar SLB-50ms custom (3 m × 0.25 mm × 0.25 µm) was used in the second dimension. The flow rates were 0.6 mL/min in the first dimension and 16 mL/min in the second one. The second-dimension flow was then split using a passive splitter connected to the MS through a capillary of 1.1 m × 0.18 mm and 0.2 mm × 0.25 mm i.d. and to the VUV detector through a 20 cm x 0.25 mm i.d. (data not used here). The auxiliary bleed line (2 × (1 m × 0.1 mm) with an auxiliary flow controller) flow was 0.6 mL/min. The loop dimensions were 0.53 mm i.d. × 22.665 mm, resulting in a loop volume of 50 µL. The modulation period (PM) was 2.7 s, with 150 ms of flush time, which was held constant throughout the entire duration of the run. The GC oven was set at 35 °C and held for 3 min. Then, the temperature was increased to 280 °C at a rate of 5 °C/min, and held for 1 min, resulting in a total run of 53 min. The transfer line and the ion source temperature were maintained at 250 °C and 200 °C, respectively. The ionization was realized in electronic impact (EI) at 70 eV. The qMS was operated in scan mode with a data acquisition rate of 50 Hz for the mass range of 35-350 m/z.

Data acquisition was performed using GCMS solution v4.50 (Shimadzu). Raw data files were converted to ".cdf" files and imported into ChromSpace software v 2.1.7. NIST17 and FFNSC 3.0 MS commercial libraries were used for identification. Putative identification was based on the combination of the MS similarity (≥80%) and confirmed using experimental linear retention index (LRI) within a ±15 range.

1.3.5. Data elaboration and statistical analysis

Chromatograms were aligned to one user-selected reference chromatogram in ChromSpace software (SepSolve). The alignment algorithm was used to overcome possible retention time drifts across the dataset. The algorithm used the available spectral information to align each chromatogram in the dataset to a single "reference" chromatogram. No further data pre-treatment was required for alignment.

The compounds identified as volatile quality markers in the European Project OLEUM were selected to evaluate their discrimination ability [22]. The list of compounds is reported in Table 6-2. A sub-group of these compounds covering a broad volatility and polarity range was used to directly compare the different sampling conditions investigated (in italic in Table 6-2), plus α-farnesene.

The data matrices with 18 markers were normalized (using z-score normalization) and log-transformed. A 75% frequency of observation within a group cutoff was

applied before performing a hierarchical cluster analysis based on the complete distance of Pearson correlation.

Untargeted tile-based approach for cross-sample comparison

A tile-based approach was applied to the aligned chromatograms to enable the raw data to be imported into the chemometrics platform directly without applying any preprocessing methods. Each chromatogram was divided into small sections or "tiles" (in this case, 13.5 s in the first dimension (equivalent to 4 modulations) and 0.9 s in the second dimension (equivalent to 1/3 of a modulation) with a 20% overlap). The signal for every m/z channel was summed for each tile for comparison across every chromatogram in the dataset. This resulted in thousands of analytical features labelled according to the retention time of the tile they were located in and the specific m/z channel. The data matrix was then cleaned from artifacts, such as siloxanes, through careful comparison with blank samples. An intensity cutoff was applied to eliminate the noise generated by very low m/z signals and a frequency of observation within a group of 75% was applied prior to further statistical elaboration.

The data matrix resulting from the olive oil samples analysis was first normalised using probabilistic quotient normalization based on the median. Then, the data underwent a log10 transformation. Data reduction was then performed using the proprietary feature selection algorithm in ChromCompare+ software (SepSolve Analytical). The algorithm uses a multivariate method to consider the covariance between features. This enabled the top 100 most significant differentiators of the known sample classes (i.e., EVO, VO, and LO) to be found. The tile-based software allows data reduction and preliminary statistical evaluation to be performed independently from identifying each feature, significantly simplifying the overall workflow of data elaboration. However, each feature is correlated with a specific tile. Thus, the retention time and m/z information are retained, allowing identification of the most significantly contributing peaks from the original chromatogram. Nevertheless, the number of features still outweighed the number of samples. Therefore, a machine learning algorithm, namely random forest, was applied to build models and select the most discriminatory core features. Visualization of the results was done using principal component analysis using MetaboAnalyst 5.0 [31] and a hierarchical cluster analysis based on the complete distance of Pearson correlation using Morpheus® (https://software.broadinstitute.org/morpheus/).

The remaining elaborations were performed using Excel® (Microsoft Office, version 2016).

1.4. Results and discussion

1.4.1. Conditions verifications

To implement Vac-MCT-HS-SPME, the applied vacuum (7 mbar) must remain stable after repeated extractions from the same vial. To verify this, the pressure was

measured after three extractions. No changes were observed, proving that the septum was properly resealing the vial after each extraction (Figure 6-1).

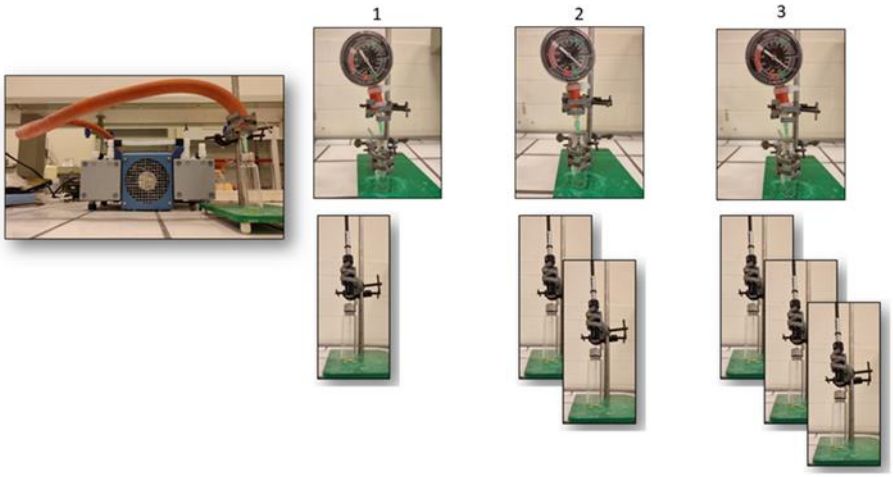

Figure 6-1: *Schematic of the verification of vacuum stability after repeated extractions.*

Preliminary tests showed that using vacuum conditions with 1.5 g of a sample, as in [18] caused a severe overload of the cryogenic trap in this analytical platform. Moreover, our previous studies on the use of MCT-HS-SPME [19,20] showed that the typical oil sample amount reported in the literature (i.e., 1.5-2.0 g) caused saturation of the HS, affecting the reliability of the observed results in mimicking the volatile distribution in the HS. Therefore, 0.1 g of sample was used to avoid HS saturation under regular conditions. Hence, the adaptation of the method and verification of the linearity conditions of the HS were necessary before further tests. Three repeated extractions of 0.1 g of oil sample were performed, confirming the exponential decrease of the signal and the absence of carry-over after each extraction and after the 3-times cumulative one.

The optimal conditions obtained by [18] using 1.5 g of oil sample had also to be verified for the use of 0.1 g of sample. Considering that the use of Vac-HS-SPME significantly improves the extraction kinetics and that the 1.5 g of sample previously used may have altered the result of the optimization due to a severe overload of the HS, the optimal conditions using 0.1 g (no saturation of the HS) and 1.5 g (saturation of the HS) were verified. For this, a CCD was used in the 5-30 min and 30-55 °C ranges. The overall extraction profile was modeled by a response surface of the total summed peak areas (Figure 6-2). The profiles of the response surface were comparable using 0.1 or 1.5 g of sample, showing a maximum response at 30 min and at about 45 °C. Therefore, 30 min extraction at 43 °C was selected as a

working condition, allowing a direct comparison with the results obtained in a previous work [18,32].

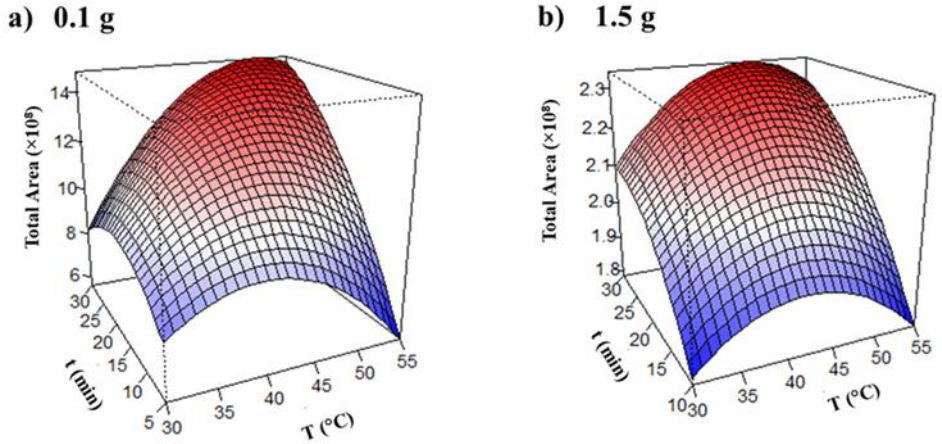

Figure 6-2: *Comparison extraction profile using single Vac-HS-SPME and different sample size, namely a) 0.1 g and b) 1.5 g of oil.*

1.4.2. Comparison of Vac-HS-SPME, MCT-HS-SPME and Vac-MCT-HS-SPME

Previous optimization of regular pressure MCT-HS-SPME showed that optimal performanc-es for the overall pattern recognition analysis (between virgin olive oil of different commer-cial categories) were obtained by performing three consecutive extractions of 10 min [21]. This condition also allowed for an interesting comparison between the single 30 min extrac-tion (optimal extraction time according to the CCD) and the overall same extraction time but divided into 3-times 10 min. Theory and previous results showed how MCT-HS-SPME allowed for substantially higher extraction of the less volatile analytes (up to ~3.5-fold more) [21]. Therefore, the same comparison was performed using Vac-HS-SPME (i.e., 1×30min and 3×10min-Vac-MCT- extractions). Moreover, the results were compared with the previously optimized atmospheric pressure 3×10min-MCT-HS-SPME. The comparison was performed on a sub-group of the quality markers (indicated in italic in Table 6-2) according to the OLEUM Project plus α-farnesene, which previously showed a highly significative gain in extraction using Vac-HS-SPME [18].

Table 6-2: List of the quality marker compounds reported in the literature [21], along with their CAS number, their octanol air partition value (Koa), experimental linear retention index (LRIexp) and the LRI reported in the library (LRIlib). Moreover, the odor and taste descriptors, as reported in http://www.thegoodscentscompany.com/.

Compound	CAS	LRI_{exp}	LRI_{lib}	Log K_{oa}	Odor description	Taste description
Ethanol	*64-17-5*	*459*	*463*	3.779	*alcoholic, ethereal*	*alcoholic*
Ethyl acetate	*141-78-6*	*616*	*586*	*2.991*	*ethereal, fruity*	*ethereal, fruity*
Acetic acid	*64-19-7*	*634*	*667*	*5.218*	*pungent acidic, dairy-like*	*acidic, dairy, fruity*
Ethyl propanoate	105-37-3	706	708	*3.199*	*fruity, sweet*	*ethereal, fruity*
Propanoic acid	79-9-4	*721*	676	5.07	*acidic, pungent, vinegar*	*acidic, dairy, fruity*
3-Methylbutanol	123-51-3	743	729	4.399	alcoholic, fusel, pungent	fusel, fermented, fruity
Octane	*111-65-9*	*800*	*800*	*3.062*	*na*	*na*
Hexanal	*66-25-1*	*809*	*806*	*3.84*	*fresh, green, fatty, aldehydic, grass*	*green, woody, grassy*
(E)-2- Hexenal	*6728-26-3*	*865*	*850*	*4.279*	*green, leafy*	*green, fruity*
1-Hexanol	*111-27-3*	*877*	*867*	*5.185*	*green, alcoholic, oily*	*green, fruity, oily*
Pentanoic acid	*109-52-4*	*888*	*875*	*6.105*	*acidic, rancid*	*acidic, dairy*
(E,E)-2,4-Hexadienal	*142-83-6*	*927*	*914*	*4.768*	*fatty, aldehydic, spicy*	*green, creamy*
(E)-2-Heptenal	18829-55-5	966	956	*4.341*	pungent, green, fatty	green, fruity, fatty, sweet
6-Methyl-5-hepten-2-one	110-93-0	995	986	4.122	citrus, green, musty	green, musty
1-Octen-3-ol	3391-86-4	*988*	969	5.625	*mushroom, earthy*	*mushroom, earthy*
(Z)-3-Hexenyl acetate	3681-71-8	1013	1008	4.195	fresh, green, sweet, fruity, grassy	green, fruity
Nonanal	*124-19-6*	*1114*	*1107*	*4.793*	*waxy, aldehydic, orange, fatty*	*aldehydic, citrus*
(E)-2- Decenal	3913-81-3	*1276*	1265	5.451	*waxy, fatty*	*waxy, fatty*

α-Farnesene*	*502-61-4*	*1510*	*1504*	*5.067*	*citrus, herbal*	*fresh, green*

in *italic* the compounds used to compare the sampling conditions; * not included in the 18 markers from [21] but added for direct comparison with previous Vac-HS-SPME.

Figure 6-3 shows the comparison of the two-dimensional chromatograms using the different conditions tested for a visual comparison of the performance.

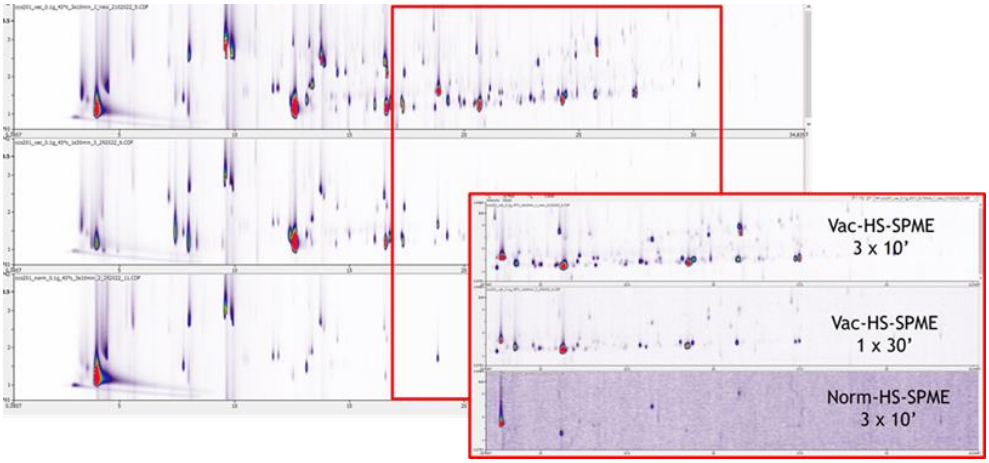

Figure 6-3: *Comparison of the two -dimensional chromatograms obtained using MCT-HS-SPME (Norm-HS-SPME 3×10'); Vac-HS-SPME (1×30') and Vac-MCT-HS-SPME (3×10'). Explosion of the elution zone of the less volatile compounds.*

Figure 6-4 shows the comparison of the two-dimensional chromatograms using the different conditions tested for a visual comparison of the performance. Figure 6-4 shows the relative comparison versus the 3×10min MCT-HS-SPME condition. Values of 1 indicate similar extraction re-sponses, while values >1 indicate higher response with the specific extraction condition. As previously observed [18], the application of Vac-HS-SPME causes an increase in the varia-bility of the obtained results compared to regular pressure extraction. This was explained considering the high viscosity of edible oil, which hindered the mass transfer in the liquid phase, delaying the diffusion at the interface between liquid and air, and thus, the replenish-ing of the depleted HS. Additionally, the variability generally increased with the reduced volatility of the targeted compound. Not surprisingly, the repeated extraction caused an ad-ditional increment of the variance. The median of the relative standard deviation (RSD) was 11%, 24%, and 23% for MCT-, Vac-MCT-, and Vac- HS-SPME, respectively. Therefore, the use of 2×15 min extraction was tested to evaluate a possible reduction of the RSD%, howev-er this was not successful. Indeed, the median RSD was 24%. Moreover, the recovery incre-ment gain was reduced in comparison to the 3×10 min-Vac-MCT-HS-SPME. Therefore, the extraction based on 2×15min-Vac-HS-SPME was not considered for further

evaluation since it showed intermediate results between 1×30min-Vac-, and 3×10min-Vac- HS-SPME in terms of response and no improvement in terms of repeatability.

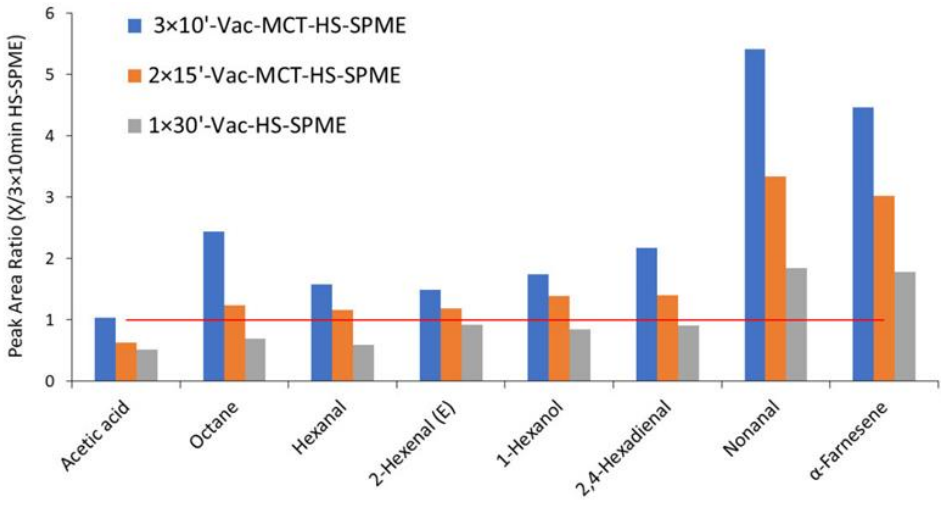

Figure 6-4: *Change in extraction efficiency for 3×10 min-Vac-MCT-, 2×15min Vac-MCT- and 1×30min -Vac- HS-SPME versus 3×10min -MCT-HS-SPME. The red line indicates the value of 1.*

Interestingly, Vac-HS-SPME and atmospheric pressure MCT-HS-SPME show similar extraction responses, being their ratio slightly below 1 for the most volatile compounds and slightly above 1 for less volatile compounds (max. 1.8 for nonanal). Both MCT- and Vac- HS-SPME showed a clear incremental trend towards the less volatile compounds (Figure 6-4). The increment in Vac-HS-SPME is also higher for repeated shorter times (3×10min-Vac-MCT-HS-SPME) compared to a single longer extraction (1×30min-Vac-HS-SPME). In the case of Vac-HS-SPME, only the kinetics of extraction is positively impacted, which means that the longer extraction time (closer to the equilibrium condition for less volatile compounds) reduced the gain compared to atmospheric pressure HS-SPME, tending to null.
On the other hand, MCT-HS-SPME depletes the HS from the most volatile compounds in the first extraction, thus favoring their mass transfer into the HS and, at the same time, reducing the possible displacement effect. These peculiar features also explain why the most volatile compounds (i.e., acetic acid, octane, hexanal) showed a ratio significantly below 1 (i.e., 0.5-0.7) for 1×30min-Vac-HS-SPME. In fact, 3×10min-MCT-HS-SPME logarithmically incremented the amount of the most volatiles, which very rapidly reached the equilibrium, while 1×30min-Vac-HS-SPME can only extract the quantity at (or closer to) the equilibrium condition.

The recovery gain obtained using Vac-MCT-HS-SPME is remarkably higher (particularly for 3×10min-Vac-MCT-HS-SPME), reaching ratios compared to 3×10min HS-SPME above a value of 4 for the less volatile compounds (5.4, and 4.5 for nonanal and α-farnesene, respectively). This behaviour is a synergic combination of the effects observed for Vac- and MCT- HS-SPME alone.
Despite Vac-MCT-HS-SPME showing superior extraction yield, the question of whether the enhanced signal was beneficial to answer more complex questions or if it was only increasing the information noise (as observed for too many repeated MCT-HS-SPME [19]) remained unanswered, and it is addressed in the next sections.

1.4.3. Cross sample comparison

A cross-sample comparison based on pattern recognition technique was carried out to assess the improvement in the overall information extractable using the MCT-HS-SPME with or without vacuum and single Vac-HS-SPME. Twenty-four samples, classified according to their quality (11 EVO, 8 VO, and 5 LO), EVO and VO samples also classified according to their geographical origin, were analyzed using the conditions discussed in section 1.3.3 (i.e., 3×10min-MCT-, 1×30min-Vac-, and 3×10min-Vac-MCT- HS-SPME). Three datasets were obtained, one for each condition tested, and treated separately, as reported in section 1.3.5. A first study was performed targeting the quality markers identified and used in the European OLEUM project [22] (and reported in Table 6-2, excluding farnesene, which does not belong to this set of markers) to evaluate the ability of these compounds to discriminate among commercial categories despite the sampling approach applied. On a second study, the same datasets were treated using random forest to select the most discriminating features among EVO, VO, and LO, and the identified compounds were compared among the different conditions herein tested.

6.1.4.3.1. Targeted cross sample comparison

The 18 compound markers selected according to previous studies [22,33,34] are a reduced number of analytes that have been claimed to satisfactorily discriminate according to the commercial categories classification of virgin olive oils. These 18 compounds were tested in an interlaboratory study among three different laboratories using precisely the same analytical protocol [22]. Therefore, the goal herein is to evaluate whether the list of compounds can be confirmed as markers to support the discrimination of virgin olive oil in the commercial categories by changing the analytical protocol. The 18 compounds were identified based on their MS similarity and LRI and integrated through all the samples. The HCA results obtained using these markers in the three different datasets are shown as heatmaps in Figure 8.5.

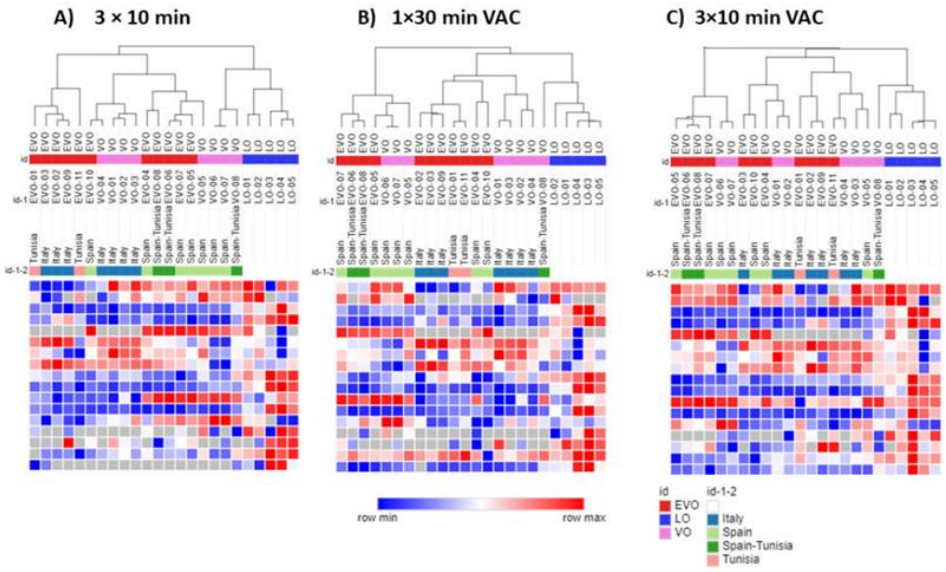

Figure 6-5: *Heat-maps and hierarchical clustering analysis of olive oil samples using the targeted compounds for A) 3 × 10 min MCT-HS-SPME; B) 1 × 30 min-Vac-; C) 3 × 10 min- Vac-MCT- HS-SPME.*

It can be seen at first sight that LO was always effectively differentiated from EVO and VO, despite the sampling conditions used. However, at a closer look, VO-08 was misclassified with LO in all the sampling conditions, while when using 3×10min-MCT-HS-SPME also VO-06 and VO-07 were misclassified. Interestingly, the sensory evaluation of VO-08 presented the lowest score for the positive attributes (i.e., fruity, bitter, and pungent), except for VO-06, which had a slightly lower fruity score (i.e., 1.6 vs 1.9) but higher bitter and pungent score (i.e., 1.8 and 2 vs 1.3 and 1.4, respectively). This can be explained by the fact that the use of MCT-HS-SPME (coupled or not with Vac) enhanced the relative extraction of less volatile compounds (such as nonanal and 2E-decenal, etc.), which can be associated with negative attributes [22,33,34]. This may have caused the misalignment of some VO profiles towards a clusterization into the LO.

Despite some misclassifications, it can be observed in the HCA obtained from the three studied sampling techniques that a general clustering is obtained based on the geographical origin (mainly Spain and Italy; Tunisia was generally clusterized with Italy, as also observed previously [21]). For instance, in the 3×10 min-MCT-HS-SPME condition (Figure 6-5a), EVO and VO are clustered separately from the LO (and the 3 VO discussed before). Within the EVO-VO cluster, two main sub-classes can be observed: one cluster with only EVO from Italy and Tunisia, and a second one including EVO and VO separated into two sub-classes; one with all Italian VO and one Spanish EVO, and the other one with all the Spanish EVO and one Spanish

VO. Examining the 1×30min-Vac-HS-SPME (Figure 6-5b), three main clusters can be observed: one with the LO and the VO-08 sample previously discussed, another cluster with Spanish oils divided into two sub-clusters containing EVO and VO, respectively, and a third cluster divided into three sub-classes, one containing Italian and Tunisian EVO, one with two samples of Spanish EVO and a last one with Italian VO. Finally, looking at the 3×10min-Vac-MCT-HS-SPME condition (Figure 6-5c), we can again observe the LO and the VO-08 group well separated, with another cluster containing Spanish oils divided into VO and EVO, and a third cluster with a confused clustering between EVO and VO but with no clear bias towards the geographic origin.

Besides the technological transformation of olives into oils, the overall volatile signature of virgin olive oils is affected by many additional variables, such as the geographical origin, the botanical cultivars, and the pedoclimatic conditions, among others [35–37]. Thus, it is very difficult to differentiate among the contribution of each variable to identify the markers responsible for the commercial category alone. The results reported here suggest that changing the sampling technique may affect the ability of the proposed markers to dis-criminate between EVO and VO. Furthermore, the geographical origin appears to take major weight over the quality attributes in the statistical analysis.

From the results shown in section 1.4.2, it is clear that the volatile profile obtained by the proposed sampling techniques differs from the one obtained when defining these markers. In-deed, the extraction of the less volatile compounds is enhanced, possibly explaining the lack of accuracy in the independent discrimination between EVO and VO. Nevertheless, it is not clear whether the different volatile profile acquired better captures the sensory response to the specific compounds in comparison to classical HS-SPME as used to define the targeted markers. Moreover, the general geographical-origin-biased classification using the targeted markers with these proposed sampling conditions may also be caused by the different vola-tile profile obtained, causing a discrepancy in the clustering capability. However, the selec-tion of the markers may have been somehow affected by the main origins of the samples used to build the model. Furthermore, the clustering accuracy could also be affected by the harvesting year variations and possibly by the pedoclimatic changes, which have been more severe over the last years due to climate changes, maybe causing a general change in the volatile profile expression. Although extremely interesting, addressing these questions is out of the scope of the present work, and the limited number of samples analyzed in this work allows only for a preliminary discussion. Dedicated investigations would be needed to clarify these observations.

6.1.4.3.2. Untargeted cross sample comparison

To further investigate the ability of the proposed techniques to capture information-rich chromatographic fingerprints, an untargeted data processing was

implemented to extract the significant features for discriminating among the virgin olive oil commercial categories.

The sets of samples were further examined within the post-processing platform using the entire raw data, investigating all the m/z as different channels. The data matrices were pre-treated as described in section 1.3.5. Similar to the targeted approach, a three-cluster model was created based on the three different virgin olive oil qualities, namely EVO, VO, and LO. The 25 most significant features based on RF selection were visualised in a two-dimensional PCA (PC1 and PC2) for the three tested conditions, as shown in Figure 6-6. The out-of-bag (OOB) estimate of error rate was 4.17% for 3×10min-MCT-HS-SPME and 1×30min-Vac-HS-SPME, while 3×10min-Vac-MCT-HS-SPME showed an OOB estimate of error rate of 8.33%. According to the confusion matrices derived from RF (Table 6-3), one EVO sample is misclassified with a VO for all three tested conditions. Furthermore, 3×10min-Vac-MCT-HS-SPME shows a further misclassification of a VO sample with an EVO one. All three conditions showed a full discrimination of the LO samples. The list of the overall selected features is reported in Table 6-4.

Table 6-3: Confusion matrix derived from the random forest performed to discriminate between EVO, VO, and LO.

	3x10 min-MCT-HS-SPME				**1x30 min-Vac-HS-SPME**				**3x10 min-Vac-MCT-HS-SPME**			
	EVO	**LO**	**VO**	**class error**	**EVO**	**LO**	**VO**	**class error**	**EVO**	**LO**	**VO**	**class error**
EVO	10	0	1	0.091	10	0	1	0.091	10	0	1	0.091
LO	0	5	0	0.000	0	5	0	0.000	0	5	0	0.000
VO	0	0	8	0.000	0	0	8	0.000	1	0	7	0.125

Table 6-4: List of the top discriminatory compounds extrapolated after RF analysis to dis-criminate the three different qualities, namely EVO, VO, and LO, reported in order of elu-tion, along with the CAS number, their octanol air partition (K_{oa}), linear retention index (LRI) experimentally calculated and reported in the literature (LRI_{lib}). The different letter on the apex indicates the extraction condition from where they were selected, namely a: 3×10min-MCT-; b: 1×30min-Vac-; c: 3×10min-Vac-MCT- HS-SPME. The odor and taste descriptors are as reported in http://www.thegoodscentscompany.com/.

Compound	**CAS**	**LRI_{exp}**	**LRI_{Lib}**	**Log K_{oa}**	**Odor description**	**Taste description**
Acetic acid [b, c]	*64-19-7*	*634*	*661*	*5.218*	*pungent acidic,*	*acidic, dairy, fruity*

					dairy-like	
Heptane [c]	*142-82-5*	*703*	*700*	*2.747*	*na*	*na*
Pentanal a, b, c	*110-62-3*	*707*	*707*	*3.531*	*fermenty, bready, fruity*	*winey, fermented, bready*
Butanoic acid, methyl ester [c]	*623-42-7*	*717*	*718*	*3.367*	*Pungent, ethereal, fruity*	*fusel, fruity*
Unknown [a]	*na*	*728*	*na*	*na*	*na*	*na*
Unknow ketone [c]	*na*	*756*	*na*	*na*	*na*	*na*
2-Penten-1-ol [c]	*1576-95-0*	*778*	*769*	*4.44*	*green*	*green, ethereal*
Octane [b, c]	*111-65-9*	*800*	*800*	*3.062*	*na*	*na*
Hexanal [a, b, c]	*66-25-1*	*809*	*806*	*3.84*	*fresh, green, fatty, aldehydic, grass*	*green, woody, grassy*
2-Octene [a, c]	*111-67-1*	*815*	*824*	*3.026*	*na*	*na*
1-Methoxyhexane [b]	*4747-07-3*	*830*	*821*	*3.358*	*na*	*na*
Unknown alkane [c]	*na*	*880*	*na*	*na*	*na*	*na*
2-Heptanone [a, b, c]	*110-43-0*	*899*	*898*	*4.141*	*fruity, creamy, cheesy*	*cheesy, fruity*
Styrene [b, c]	*100-42-5*	*902*	*891*	*3.899*	*na*	*na*
Heptanal [b]	*111-71-7*	*911*	*906*	*4.247*	*green, aldehydic, fatty*	*green, aldehydic, oily*
(E,E)-2,4-Hexadienal [b]	*142-83-6*	*927*	*914*	*4.768*	*fatty, aldehydic, spicy*	*green, creamy*
Hexanoic acid, methyl ester [c]	*106-70-7*	*931*	*922*	*4.164*	*fruity, ethereal*	*fruity*
Unknown alkane [a]	*na*	*954*	*na*	*na*	*na*	*na*
6-Methyl-5-hepten-2-one [b,c]	*110-93-0*	*994*	*986*	*4.122*	*citrus, green, musty*	*green, musty*

Octanal [b]	*124-13-0*	*1013*	*1006*	*4.457*	*aldehydic, waxy*	*aldehydic, waxy, citrus*
Nonanal [b]	*124-19-6*	*1114*	*1014*	*4.793*	*waxy, aldehydic, orange, fatty*	*aldehydic, citrus*
Nonanoic acid [a]	*112-05-0*	*1277*	*1272*	*7.748*	*waxy, dairy*	*fatty, waxy*
Copaene [a]	*3856-25-5*	*1385*	*1375*	*4.458*	*woody*	*na*

Overall, superior discrimination was proven for atmospheric pressure 3×10min HS-SPME compared to the previous results reported in the literature [21], probably thanks to the superior separation power achieved by using GC×GC compared to monodimensional GC, and thus to the more reliable and efficient blueprint determination using untargeted approaches.

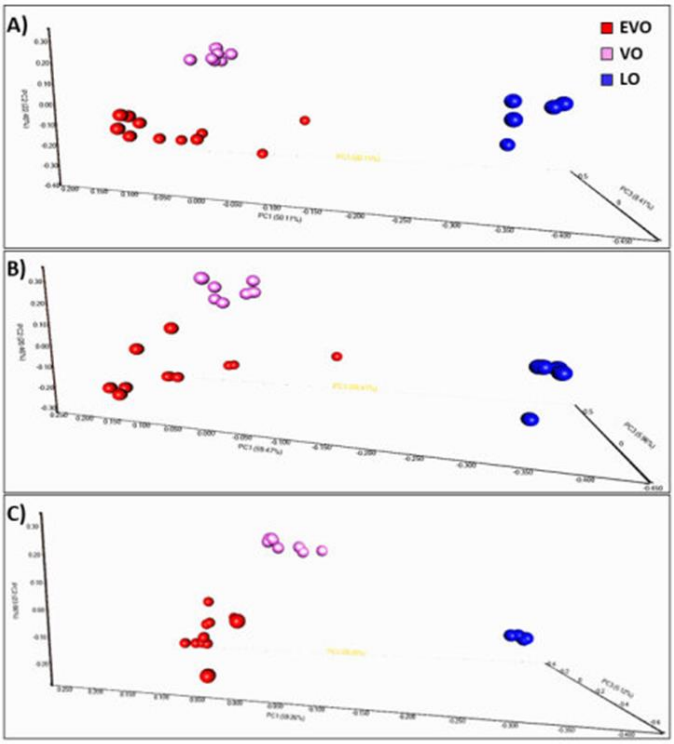

Figure 6-6: *Principal component analysis obtained using the top discriminatory features obtained with RF of the entire set of samples by A) 3 × 10 min-MCT-; B) 1 × 30 min-Vac-; C) 3 × 10 min-Vac-MCT- HS-SPME.*

From the selected features, 23 compounds were tentatively identified based on the MS simi-larity match over 80% and the LRI match with data reported in the commercial libraries used (Table 6-4). Out of the 23 compounds, 6 overlapped with those used for the target analysis (i.e., acetic acid, octane, hexanal, (E,E)-2,4-hexadienal, 6-methyl-5-hepten-2-one, nonanal); all of them recalling defects in sensory perception.

Three compounds were identified in all the conditions, namely butanoic acid methyl ester, hexanal, and 2-heptanone. Eight compounds were identified as significant by using 3×10min-MCT-HS-SPME, they are the three compounds in common with all the conditions, 2-octene (in common with 3×10min-Vac-MCT-HS-SPME), nonanoic acid, copaene, and two unknown. Using 1×30min Vac-HS-SPME 12 compounds were identified, three in common with the other conditions, 4 in common only with 3×10min Vac-MCT-HS-SPME (i.e., acetic acid, octane, styrene and 6-methyl-5-hepten-2one), and 5 significant only for this condition, namely, 1-methoxyhexane, heptanal, (E,E)-2,4-hexadienal, octanal, and nonanal. Finally, 6 compounds were significant only when using 3×10min-Vac-MCT-HS-SPME, i.e., heptane, butanoic acid methyl ester, 2-penten-1-ol, hexanoic acid methyl ester, an unknown ketone, and an unknown alkane.

The first two PCs reported over 70% of the total explained variance for the different extraction techniques. Regardless of the conditions, the separation between the three virgin olive oil categories was overweighted by LO because of their high content of compounds related to defects. From a quality viewpoint, it is more critical to support the discrimination between EVO and VO. Therefore, the data were reprocessed by removing LO and performing the same RF procedure for selecting the most significant features and performing a hierarchical cluster analysis, as shown in the heatmaps of Figure 6-7.

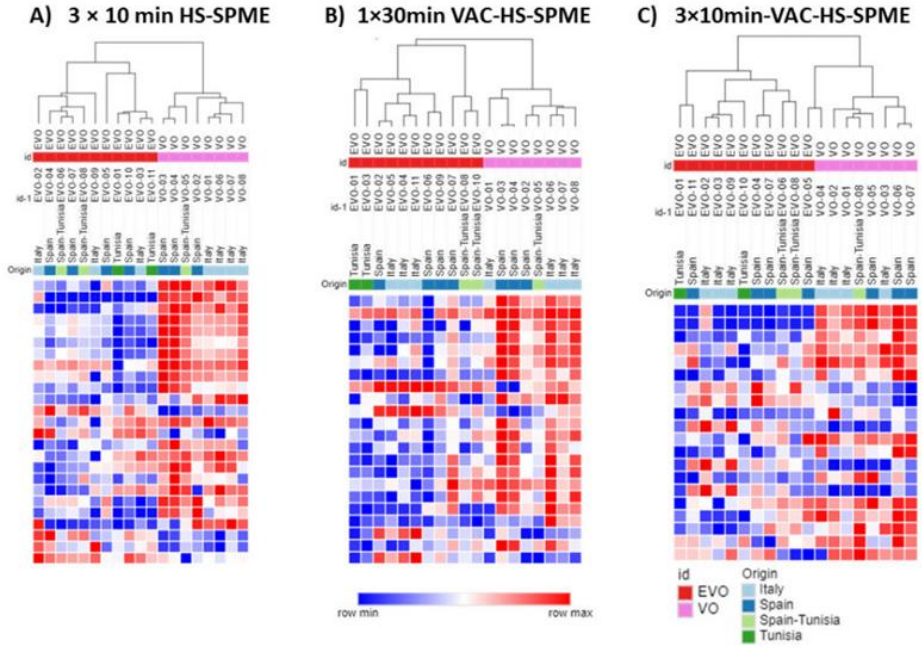

Figure 6-7: *Heatmaps and hierarchical cluster analysis of EVO and VO using RF feature selection for A) 3 × 10 min-MCT- HS-SPME; B) 1 × 30 min-Vac-HS-SPME; C) 3 × 10 min-Vac-MCT-HS-SPME.*

3×10min-MCT-HS-SPME and 1×30min-Vac-HS-SPME showed excellent discrimination between EVO and VO, while a 3×10min-Vac-MCT-HS-SPME showed a misclassification of one EVO (EVO-05) into the VO cluster. Random forest resulted in an OOB estimate of error rate of 0% for 3×10 min-MCT-HS-SPME and 1×30min-Vac-HS-SPME, while 3×10min-Vac-MCT-HS-SPME showed an OOB estimate of error rate of 5.3%. The confusion matrices (Table 6-5) derived from RF confirm the misclassification of one EVO with a VO on the 3×10min-Vac-MCT-HS-SPME.

Table 6-5: Confusion matrix derived from the random forest performed to discriminate between EVO and VO.

	3x10 min-MCT-HS-SPME			1x30 min-Vac-HS-SPME			3x10 min-Vac-MCT-HS-SPME		
	EVO	VO	class error	EVO	VO	class error	EVO	VO	class error
EVO	11	0	0	10	1	0	10	1	0.09
VO	0	8	0	0	8	0	0	8	0

In this case, although not as clear as previously reported for the targeted compounds, a certain clustering degree based on the geographical origin can be observed without building an ad hoc model as in the previous work we published [21]. It can be hypothesized that a more powerful classification can be obtained using a higher number of samples and an ad hoc sampling design.

Of the overall 13 compounds identified (Table 6-6), 6 were shared in all the conditions (i.e., ethyl acetate, acetic acid, penten-3-one, 1-hexanol, hexanal, and pentanal), while hexane was discriminatory when using 3×10min-MCT-HS-SPME and 1×30min-Vac-HS-SPME, but not in 3×10minVac-MCT-HS-SPME. Two compounds, 2-penten-1ol and 3-methylbutanol, were discriminant only when 3×10min-MCT-HS-SPME was used. Whilst 2-butoxyethanol was discriminant only when using 3×10 min-Vac-MCT-HS-SPME, whereas butanoic acid and 1-penten-3-ol showed power of discrimination in 3×10min-Vac-MCT- and 1×30min-Vac- HS-SPME. Among the selected features, only 5 compounds were in common with the previously targeted compounds: acetic acid, ethyl acetate, 3-methylbutanol, 1-hexanol, and hexanal. It is noteworthy that 1-hexanol is the only compound associated with a fruity attribute that is in common with the targeted markers in the OLEUM project. Nevertheless, other compounds responsible for positive attributes and derived from the lipoxygenase pathway were selected, namely penten-3-one, 2-penten-1-ol, pentanal, hexanal, 3-pentanone, and 1-penten-3-ol. Compounds related to specific defects were also selected, such as ethyl acetate, acetic acid and 3-methylbutanal for the winery-vinegar defect; pentanal and hexanal responsible for the rancidity perception (depending on their relative concentration), butanoic acid related to the perception of muddy sediment defect [38]

All the considered compounds are consistent with the discrimination observed and have been reported in the literature as related to the overall description of virgin olive oils, either as positive or as negative attributes. The standing difficulty is to determine a “universal” blueprint, which should be robust despite the analytical technique used, the chemometric algorithm applied, and the set of samples investigated. Only once this goal will be achieved, it will be possible to develop a rapid analytical method able to support the panel test.

Table 6-6: List of the top discriminatory compounds extrapolated after RF analysis to discriminate between EVO and VO, reported in order of elution, along with the CAS number, their octanol air partition (Koa), linear retention index (LRI_{exp}) experimentally calculated and reported in the literature (LRI_{lib}). From which

conditions they were selected is indicated with different letters in apex, which are: a: 3×10min-MCT-; b: 1×30min-Vac-; c: 3×10min-Vac-MCT- HS-SPME.

Compound	CAS	LRI_{exp}	LRI_{lib}	Log K_{oa}	Odor description	Taste description
Hexane [a,b]	*110-54-3*	*600*	*600*	*2.033*	*na*	*na*
Ethyl acetate [a,b,c]	*141-78-6*	*605*	*606*	*2.991*	*ethereal, fruity*	*ethereal, fruity*
Acetic acid [a,b,c]	*64-19-7*	*634*	*661*	*5.218*	*pungent acidic, dairy-like*	*acidic, dairy, fruity*
Penten-3-one [a,c]	*1629-58-9*	*696*	*677*	*3.748*	*pungent, peppery, garlic, etherial*	*ethereal*
2-Penten-1-ol [a]	*1576-95-0*	*778*	*769*	*4.44*	*green*	*green, ethereal*
Pentanal [a,b,c]	*110-62-3*	*707*	*707*	*3.531*	*fermenty, bready, fruity*	*winey, fermented, bready*
3-Methylbutanol [a]	*123-51-3*	*743*	*729*	*4.399*	*alcoholic, fusel, pungent*	*fusel, fermented, fruity*
Hexanal [a,b,c]	*66-25-1*	*809*	*806*	*3.84*	*fresh, green, fatty, aldehydic, grass*	*green, woody, grassy*
1-Hexanol [a,b,c]	*111-27-3*	*877*	*867*	*5.185*	*green, alcoholic, oily*	*green, fruity, oily*
3-Pentanone [b]	*96-22-0*	*697*	*697*	*3.43*	*ethereal, fruity*	*na*
Butanoic acid [b,c]	*107-92-6*	*762*	*773*	*5.45*	*acetic, cheesy, fruity*	*fruity, dairy*
1-Penten-3-ol [b,c]	*616-25-1*	*692*	*680*	*4.514*	*green, radish, fruity*	*green, fruity*
2-Butoxyethanol [c]	*111-76-2*	*927*	*936*	*5.014*	*na*	*na*

1.4.4. Evaluation of method greenness and practicality

Over the last years the evaluation of any analytical method according to the general principles of green analytical chemistry [39] has become fundamental and several metrics have been developed for evaluating their performance. Among the metrics proposed, White Analytical Chemistry (WAC) is the most comprehensive one as it considers not only the green aspects of the method, but also the efficiency (red) and the practical/economical efficiency (blue) of a method [40]. The latter has been further extended into the recently introduced blue applicability grade index (BAGI), named "blue" in reference to the WAC metric [41]. Regarding the green aspects many metrics have been proposed [42]. AGREEprep calculates the impact of

sample preparations giving different scores for sample preparation place (ex-situ, in-situ, on-line, or in-line), hazardous materials, their renewability, amount of waste, size of the sample, number of samples prepared per hour, automation, energy consumption, type of instrument for analysis and operator safety [43].

In the present work AGREEprep and BAGI were considered to evaluate the greenness and applicability potential of the methods (i.e., HS-SPME, Vac-HS-SPME, MCT-HS-SPME, and Vac-MCT-HS-SPME). Comparative analysis was avoidedsince all methods fall within the same evaluation parameters. This would have resulted in identical scores in both AGREEprep and BAGI. The resulting pictograms are reported in Figure 6-8.

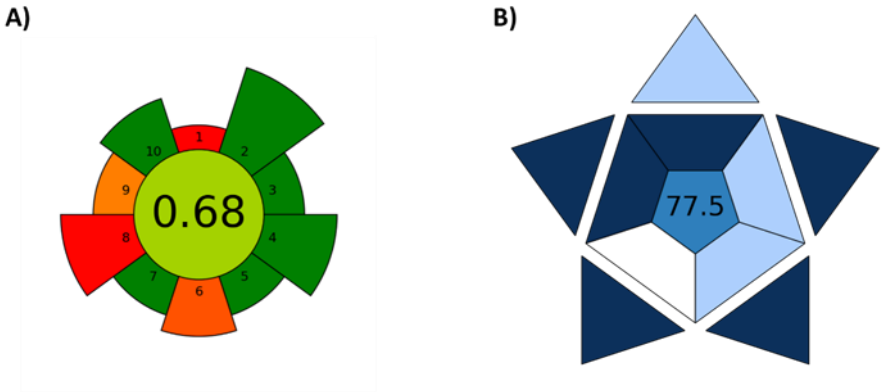

Figure 6-8: *AGREEPrep (A) and BAGI (B) pictograms with scores obtained for the proposed method.*

Although in the present work the proposed methods were not used for absolute quantification, in the first criterium of the BAGI index (i.e., type of analysis) both quantitative and confirmatory analysis type was selected as it can be easily implemented. The BAGI index was negatively impacted by the instruments used (Figure 6-8b). It is worth mention that the specific autosampler able to perform the MCT and the GC×GC chromatographical equipment are still niche analytical products found in a small number of laboratories. The other parameters in light blue were related to the sample throughput (i.e., “simultaneous sample preparation” and “samples per h”) and the type of sample preparation. For the latter, the maximum is reached when no sample preparation is applied at all. Regarding sample throughput, the proposed method can analyzed 2 samples/h (circa 30 minutes extraction and chromatographic run time). As for the nature of the analysis itself and the automation procedure, it is obviously not possible to analyse more samples simultaneously. The time required for the sample pretreatment is limited by the GC run. Thus, the throughput is not determined by the sample preparation itself but by

the time required by the instrumental determination. Nevertheless, the samples can be prepared all together, requiring weighting them into the vial (and in the case of the Vac-HS-SPME, to evacuate the air for 1 min) and then leave them in the autosampler to be analyzed. Therefore, in reality, the operator's time is very limited. Similarly, the sample throughput over-reduced the results of the AGREEprep index (parameter 6). The other parameters scoring low (reddish) are the sample preparation placement (parameter 1, ex-situ), and the energy consumption-related criteria (i.e., parameters 8 and 9) penalized by the use of a GC- and MS-based technique (Figure 6-8a).

Despite a few weaknesses, seven of the parameters showed green color for the AGREEprep index and six were in blue color for the BAGI, and the overall scores were 0.68 and 77.5 for AGREEprep and BAGI, respectively. Therefore, the proposed methods show greenness and practicality based on the general principles of green analytical chemistry.

1.5. Conclusion

The use of Vac-HS-SPME and MCT-HS-SPME were explored as sampling alternatives to classical HS-SPME for the analysis of virgin olive oils. Furthermore, the synergic combination of these two innovative techniques was investigated by the successful implementation of Vac-MCT-HS-SPME. All the proposed techniques showed a superior extraction of semi-volatiles. The use of GC×GC-MS for the analysis of the extracted analytes contributed to an enhanced separation of the constituents and a better definition of the blueprint.

When targeting the analytes that have been previously identified as quality markers and processing the results obtained by each sampling technique, the HCA analysis showed a good discrimination of LO samples, with some justifiable misclassifications due to low-scoring samples. Nevertheless, VO and EVO samples could not be satisfactorily separated. Despite the method applied a geographical origin clustering tendency was observed. Although different hypotheses were presented, they were out of the scope of the present work, and they should be further investigated separately with a significantly higher number of samples.

In order to fully explore the classification capability of the proposed sampling techniques, an untargeted analysis of the obtained chromatograms was performed. Different sets of features were selected by RF for each technique, and a better classification of samples by commercial categories was obtained for all techniques, proving the great potential of Vac-, MCT- and Vac-MCT- HS-SPME in combination with GC×GC for a comprehensive analysis of virgin olive oil samples. Nevertheless, it should be noted that the number of samples was limited in this case, and the selected features should be confirmed by examining a much larger variety of virgin olive oils from different geographical origins and harvesting years.

As aforementioned, it is the authors' opinion that to achieve the goal of supporting the panel test in the classification of EVO and VO, it is vital to select markers able to perform robustly despite the analytical technique applied and the sample set

investigated. Furthermore, using the BAGI and AGREEprep indices, the ‘greenness’ and praticability of the methods was assessed with favourable scores.

1.6. References

[1] C.L. Arthur, J. Pawliszyn, Solid phase microextraction with thermal desorption using fused silica optical fibers, Anal. Chem. 62 (1990) 2145–2148. https://doi.org/10.1021/ac00218a019.

[2] É.A. Souza-Silva, E. Gionfriddo, J. Pawliszyn, A critical review of the state of the art of solid-phase microextraction of complex matrices II. Food analysis, TrAC - Trends in Analytical Chemis-try (2015). https://doi.org/10.1016/j.trac.2015.04.018.

[3] C.H. Xu, G.S. Chen, Z.H. Xiong, Y.X. Fan, X.C. Wang, Y. Liu, Applications of solid-phase microex-traction in food analysis, TrAC - Trends in Analytical Chemistry 80 (2016) 12–29. https://doi.org/10.1016/j.trac.2016.02.022.

[4] P.Q. Tranchida, G. Purcaro, M. Maimone, L. Mondello, Impact of comprehensive two-dimensional gas chromatography with mass spectrometry on food analysis, Journal of Separa-tion Science 39 (2016) 149–161. https://doi.org/10.1002/jssc.201500379.

[5] M.E.I. Badawy, M.A.M. El-Nouby, P.K. Kimani, L.W. Lim, E.I. Rabea, A review of the modern principles and applications of solid-phase extraction techniques in chromatographic analysis, Springer Nature Singapore, 2022. https://doi.org/10.1007/s44211-022-00190-8.

[6] C. Lancioni, C. Castells, R. Candal, M. Tascon, Headspace solid-phase microextraction: Funda-mentals and recent advances, Advances in Sample Preparation 3 (2022) 100035. https://doi.org/10.1016/j.sampre.2022.100035.

[7] T. Górecki, J. Pawliszyn, Effect of Sample Volume on Quantitative Analysis by Solid-phase Micro-extractionPart 1. Theoretical Considerations, The Analyst 122 (1997) 1079–1086. https://doi.org/10.1039/a701303e.

[8] M.J. Trujillo-Rodríguez, V. Pino, E. Psillakis, J.L. Anderson, J.H. Ayala, E. Yiantzi, A.M. Afonso, Vacuum-assisted headspace-solid phase microextraction for determining volatile free fatty acids and phenols. Investigations on the effect of pressure on competitive adsorption phenomena in a multicomponent system, Analytica Chimica Acta 962 (2017) 41–51. https://doi.org/10.1016/j.aca.2017.01.056.

[9] N.P. Brunton, D.A. Cronin, F.J. Monahan, The effects of temperature and pressure on the per-formance of Carboxen/PDMS fibres during solid phase microextraction (SPME) of headspace volatiles from cooked and raw turkey breast, Flavour and Fragrance Journal 16 (2001) 294–302. https://doi.org/10.1002/ffj.1000.

[10] E. Psillakis, E. Yiantzi, L. Sanchez-Prado, N. Kalogerakis, Vacuum-assisted headspace solid phase microextraction: Improved extraction of semivolatiles by non-equilibrium headspace sampling under reduced pressure conditions, Analytica Chimica Acta 742 (2012) 30–36. https://doi.org/10.1016/j.aca.2012.01.019.

[11] E. Psillakis, Vacuum-assisted headspace solid-phase microextraction: A tutorial review, Analytica Chimica Acta 986 (2017) 12–24. https://doi.org/10.1016/j.aca.2017.06.033.

[12] N. Solomou, C. Bicchi, B. Sgorbini, E. Psillakis, Vacuum-assisted headspace sorptive extraction: Theoretical considerations and proof-of-concept extraction of polycyclic aromatic hydrocar-bons from water samples, Analytica Chimica Acta 1096 (2020) 100–107. https://doi.org/10.1016/j.aca.2019.10.050.

[13] E. Yiantzi, N. Kalogerakis, E. Psillakis, Design and testing of a new sampler for simplified vacuum-assisted headspace solid-phase microextraction, Analytica Chimica Acta 927 (2016) 46–54. https://doi.org/10.1016/j.aca.2016.05.001.

[14] M. Vakinti, S.M. Mela, E. Fernández, E. Psillakis, Room temperature and sensitive determination of haloanisoles in wine using vacuum-assisted headspace solid-phase microextraction, Journal of Chromatography A 1602 (2019) 142–149. https://doi.org/10.1016/j.chroma.2019.03.047.

[15] E. Psillakis, E. Yiantzi, N. Kalogerakis, Downsizing vacuum-assisted headspace solid phase micro-extraction, Journal of Chromatography A 1300 (2013) 119–126. https://doi.org/10.1016/j.chroma.2013.02.009.

[16] E. Yiantzi, N. Kalogerakis, E. Psillakis, Vacuum-assisted headspace solid phase microextraction of polycyclic aromatic hydrocarbons in solid samples, Analytica Chimica Acta 890 (2015) 108–116. https://doi.org/10.1016/j.aca.2015.05.047.

[17] E. Psillakis, N. Koutela, A.J. Colussi, Vacuum-assisted headspace single-drop microextraction: eliminating interfacial gas-phase limitations, Analytica Chimica Acta 1092 (2019) 9–16.

[18] S. Mascrez, E. Psillakis, G. Purcaro, A multifaceted investigation on the effect of vacuum on the headspace solid-phase microextraction of extra-virgin olive oil, Analytica Chimica Acta 1103 (2020) 106–114. https://doi.org/10.1016/j.aca.2019.12.053.

[19] S. Mascrez, G. Purcaro, Exploring multiple-cumulative solid-phase microextraction for olive oil aroma profiling, Journal of Separation Science 43 (2020) 1934–1941.

[20] S. Mascrez, G. Purcaro, Enhancement of volatile profiling using multiple-cumulative trapping solid-phase microextraction. Consideration on sample volume, Analytica Chimica Acta 1122 (2020) 89–96. https://doi.org/10.1016/j.aca.2020.05.007.

[21] N.D. Spadafora, S. Mascrez, L. McGregor, G. Purcaro, Exploring multiple-cumulative trapping solid-phase microextraction coupled to gas chromatography–mass spectrometry for quality and authenticity assessment of olive oil, Food Chemistry 383 (2022) 132438. https://doi.org/10.1016/j.foodchem.2022.132438.

[22] E. Casadei, E. Valli, R. Aparicio-Ruiz, C. Ortiz-Romero, D.L. García-González, S. Vichi, B. Quinta-nilla-Casas, A. Tres, A. Bendini, T.G. Toschi, Peer inter-laboratory validation study of a harmo-nized SPME-GC-FID method for the

analysis of selected volatile compounds in virgin olive oils, Food Control 123 (2021). https://doi.org/10.1016/j.foodcont.2020.107823.

[23] L. Cecchi, M. Migliorini, E. Giambanelli, A. Rossetti, A. Cane, F. Melani, N. Mulinacci, Headspace Solid-Phase Microextraction-Gas Chromatography-Mass Spectrometry Quantification of the Volatile Profile of More than 1200 Virgin Olive Oils for Supporting the Panel Test in Their Classi-fication: Comparison of Different Chemometric Approaches, Journal of Agricultural and Food Chemistry 67 (2019) 9112–9120. https://doi.org/10.1021/acs.jafc.9b03346.

[24] R. Aparicio-Ruiz, D.L. García-González, M.T. Morales, A. Lobo-Prieto, I. Romero, Comparison of two analytical methods validated for the determination of volatile compounds in virgin olive oil: GC-FID vs GC-MS, Talanta 187 (2018) 133–141. https://doi.org/10.1016/j.talanta.2018.05.008.

[25] M. Fortini, M. Migliorini, C. Cherubini, L. Cecchi, L. Calamai, Multiple internal standard normali-zation for improving HS-SPME-GC-MS quantitation in virgin olive oil volatile organic compounds (VOO-VOCs) profile, Talanta 165 (2017) 641–652. https://doi.org/10.1016/j.talanta.2016.12.082.

[26] E. Valli, F. Panni, E. Casadei, S. Barbieri, C. Cevoli, A. Bendini, D.L. García-González, T.G. Toschi, An HS-GC-IMS method for the quality classification of virgin olive oils as screening support for the panel test, Foods 9 (2020) 1–15. https://doi.org/10.3390/foods9050657.

[27] S. Barbieri, C. Cevoli, A. Bendini, B. Quintanilla-Casas, D.L. Garcia-Gonzalez, T.G. Toschi, Flash Gas Chromatography in Tandem With Chemometrics: a Rapid Screening Tool for Quality Grades of Virgin Olive Oils, Rivista Italiana Delle Sostanze Grasse 98 (2021) 277–279.

[28] B. Quintanilla-Casas, M. Marin, F. Guardiola, D.L. García-González, S. Barbieri, A. Bendini, T.G. Toschi, S. Vichi, A. Tres, Supporting the sensory panel to grade virgin olive oils: an in-house-validated screening tool by volatile fingerprinting and chemometrics, Foods 9 (2020) 1–14. https://doi.org/10.3390/foods9101509.

[29] B. Quintanilla-Casas, S. Bertin, K. Leik, J. Bustamante, F. Guardiola, E. Valli, A. Bendini, T.G. Toschi, A. Tres, S. Vichi, Profiling versus fingerprinting analysis of sesquiterpene hydrocarbons for the geographical authentication of extra virgin olive oils, Food Chemistry 307 (2020). https://doi.org/10.1016/j.foodchem.2019.125556.

[30] IOC, Sensory Analysis of Olive Oil - Method for the Organoleptic Assessment of Virgin Olive Oil, International Olive Council (2018).

[31] Z. Pang, J. Chong, G. Zhou, D.A. De Lima Morais, L. Chang, M. Barrette, C. Gauthier, P.É. Jacques, S. Li, J. Xia, MetaboAnalyst 5.0: Narrowing the gap between raw spectra and functional insights, Nucleic Acids Research 49 (2021) W388–W396. https://doi.org/10.1093/nar/gkab382.

[32] G. Purcaro, C. Cordero, E. Liberto, C. Bicchi, L.S. Conte, Toward a definition of blueprint of virgin olive oil by comprehensive two-dimensional gas

chromatography, Journal of Chromatography A 1334 (2014) 101–111. https://doi.org/10.1016/j.chroma.2014.01.067.

[33] C. Oliver-Pozo, D. Trypidis, R. Aparicio, D.L. Garciá-González, R. Aparicio-Ruiz, Implementing Dynamic Headspace with SPME Sampling of Virgin Olive Oil Volatiles: Optimization, Quality Ana-lytical Study, and Performance Testing, Journal of Agricultural and Food Chemistry 67 (2019) 2086–2097. https://doi.org/10.1021/acs.jafc.9b00477.

[34] M. Fortini, M. Migliorini, C. Cherubini, L. Cecchi, L. Calamai, Multiple internal standard normali-zation for improving HS-SPME-GC-MS quantitation in virgin olive oil volatile organic compounds (VOO-VOCs) profile, Talanta 165 (2017) 641–652. https://doi.org/10.1016/j.talanta.2016.12.082.

[35] G. Luna, M.T. Morales, R. Aparicio, Characterisation of 39 varietal virgin olive oils by their vola-tile compositions, Food Chemistry 98 (2006) 243–252. https://doi.org/10.1016/j.foodchem.2005.05.069.

[36] F. Angerosa, R. Mostallino, C. Basti, R. Vito, Virgin olive oil odour notes: Their relationships with volatile compounds from the lipoxygenase pathway and secoiridoid compounds, Food Chemis-try 68 (2000) 283–287. https://doi.org/10.1016/S0308-8146(99)00189-2.

[37] M. Greco, N. Spadafora, M. Shine, A. Smith, A. Muto, I. Muzzalupo, A. Chiappetta, L. Bruno, C. Müller, H. Rogers, M.B. Bitonti, Identifying volatile and non-volatile organic compounds to dis-criminate cultivar, growth location, and stage of ripening in olive fruits and oils, Journal of the Science of Food and Agriculture 102 (2022) 4500–4513. https://doi.org/10.1002/jsfa.11805.

[38] A. Genovese, N. Caporaso, R. Sacchi, Flavor chemistry of virgin olive oil: An overview, Applied Sciences (Switzerland) 11 (2021) 1–21. https://doi.org/10.3390/app11041639.

[39] A. Gałuszka, Z. Migaszewski, J. Namieśnik, The 12 principles of green analytical chemistry and the SIGNIFICANCE mnemonic of green analytical practices, TrAC - Trends in Analytical Chemistry 50 (2013) 78–84. https://doi.org/10.1016/j.trac.2013.04.010.

[40] P.M. Nowak, R. Wietecha-Posłuszny, J. Pawliszyn, White Analytical Chemistry: An approach to reconcile the principles of Green Analytical Chemistry and functionality, TrAC - Trends in Analyti-cal Chemistry 138 (2021). https://doi.org/10.1016/j.trac.2021.116223.

[41] N. Manousi, W. Wojnowski, J. Płotka-Wasylka, V. Samanidou, Blue applicability grade index (BAGI) and software: a new tool for the evaluation of method practicality, Green Chemistry 25 (2023) 7598–7604. https://doi.org/10.1039/d3gc02347h.

[42] M. Locatelli, A. Kabir, M. Perrucci, S. Ulusoy, H.I. Ulusoy, I. Ali, Green profile tools: Current sta-tus and future perspectives, Advances in Sample Preparation 6 (2023) 100068. https://doi.org/10.1016/j.sampre.2023.100068.

[43] W. Wojnowski, M. Tobiszewski, F. Pena-Pereira, E. Psillakis, AGREEprep – Analytical greenness metric for sample preparation, TrAC - Trends in Analytical Chemistry 149 (2022) 116553. https://doi.org/10.1016/j.trac.2022.116553.

Chapter 7

Discussion and perspectives

1. Conclusion

Among the five human senses, opposite to sight and hearing, touch, taste, and smell are the most complex to quantify objectively. This is particularly the case for the foods we consume and the hedonic value we attribute to them. Touch is related to the texture of foods, while taste and smell jointly appreciate the flavor. In general, "measuring flavor, assigning it a numerical score, is a real challenge that still sparks considerable scientific debate." Indeed, the modern literature on the subject is as plentiful as it is controversial. However, various approaches are feasible today: the use of sensors embedded in "electronic noses," sensory analysis, and separation-identification techniques.

In the early nineties, the first "electronic nose" was developed at the engineering school of the University of Warwick (UK). Since then, numerous devices have been commercialized for applications in food, environmental, and healthcare fields. These "artificial noses" all rely on the combination of more or less specific sensors with a central computing device that consolidates the "perceived" electrical information. The aim of such instruments is to enable automatic recognition simulating human olfaction through software replacing the human brain. Through this means, it is possible to generate "shape" data, that is, to provide overall, relatively holistic information, rather than distinguishing at the molecular level the occurrence of one or more specific compounds among the entire set of compounds released. Nevertheless, their use makes possible a certain objectification of food flavor via three complementary or even synergistic approaches:

i) a classification according to defined criteria, whether it be basic constituents or formulated food products

ii) the definition/verification of a geographical origin

iii) characterization of the quality of a food or its evolution over shelf-life

Technical mastery of electronic flavor perception systems (such as electronic noses and even electronic tongues) is relatively straightforward; however, the often "black-box" nature of the software makes them rigid and less usable for a significant number of applications or products.

In contrast to instrumental approaches, sensory analysis remains the method of choice for evaluating foods. This approach to flavor (smell and taste) relies on the opinions of human panels and, depending on the objectives, utilizes a panel of experts who are particularly well-trained. According to the French standard NF ISO 5492, sensory analysis is defined as "the examination of the organoleptic properties of a product by the sense organs." Thus, it involves using the human being as a sort of measuring instrument in areas where the senses provide added value compared to usual physicochemical measurements. Sensory analysis revolves around three types of tests: discriminative, descriptive, and hedonic. Its scope extends beyond the agri-food domain, particularly towards environmental studies where odor detection is necessary (olfactory pollution). In this technique, the obtained results have a similar objective to electronic noses as specified above, but they reflect a much more

pronounced "human sensitivity": humans act as direct producers of information; statistical treatments allow for the extraction of trends with a simultaneous estimation of their reliability.

Sensory analysis is of considerable importance in the characterization of olive oils. To this end, the International Olive Council sets no fewer than 11 recommendations in its “Organoleptic Assessement Methods and Standards”. All aim to standardize the procedures to be applied in accordance with strict norms. Great attention is paid to the classification of oils according to their production method and geographical origin. The sensory analysis of olive oil involves a panel test methodology where trained tasters evaluate the aroma and taste of the oil based on predefined attributes. This method is regulated to ensure standardization. Panellists assess the intensity of both positive and negative attributes, and the results are used to grade the oil. It allows to take into account the complex interactions between compounds in the organoleptic perception. However, sensory analysis is subjective and time-consuming, limited by taster fatigue and potential inter panel variability. Moreover, sensory analyses are costly considering the panellist training and the limited number of analyses per day.

Gas chromatography coupled with mass spectrometry is the preferred technique for studying the constituent molecules of food aromas. Nowadays, with the highly efficient capabilities offered by two-dimensional separation methods combined with the performance of spectrometric couplings, multidimensional systems provide up-to-date means of molecular characterization. Nevertheless, aroma evaluation still requires the most representative sampling possible. The present thesis has been framed within the broader perspective of instrumentally characterizing/classifying olive oils with the aim of estimating quality criteria.

In this regards, the aim of this Ph.D. thesis was to investigate a comprehensive HS sampling technique targeting of broadening the range of extractable compounds, enhancing the information that can be derived from the volatile profile, especially by the sensitivity increasing of the less volatile compounds. In this regard, two main approaches were explored: vacuum-assisted HS-SPME (Vac-HS-SPME) and multiple-cumulative trapping HS-SPME (MCT-HS-SPME), closing the study with the investigation of the combination of the two techniques.

The first work explores the impact of vacuum conditions during HS extraction of the volatile profile of virgin olive oils (Chapter 4 section 1). The study employed a comprehensive approach to assess various parameters (temperature, extraction time, viscosity and pressure) affecting the extraction efficiency of volatile compounds from the samples. The experiments were conducted using different pressures (atmospheric and at 7 mbar) and the extracted volatile compounds were analyzed using GC-MS. Lower pressures were found to enhance the extraction efficiency, particularly for compounds with higher vapor pressure (semi-volatiles). Moreover, differently from previous studies on aqueous matrices, the study highlights the importance of temperature on viscous matrices, differently from previous studies on aqueous samples. Indeed, a higher temperature significantly increases the diffusion coefficient of the analytes inside the sample, thus significantly increasing the kinetic

extraction of semi-volatiles. However, the use of higher temperatures should always be applied with care, considering the matrix analysed. For instance, in the evaluation of edible oil quality an excessive temperature can lead to degradation and oxidation phenomena.

Considering the significant improvement of the extraction kinetics using low-pressure conditions for oil samples and the positive synergism of temperature, the use of sub-ambient temperature (5 °C) was investigated. However, due to the partial crystallization of the oil at low temperatures, it was decideded to consider a perishable food commodity as fish, for which low temperature is crucial (Chapter 4 section 2). The comparison between the combination of sub-ambient temperature and vacuum and the one using 30°C and atmospheric pressure showed how the use of cool-temperature sampling led to a more efficient extraction yield compare to the second one, possibly preventing degradation of the sample's volatile profile in such kind of matrices.

The second technique investigated in the context of this thesis was the application of multiple-cumulative trapping solid-phase microextraction (MCT-SPME) for the profiling of aroma compounds in olive oil. This study explores this novel approach to enhance the sensitivity and efficiency extraction of the olive oil aroma. For the sake of comparison and consistency with Vac-HS-SPME, olive oil was maintained as a case study for the MCT applications. In the present study (Chapter 5 section 1) compared classical SPME conditions for olive oil aroma profiling, found in the literature (in terms of extraction time temperature and sample mass). The study demonstrates the effectiveness of MCT-SPME in extracting a broader range of volatile compounds from olive oil compared to conventional SPME methods. The enhanced sensitivity and coverage provided by MCT-SPME enable more comprehensive aroma profiling and characterization of olive oil samples.

Nevertheless, it was proved that the quantity used was way too much, causing the saturation of the headspace. Therefore, a second study was oriented toward the investigation of the impact of the sample quantity on the overall profile obtained and how to better exploit it in this context to demonstrate (Chapter 5 section 2). Then, the work was oriented toward the investigation of MCT-SPME in order to determine sample quantity which does not saturate the headspace. Indeed, selecting an appropriate sample volume to avoid headspace (HS) saturation leads to a marginally heightened sensitivity and notably richer HS fingerprinting. Through the utilization of MCT-SPME, it became feasible to enhance both these aspects, thereby amplifying the volume of information while augmenting sensitivity for semi-volatile compounds.

Following the optimization of multiple-cumulative trapping (MCT) conditions as detailed in the initial explorative study, and the determination of the optimal sample volume as elaborated in the subsequent research, the investigation focused on integrating these refined parameters. This involved the assessment of the quality and authenticity of olive oil on a larger number of samples (Chapter 5 section 3). Through experimental results, the effectiveness of MCT-SPME has been demonstrated in discriminating between different commercial categories of olive oil

and, within the extra virgin olive oils, between the different geographical origins, all based on their volatile composition. The technique proves valuable for detecting markers indicative of quality.

The focus of this thesis was around the advancement of two methodologies designed to enhance the detection of semi-volatile organic compounds, with a specific emphasis on their application to olive oil analysis. Similarly, both methods exhibited a common trait: an augmentation in the extraction of semi-volatile compounds. To explore potential synergies, their integration was explored in the last work of this thesis (Chapter 6).

The first part of this study aimed to compare separately the two techniques and together coupled to comprehensive gas chromatography. It effectively showed the synergistic effect of the merged techniques. As for the previous studies on MCT, a cross-sample study has been realized using the different developed conditions (Vac-, MCT- and Vac-MCT-HS-SPME) in order to demonstrate their potential to separate the samples according to their commercial categories. However, a more systematic approach was used. The volatile profiles obtained with the different techniques were evaluated based on their ability to differentiated the sample on their commercial category. Firstly, a targeted approach was applied using the markers selected as quality markers by the European Union project named OLEUM. Regardless of the technique, a common trend was observed. The origin of extra virgin and virgin olive oils had a more significant discriminating power than the quality. It was postulated that the extraction methods might introduce a bias in the overall profile of these compounds compared to the expected profile defined in the OLEUM project. Hence, an untargeted approach was employed to mitigate any potential bias associated with the selection of compounds. The features selected based on an independent feature on an independent feature selection performed on our samples showed only a limited overlap with the previously proposed quality markers, but allowed for a perfect clustering of the samples according to the commercial categories.

2. Perspectives

The goal of this thesis is to propose new innovative approaches using SPME in the case of oil quality analysis. However, the work focused solely on the development of the method and highlighting its analytical potential. The next step in this work should be the application of this method with a determined analytical objective, for example, in a more qualitative and quantitative approach.

Firstly, parameters concerning the equipment and protocol should be controlled. The part where an operator is required is the one concerning vacuum sealing the vial and adding the olive oil sample. As presented in the chapters involving vacuum usage, the procedure is simple and quick. First, screw the vacuum-specific cap along with an appropriate septum, then pump the air inside the vial using a vacuum pump connected to a needle piercing the septum. Then comes the addition of the olive oil sample. This step can be a significant source of variability in the development of a robust method. The flow of olive oil through the syringe can pose a problem for

quantitative transfer into the vial. Residual oil may indeed remain in contact with the syringe. Even worse, the residual oil could come into contact with the septum during syringe removal, potentially leading to septum contamination. The septa used for vacuum applications can be reused. However, even if they are airtight, they are porous materials that can absorb compounds and release them during subsequent analyses. In such cases, these septa should be for single use only. Investigations could focus on different types of syringes to achieve a homogeneous and repeatable sample deposition.

The second point requiring further investigation concerns the sample homogeneity. Method optimization led to a significant reduction of the sample quantity. Even though 0.1 g of olive oil yields better results in terms of semi-volatile extraction, it is conceivable that this small quantity may not be representative within a sample as complex as olive oil. To address this issue, further investigations could include studies on intra-sample variability. This could involve collecting samples at different depths or sampling points within the olive oil container to assess the variability of the chemical composition across the sample. Additionally, validation studies could be undertaken to determine the minimum sample quantity required to obtain reliable and representative results. This could involve comparisons between different sample quantities and evaluating the reproducibility of the results obtained.

Still for a quantitative purpose, the addition of an internal standard would be necessary. This does not only reduce the analysis time to a single GC cycle but also provides a sensitivity gain due to the concentration factor in the autosampler which would allow the quantification of low-concentrated coupounds. The key factor in this step would focus on how to add the standard because homogenizing an internal standard in a viscous matrix like olive oil can be challenging due to the oil's viscosity and its resistance to solute dispersion.

Finally, the operator's role needs to be evaluated to enable the use of the method in any routine laboratory. Even though the use of vacuum coupled with MCT is straightforward and requires minimal manipulation, thus limiting sources of errors, it is essential to consider the previously mentioned error sources . To address this, one could envision the development of an intra- and inter-laboratory study to evaluate the repeatability using the same set of samples. Additionally, specifying the use of the same equipment that could potentially cause variability in the analyses (such as the syringe used for sample and standard addition, and the same vacuum pump) would be important.

The aim of the thesis primarily focuses on the quality of olive oil. However, a secondary criterion has also been evaluated, which is authenticity. The authenticity of olive oil is essential to maintain consumer trust and ensure food quality, protect local producers and producing regions, and to comply with regulations and origin designations. It also ensures the preservation of traditional production methods and promotes a sustainable economy. For this purpose, an interesting approach would fit perfectly with Vac-MCT because the sesquiterpenes, as secondary metabolites present in olive oil, are influenced by environmental and agro-climatic conditions, leading to variations in their composition and content. Their presence and quantity

have been recognized as valuable markers of olive oil origin. Being semi-volatile compounds with a C15 structure, sesquiterpenes are ideal candidates for using the Vac-MCT technique. Directing the analytical method towards this application could provide valuable information on the specific composition of sesquiterpenes, thus contributing to the characterization and authentication of olive oil based on its origin.

Chapter 8

List of Publications and scientific communications

1.1. Papers related to the PhD work

S. Mascrez, E. Psillakis and G. Purcaro, A multifaceted investigation of the effect vacuum on the headspace solid-phase microextraction of extrac-virgin olive oil, Analytica Chimica Acta, 1103 (2020) 106-114.

N. Delbecque, S. Mascrez, E. Psillakis and G. Purcaro, Sub-ambient temperature sampling of fish volatiles using vacuum-assisted headspace solid phase microextraction: Theoretical considerations and proof of concept, Analytica Chimica Acta, 1192 (2022) 339365.

S. Mascrez and G. Purcaro, Exploring multiple-cumulative trapping solid-phase microextraction for olive oil aroma profiling, Journal of Separation Science, 43 (2020) 1934-1941.

S. Mascrez and G. Purcaro, Enhancement of volatile profiling using multiple-cumulative trapping solid-phase microextraction. Consideration on sample volume, Analytica Chimica Acta, 1122 (2020) 89-96.

N. Spadafora, S. Mascrez, L. McGregor and G. Purcaro, Exploring multiple-cumulative trapping solid-phase microextraction coupled to gas chromatography-mass spectrometry for quality and authenticity assessment of olive oil, Food Chemistry, 383 (2022) 132438.

S. Mascrez, J. Aspromonte, N. Spadafora, and G. Purcaro, Vacuum-assisted and multi-cumulative trapping in headspace solid-phase microextraction combined with comprehensive multidimensional chromatography-mass spectrometry for profiling olive oil aroma, Food Chemistry (2024) 138409.

J. Aspromonte, S. Mascrez, D. Eggermont, G. Purcaro, Solid-phase microextraction coupled to comprehensive multidimensional gas chromatography for food analysis. Analytical and Bioanalytical Chemistry (2023). https://doi.org/10.1007/s00216-023-05048-0.

S. Mascrez, D. Eggermont and G. Purcaro, SPME and chromatographic fingerprints in food analysis, The Royal Society of Chemistry (book chapter), published on 24/03/2023.

1.2. Papers related to side projects

S. Mascrez, S. Danthine, G. Purcaro, Microwave-assisted saponification method followed by solid-phase extraction for the characterization of sterols and dialkyl ketones in fats, Foods, 10 (2021) 445, https://doi.org/10.3390/foods10020445.

M. C. Rosso, F. Stilo, S. Mascrez, C. Bicchi, G. Purcaro and C. Cordero, Shelf-Life Evolution of the Fatty Acid Fingerprint in High-Quality Hazelnuts (Corylus avellana L.) Harvested in Different Geographical Regions, Foods, 10 (2021) 685, https://doi.org/10.3390/foods10030685.

S. Dantine, S. Closset, J. Maes, S. Mascrez, C. Blecker, G. Purcaro and V. Gibon, Enzymatic interesterification to produce zero-trans and dialkylketones-free fats from

rapeseed oil, Oilseeds & fats Crops and Lipids, 29 (2022) 36, https://doi.org/10.1051/ocl/2022029.

A. Fina, S. Mascrez, M. Beccaria, C. De Luca, J. Aspromonte, C. Cordero and G. Purcaro, A high throughput method for fatty acid profiling using simultaneous microwave-assisted extraction and derivatization followed by reversed fill/flush flow modulation comprehensive multidimensional gas chromatography, Advances in Sample Preparation, 4 (2022) 100039.

D. Zanella, A. Henin, S. Mascrez, PH. Stefanuto, F. A. Franchina, JF. Focant, G. Purcaro, Comprehensive two-dimensional gas chromatographic platforms comparison for exhaled breath metabolites analysis, Journal of Separation Science, 45 (2022) 3542-3555.

1.3. Scientific communications

1.3.1. Oral presentations

S. Mascrez, E. Psillakis, G. Purcaro, A comprehensive study on the effect of vacuum of targeted volatile compounds on HS-SPME in a complex matrix: A softer efficient method to profile olive oil aromas, Euro Analysis, September 1-5 2019, Istanbul, Turkey (COST-Action session).

S. Mascrez, G. Purcaro, Determination of dialkyl ketones (DAK) in interesterified lipids by GC-FID and GC-MS, ILSI (International Life Sciences Institute) seminar, 17th November 2019, Gembloux, Belgium.

S. Mascrez, G. Purcaro, Bursting the chromatographic fingerprint by combining vacuum-assisted headspace, multi-cumulative trapping SPME, and GC×GC, 14th Multidimensional Chromatography Workshop, 30 January-1st February 2023, Liège, Belgium.

S. Mascrez, G. Purcaro, Coupling vacuum-assisted headspace and multiple cumulative trapping SPME with GC GC-MS to enhance the chromatographic profiling, 2nd Advances in Separation Sciences, 28-29th June 2023, Gembloux, Belgium.

1.3.2. Posters

S. Mascrez, E. Psillakis, G. Purcaro, A comparative study on the effect of vacuum on HS-SPME of olive oil volatiles, 43rd ISCC & 16th GCxGC Symposium; 13-17 May 2019, Texas, USA.

S. Mascrez, M. Collard, S. Panto, G. Purcaro, Comprehensive multidimensional gas chromatography coupled with dual detection for MOSH&MOAH determination in food, Euro Analysis, September 1-5 2019, Istanbul, Turkey.

S. Mascrez, E. Psillakis, G. Purcaro, Exploring the performance of vacuum-HS-SPME for volatile profiling of olive oil, 9th International Symposium on Recent Advances in Food Analysis (RAFA 2019), 5-8 November 2019, Prague, Czech Republic.

S. Mascrez, S.Moret, G. Purcaro, Direct Immersion-Solid-phase microextraction (DI-SPME) as a highly efficient technique for polycyclic aromatic determination in edible oil, ILSI (International Life Sciences Institute) seminar, 17th November 2019, Gembloux, Belgium.

S. Mascrez, E. Psillakis, G. Purcaro, Vacuum-Assisted HSSPME, An Innovative Sampling Approach, For Food Applications, 25th National Symposium for Applied Biological Science (NSABS), 31st January 2020, Gembloux, Belgium.

S. Mascrez, G. Purcaro, Enhanced Fingerprinting of Extra Olive Oil by Multiple-Cumulative SPME and GC×GC, 12th Multidimensional Chromatography Virtual Workshop, 1-3 February 2021, online organised by University of Liège.

S. Mascrez, E. Psillakis, G. Purcaro, Vacuum-Assisted Headspace SPME: A Powerful Tool For Extra Virgin Olive Oil Profiling Enhancement, EuChemS Sample Preparation, 11-12 March 2021, online.

S. Mascrez, S. Danthine, G. Purcaro, Microwave-Assisted Saponification and SPE for the Simultaneous or Alternative Analysis of Dialkyl ketones and Sterols in Fats, EuChemS Sample Preparation, 11-12 March 2021, online.

S. Mascrez, G. Purcaro, Multi-Cumulative Trapping HS-SPME to enhance the volatile profile of extra-virgin olive oil, AOCS Annual meeting & expo, 3-15 May 2021, online.Winner of a price for the 2nd place of Poster presentation contest.

S. Mascrez, S. Danthine, G. Purcaro, A rapid and efficient method for dialkyl ketones and sterols determination in fat, AOCS Annual meeting & expo, 3-15 May 2021, online.

S. Mascrez, A. Fina, G. Purcaro, A rapid single step microwave-assisted extraction and derivatization method for the analysis of fatty acid in food by GC×GC-FID, EuChemS Sample Preparation, 14-16 March 2022, online.

S. Mascrez, A. Fina, G. Purcaro, Increase the throughput and reliability of fatty acid characterization in food by using a rapid single step microwave-assisted extraction and derivatization method followed by GC×GC-FID, AOCS Annual meeting & expo, 1-4 May 2022, online.

S. Mascrez, G. Purcaro, Enhance HS-SPME extraction kinetics by vacuum-assisted headspace and multi-cumulative trapping SPME and the combination of them for olive oil volatile profiling, AOCS Annual meeting & expo, 1-4 May 2022, online. Winner of a price for the 2nd place of Poster presentation contest.

S. Mascrez, G. Purcaro, Enhancing the olive oil fingerprint by combining vacuum assisted and multi cumulative trapping SPME, 19th GC×GC Symposium, 29 May-2 June 2022, online.